Imperial College London

cep

Centre for Process Systems Engineering

Developing a framework for the optimal deployment of negative emissions technologies

by Mathilde Clémence Fajardy

Centre for Environmental Policy
Centre for Process Systems Engineering
Imperial College London

London, April 2020

Submitted in part fulfilment of the requirements for the degree of
Doctor of Philosophy of Imperial College London and the
Diploma of Imperial College London.

Supervision: Dr. Niall Mac Dowell
Financial support: Imperial College President's PhD scholarship

Declaration of Originality
I certify that all material in this dissertation which is not my own work has been appropriately referenced.

The copyright of this thesis rests with the author. Unless otherwise indicated, its contents are licensed under a Creative Commons Attribution-Non Commercial 4.0 International Licence (CC BY-NC). Under this licence, you may copy and redistribute the material in any medium or format. You may also create and distribute modified versions of the work. This is on the condition that: you credit the author and do not use it, or any derivative works, for a commercial purpose. When reusing or sharing this work, ensure you make the licence terms clear to others by naming the licence and linking to the licence text. Where a work has been adapted, you should indicate that the work has been changed and describe those changes. Please seek permission from the copyright holder for uses of this work that are not included in this licence or permitted under UK Copyright Law.

Abstract

In delivering on the world's climate goals, removing carbon dioxide from the atmosphere is required in addition to deep mitigation efforts. As no carbon dioxide removal method stands out as an obvious winner, which, how, and how much of these technologies should be deployed to guarantee efficient, sustainable and permanent carbon dioxide removal remains a fundamental research challenge. One potential option, bioenergy with carbon capture and storage (BECCS) is likely to play an important role. BECCS's ability to sustainably remove carbon dioxide from the atmosphere is, however, controversial. Given the range of potential outcomes, it is crucial to understand how, if at all, this technology can be deployed in a way which minimises its cost and impact on natural resources and ecosystems, while maximising both carbon removal and energy production. In this dissertation, we explore the regional drivers of BECCS sustainability and cost, and provide insights into the where, when, and extent of environmentally sustainable and economically viable BECCS deployment. We conclude that the total quantity of atmospheric carbon dioxide removal and energy production over the lifetime of a BECCS project, and the time required to start removing carbon dioxide from the atmosphere will likely vary from project to project. This has profound implications for the policy frameworks required to incentivise and regulate the widespread deployment of BECCS technology. When optimising regional biomass supply chains, we find that a myopic focus on energy generation and carbon dioxide removal can result in negative consequences for the broader environment, which warrants consideration for all impacts when assessing the performance of a BECCS project. Finally, when exploring least-cost BECCS deployment pathways to meet global carbon dioxide removal targets, an important finding is that inter-regional cooperation and collaboration are central to sustainably and affordably meeting these targets, with important value creation opportunities for key providers of carbon dioxide removal.

Acknowledgement

First and foremost, I would like to thank my advisor, Niall Mac Dowell, for his incredible presence, guidance and kindness over the course of my PhD. Niall, you have raised my game by constantly pushing me onto the next challenge, and always been there for advice, far beyond the scope of supervision.

I would also like to express my thanks to all the researchers who have enriched my PhD experience. Alyssa Gilbert and Alexandre Koberle from the Grantham Institute, thank you for helping me put my research in a broader context. Sergey Paltsev and Jennifer Morris at the Joint Program at MIT, thank you for giving me the opportunity to expand my research scope and learn new skills. Last but not least, thank you, to Piera Patrizio from IIASA. I greatly value our friendship and research collaboration, and I am looking forward to seeing it flourish in the years to come.

I also consider myself very lucky to have shared by PhD day-to-day life with a wonderful group of people at Imperial. Be it in the office or in trips around the world, thank you to the Cleanfab group for all the memories we have shared. I wish you all the best in the future. A special thank you to my dear Imperial friends, Clara, Clea, Praveen, Shayne, Ricardo and Tim, whose consistent presence over the last four years has been an incredible source of joy and comfort.

Finally, I could not have undertook this PhD without the most important people in my life. Thank you to my parents, Isabelle and Philippe, for leading by example and always providing the right advice. To my three amazing sisters, Marion, Claire and Noëlle, thank you for being a great source of inspiration. And to Alexandre, thank you for making our life so special.

Table of Contents

Abstract **4**

Acknowledgement **5**

List of Figures **12**

List of Tables **15**

Nomenclature **18**

1 Introduction **32**

1.1 Motivation 32

1.2 Objectives 33

1.3 Structure 33

2 Overview of bioenergy with carbon capture and storage **35**

2.1 The need for atmospheric carbon dioxide removal 35

2.2 The history of BECCS 36

2.3 Global deployment status of BECCS 37

2.4 Overview of BECCS technologies 37

2.5 Challenges to BECCS large scale deployment 40

2.5.1 BECCS technical challenges 40

2.5.2 CO_2 negativity 41

2.5.3 Land use and land use change 42

2.5.4 CO_2 breakeven time 42
2.5.5 Energy requirement 43
2.5.6 The water concern 44
2.6 BECCS global potential 44
2.6.1 Geophysical constraints 44
2.6.2 Broader sustainability constraints 45
2.6.3 The case of marginal lands 45
2.6.4 Agricultural residues 47

3 The Modelling and Optimisation of Negative Emissions Technologies (MONET) framework 49

3.1 Objectives and overview of the MONET framework 49
3.2 BECCS supply chain modelling framework 50
3.2.1 Supply chain model overview 50
3.2.2 Supply chain sub-models 55
3.2.3 BECCS water balance 61
3.2.4 BECCS energy balance 65
3.2.5 BECCS carbon balance 74
3.2.6 BECCS cost model 80
3.2.7 BECCS land balance 84
3.2.8 Key outputs for the optimisation framework 84
3.3 BECCS deployment optimisation framework 86
3.3.1 Overview 86
3.3.2 Objective functions 86
3.3.3 Constraints 88
3.3.4 Pareto-front analysis 92
3.3.5 Integrating alternative CO_2 removal methods in MONET 92
3.4 Data collection and curation 93
3.4.1 Type of data 93
3.4.2 Data source 94

3.5 Modelling and optimisation scenarios 102
3.5.1 Bioenergy availability: preventing land use change and water stress 102
3.5.2 Supply chain assumptions 102

4 Carbon balance and resource efficiency of selected BECCS value chains 104
4.1 Introduction 104
4.1.1 Objectives of the chapter 104
4.1.2 Bioenergy supply chain modelling in the literature 105
4.1.3 BECCS water footprint in the literature 105
4.2 The water-land-carbon nexus of BECCS 106
4.2.1 Case study 106
4.2.2 BECCS water intensity 106
4.2.3 BECCS carbon intensity 112
4.2.4 BECCS net carbon intensity 115
4.2.5 BECCS net carbon efficiency 118
4.3 BECCS dynamic GHG emissions profile 119
4.3.1 Single dynamic balance 119
4.3.2 Multiple dynamic balances 121
4.3.3 Sensitivity analysis and alternative scenarios 123
4.4 Implications for resource mobilisation 125
4.5 Comparison with other carbon dioxide removal methods 128
4.6 Preliminary conclusions and discussion 129

5 Is BECCS a threat to energy security? 131
5.1 Introduction 131
5.1.1 Objectives of the chapter 131
5.1.2 EROI for technology valuation 132
5.1.3 The EROI of bioenergy 133
5.1.4 The UK as a case study 134
5.2 BECCS net electricity balance 135

5.2.1 Thought experiment . . . 135
5.2.2 Energy model validation . . . 136
5.2.3 Cumulative energy demand of BECCS . . . 139
5.2.4 E_IROI and Net Electricity balance . . . 141
5.3 Improving BECCS net electricity balance . . . 145
5.3.1 BECCS plant base efficiency . . . 145
5.3.2 Identification of main energy losses . . . 145
5.3.3 Power generation efficiency improvement and implications for resource mobilisation . . . 147
5.4 Preliminary conclusions and discussion . . . 149

6 Environmental trade-offs between optimal biomass supply chains in selected regions 152
6.1 Introduction . . . 152
6.1.1 Objectives of the chapter . . . 152
6.1.2 Biomass supply chain design is a multi-criteria optimisation problem 153
6.2 Optimal biomass supply chain in the water-land-carbon nexus . . . 154
6.3 Trade-offs within the water-carbon-land nexus . . . 157
6.4 Sensitivity analysis . . . 159
6.4.1 Limiting supply . . . 159
6.4.2 Ramping up the carbon removal target . . . 162
6.5 Energy production or resource conservation? . . . 163
6.6 Preliminary conclusions and discussion . . . 167

7 Cost-optimal and sustainable BECCS deployment to meet global targets 168
7.1 Introduction . . . 168
7.1.1 Objectives of this chapter . . . 168
7.1.2 Regional allocation of BECCS deployment . . . 168
7.1.3 BECCS cost in the literature . . . 170
7.2 Drivers of BECCS cost . . . 172
7.2.1 BECCS cost in different regions . . . 172

7.2.2 BECCS deployment: where, when and how much? 174
7.2.3 BECCS cost curve 178
7.2.4 Does electricity generation matter? 180
7.3 CO_2 removal: *cui bono?* 180
7.4 Sensitivity to CO_2 storage capacity 184
7.5 Preliminary conclusions and discussion 186

8 Conclusions 188

8.1 Conclusions and contributions made 188
8.1.1 Does BECCS deliver resource efficient negative emissions? . . . 188
8.1.2 Does BECCS provide energy? 190
8.1.3 What are the trade-offs within the BECCS resource nexus? . . . 191
8.1.4 What are the geophysical and geopolitical drivers of BECCS cost-optimal deployment? 193
8.2 Limitations of the thesis and future work 194
8.2.1 Biomass-to-x 194
8.2.2 Co-deployment of CDR methods 195
8.2.3 Biomass growth model 195
8.2.4 Multi-objective optimisation of BECCS value chain 195
8.2.5 Dynamic modelling in MONET 196
8.2.6 Broadening the scope of feedstock and regions 197
8.2.7 BECCS deployment: possible *vs.* probable 197
8.2.8 Accounting for BECCS social impact 197

References 198

A Appendix: Biomass drying model 233

B Appendix: MONET input data **236**

B.1 Energy, GHG and cost data 236

B.2 Biomass data 242

B.3 Land cover data 249

B.4 Electricity data 253

B.5 CO_2 storage data 257

List of Figures

2.1 Different CDR methods, different challenges 36
2.2 Illustration of different BECCS pathways 38
2.3 Global bioenergy requirement and potential 45

3.1 Schematic of the NETs trilemma 50
3.2 Illustration of the MONET framework 50
3.3 Overview of BECCS value chain modelling framework 52
3.4 Sub-regions and ports considered in MONET 53
3.5 Illustration of a crop growth cycle 62
3.6 Overview of the BECCS dynamic energy model 74
3.7 Methodology of direct and indirect land use change effects accounting . 76
3.8 Methodology for the derivation of ILUC conversion factors 77
3.9 Overview of the BECCS deployment optimisation framework 86
3.10 Length and scatter of biomass and GHG and energy normalised data series 95
3.11 CO_2 removal target profile in MONET 99

4.1 Blue and grey water footprints of four crops in different regions 109
4.2 BECCS water intensity as a function of capture rate and biomass co-firing proportion 110
4.3 BECCS water intensity as a function of capture rate and co-firing proportion, with and without supply chain 111
4.4 Carbon footprint of pellets without land use change 114
4.5 Carbon footprint of pellets including land use change 115

4.6 BECCS carbon intensity as a function of capture rate and biomass co-firing proportion . . . 115
4.7 BECCS carbon intensity as a function of capture rate and co-firing proportion, with and without supply chain, without land use change 116
4.8 BECCS carbon intensity as a function of capture rate and co-firing proportion, with and without supply chain, with land use change 117
4.9 BECCS CO_2 efficiency diagram with and without land use change . . . 119
4.10 BECCS cumulative emissions over 50 years for different land types, with land use change . . . 120
4.11 BECCS cumulative emissions over 50 years for case studies A-D 122
4.12 Sensitivity of BECCS dynamic GHG balance towards eight parameters . 124
4.13 Resource mobilisation to remove 12 $GtCO_2/yr$ via different CDR methods 128

5.1 Case study and input data considered for the EROI analysis 136
5.2 Cumulative energy demand of different BECCS value chains for three system boundaries: energy carrier, primary energy and electrical energy equivalent . . . 139
5.3 Dynamic EROI of biomass pellets and dynamic E_1ROI of BECCS 142
5.4 Lifetime EROI of biomass pellets and lifetime E_1ROI of BECCS 143
5.5 Cumulative net electricity balance of a BECCS facility using different feedstock . . . 144
5.6 BECCS plant power generation efficiency as a function of capture rate and biomass co-firing proportion . . . 145
5.7 Energy flow diagram of BECCS value chain for domestic and imported bioenergy pellets . . . 146
5.8 Mean net electricity balance, water use, land use as a function of CO_2 removed per unit per year and capacity requirement 148

6.1 Optimal biomass supply chain under different objective functions in the median scenario . . . 155
6.2 Optimal biomass supply chain under different objective functions in the optimistic scenario . . . 156
6.3 Optimal biomass supply chain under different objective functions in the optimistic scenario . . . 157

6.4 Pareto lines between water use, land use, and CO_2 efficiency, in the median scenario 158
6.5 Total land use and land use change under different objective functions . 160
6.6 Sensitivity of BECCS water-optimal value chain to marginal land availability 161
6.7 BECCS minimal water use, minimal land use and maximal CO_2 efficiency under different impact scenarios 162
6.8 Total water use, land use, and CO_2 efficiency and land use change under different objective functions and input data scenarios 164
6.9 BECCS total electricity generated under different land constraints, under different objective functions 166

7.1 Break-down of BECCS cost in different regions 173
7.2 Map of BECCS cost-optimal deployment by 2100 176
7.3 Map of cost-optimal BECCS deployment in 2100 under optimistic and pessimistic supply chain scenarios 177
7.4 BECCS cost and negative emissions credit curves in 2100 179
7.5 Map of BECCS least negative emissions credit deployment by 2100 . . . 180
7.6 CO_2 removal surplus and cost over time 181
7.7 The impact of collaboration on global CO_2 removal via BECCS 182
7.8 Map of BECCS cost-optimal deployment by 2100 under a high CO_2 storage capacity scenario 184
7.9 The impact of collaboration on global CO_2 removal via BECCS under a high CO_2 storage capacity scenario 185

A.1 Drying model 233

B.1 Regional BECCS plant CAPEX over time 239
B.2 Map of land cover, marginal land area and harvested wheat area in MONET 249

List of Tables

2.1 Literature review on marginal land availability 47

3.1 Regional cumulative GHG emissions and shares of global CO_2 removal targets in MONET 99

4.1 Regions and climates selected in the model 106

4.2 Water footprint model comparison with literature results 107

4.3 Comparison of IECM water intensity calculations with literature for a pulverized coal power plant with a wet cooling tower and no CCS . . . 107

4.4 Carbon footprint model comparison with literature results 113

4.5 Case studies dynamic GHG balance results repartition 121

4.6 Alternative scenarios effect on BECCS carbon intensity over 50 years . . 125

4.7 Resource mobilisation to remove 12 $GtCO_2/yr$ via BECCS 127

4.8 BECCS, afforestation and DACCS performance comparison to remove 12 $GtCO_2/yr$ 129

5.1 EROI values in the literature 134

5.2 Energy model key input data 137

5.3 Embodied energy model comparison with literature results 138

B.1 Mean values and ranges of uncertainty of energy data 236

B.2 Mean values and ranges of uncertainty of GHG data 237

B.3 Mean values and ranges of uncertainty of miscellaneous data 238

B.4 Country-level cost data 240

B.5 Biomass production and transport costs 241
B.6 Other regional cost assumptions 241
B.7 Mean values and ranges of uncertainty of wheat straw data 242
B.8 Mean values and ranges of uncertainty of miscanthus data 243
B.9 Mean values and ranges of uncertainty of switchgrass data 244
B.10 Mean values and ranges of uncertainty of short rotation coppice willow data 245
B.11 Regional road tortuosity and biomass yield (Brazil and China) 246
B.12 Regional road tortuosity and biomass yield (EU and India) 247
B.13 Regional road tortuosity and biomass yield (US) 248
B.14 Land cover, marginal land and harvested wheat harvested area (Brazil and China) 250
B.15 Land cover, marginal land and harvested wheat harvested area (EU and India) 251
B.16 Land cover, marginal land and harvested wheat area (US) 252
B.17 Electricity cost and carbon intensity over time (1/3) 253
B.18 Electricity cost and carbon intensity over time (2/3) 254
B.19 Electricity cost and carbon intensity over time (3/3) 255
B.20 Energy conversion factors 256
B.21 CO_2 storage capacity in the BAU and high scenarios in Brazil and China 258
B.22 CO_2 storage capacity in the BAU and high scenarios in the EU and India 259
B.23 CO_2 storage capacity in the BAU and high scenarios in the USA 260

Nomenclature

Mathematical Symbols

Sets and indices

Symbol	Unit	Description
Sets		
c,c'	-	country for biomass production/BECCS plant (biomass conversion and CO_2 storage) $r \in$ {Brazil, China, Europe, India, US}
sr,sr'	-	sub-region for biomass production/BECCS plant (biomass conversion and CO_2 storage), $(sr,sr') \in$ {Acre, ... Wyoming}
b	-	type of biomass, $b \in$ {miscanthus, switchgrass, wheat straw, short rotation coppice willow (SRC willow)}
l	-	type of land, $l \in$ {cropland, grassland, forest, marginal land},
p,p'	-	ports considered for biomass shipping from sub-region sr to sr', $p \in$ {Belem,...Norfolk}
t	-	transport method, $t \in$ {AllRoad, RoadSeaRoad, Notransport}
e	-	energy method considered for energy balance calculation, $e \in$ {EC,PE,EEQ} or {Energy Carrier, Primary Energy, Electrical Energy Equivalent}
d	day	daily time step, $d \in \{1,2,...,360\}$
m	month	monthly time step, $m \in \{1,2,...,12\}$
a	year	annual time step for biomass production (50 year lifetime project), $a \in \{1,2,...,50\}$

$time$	year	decadal time step for BECCS deployment, $time \in \{2030,2040,...2100\}$
Indices		
k	-	biomass value chain stage, $k \in$ {size reduction, drying, grinding, pelleting, cooling, road transport 1, sea transport, road transport 2, pellet grinding} or {SR, D, G, P, C, RT1, ST, RT2, PG}
i	-	input product at the field level, $i \in$ {nitrogen, phosphorous, potassium, lime, seed, pesticide} or {N, P_2O_5, K_2O, lime, seed, pesticide}
j	-	fuel or power input, $j \in$ {diesel, biodiesel, natural gas, wood pellets, coal, electricity} or {diesel, bioD, NG, wood, coal, elec}
f	-	biomass transport format, $f \in$ {pellet, chip, bale}

Selected input parameters

Symbol	Unit	Description
Sub-region parameters		
$Lat(sr)$	°	latitude of the centroid of sub-region sr
$Long(sr)$	°	longitude of the centroid of sub-region sr
$Area(sr)$	ha	Geographic area of sub-region sr
$WH_{Area}(sr)$	ha	Wheat harvested area of sub-region sr
$t(sr)$	-	Average road tortuosity in sub-region sr
$Ind_{RoadAccess}(sr,sr')$	-	Binary parameter indicating if road access between sr and sr'
$OWR(sr)$	-	Overall water stress
$Ind_{storage}(sr)$	-	Binary parameter indicating if storage available
$cap(sr)$	tCO_2	CO_2 storage capacity
Time parameters		
$CO2target_{P2}(time)$	tCO_2/yr	CO_2 removal target in scenario P2
$CO2target_{P3}(time)$	tCO_2/yr	CO_2 removal target in scenario P3

$Decarb_{elec}(sr,time)$	$\%_{\text{BAU}}$	Electricity decarbonisation rate
$CAP_{PP}(sr,time)$	$	Capital cost of a 500 MW BECCS plant
Port parameters		
$PortLat(p)$	°	latitude of the port p
$PortLong(p)$	°	longitude of the port p
$SD_p(p,p')$	km	Sea distance from port p to port p'
$Ind_{PortAccess}(sr,p)$	-	Binary parameter indicating if road access between sr and p
$Ind_{port}(p)$	-	Binary parameter indicating if road access between port p and location of plant (and storage) sr
Biomass parameters		
$HHV_{bio}(b)$	MJ/kg_{DM}	Higher heating value of dry biomass (DM)
$MC_{bio,h}(b)$	$\%_{\text{WM}}$	Moisture content of wet biomass (WM) at harvest
$C_{bio}(b)$	$\%_{\text{DM}}$	Carbon content of dry biomass
$N_{bio}(b)$	$\%_{\text{DM}}$	Nitrogen content of dry biomass
$P_{bio}(b)$	$\%_{\text{DM}}$	Phosphorus content of dry biomass
$K_{bio}(b)$	$\%_{\text{DM}}$	Potassium content of dry biomass
Crop parameters		
$Yield_{th}(sr,b)$	$\text{t}_{\text{DM}}\text{/ha/yr}$	Theoretical dry crop yield at harvest
$HR(sr,b)$	yr/harvest	Harvest rotation
$HP_1(b)$	$\%_{\text{Yield}}$	Proportion of full yield harvested the first harvest
$HP_2(b)$	$\%_{\text{Yield}}$	Proportion of full yield harvested the second harvest
$CL(sr,b)$	yr	Crop lifetime
$NoH(sr,b)$	-	Number of harvests
$FDoH(sr,b)$	-	First day of harvest (1st or 15th of the month)
$FMoH(sr,b)$	-	First month of harvest
$St1(sr,b)$	d	Length of growth stage 1
$St2(sr,b)$	d	Length of growth stage 2
$St3(sr,b)$	d	Length of growth stage 3
$St4(sr,b)$	d	Length of growth stage 4
$Kc_{ini}(sr,b)$	-	Initial stage growth coefficient
$Kc_{mid}(sr,b)$	-	Mid-season stage growth coefficient
$Kc_{late}(sr,b)$	-	End stage growth coefficient

$K_c(d)$		Daily crop coefficient function
$R_i(b)$	kg/ha	Application rate of input $i \in$ {lime, seed}
$R_{i'}(b)$	kg/ha/yr	Annual application rate of input $i' \in$ {pesticide}
$FR_{landprep}(b)$	L/ha	Fuel requirement of land preparation (once in a crop lifetime)
$FR_{Harvest}(b)$	L/ha/harvest	Fuel requirement for crop maintenance and harvest
ER_{irrig}	MJ/mm	Irrigation energy requirement
$Cap_{mach}(sr,b)$	$ per ha per yr	Cost of machinery use
$Lab_{farm}(sr,b)$	hrs per ha	Labour use
D_{farm}	km	Driving distance within farm
$ER_{SR}(b)$	MJ/t_{WM}	Energy requirement (fuel) for biomass size reduction (b)
$ER_k(b)$	MJ/t_{WM}	Power requirement for process $k \in$ {D, G, P, C, PG}
Agricultural residues parameters		
$RR(b)$	$\%_{DM}$	Residue recovery if b agricultural residue
$CR(b)$	$\%_{DM}$	Residue collection rate if b agricultural residue
N_{av}	$\%_{N}$	Fraction of nitrogen in residue available to the field
P_{av}	$\%_{P}$	Fraction of phosphorous in residue available to the field
K_{av}	$\%_{K}$	Fraction of potassium in residue available to the field
Climate parameters		
$T_{low}(sr,m)$	°	Monthly average low temperature
$T_{high}(sr,m)$	°	Monthly average high temperature
$n_s(sr,m)$	hrs	Monthly average daily sunshine hours
$u_{2m}(sr,m)$	m/s	Monthly average wind speed at 2 meters
$RH_{mean}(sr,m)$	%	Monthly mean humidity
$P(sr,m)$	%	Monthly precipitations
$z(sr)$	m	Elevation of weather station
$\Phi(sr)$	°	Latitude of weather station
Energy parameters		

EE_i	MJ/kg	Embodied energy in input product $i \in$ {N, P_2O_5, K_2O, lime, seed, pesticide}
$EE_j(e)$	MJ/unit	Embodied energy in fuel $j \in$ {diesel, biodiesel, wood pellets, natural gas, coal, HFO}
LHV_j	MJ/unit	Lower heating value of fuel $i \in$ {diesel, biodiesel, coal, natural gas, wood pellets}
$ER_{SupTrans}$	MJ/kg	Fuel use for the transport of supplies
$FE_{RT,f}$	L/(km.t_{WM})	Fuel efficiency in road transport for biomass format $f \in$ {pellet, chip, bale}
FE_{STHFO}	MJ/(km.t_{WM})	HFO efficiency in pellet sea transport
N_2O emissions parameters		
$EF_{N,add}$	kg_{N_2O-N}/kg_N	N_2O-N emission factor for N addition
$EF_{N,volatilized}$	kg_{N_2O-N} $/kg_{NH_3-N+NO_x-N}$	N_2O-N emission factor for N volatization
$EF_{NH_3-N+NO_x-N}$	$kg_{NH_3-N+NO_x-N}$ $/kg_N$	NH_3-N+NO_x-N emission factor for N addition
$EF_{N,leaching}$	kg_{N_2O-N}/kg_N	N_2O-N leaching factor for N addition
$N_{Leaching}$	kg_N/kg_N	N fraction leaching in the ground water
Carbon parameters		
CF_i	$kgCO_2$/unit	Carbon footprint of input $i \in$ {N,P_2O_5, K_2O, lime, seed, pesticide}
$CF_{elec,BAU}$	MJ/unit	Carbon footprint of electricity in the BAU scenario (before decarbonisation)
EF_j	$kgCO_2$/L	Emission factor (direct emission + carbon footprint) of fuel $j \in$ {diesel, bioD, NG, HFO, wood}
$EF_{SupTrans}$	$kgCO_2$/kg	Emission factor for the transport of supplies
$EF_{RT,f}$	$kgCO_2$/(km.t_{WM})	Emission factor of road transport of biomass format $f \in$ {pellet, chip, bale}
EF_{STHFO}	$kgCO_2$/(km.t_{WM})	Emission factor of sea transport of biomass pellet
$ILUC(l)$	$kgCO_2$/ha	Indirect land use change emission coefficient
$LUC(l)$	$kgCO_2$/ha	Direct land use change emission coefficient

EF_{TS}	$\%_{\text{CO2captured}}$	Emission factor from CO_2 transport and storage
Power plant parameters		
$FIT_{F_{fuel}}(b)$		Fit function of fuel flowrate in power plant
$FIT_{F_{water}}(b)$		Fit function of water flowrate in power plant
$FIT_{NPO}(b)$		Fit function of the power plant net power output
C_f	$\%_{\text{WM}}$	Coal-biomass co-firing proportion
R_{CCS}	%	CCS capture rate
$LoadFactor$	%	Power plant load factor
C_{coal}	$\%_{\text{WM}}$	Coal carbon content
HHV_{coal}	MJ/kg_{DM}	Coal HHV
$Area_P$	ha	Power plant area
Financial parameters		
IR_m	-	interest rate of infrastructure $m \in$ {pellet plant, power plant, CO_2 transport network} or {PeP, PP, CO2T}
PL	yrs	BECCS project lifetime
LT_m	yrs	lifetime of infrastructure $m \in$ {pellet plant, power plant, CO_2 transport network} or {PeP, PP, CO2T}
Cost parameters		
$Cost_i(sr)$	\$/unit	Cost of input $i \in$ {N,P_2O_5, K_2O, lime, seed, pesticide}
$Cost_{lab}(sr)$	\$/hr	Agricultural labour cost
$Cost_{land}(sr,l)$	\$/ha/yr	Land rent cost
$Cost_j(sr)$	\$/L	Cost of fuel $j \in$ {diesel, biodiesel}
$Cost'_j(sr)$	\$/kg	Cost of fuel $j' \in$ {NG,wood,coal}
$Cost_{RT,f}$	$\$/(km.t_{\text{WM}})$	Cost of road transport of biomass format $f \in$ {pellet, chip, bale}
$Cost_{STHFO}$	$\$/(km.t_{\text{WM}})$	Cost of sea transport of biomass pellet
$CAP_m(sr)$	$\$t_{\text{WM}}$	Capital cost of infrastructure $m \in$ {pellet plant, dryer, CO_2 transport network} or {PeP, D, CO2T}

$OM_D(sr)$	$\$t_{WM}$	operational cost of infrastructure $m \in$ {pellet plant, dryer, CO_2 transport network, power plant} or {PeP, D, CO2T, PP}
$capa_{co2}t(sr)$	tCO_2/yr	Capacity CO_2 transport network
Miscellaneous parameters		
$C_{N_2O-N \rightarrow N_2O}$		Conversion factor N_2O-N-N_2O to N_2O
$C_{P \rightarrow P_2O_5}$		Conversion factor P to P_2O_5
$C_{K \rightarrow K_2O}$		Conversion factor K to K_2O
$C_{C \rightarrow CO_2}$		Conversion factor C to CO_2
GWP_{N_2O}	$kgCO_2/kg_{N_2O}$	Global warming potential of N_2O
SR_k	$\%_{DM}$	Solid recovery of process $k \in$ {SR,D,G,P,T}
ML_k	$\%_{DM}$	Moisture loss during process $k \in$ {SR,D,G,P,T}
TMC_{drying}	$\%_{WM}$	Target moisture content after drying
$HR_{evap,drying}$	$MJ/t_{H_2O,evap}$	Drying heat requirement
$\eta_{boiler,NG}$	$\%_{LHV}$	Drying boiler efficiency with natural gas
$\eta_{boiler,bio}$	$\%_{LHV}$	Drying boiler efficiency with biomass
$C_{Elec \rightarrow PE}(sr,e)$		Power to primary energy conversion
$C_{j \rightarrow Elec}(sr,e)$	-	Fuel $j \in$ {diesel, bioD, NG, HFO, wood} conversion to electricity conversation efficiency

In the following table, $set1 = (sr,sr',b,p,p',t)$, $set2 = (sr,sr',b,l,p,p',t)$, $set3 = (sr,sr',b,l,p,p',t,e)$.

Selected calculated parameters

Symbol	Unit	Description
Crop yield		
$Ind_{Harv}(yr)$	-	Harvest indicator
$Ind_{Landprep}(yr)$	-	Land preparation indicator
$Yield(sr,b,a)$	$t_{WM}/ha/yr$	Biomass annual dry mass yield
$tYield(sr,b)$	t_{DM}/ha	Total dry mass biomass yield over project lifetime
Biomass yield model		
$Bio_{proc,k}$	$t_{DM}/ha/yr$	Dry biomass processed at stage k

$MC_{proc,k}$	-	Moisture content of biomass at stage k
$Pellet(sr,b,a)$	$t_{DM}/ha/yr$	Dry pellet production
$CPellet(sr,b,a)$	$t_{WM}/ha/yr$	Cumulative pellet production
$tPellet(sr,b)$	t_{WM}/ha	Pellet production over project lifetime
Drying and N_2O emissions model		
EF_{N_2O}	kg_{N_2O}/kg_N	N_2O emissions per N applied
$ER_{drying}(sr,b,e)$	MJ/t_{DM}	Drying energy demand per ton of dry biomass
BECCS power plant model		
C_{fuel}	$\%_{WM}$	BECCS plant input fuel carbon content
HHV_{fuel}	MJ/kg_{WM}	BECCS plant input fuel HHV
NPO	MW_e	BECCS plant net power output
F_{fuel}	t_{WM}/hr	BECCS plant fuel flowrate
F_{water}	t/hr	BECCS plant water flowrate
η	$\%_{HHV}$	BECCS plant power generation efficiency
$WU_{PP,hour}$	m^3/hr	BECCS plant water use per hour
WI_{PP}	m^3/MWh_e	BECCS plant water intensity
$WF_{PP}(sr,b)$	m^3/t_{DM}	BECCS plant water footprint
$CO2_{PP,hour}(sr,b)$	tCO_2/hr	BECCS plant CO_2 emitted per hour
CI_{PP}	$kgCO_2/MWh_e$	BECCS plant carbon intensity
$LU_{PP,hour}(sr,b)$	yr.ha/hr	BECCS plant land use per hour
LI_{PP}	ha/MWh_e	BECCS plant land intensity
$LF_{PP}(sr,b)$	ha/t_{DM}	BECCS plant land footprint
Transport model		
$RD1(set1)$	km	Biomass transport road distance from sr to sr' or p (first leg)
$SD(set1)$	km	Biomass transport sea distance from p and p'
$RD2(set1)$	km	Biomass transport road distance from p' to sr' (second leg)
Land footprint model		
$LF_{SC}(sr,sr',b,t)$	ha/t_{DM}	Biomass pellet land footprint
$LF_{PP}(sr,b)$	ha/t_{DM}	BECCS plant land footprint
$LF(sr,sr',b,t)$	ha/t_{DM}	BECCS total land footprint
Water footprint model		
$ET_0(sr,m)$	mm/day	Monthly average of daily reference crop evapotranspiration
$ET_{0,day}(sr,d)$	mm/day	Daily reference crop evapotranspiration
$ET_{0,a}(sr,d)$	mm/day	Yearly reference crop evapotranspiration

Pr_{day}	mm/day	Daily precipitation
Pr_e	mm/day	Monthly effective precipitation
$Pr_{e,day}$	mm/day	Daily effective precipitation
$tPr(sr)$	mm/growing cycle	Total water precipitation over the crop growth cycle
$CWR(wr,b)$	mm/yr	Crop water requirement
$IN(Sr,b)$	mm/yr	Crop irrigation need
$BlueWF_{SC}(sr,sr',b,t)$	m^3/t_{DM}	Biomass pellet blue water footprint
$GreenWF_{SC}(sr,sr',b,t)$	m^3/t_{DM}	Biomass pellet green water footprint
$GreyWF_{SC}(sr,sr',b,t)$	m^3/t_{DM}	Biomass pellet grey water footprint
$WF_{SC}(sr,sr',b,t)$	m^3/t_{DM}	Biomass pellet water footprint
$MWF_{SC}(sr,sr',b,t)$	m^3/t_{DM}	Marginal biomass pellet water footprint
WI	m^3/MWh_e	BECCS net water intensity
MWI	m^3/MWh_e	BECCS marginal water intensity
Energy demand model		
$ED_{k,ha}(set3,a)$	MJ/ha	Energy demand of stage k per hectare in year a
$ED_{SC,ha}(set3,a)$	MJ/ha	Total supply chain energy demand per hectare in year a
$CED_{SC,ha}(set3,a)$	MJ/ha	Cumulative supply chain energy demand per hectare in year a
$tED_{SC}(set3,e)$	MJ/t_{DM}	Cumulative supply chain energy demand per ton of pellet over the project lifetime
$ED_{coal,ha}(sr,sr',b,t,e,a)$	MJ/ha	Energy demand per hectare from coal use in the power plant in year a
$EG_{PP,ha}(sr,sr',b,t,a)$	MJ/ha	Total electricity production per hectare at year a
$CEG_{PP,ha}(sr,sr',b,t,a)$	MJ/ha	Cumulative electricity production per hectare at year a
$tEG_{PP}(sr,sr',b,t)$	MJ/t_{DM}	Cumulative electricity production per ton of pellet over the project
$ED_{ha}(set3,a)$	MJ/ha	Total BECCS energy demand per hectare in year a
$CED_{ha}(set3,a)$	MJ/ha	Cumulative energy demand per hectare in year a
$EB_{ha}(set3,a)$	MJ/ha	Net energy balance per hectare in year a
$E_lB_{ha}(set3,a)$	MJ/ha	Net electricity balance per hectare in year a
$CEB_{ha}(set3,a)$	MJ/ha	Cumulative net energy balance per hectare at year a

$CE_lB_{ha}(set3,a)$	MJ/ha	Cumulative net electricity balance per hectare at year a
$tEB_{ha}(set3)$	MJ/ha	Total net energy balance per hectare over the project lifetime
$tE_lB_{ha}(set3)$	MJ/ha	Total net electricity balance per hectare over the project lifetime
$tEB(set2)$	$MJ/_{DM}$	Total net energy balance per ton of pellet over the project lifetime
$tE_lB(set2)$	$MJ/_{DM}$	Total net electricity balance per ton of pellet over the project
$EG_{bio,ha}(sr,b,a)$	MJ/ha	Bioenergy production in the form of raw biomass per hectare in year a
$CEG_{bio,ha}(sr,b,a)$	MJ/ha	Cumulative bioenergy production (raw biomass) per hectare at year a
$EG_{pellet,ha}(sr,sr',b,t,a)$	MJ/ha	Bioenergy production in the form of pellets per hectare in year a
$CEG_{pellet,ha}(sr,sr',b,t,a)$	MJ/ha	Cumulative bioenergy production (pellets) per hectare in year a
$EROI(set2)$	-	Biomass pellet energy return on investment
$E_lROI(set2)$	-	BECCS electricity return on investment
$BET_E(set2)$	years	BECCS energy breakeven time
$\eta_{net}(set2)$	$\%_{HHV}$	BECCS net efficiency
Carbon footprint model		
$CF_{k,ha}(set2,a)$	$kgCO_2/ha$	GHG emissions of stage k
$CF_{SC,ha}(set2,a)$	$kgCO_2/ha$	Total supply chain emissions per hectare at year a
$CF_{coal,ha}(sr,sr',b,t,a)$	$kgCO_2/ha$	Power plant coal emissions per hectare at year a
$CF_{CCS,ha}(sr,sr',b,t,a)$	$kgCO_2/ha$	Emissions from CO_2 transport and injection per hectare in year a
$CF_{ha}(set2,a)$	$kgCO_2/ha$	Total emissions from BECCS per hectare in year a
$CCF_{SC}(set2,a)$	$kgCO_2/ha$	Cumulative supply chain emissions per hectare in year a
$CCF(set2,a)$	$kgCO_2/ha$	Cumulative BECCS emissions per hectare in year a
$tCF_{SC,ha}(set2,a)$	$kgCO_2/ha$	Total supply chain emissions per hectare over the project lifetime

$tCF_{ha}(set2,a)$	$kgCO_2/ha$	Total BECCS emissions per hectare over the project lifetime
$tCF_{SC}(set2,a)$	$kgCO_2/_{DM}$	Total supply chain emissions per ton of pellet over the project lifetime
$tCF(set2,a)$	$kgCO_2/_{DM}$	Total BECCS emissions per ton of pellet over the project lifetime
$BioCO2_{P,ha}(sr,b,a)$	$kg_{CO_2}/ha/yr$	Amount of biogenic CO_2 emitted from the plant at year a
$CoalCO2_{P,ha}(sr,sr',b,t,a)$	$kg_{CO_2}/ha/yr$	Amount of coal CO_2 emitted from the plant at year a
$SCO2_{ha}(sr,sr',b,t,a)$	$kg_{CO_2}/ha/yr$	Amount of CO_2 captured and stored in geological formations at year a
$CSCO2_{ha}(sr,sr',b,t,a)$	kg_{CO_2}/ha	Cumulative amount of CO_2 captured and stored in geological formations at year a
$tSCO2_{ha}(sr,sr',b,t)$	kg_{CO_2}/ha	Total CO_2 geologically stored per hectare over project lifetime
$RCO2_{ha}(set2,a)$	$kg_{CO_2}/ha/yr$	Net CO_2 removed at year a
$CRCO2_{ha}(set2,a)$	kg_{CO_2}/ha	Cumulative net CO_2 removed per hectare in year a
$tRCO2_{ha}(set2,a)$	kg_{CO_2}/ha	Total net CO_2 removed per hectare over project lifetime
$tRCO2(set2,a)$	$kg_{CO_2}/_{DM}$	Total net CO_2 stored per ton of pellet the project lifetime
$SCO2_{bio,ha}(sr,b,a)$	$kg_{CO_2}/ha/yr$	Amount of CO_2 biologically stored at year a
$CSCO2_{bio,ha}(sr,b,a)$	kg_{CO_2}/ha	Cumulative CO_2 biologically stored per hectare at year a
$tSCO2_{bio,ha}(sr,b)$	kg_{CO_2}/ha	Total CO_2 biologically stored per hectare over the project lifetime
$\eta_{CO2}(set2)$	-	CO_2 efficiency *i.e* the ratio of net CO_2 removed to the amount of CO_2 stored in the biomass,
$BET_{CO2}(set2)$	years	CO_2 breakeven time *i.e.* the numbers of years required for the system to reach net CO_2 negativity.
$CI(set2)$	$kgCO_2/MWh_e$	BECCS net carbon intensity
$RCO2_{hour}(set2)$	tCO_2/hr	Net CO_2 stored per hour
$tRCO2_{unit,year}(set2)$	$tCO_2/unit/yr$	Net CO_2 stored per unit per year
$Unit_{CO2}(set2)$	$1/t_{CO_2}$	Number of BECCS 500MW units per tCO_2 removed

$RCO2_{CO2}(set2,a)$	-	Net CO_2 removed per year per ton of CO_2 removed
Cost model		
$cost_{n,ha}(set2)$	\$/ha/yr	annual cost per hectare of item $n \in$ {land, inputs, farm, PeP, RT1, ST, RT2,PG }
$tcost_{SC}(set2)$	\$/ton	Total biomass supply chain cost per ton of pellet
CRF_m		Capital recovery factor of infrastructure $m \in$ {PP,CO2T }
$cost_{PP,MWh}(sr,sr',b,time)$	\$/MWh	BECCS plant cost per MWh (CAPEX - O&M)
$cost_{CO2T,SCO2}(sr)$	\$/tCO_2	CO_2 transport cost
$tcost_{PP}(sr,sr',b,t,time)$	\$/ton	BECCS plant total cost per ton of pellet
$tcost_{CO2TS}(sr,sr',b,t,time)$	\$/ton	CO_2 t&S cost per ton of pellet
$rev_{PP}(set2)$	\$/ton	BECCS plant total revenue per ton of pellet
CRF_m		Capital recovery factor of infrastructure $m \in$ {PP,CO2T}
$tcost(set2)$	\$/ton	BECCS total cost per ton of pellet
$tCB(set2)$	\$/ton	BECCS total cost balance per ton of pellet
$BE_{NEC}(set2)$	\$/tCO_2	Breakeven negative CO_2 credit
Output for optimisation		
$Unit_{CO2}(set2)$	1/tCO_2	Number of 500 MW BECCS units per ton of CO_2 removed
$SCO2_{CO2}(set2)$	tCO_2/tCO_2	Tons of stored CO_2 per ton of CO_2 removed
$WU_{CO2}(set2)$	m^3/tCO_2	BECCS water use per ton of CO_2 removed
$MWU_{CO2}(set2)$	m^3/tCO_2	BECCS marginal water use per ton of CO_2 removed
$LU_{SC,CO2}(set2)$	ha/tCO_2	BECCS field land use per ton of CO_2 removed
$LU_{PP,CO2}(set2)$	ha/tCO_2	BECCS power plant land use per ton of CO_2 removed
$LU_{CO2}(set2)$	ha/tCO_2	BECCS total land use per ton of CO_2 removed
$PU_{CO2}(set2)$	t_{DM}/tCO_2	BECCS pellet use per ton of CO_2 removed
$BU_{CO2}(set2)$	t_{DM}/tCO_2	BECCS biomass use per ton of CO_2 removed
$EB_{CO2}(set2)$	MJ/tCO_2	BECCS net electricity balance per ton of CO_2 removed

$cost_{CO2}(set2)$	$/tCO$_2$	BECCS cost per ton of CO_2 removed
$CB_{CO2}(set2)$	$/tCO$_2$	BECCS cost balance per ton of CO_2 removed

Optimisation variables

Symbol	Unit	Description
$RCO2_{opt}(set2,time)$	tCO_2/yr	Net CO_2 removed per year per configuration
$tRCO2_{opt}(set2,time)$	tCO_2	Net CO_2 removed over the time horizon
$tWU_{opt}(set2,time)$	m^3	Total water use over the time horizon
$tMWU_{opt}(set2,time)$	m^3	Total marginal water use over the time horizon
$tLU_{opt}(set2,time)$	ha	Total land use over time horizon
$tBioCO2_{opt}(set2,time)$	DM	Total CO_2 stored in biomass over the time horizon
$tEB_{opt}(set2,time)$	MJ	Total net electricity balance over the time horizon
$t\eta_{CO2}(set2,time)$	-	Total CO_2 efficiency
$SCO2_{opt,reg}(set2,time)$	tCO_2/yr	CO_2 stored per year per region sr'
$CSCO2_{opt,reg}(set2,time)$	tCO_2	Cumulative CO_2 stored per region sr' at time $time$

Acronyms

BECCS	Bioenergy with carbon capture and storage
CAPEX	capital expenditures
CCS	Carbon capture and storage
CDR	Carbon dioxide removal
EROI	Energy return on Investment
FAO	Food and Agriculture Organisation
GHG	Greenhouse gas
IAM	Integrated assessment model
IEA	International Energy Agency
IGCC	Integrated gasification combined cycle
ILUC	Indirect land use change
LUC	Land use change

NET	Negative emissions technology
NEC	Negative emissions credit
OPEX	Operational expenditures
WM	wet mass (biomass)
DM	dry mass (biomass)

Chapter 1

Introduction

1.1 Motivation

Human-induced climate change, in the form of extreme weather events, global temperature rise, or ocean level rise, has dramatically worsened since first impacts were quantified in the seventies [1]. Global awareness acknowledging the gravity of the situation, and international efforts to fight it has, however, been much slower to follow. In 2015, in a landmark agreement in Paris, 187 countries agreed to limit global warming 'well below' 2°C, and pursue efforts towards 1.5°C. Notwithstanding this agreement, global carbon dioxide (CO_2) emissions have reached their highest level yet in 2018, suggesting the inadequacy of national pledges and their implementation [2]. In 2019, as the Amazon forest is burning at an alarming rate, international cooperation and collaboration in tackling this crisis is needed more than ever.

According to integrated assessment modelling (IAM), unprecedented changes in the energy system are required to limit global warming to 1.5°C by the end of the century [3]. In addition to deep mitigation of emissions, net removal of carbon dioxide from the atmosphere has become indispensable in meeting these goals. Carbon dioxide removal (CDR) methods is a general term used to refer to both natural solutions, which focus on enhancing natural CO_2 sinks such as land or forests, and engineered solutions, which are technologies designed to remove and store CO_2, also referred to as 'Negative emissions technologies' (NETs), in the literature. So far, however, no option stands out as a 'silver bullet', and a portfolio approach is likely to be the best way forward to deliver sustainable and cost effective CDR. One potential technology, bioenergy with carbon capture and storage (BECCS) is, in principle, valuable to both CO_2 mitigation – by providing low carbon energy – and to CO_2 removal. This has resulted in BECCS being consistently and largely deployed in scenarios compatible with a 1.5-2°C target. BECCS's omnipresence in IAMs has sparked controversy around BECCS competition for arable

land and fresh water, in addition to questions concerning its ability to actually remove CO_2 from the atmosphere. Additionally, the scale at which BECCS can be sustainably deployed, and the regional drivers of BECCS sustainability and cost over time, remain broadly unknown.

With this dissertation, I aim at understanding the conditions leading to BECCS providing net CO_2 removal from the atmosphere, at low energy, resource and financial costs. Considering the complexity of impacts associated with the large scale deployment of the technology, we adopt a multi-level, spatially and temporarily explicit, systems modelling and optimisation approach to represent the deployment of the technology with the evolution of CO_2 removal targets and the energy system. Whilst the case studies in this dissertation focus exclusively on BECCS, we present a framework which could be used to explore the optimal deployment of negative emissions technologies in general (see Section 3.3.5 in Chapter 3).

1.2 Objectives

The overarching objectives of this thesis can be articulated as follows:

1. Identify the conditions leading to BECCS being a net provider of CO_2 removal, at a low resource – land and water – cost, and in a timely fashion,
2. Determine the conditions leading to BECCS being a net provider of energy, and discuss the trade-offs between the two services provided by BECCS, energy production and CO_2 removal,
3. Quantify the regional trade-offs between BECCS sustainability indicators,
4. Identify the competitive advantages – geopolitical context, sustainable biomass availability, storage availability, cost – and the value opportunities of different regions for least cost BECCS deployment, and how these evolve with increasing CO_2 removal targets and the decarbonisation of the energy system.

1.3 Structure

The dissertation is structured as follows. Chapter 1 introduces the thesis motivation and objectives. Chapter 2 provides an overview of the BECCS technology and its main challenges. Chapter 3 presents the Modelling and Optimisation of Negative Emissions Technologies (MONET) framework, developed for the purpose of this dissertation. The following chapters then apply MONET to four case studies so as to explore key questions related to BECCS large scale deployment. Chapter 4 discusses the biomass supply chain conditions leading to BECCS being a net provider of negative emissions, in a

relevant time frame, at a low land and water cost. Chapter 5 explores BECCS capacity to generate energy, and the trade-offs between BECCS energy generation and CO_2 removal. Based on these identified conditions, Chapter 6 explores the trade-offs within the BECCS trilemma – energy generation and CO_2 removal, resource minimisation and limited impacts on ecosystems, in resource optimal regional biomass supply chains. Chapter 7 determines the cost-optimal deployment of BECCS and quantifies the value of international collaboration in meeting global CO_2 removal targets. Finally, Chapter 8 concludes on the technical, economic and policy implications of these findings, and discusses the limitations of this thesis as well as future axis of research.

The following peer-reviewed journal papers and reports were used in writing this study. Below is indicated which chapter the papers mostly contribute to.

1. M Fajardy, N Mac Dowell, 2017, *Can BECCS deliver sustainable and resource efficient negative emissions?*, Energy & Environmental Science, 10(6): 1389-1426 [4] (Chapter 4)
2. M Fajardy, N Mac Dowell, 2018, *The Energy Return On Investment of negative emissions: is BECCS a threat to energy security?*, Energy & Environmental Science, 11(6): 1581-1594 [5] (Chapter 5)
3. M Fajardy, S Chiquier, N Mac Dowell, 2018, *Investigating the BECCS resource nexus: delivering sustainable negative emissions*, Energy & Environmental Science, 11(12): 3408-3430 [6] (Chapter 6)
4. M Fajardy, N Mac Dowell, 2020, *Recognising the value of collaboration in delivering carbon dioxide removal*, (*in peer review*) (Chapter 7)
5. M Fajardy, A Daggash, P Patrizio, N Mac Dowell, 2019, *Negative Emissions: Priorities for Research and Policy Design*, Frontiers in Climate, 1 [7] (Chapter 2)
6. H Daggash, M Fajardy, P Heptonstall, N Mac Dowell, R Gross, 2019, *Bioenergy with carbon capture and storage, and direct air carbon capture and storage: Examining the evidence on deployment potential and costs in the UK*, a UKERC Technology and Policy Assessment, available at `http://www.ukerc.ac.uk/programmes/technology-and-policy-assessment/bioenergy-with-ccas.html` [8] (Chapter 2)
7. M Fajardy, A Koberle, N Mac Dowell, A Fantuzzi, 2019, *BECCS deployment: a reality check*, Grantham Institute Briefing paper No 28, available at `https://www.imperial.ac.uk/media/imperial-college/grantham-institute/public/publications/briefing-papers/BECCS-deployment---a-reality-check.pdf` [9] (Chapter 2)

Chapter 2

Overview of bioenergy with carbon capture and storage

2.1 The need for atmospheric carbon dioxide removal

Transitioning from a 2°C to a more stringent 1.5°C target has rendered atmospheric carbon dioxide removal indispensable, with between 190 and 1,190 $GtCO_2$ cumulative removal required before the end of the century, depending on the pace and extent of climate change mitigation efforts [10, 11]. Several methods have been identified as capable of delivering CDR at scale. A first category includes methods enhancing natural carbon sinks, such as forests, via afforestation/reforestation (AR/RE), land, via biochar, soil carbon sequestration, and oceans, via ocean liming and/or fertilisation. A second category involves enhancing mineral sinks, through enhanced weathering of minerals. Finally, the last category involves geological storage of CO_2, captured from bioenergy plants (BECCS) or directly from the air (DACCS) [12]. Whilst these technologies differ in terms of cost, potential scale, and side-effects, none appears to be an obvious and unique winner to deliver large-scale CDR [13]. Key strengths and challenges of selected CDR methods are represented in Figure 2.1.

The scale of BECCS deployment in IAMs is highly dependent on the scale and pace of greenhouse gas emissions mitigation. In the latest IPCC report on limiting global warming of 1.5°C, BECCS reaches a deployment level as high as 22 $GtCO_2$/yr by the end of the century in a fossil fuel intensive scenario (P4), and as low as zero in a low energy demand scenario (P1), where all the need for carbon dioxide removal can be fulfilled by better land management and afforestation/reforestation (AFOLU). In the middle-of-the-road scenario (P3), BECCS capacity reaches 12 $GtCO_2$/yr [10, 11].

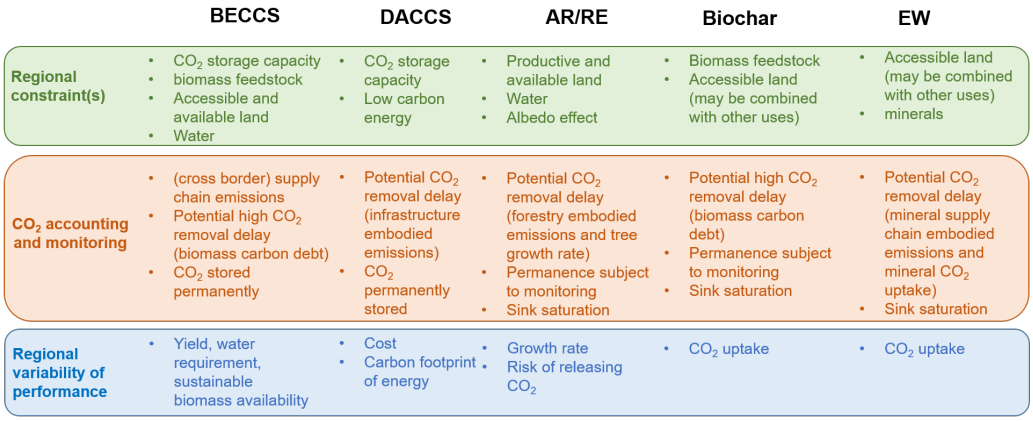


Figure 2.1: Summary of key strengths and challenges of different carbon dioxide removal methods.

Whether these levels of CDR will be achieved solely via BECCS, or with a combination of alternative CDR methods, is yet to be determined.

2.2 The history of BECCS

Bioenergy with carbon capture and storage is the combination of two well-known technologies for climate change mitigation. Carbon capture and sequestration (CCS) as a means to mitigate CO_2 emissions arising from the power and industrial sectors has been widely investigated in the literature (see Bui *et al.* for a review [14]), and the use of biomass as an energy source is ubiquitous throughout human history. Their combination was first identified as a negative emission technology by Williams *et al.* for the production of hydrogen [15], and by Herzog for power generation [16] in 1996. In 2001, Obersteiner *et al.* acknowledged the key role of CO_2 removal via bioenergy with carbon capture and storage for climate risk management [17]. However, the combination of bioenergy and carbon capture and storage was not referred to as 'BECCS' or 'BECS' until 2003 when Kraxner *et al.* first coined the term [18]. A core element of the utility of BECCS is its potential to remove CO_2 from the atmosphere [18–26], and in so doing permits the offsetting, or mitigation, of otherwise hard to reach point sources such as transport or sources which are remote from CO_2 transport and storage infrastructure [27].

However, despite its potential advantages, BECCS is not without controversy. Land competition for food production [28–31], as well as CO_2 emissions associated with biomass cultivation, harvesting and processing [32–34] cast doubt on the general ability of a BECCS facility to actually result in a net removal of CO_2 from the atmosphere

[35, 36]. This has led some to suggest that relying so heavily on CDR techniques in general, and BECCS in particular, could represent a moral hazard, preventing us from taking active steps towards climate mitigation today [37]. In addition to contributing to carbon removal, BECCS is also projected to significantly contribute to global energy supply, providing up to 430 EJ/yr to the primary energy mix [10, 11]. If negative emissions are to be achieved via BECCS, in a way that is both sustainable and resource efficient, it is important to understand under which conditions BECCS can be deployed such that it is simultaneously net CO_2 negative, resource efficient, and net energy positive. It is recognised [38] that a detailed assessment of the water, land and carbon intensity of the biomass supply chain and conversion technology is vital to quantitatively addressing the uncertainty in this area, identifying key points for improvement and thus facilitating the large scale deployment of BECCS.

2.3 Global deployment status of BECCS

At the time of writing, the installed BECCS CO_2 removal capacity reaches just above 1 $MtCO_2$ per year. The first BECCS plant, operating since 2017, is the Decatur corn-based bioethanol plant in Illinois, which captures around 1 Mt of CO_2 per year, storing the CO_2 in a sandstone reservoir underneath the plant [39]. In early 2019, the DRAX thermal power plant in the UK, which has converted four of its six 660 MW boilers to dedicated biomass combustion, started a BECCS pilot project with the company C-capture to capture 1 tCO_2 a day [40]. No storage site or utilisation of this captured CO_2 has however been identified yet. Other BECCS projects in planning include the North Dakota BIGCC plant with CCS and a bioethanol plant with CCS in Kansas. CCS projects including capture from both fossil and biogenic sources capture about 30 Mt of CO_2 per year [41]. Even when considering all CCS projects, these values are still orders of magnitude below the gigatone-scale requirement of carbon dioxide removal forecasted by climate models. A drastic ramp up of BECCS and CCS deployment is therefore required.

2.4 Overview of BECCS technologies

BECCS encompasses any technological route combining the conversion of a biomass feedstock to energy, with the capture and geological storage of the CO_2 released upon this conversion. Considering the variety of biomass feedstock types (*e.g.*, sugar and starch crops, lignocellulosic biomass, organic wastes), biomass conversion routes (*e.g.*, gasification, combustion, fermentation), and capture options (*e.g.*, pre-, post- or oxy-combustion capture), there is not one single BECCS technology. BECCS technologies

can be categorised in three pathways:

- BECCS to power via combustion in pulverised combustion (PC) plants, fluidised bed combustion (FBC) plants, chemical looping combustion plants (CLC) and combined heat and power (CHP) plants to produce heat in addition to power, or via gasification in an integrated combined cycle (IGCC).
- BECCS to gaseous or liquid biofuels via fermentation (bioethanol), or gasification (bio syngas or bio-sng) followed by Fischer-Tropsch conversion (biodiesel).
- BECCS to biohydrogen via fermentation, gasification or pyrolysis.

CO_2 capture, transport and geological storage can be applied to all conversion pathways. The CO_2 capture technology applied however depends on the conversion pathway. In pathways involving biomass combustion, the CO_2 can be captured via a post-combustion system when combustion happens in air, an oxy-combustion system for combustion in oxygen, and a chemical loop integrated to the combustion technology in the CLC technology. In the case of biomass gasification, the CO_2 is captured with a pre-combustion system from the syngas. Upon biomass fermentation, pure CO_2 ($>$ 99% purity) is released during fermentation, and can be directly captured. Figure 2.2 summarises these pathways.

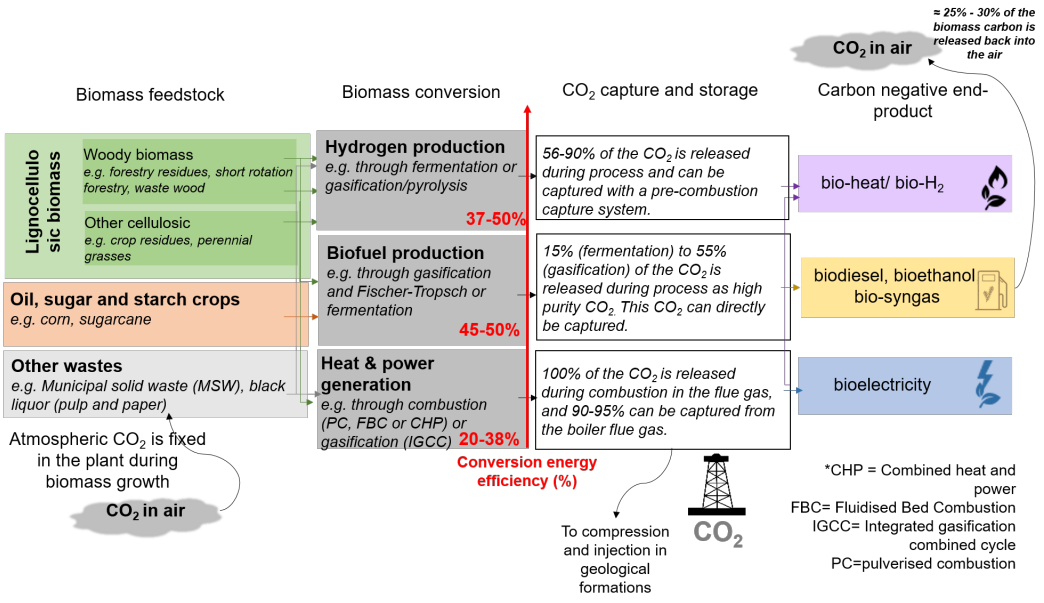


Figure 2.2: Illustration of different BECCS pathways. Pathways provide different value to the energy system: whilst BECCS via biofuels provide less negative emissions than BECCS via bioelectricity, it potentially provides more useful energy to a hard-to-decarbonise sector.

Each technological option differs in their performance and energy product output. Key metrics to measure the performance of a BECCS technology include cost, conversion en-

ergy efficiency (useful energy generated from the raw biomass energy), and CO_2 capture efficiency (how much of the biomass feedstock CO_2 is captured during the conversion). Conversion energy efficiencies are typically higher for the BECCS via biofuels or hydrogen pathways, at around 29-44% [42–44] for biofuels, and 37-50% for hydrogen [45–47]. Conversely, the efficiency of BECCS via power can be found anywhere between 20% [48] and 38% [49], including the CO_2 capture system efficiency penalty. This results in varying operating costs for each technology, and different quantity of energy products generated, hence in the BECCS technology having a different value within the energy system it is operating in. Given the same amount of biomass feedstock, the BECCS to biofuel pathway, for example, can generate more useful energy in the form of biofuel, than the BECCS to power pathway yields bioelectricity. If displacing conventional diesel, biofuels could therefore result in more CO_2 emissions being avoided, than bioelectricity [32]. This is however largely dependent on the structure and carbon intensity of the energy system with which a given BECCS system interacts. From a cost perspective, the CO_2 released during from pathways involving biomass fermentation is more concentrated and therefore cheaper to capture, than in pathways involving biomass gasification, for which the CO_2 is captured from the syngas, or to a greater extent biomass combustion, for which the CO_2 is captured from the boiler exhaust gas.

From a CO_2 capture efficiency perspective, however, only 15% – for fermentation [42] – to 56% – for gasification [43] – of the biomass feedstock carbon is released into CO_2 during the process, whilst 25 to 30% remains in the biofuel and will be re-emitted back into the atmosphere upon end-use of the biofuel. In the BECCS via power pathway, close to 100% of the biomass carbon can be released upon combustion, of which 90 to 95% can be captured from the flue gas and stored. In the biomass to hydrogen pathway, the CO_2 capture efficiency of the overall process depends on the CO_2 capture point and the performance of the absorption process [46, 50]. When the CO_2 is captured directly from the shifted syngas, capture efficiencies between 56% [50] and 90% [46] can be achieved. Overall, BECCS via power typically leads to more negative emissions per unit of biomass feedstock than BECCS via biofuels or biohydrogen.

Finally, the energy product generated by each pathway can have different value to the energy system. Whilst low carbon alternatives to decarbonise the power sector already exist – for example wind and solar, some sectors such as heat and transport have currently fewer alternatives. The production of biofuels or biohydrogen to decarbonise the heat and transport sector, by producing aviation biofuels for example [51], may therefore have more value in decarbonising the energy system, than producing bioelectricity.

Other BECCS opportunities include the integration of CCS in pulp and paper plants, whose on-site energy generation largely relies on biomass feedstock [52], and the integration of biomass and CCS in industrial processes such as steel making [53]. Whilst negative emissions might be limited in the latter application, the value of BECCS can

be important in the context of industrial decarbonisation.

2.5 Challenges to BECCS large scale deployment

Regardless of the pathway chosen, biomass feedstock needs to be produced or collected, upgraded to a proper fuel – dried, pelleted, and/or ground – and transported to the location of the conversion plant. This is referred to as the biomass supply chain, and has been identified as being the key driver of the sustainability of a bioenergy or BECCS process [36, 54–56]. The potentially high resource and carbon intensity of the BECCS value chain has sparked a controversy around the actual ability of BECCS to deliver negative emissions and energy, without having detrimental consequences on the wider economy and ecosystem [35, 37, 57, 58]. Within this context, various potential challenges and metrics are important to consider when assessing BECCS performance.

2.5.1 BECCS technical challenges

One category of challenges BECCS faces relates to biomass conversion and CO_2 capture technologies. In a post-combustion capture system, steam is taken out of the steam cycle to regenerate the solvent. This imposes a first energy penalty on the system, on the order of 20% with conventional technologies at 90% capture, or 9% in efficiency points [46] with conventional solvents (*i.e.*, alkanolamines). Using state-of-the-art solvents could bring the heat requirement to values as low as 2.3 GJ/tCO_2 [59, 60], or even 2 GJ/tCO_2 in the case of biphasic solvents [61]. Bui *et al.* investigated the impact of solvent heat duty on the system efficiency and carbon intensity, and showed that using advanced solvents combined with heat recovery from the boiler exhaust gases could reduce the efficiency penalty associated with solvent regeneration to zero [49].

This efficiency penalty is further increased by the use of a potentially lower quality fuel – biomass – in complement or supplement to coal. Whilst the average higher heating value (HHV) of bituminous coal is approximately 27 MJ/t_{WM} at 11% moisture and 64% carbon content [62], raw biomass, with a higher moisture content – up to 50% with woody biomass [63] – and a lower carbon content – around 48% dry mass – tend to exhibit an HHV around 18-20 MJ/t_{DM} [64–69]. In addition to the efficiency loss at the boiler, the physical properties of biomass will increase the costs associated with fuel storage, handling and size reduction. In the case of high moisture biomass, drying will automatically represent a substantial energy cost. Furthermore, as shown in Williams *et al.* [70], biomass grindability is significantly lower than that of coal, resulting in a grinding energy cost up to four to five times higher on a mass basis. On an HHV basis, grinding energy cost can be up to seven times higher for biomass relative to coal,

with an energy requirement of 20 kWh/MWh_{HHV} in the case of wood pellets, against 3 kWh/MWh_{HHV} in the case of coal.

In addition to a reduction in efficiency associated with increased fuel processing costs, another concern is associated with transitioning from dedicated coal to dedicated biomass combustion and the resulting impact on the boiler technology. Experimental studies [71] and recent reports from DRAX power station, which started converting its 660 MW units to dedicated biomass in 2014 (today four out of six [40]), demonstrate that large scale biomass firing is feasible with no major change, providing modern boiler technology is used, and biomass feedstock comes with the right specification. Utility-scale biomass-fired power plants are inherently more costly than their coal-fired counterparts, primarily as a result of the more costly fuel handling and storage infrastructure. In addition to the capital cost, the ongoing operating cost associated with providing a nitrogen-rich atmosphere for the biomass is also an important consideration. Moreover, an improved understanding of the impact of ash formation and slagging behaviour, as well as corrosion, on boiler efficiency and maintenance [72, 73] costs is also necessary.

However, Mac Dowell and Fajardy showed that BECCS facilities that are less efficient at converting biomass to electricity could remove more CO_2 at a lower cost than their more efficient counterparts [74]. This paradoxical observation has important implications for the way in which CDR technologies will be integrated with the broader energy system.

2.5.2 CO_2 negativity

The underpinning assumption behind BECCS delivering negative emissions, is that bioenergy is carbon neutral. This assumption can be challenged when considering the greenhouse gases emissions occurring along the biomass supply chain from energy use, direct and indirect land use change – the conversion of a land to bioenergy production causing further land conversion elsewhere [75–77], and field nitrous oxide emissions [36] from fertiliser application. A first issue often raised involves biomass sourcing and transportation related emissions. There are several biogeophysical and geopolitical constraints to consider: all geological storage sites do not coincide with available land for biomass production, or thermal power plant locations. The deployment of BECCS at the scale envisioned by IAM solutions will likely require a multi-national biomass supply chain, with stakeholders based in different regions acting to provide a reliable supply of sustainably sourced biomass, or consume this biomass and store the CO_2. In 2018, over 80% of UK DRAX power plant biomass supply was imported from North America, incurring a carbon cost of 31 gCO_2/MJ of electricity produced [40]. For a BECCS system to be carbon negative *i.e.* delivering negative emissions, biomass supply chain emissions need to be kept to minimum, not to outweigh the CO_2 captured at the conversion plant. In a study by Smith *et al.*, the authors showed that if CO_2 leakages along the whole

BECCS value were accounted for, removing 1 ton of CO_2 from the atmosphere actually meant capturing 2.11 tons of CO_2 from the atmosphere [56]. In this case, the CO_2 efficiency of the system – the fraction of biomass CO_2 which is actually removed from the atmosphere, is only 47%.

2.5.3 Land use and land use change

When relying on land-based bioenergy – feedstock from agriculture or forestry, BECCS land intensity has been identified as a one of the central challenges of BECCS deployment. Levels of BECCS requirements in climate models could require between 100 and 800 Mha of land [10, 11]. To put these numbers in context, total cropland area in 2017 was 1,600 Mha [78]. Such land conversions could bring about economic-environmental impacts including food price increases [28–30] and biodiversity losses [79]. Using residual biomass from forestry and agriculture can be considered as alternatives, providing the biomass collection rate is sustainable, and does not cause, for *e.g.*, soil depletion [80]. Other opportunities such as using municipal solid wastes [81], agricultural residues, remediating abandoned land with high yielding grasses [56, 82, 83], or using marine biomass [84] are being investigated to decrease BECCS pressure on land use.

In addition to economic impacts, such land use change may also impact BECCS carbon balance. Direct land use change, as defined by Fargione *et al.*, encompasses the direct emissions released during the initial plant combustion and eventual roots and leaves decomposition, the carbon converted into charcoal, and the carbon incorporated in merchantable forestry products (considered to have a half life of 30 years) [76]. Land conversion factors are a strong function of the land type converted, and are reported to be in the range 0 - 70 $kgCO_2/ha$ for marginal land, 350-120 tCO_2/ha for forest or even up to 3450 tCO_2/ha for wetland [76, 85]. However, some studies argue that this accounting method cannot be complete without taking into account the indirect effects of altering a land economic function (*e.g.*, agriculture, grazing) by converting part of it for biomass production [36, 86, 87]. Models evaluating those effects do exist, but their level of specificity limit their applicability to a case-to-case basis [77, 85, 88, 89]. Plevin *et al.* evaluated indirect emission factors to range from 10 to 340 gCO_2eq/MJ of liquid biofuel, with a strong sensitivity to socio-economic activity and time horizon within a specific region [85].

2.5.4 CO_2 breakeven time

This dependence on time also raises the question of dynamic accounting of carbon emissions [90]. Some studies indicate that on a transient basis, the 'carbon debt' initiated by land conversion to biomass production cannot offset CO_2 savings from displacing

coal, or only over a period of time that is greater than to the power plant lifetime [91, 92]. This is referred to as 'carbon payback time', or carbon breakeven time, and can be understood as the amount of time required for a system to reach carbon neutrality. In those studies however, biofuels pay back this initial carbon debt by offsetting fossil fuels related emissions, and carbon breakeven time thus has to be calculated relatively to a given fossil fuel. In BECCS case, because it physically captures carbon from the atmosphere, we could define the CO_2 breakeven time as the time required for a BECCS powerplant to become net CO_2 negative, in absolute terms. Delayed carbon removal could have significant implications to 1) the way CO_2 removal is credited, and 2) BECCS' ability to compete with alternative CDR methods with a potentially lower initial carbon debt, and therefore shorter CO_2 removal delay.

2.5.5 Energy requirement

Another key assumption when deploying BECCS technologies in climate scenarios is that BECCS produces energy in addition to removing CO_2 from the atmosphere. However, the energy intensity of biomass supply chains could represent a challenge to this assumption [55]. Additionally, the conversion of a lower quality fuel – biomass – combined with CO_2 capture and storage, impose an energy penalty on the system, relative to conventional fossil power generation, resulting in a potentially low power generation efficiency [49]. In their review, Moriarty *et al.* say that there is uncertainty as to the capability of bioenergy to be a net provider of energy, and further argue that were it to pass the 'energy test', it might not deliver emissions reduction [93]. Vaughan *et al.* identified seven BECCS assumptions with both high uncertainty and great impact on BECCS performance, and highlighted BECCS total contribution to the energy system as one of them [35]. Smith *et al.* presented a high level analysis showing that BECCS had a positive net energy balance on average, with energy production ranges of 0.8–11 GJ/tCO_2 for energy crops (3–40 GJ/tons of carbon in the study) [36]. However, the analysis also pointed out the possibility of energy negative scenarios with an energy consumption up to 2.3 GJ/tCO_2 (8.7 GJ per ton of carbon in the study). Nevertheless, BECCS is still consistently represented as a net source of both negative emissions and energy (fuel, power or hydrogen) in IAMs, which explains its prevalence in these models [94]. From an energy return on investment perspective (which measures the energy output over the energy input of a system), this potential large energy usage could result in BECCS having a very low energy return. This metric, partly correlated with BECCS carbon negativity, also needs to be carefully measured when deploying BECCS value chains. Understanding the circumstances under which BECCS deployment might lead to a negative energy balance, and the implications for the energy system, is thus crucial

to the design of BECCS systems that will make a net positive contribution to climate change mitigation.

2.5.6 The water concern

Agriculture and power generation are highly water intense, accounting for 70% [95] and 15% [96] of the world's total freshwater withdrawal (*i.e.*, total water use). Thus the sustainability of BECCS warrants close scrutiny [36]. According to the Food and Agriculture Organisation (FAO), 1.2 billion people already live in absolute water scarcity, and this number could be further increased by the additional 1.6 billion who are currently facing water shortages [97]. As agriculture is responsible for up to 90% of water withdrawal in the Asia-Pacific region [98], the combination of population growth and climate change has the potential to further exacerbate this situation [99, 100]. Due to water use both at the crop level and the power plant level, BECCS is considered as the most water intense within the portfolio of CDR methods [36]. Considering BECCS water use and potential water constraints to its sustainable deployment is crucial [101].

2.6 BECCS global potential

The literature estimates BECCS maximal deployment potential between 5 and 15 $GtCO_2/yr$ [13, 36, 102–106], depending on the geophysical, technical and socio-economic constraints potentially considered in these assessments.

2.6.1 Geophysical constraints

CO_2 storage is generally not considered as a global bottleneck, with over 11,700 $GtCO_2$ identified available storage with a 75-100% confidence, and 14,000 $GtCO_2$ with a confidence of 56% and higher. However, regional assessments may substantially vary in capacity and in reliability [41].

Global technical and/or sustainable bioenergy potential have been identified as potential bottlenecks. Such assessments much depend on assumptions as to what is, in fact, considered sustainable, and are therefore found within a wide range in the literature [34, 103, 107–110]. Whilst pessimistic assessments find the global potential to be around 60 EJ/yr, and optimistic assessments over 350 EJ/yr [103], there tends to be a broader agreement of the literature around 100 EJ/yr [34]. Figure 2.3 illustrates the potential gap between what is required in climate models (left) and ranges of global potential per feedstock type across the literature (right).

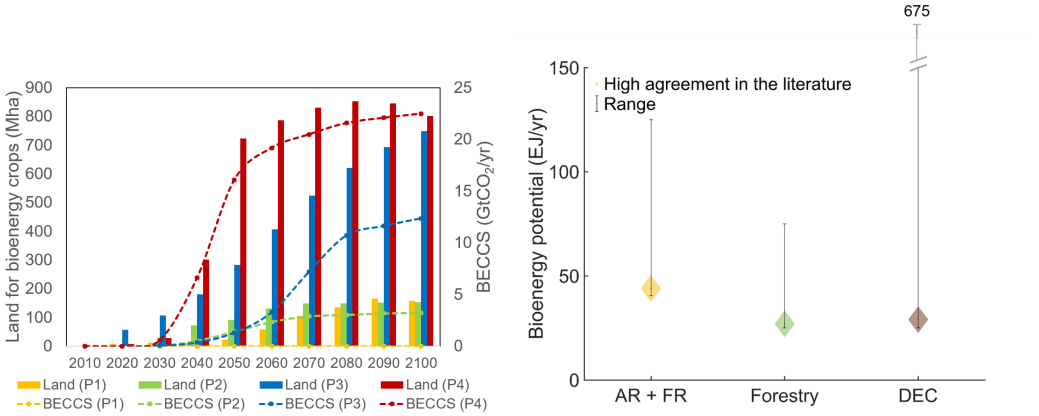


Figure 2.3: Global bioenergy requirement in climate models (adapted from [10, 11] (left) and technical bioenergy potential (adapted from [34]) (right). Whilst up to 400 EJ of bioenergy are required annually by the end of the century of bioenergy, agreement around global technical bioenergy potential within the literature tends to lie around 100 EJ/yr.

2.6.2 Broader sustainability constraints

How this technical bioenergy supply translates into carbon removal potential via BECCS depends on assumptions as to BECCS pathway, characteristics of the biomass feedstock and performance of the BECCS value chain. A handful of bottom up assessments have also investigated how the consideration of planetary boundaries [111] could further limit the deployment of BECCS [79, 101, 112], resulting in a sustainable potential of BECCS, much lower than the technical potential of BECCS. In Heck *et al.* limiting BECCS deployment within a 'safe' zone of a subset of planetary boundaries, including biochemical flows, biodiversity loss, land use change and water use – limited global carbon dioxide removal to 0.2 $GtCO_2/yr$, which is two orders of magnitude lower than what is required by the end of the century in most scenarios [79]. In Seferian *et al.*, authors quantified that considering water constraints would reduced BECCS deployment by 90% relative to the level of deployment modelled in 1.5°C scenarios. More recently, the IPCC special report on land use warned on BECCS potential detrimental on ecosystems, and identified 5 $GtCO_2/yr$ as being an upper limit for BECCS sustainable deployment [102].

2.6.3 The case of marginal lands

To avoid potential land use change and competition with other land uses, there have been many attempts to evaluate the amount of marginal, yet suitable, land for bioenergy production. The main caveat comes from the difficulty in defining the nature of marginal land (MAL). Edrisi *et al.* differentiates wastelands for biomass cultivation by two views:

the suitability/quality of the land, and the socio-economic value of the land [113]. In this context, marginal land is considered to be at the intersection of under-utilised lands and neglected unused land. The definition of marginal land can also vary in time. A farmer might choose to use a parcel of marginal land one year, and leave it unused the next, depending on the profitability of this land in this specific year.

This diversity in definition results in a variety of marginal land evaluation. In 2011, Cai *et al.* provided an extensive mapping of marginal land, by quantifying the mixed crops, natural vegetation land, cropland, scrubland, savannah and grassland with marginal productivity [114]. This work resulted in the spatial determination of marginal land availability with a spatial resolution of 30 arc second geographic. Total world marginal land availability was quantified between 320 and 1,107 Mha, with between 108 and 256 Mha in South America, 18 and 151 Mha in India, 33 and 111 Mha in Europe, 52-152 Mha in China, and 66-314 Mha in Africa. This evaluation was later on downscaled by Fritz *et al.* to 56 to 1035 Mha, with adjustments made to land cover and human impact assumptions [115]. Several studies were also performed at the regional level. In Brazil, Lossau *et al.* evaluated the spatial distribution of marginal land in Brazil by calculating the residual land from cropland, pastures, forest, build up, barren, water bodies, and the protected Amazon biome area [82]. The residual area was then overlayed with the FAO/IIASA land suitability modelling framework to assess its suitability [116]. A total of 37.8 Mha was found to be available and unprotected, with approximately 20% of this land was considered very suitable for biofuel production. It is worth noting however that the suitability modelling framework was used for conventional oil and grain crops production, and perennial grasses such as miscanthus and switchgrass could potentially be more resilient. In China, marginal land including saline land, steep hillside and idle land was evaluated at 35-75 Mha [117], while another study pointed to 44 Mha exploitable for energy crops [118]. A more detailed study on miscanthus production in China evaluated at only 17 Mha the potential miscanthus production area in China, with yields as low as 2 t/ha in bare areas [119]. In Europe, a study by Strapasson *et al.* based on FAO land cover and land use data quantified the land available in the EU for bioenergy production to 20 Mha [120]. In India, a study by Edrisi *et al.* evaluated the potential of MAL for bioenergy production to 39 Mha, providing suitable soil amendments and agro-technologies are used to improve the fertility/productivity of the various wasteland considered [113]. Table 2.1 summarises these findings, highlighting the great range in marginal land availability assessments in the literature.

Table 2.1: Literature review on marginal land availability

Region	year	MAL (Mha)	Sources
South America	2011	108[a]-256[b]	[114]
Brazil	2015	10[c]-38[d]	[82]
China	2009	35-75[e]	[117]
China	2011	44[f]	[118]
China	2011	52[a]-152[b]	[114]
China	2016	8[g]-21[h]	[119]
UK	2009	1.4[j]	[121]
England and Wales	2010	0.6[k]	[122]
UK	2015	3.4[l]	[123]
Europe	2011	33[a]-111[b]	[114]
EU28	2016	20[i]	[120]
India	2011	18[a]-151[b]	[114]
India	2016	39[g]-47[e]	[113]
USA	2011	43[a]-123[b]	[114]
World	2011	320[a]-1,107[b]	[114]
World	2013	56[m]-1,035[m]	[115]

[a]Mixed crop and natural vegetation land with marginal productivity.
[b]Mixed crops and natural vegetation land, cropland, scrubland, savanna and grassland with marginal productivity, discounting the total pasture land.
[c]Total protected MAL suitable or very suitable for conventional oil and grain crops.
[d]Total unprotected MAL.
[e]Total MAL including saline, steep and idle land.
[f]Total MAL.
[g]Fraction of the MAL which is suitable.
[h]Total MAL for Miscanthus.
[i]Total MAL for bioenergy based on FAO land use/land cover data.
[j]Relatively high quality land for perennial crops.
[k]0.2 for miscanthus, 0.4 for SRC willow from agricultural land quality and yield map.
[l]Total available arable and grassland for bioenergy in 2030.
[m]Cai *et al.* MAL values downscaled after land cover and human impacts corrections.

2.6.4 Agricultural residues

Using agricultural residues could represent an alternative to using marginal land, while still avoiding land use change. However, mismanagement or over-utilisation of agricultural residues could led to various negative impacts among increased water evapotranspiration, soil depletion, productivity loss, erosion [124, 125]. The use of agricultural residues to reduce BECCS's impact on land use, water use and land use change, therefore needs to be carefully monitored.

In an attempt to address these issues, Chapter 3 presents the Modelling and Optimisation of Negative Emissions Technologies (MONET), a BECCS value chain modelling and optimisation framework, which can be used to quantify the water, land, energy,

carbon and financial costs of BECCS value chain, and identify the regional drivers of the cost and sustainability of BECCS deployment.

Chapter 3

The Modelling and Optimisation of Negative Emissions Technologies (MONET) framework

3.1 Objectives and overview of the MONET framework

In order to sustainably contribute to climate change mitigation, negative emissions technologies must 1) deliver the service(s) for which they were deployed, *i.e.*, CO_2 removal and, in the case of BECCS, energy production, 2) at a low resource cost, and 3) with limited indirect impact on the markets and ecosystems. We have designated this as the NETs trilemma, illustrated in figure 3.1. The NETs key performance indicators (KPIs) include net CO_2 removal, $tRCO2$, and electricity production, tEB, cost, $tcost$, to evaluate techno-economic performance, water use, tWU, land use, tLU, and biomass use, tBU, to evaluate resource efficiency, and agricultural residue use, tRU, and land use change, $tLUC$, to evaluate BECCS environmental impacts.

In order to position BECCS within this performance trilemma, we designed the MONET framework which comprises 1) a BECCS value chain model which calculates the water use, land use, net CO_2 removed, CO_2 breakeven time, net electricity produced, net CO_2 efficiency and cost of different BECCS value chains, and 2) a linear optimisation model which determines BECCS optimal deployment – type of biomass used, location of biomass supply regions, transport route/mode, location of BECCS plant/CO_2 storage – from 2030 to 2100 with a decadal time step, subject to global or regional CO_2 removal targets, land, biomass, CO_2 storage availability, and BECCS plant build rate constraints.

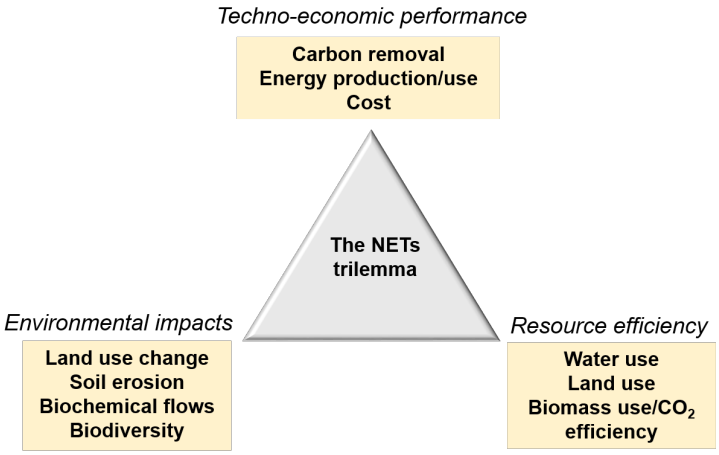


Figure 3.1: NETs key performance indicators are reassembled in three categories: techno-economic performance – net CO_2 removal, electricity production and cost, resource efficiency – water, land and biomass use (equivalent to CO_2 efficiency), and environmental impacts – land use change and agricultural residues use (with potential impact on soil productivity and erosion).

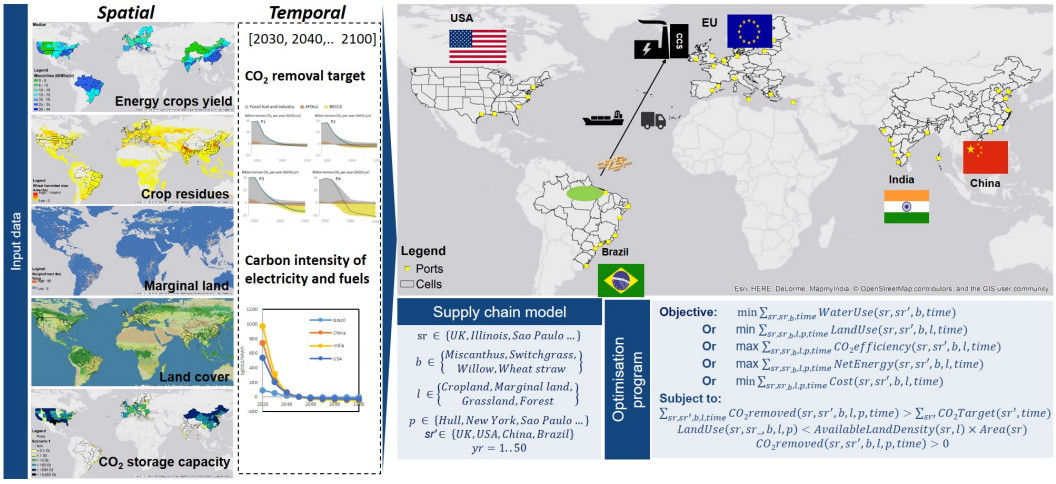


Figure 3.2: Illustration of the MONET framework

3.2 BECCS supply chain modelling framework

3.2.1 Supply chain model overview

The value chain model specifically accounts for biomass cultivating, harvesting, pelleting, transport to a given region and conversion in a pulverised combustion plant combined with post-combustion CO_2 capture and subsequent storage in the vicinity of

the power plant.

Sets

The value chain configurations are characterised by distinct:

- biomass feedstock, b: miscanthus, switchgrass and short rotation coppice willow as archetypal dedicated energy crops, and wheat straw as an archetypal agricultural residue,
- sub-region, sr, from which the biomass is imported: Brazil, China, EU, India and the USA are considered as potential regions of import, and discretised at the state/province level, resulting in 169 potential cells for biomass farming and import to the UK. Each cell is defined by its area and the position of its centroid,
- sub-region, sr', where the biomass is converted in a BECCS plant and CO_2 is stored in a nearby storage. Locations of BECCS plants are therefore constraints by CO_2 storage availability.
- land type, l, on which the biomass is grown: cropland, grassland, forest and marginal land. The different land scenarios are included to account for direct (LUC) and indirect (ILUC) land use change, *i.e.*, the direct and indirect CO_2 emissions associated with the conversion of a certain land type to bioenergy production. Different types of land are associated with distinct LUC and ILUC, and the resulting emissions are highly dependent on the biomass type, economic use of the land, region, timeframe considered, *etc.* As a simplification in this study, LUC and ILUC values, within a range of uncertainty, are attributed to the different land types, regardless of the region and biomass type. It was therefore considered that no LUC/ILUC was attributed to marginal land, medium LUC and high ILUC were attributed to cropland and grassland, as using these managed lands means an activity must be re-allocated elsewhere, and high LUC and no ILUC were attributed to forests. Converting a low vegetation land such as a marginal land, to a managed bioenergy crop with deep rooted perennial grasses, could result in negative land use change, *i.e.* net soil CO_2 sequestration [92]. While these effects could improve BECCS CO_2 balance, we adopted the conservative approach of not considering them, given the uncertainty around their amplitude and permanence.
- transport mode, t: different transport modes are considered included all road transport in hauling trucks if there is a road access between sr and sr', a combination of road transport and sea transport in bulk carriers, or only local transports in hauling trucks in the BECCS plant is collocated with biomass production farms ($sr = sr'$).
- port, p,p', which is used for shipping the biomass from its region of origin to the region of conversion and sequestration. Each sub-region sr (or sr') has access to

a port p (or p') as long as there is a road access to this port.

- energy method, e, in which the energy balance is expressed: energy carrier, or 'EC' (*e.g.*, heat, electricity, fuel), primary energy, or 'PE', where all energy inputs and outputs are converted into primary energy equivalent, and electricity equivalent, or 'EEQ', where all energy inputs and outputs are converted into electricity equivalent. This set is only used for the purpose of the energy balance and the energy return on investment analysis (see Chapter 4).
- annual time step, a, which is used to calculate the water, GHG, energy, cost and land balances of a BECCS project.
- decade, $time$, which is used to model the optimal deployment of BECCS plants between 2030 (assumed start date of deployment) and the end of the century.

Figure 3.3 provides an overview of the key inputs/outputs of the BECCS supply chain modelling framework.

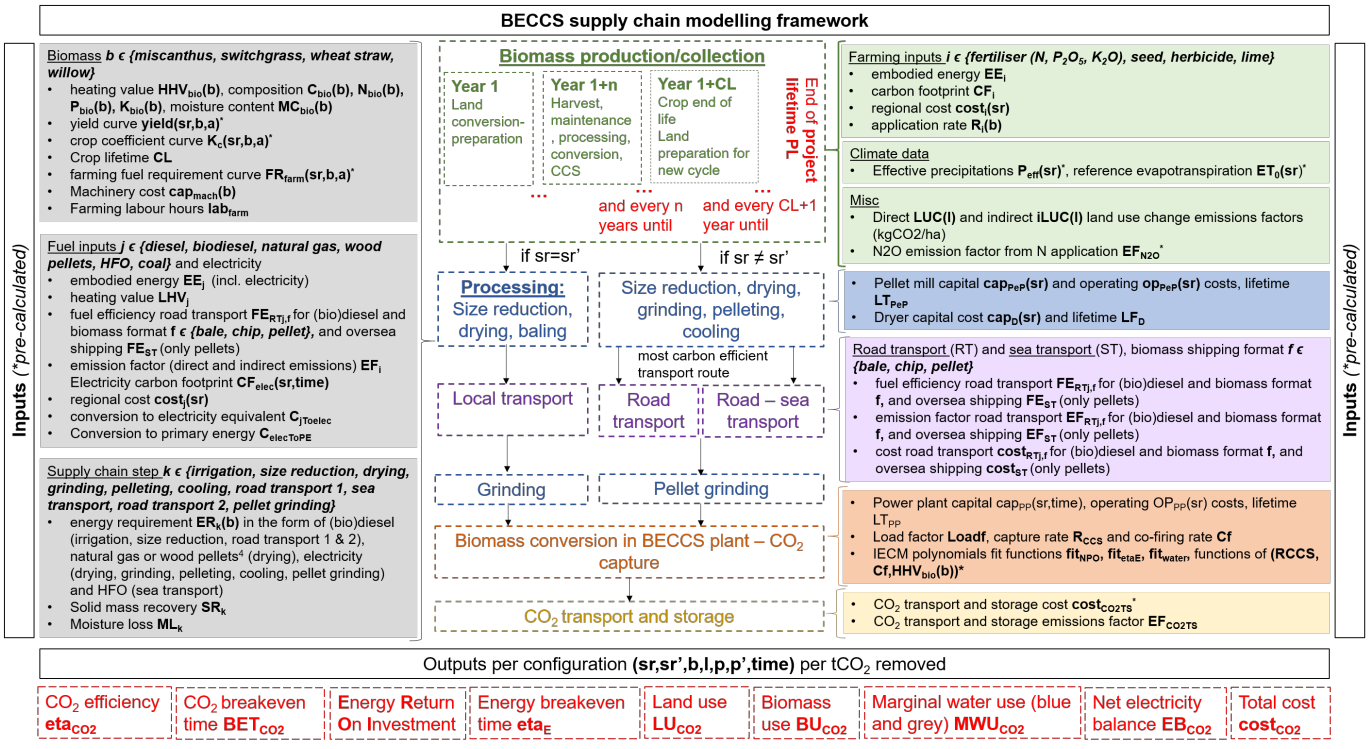


Figure 3.3: BECCS water, carbon, energy and cost balance is evaluated over 50 years (to account for land use change). Biomass production or collection, processing, transport, conversion and CO_2 capture, transport and storage are explicitly accounted for in the modelling.

Spatial representation

The framework does not aim at predicting BECCS optimal deployment to meet global targets, but highlight trends and trade-offs, as well as identify key drivers of BECCS sustainability and cost. To limit computation time and model size, five regions of the world with potential for biomass growth and/or CO_2 storage were chosen as representative of a range of climates and economies: Europe, Brazil, USA, India and China. To capture variability in energy systems, economies and climates at the regional level, while limiting the model size, these five countries were modelled at the country level for Europe, and the state level for USA, India, China and Brazil. A schematic of the current bio-geo-physical map of the MONET model is presented in Figure 3.4, including the ports and biomass collection points. Polygon shapefiles of the administrative boundaries of each macro-region were obtained from the ArcGIS databases [126]. All shapefiles were projected in the WGS-1984 coordinate system, before being merged into one world shapefile containing 169 cells. The latitude and longitude of the centroid of each cell, as well as the cell area, were calculated using ArcGIS, and used as inputs in the model. Figure 3.4 shows the world map with the positions of the sub-regions centroid.

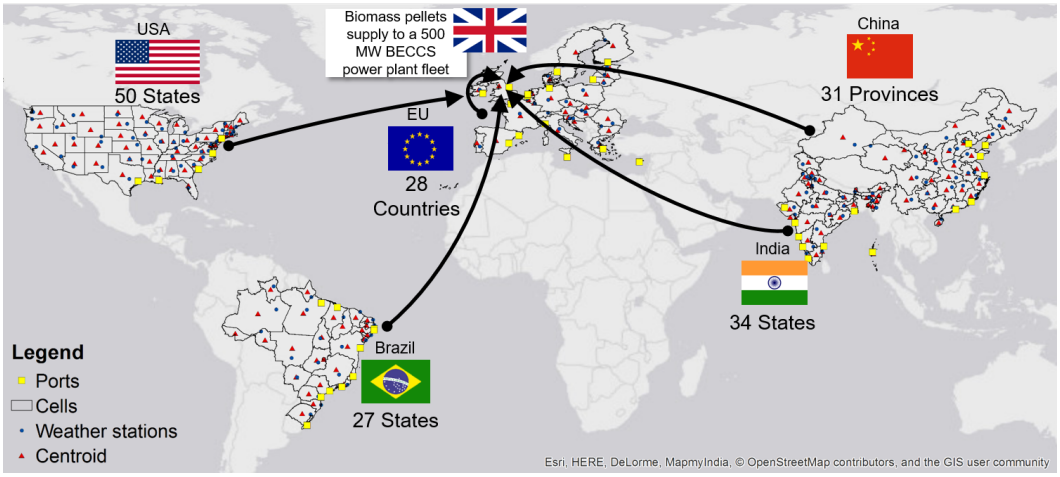


Figure 3.4: Sub-regions sr (or cells) and ports p considered for BECCS value chain modelling in MONET. Each cell is defined by its area and the position of its centroid, which were calculated using ArcGIS 10.5 [126]. The map also displays the location of the weather stations, indicated by the blue dot in each cell, and obtained from the software CLIMWAT 2.0, from which the climate data of each sub-region was collected [127]. As an example in this figure, biomass is shipped to the UK for conversion and CO_2 sequestration.

Temporal representation

Three time scales are considered in MONET: 1) a daily time scale, $d \in \{1,2,...,365\}$, over a year, 2) an annual time scale, $a \in \{1,2,...,50\}$, over the project lifetime, PL, and 3) a decadal time scale, $time \in \{2030,2040,...,2100\}$. These three time steps serve different modelling and optimisation purposes. First, the daily time step, d, is used to calculate the crop water requirement over crop growth cycle. For each crop, this daily time step allows to capture the first day of growth, the length (in days) of the different growth periods, and the monthly variation of climate data such as average temperature, precipitation or wind speed. The annual time step, a, is used to compute the BECCS water, land, energy, carbon and cost balances. The balances are performed summing the annual water use, land use, energy flows (use and generation), GHG flows (GHG emissions and CO_2 removal) and financial flows (costs and revenues) on a hectare of land. Whilst the crop lifetime (typically 15-20 years) could have been chosen as a relevant time horizon for this balance, a longer time period of 50 years was considered to capture the land use change effects occurring when converting a given type of land to a bioenergy crop. We assume that this conversion only happens one time over 50 years, and that several crop lifetime may occur during that time without reconversion of the land (see section 3.2.5). These balances are then divided by the amount of CO_2 removal achieved over this 50 year period to obtain the average water use, land use, net energy use and cost of a given BECCS configuration. Finally, the decadal time step, $time$, is used to determine the optimal allocation of biomass production and CO_2 storage sites given a starting BECCS deployment year (here assumed to be 2030) as the CO_2 removal target increases over time. We also use this time horizon to assume a decarbonisation of the energy system over time (electricity and fuels), as well as BECCS plant capital costs reductions. The modelling framework is ran as a snapshot model in different decades to account for these changes in the BECCS water, land, energy and cost balances per ton of CO_2. The dynamic aspect is therefore used to account for the evolution of the CO_2 removal target, the depletion of CO_2 storage sites, the decarbonisation of the energy system, and the capital cost reduction of BECCS plants. Given the amount of uncertainty, all other data points including yield, farming energy requirement, power plant efficiencies, are considered constant.

System boundaries for agriculture residues

For agricultural residues, it is assumed that straw is a by-product of wheat production. Whilst there are a variety of approaches to attribute the energy use and GHG emissions associated with the production of a crop, to agricultural residues [128–130], we have decided to assume that land conversion and farming contributions were not attributed to the residue. Straw carbon, energy, water and cost balances start at its collection from

the field and ends at the power plant boiler. However, as straw would have normally been left on the field to provide the crop with nutrients, additional fertilizers need to be applied to compensate for its removal. From this perspective, water consumption during wheat growth was not included in the evaluation of the water intensity of a wheat straw-based BECCS facility.

3.2.2 Supply chain sub-models

Yield and crop cycle

Regional yield potential $Yield_{th}(sr,b)$, lifetime $CL(b)$, harvest rotation $HR(b)$, and first and second harvest yield potential, $HP_1(b)$ and $HP_2(b)$ (at which the crop yield is typically lower than its full harvest potential) were gathered for each crop from the literature. An additional residue recovery factor $RR(b)$ is considered to convert wheat grain yield into wheat straw yield. Its value may vary between 0.6-2.0 [131], while it is considered to be 1 for energy crops.

The annual yield, $Yield_{th}(sr,b)$, can then be calculated:

$$Yield(sr,b,a) = \begin{cases} 0 & \text{when no harvest} \\ Yield_{th}(sr,b).HP_1(b).HR(sr,b).RR(b) & \text{at the first harvest} \\ Yield_{th}(sr,b).HP_2(b).HR(sr,b).RR(b) & \text{at the second harvest} \\ Yield_{th}(sr,b).HR(sr,b).RR(b) & \text{else} \end{cases} \tag{3.1}$$

As well as the total yield over the project lifetime, PL:

$$tYield(sr,b) = \sum_{a=1}^{PL} Yield(sr,b,a) \tag{3.2}$$

Here, and throughout the model except if otherwise specified, yield is considered dry biomass yield. The wet mass yield, $Yield_{WM}(sr,b,a)$, can be obtained with the biomass moisture content at harvest, MC_{bio},:

$$Yield_{WM}(sr,b,a) = \frac{Yield(sr,b,a)}{1 - MC_{bio}(sr)} \tag{3.3}$$

Nutrient input

We recognise that the removal of residues results in soil nutrient depletion, and needs to be compensated as a function of the residue yield [132]. It was assumed that 30% (N_{av}), 100% (P_{av}) and 100% (K_{av}) of straw nitrogen, phosphorus and potassium content respectively, was available to the field [132]. Given the composition of wheat straw, extra NPK fertilizer input was then determined and included in the model.

$$R_{N,extra}(sr,b,a) = Yield(sr,b,a).N_{bio}(b).N_{av} \text{ , for } b \text{ residue} \tag{3.4}$$

$$R_{P_2O_5,extra}(sr,b,a) = Yield(sr,b,a).P_{bio}(b).P_{av}.C_{P\rightarrow P_2O_5} \text{ , for } b \text{ residue} \tag{3.5}$$

$$R_{K_2O,extra}(sr,b,a) = Yield(sr,b,a).K_{bio}(b).K_{av}.C_{K\rightarrow K_2O} \text{ , for } b \text{ residue} \tag{3.6}$$

For energy crops, fertiliser input is calculated as a function of yield and the biomass nutrient content (N_{bio},P_{bio},K_{bio}) [133]. No prior natural deposition of nitrogen in the soil was considered.

$$R_N(sr,b,a) = Yield(sr,b,a).N_{bio}(b) \tag{3.7}$$

$$R_{P_2O_5}(sr,b,a) = Yield(sr,b,a).P_{bio}(b).C_{P\rightarrow P_2O_5} \tag{3.8}$$

$$R_{K_2O}(sr,b,a) = Yield(sr,b,a).K_{bio}(b).C_{K\rightarrow K_2O} \tag{3.9}$$

Farming fuel use

In-field operations such as harrowing, ploughing, seeding, packing, fertilizing, *etc.* during site preparation, or mowing, harvesting, baling, *etc.* during harvest, require fuel in the form of diesel. Fuel efficiency associated with land preparation, $FR_{landprep}(b)$ in L/ha, with harvest/maintenance, $FR_{harvest}(b)$ in L/ha/harvest, for each crop, and irrigation ER_{irrig} in MJ/mm, were gathered from the literature.

Biomass transport

Sub-regions are polygons represented geographically by the latitude $Lat(sr)$ and longitude $Long(sr)$ of their centroid. Similarly, ports are represented by their latitude $PortLat(p)$ and longitude $PortLong(p)$. The road distance, $RD_p(sr,p)$ between sr and p, or $RD(sr,sr')$ between sr and sr', is calculated with the euclidian distance between these two points, corrected by a region tortuosity factor $t_r(sr)$:

$$RD_p(sr,p) = t_r(sr) \times R_{earth} \times arcos(sin(\phi_{PortLat(p)})sin(Lat(sr)) +$$

$$cos(PortLat(p))cos(Lat(sr))cos(Lat(sr) - PortLat(p))) \tag{3.10}$$

$$RD(sr,sr') = t_r(sr) \times R_{earth} \times arcos(sin(\phi_{Lat(sr')})sin(Lat(sr))+ cos(Lat(sr'))cos(Lat(sr))cos(Lat(sr) - Lat(sr'))) \tag{3.11}$$

Three transport options are considered: (1) road transport by heavy duty vehicles (HDV) if there is a road access between sr and sr' ($t = 1$), (2) a combination of road and sea transport by container ship ($t = 2$), (3) and short distance transport (50k) by HDV if $sr = sr'$ ($t = 3$). For simplicity, rail and barge are not considered in this analysis. The least emitting transport route – option (1), (2) or (3), and optimal ports p and p' in option (2) – is determined prior to the optimisation program. Depending on the transport option t, different transport distances can then be computed:

$$RD1(set1) = \begin{cases} RD_p(sr,p) & \text{if } sr \neq sr' \text{ and } p \neq p' \\ & \text{and } Ind_{PortAccess}(sr,p) = 1 \\ & \text{and } Ind_{PortAccess}(sr',p') = 1 \\ & \text{and } t = RoadSeaRoad \\ RD(sr,sr') & \text{if } sr \neq sr' \text{and } p \neq p' \\ & \text{and } Ind_{RoadAccess}(sr,sr) = 1 \\ & \text{and } t = Road \\ 50 & \text{if } sr = sr' \text{and } t = NoTransport \end{cases} \tag{3.12}$$

$$SD(set1) = \begin{cases} SD_p(p,p') & \text{if } sr \neq sr' \text{ and } p \neq p' \\ & \text{and } Ind_{PortAccess}(sr,p) = 1 \\ & \text{and } Ind_{PortAccess}(sr',p') = 1 \\ & \text{and } t = RoadSeaRoad \\ 0 & \text{if } sr \neq sr' \text{and } p \neq p' \\ & \text{and } Ind_{RoadAccess}(sr,sr) = 1 \\ & \text{and } t = Road \\ 0 & \text{if } sr \neq sr' \text{and } p \neq p' \\ & \text{and } Ind_{RoadAccess}(sr,sr) = 1 \\ 0 & \text{if } sr = sr' \text{and } t = NoTransport \end{cases} \tag{3.13}$$

$$RD2(set1) = \begin{cases} RD_p(sr',p') & \text{if } sr \neq sr' \text{ and } p \neq p' \\ & \text{and } Ind_{PortAccess}(sr,p) = 1 \\ & \text{and } Ind_{PortAccess}(sr',p') = 1 \\ & \text{and } t = RoadSeaRoad \\ 0 & \text{if } sr \neq sr' \text{and } p \neq p' \\ & \text{and } Ind_{RoadAccess}(sr,sr) = 1 \\ & \text{and } t = Road \\ 0 & \text{if } sr = sr' \text{and } t = NoTransport \end{cases} \tag{3.14}$$

where $RD1(set1)$ is the distance for the first leg of the journey (from sr to sr' in option 1, from sr to p in option 2, or from the farm to the power plant if $sr = sr'$ in option 3), $SD(set1)$ is the shipping distance between p and p' in option 2, and $RD2(set1)$ the distance from p' to sr' in option 2.

The values for the fuel efficiency, emission factor and cost factors of biomass transport vary with transportation mean and biomass format.

Biomass processing

Biomass can be supplied to the power plant in various forms, such as bales, chips, pellets or briquettes. Transport costs (financial, CO_2 or energy wise) are typically lower for biomass feedstock in denser form [134]. Pelleting biomass also enables to reduce biomass loss along the supply chain. Conversely, each biomass conditioning process involves different processing stages and moisture requirements, resulting in a different supply chain energy cost. As the optimal moisture content for biomass combustion is around 10-15 wt% [135, 136], drying biomass is generally required. Pelleting biomass also requires a feedstock at around 10 wt% moisture [137]. Information on the pelleting process is extensively available in the Pellet Handbook by Obernberger & Theck [138]. In order to be condensed as a proper fuel, harvested biomass needs to have its size reduced (chopping, chipping), dried to a maximum moisture content of 15%, further milled (grinding) and go through the pelleting process (die extruder). Processing operations require energy both in the form of fuel (drying) and electrical power (size reduction, drying, grinding, pelleting, cooling). Knowing the energy requirement ER_k of each process, k, in MJ/t_{WM}, and the process biomass input $Bio_{proc,k-1,WM}$, each processing contribution to biomass embodied energy can be calculated. The energy requirement in MJ/t for biomass processing is taken from the literature (experimental and industrial data) for size reduction, grinding and pelleting. Because pelleting biomass incurs both an energy and financial penalty on the system, there is a trade-off between the gains

made over transport and dry mass loss, and the processing cost. In modelling the biomass supply chain in MONET, the following was assumed:

- If biomass transport is within a region (*i.e.*, $sr = sr'$), biomass is baled (miscanthus, switchgrass, wheat straw) or chipped (willow) at harvest, dried, and transported in this format to the power plant.
- If biomass transport is interregional (*i.e.*, $sr \neq sr'$), biomass bales or chips are dried, grinded and pelleted prior to transport.

Biomass yield loss over supply chain

At each step $k \in$ {size reduction, drying, grinding, pelleting, road transport 1, sea transport, road transport 2}, or {SR, D, G, P, RT1, ST, RT2, PG} of the value chain, we assume that some biomass is lost, either through dry mass loss or moisture loss (when heated). Moisture loss, ML_k, and solid recovery, SR_k, factors are therefore considered for each process k, and links each process's biomass input, $Bio_{proc,k-1}(sr,sr',b,a)$, and output, $Bio_{proc,k}(sr,sr',b,a)$:

$$Bio_{proc,k}(sr,sr',b,a) = Bio_{proc,k-1}(sr,sr',b,a) \times SR_k(sr,sr'),\ \forall\ stage\ k,\ sr \neq sr' \quad (3.15)$$

and

$$MC_{proc,k}(sr,sr',b,a) = MC_{proc,k-1}(sr,sr',b,a) - ML_k,\ \forall \text{ stage } k,\ sr \neq sr' \quad (3.16)$$

The final amount of dry pellets delivered at the power, $Pellet(sr,sr',b,t,a)$ plant is thus the following:

$$Pellet(sr,sr',b,t,a) = Bio_{proc,PG}(sr,sr',b,t,a) \quad (3.17)$$

and the total amount of pellets over the project lifetime:

$$tPellet(sr,sr',b,t,a) = \sum_{year=1}^{PL} Pellet(sr,sr',b,t,a) \quad (3.18)$$

BECCS plant model

The BECCS plant power generation efficiency is a function of the base plant steam cycle performance (subcritical, supercritical or ultra-supercritical), CO_2 capture system and fuel composition. As this thesis strongly focuses on the biomass supply side, conservative assumptions were made as to the performance of the BECCS base plant and capture system. A supercritical pulverised combustion power plant with post-combustion capture rate was chosen as the archetypal BECCS system for this analysis. The capture system was modelled as a 30% weight monoethanolamine solvent absorption which requires 3.6 GJ per tonne of CO_2 recovered (whilst we acknowledge that solvent regeneration heat duty of 2 GJ could be achieved with advanced solvents [14]). As this study focuses on the impact of large scale deployment of BECCS, at a low spatial resolution, a size of 500 MW (the order of magnitude of a DRAX unit) was chosen for the system size. To evaluate the impact of biomass co-firing and CO_2 capture rate on the system's energy and water efficiencies, this base plant was modelled in the Integrated Environment Control Model (IECM [62]). The Compression of CO_2 to 110 bar for transport is also included. As a reference point, In IECM, the base efficiency of the plant with 100% coal and no CO_2 capture is $38.9\%_{\mathrm{HHV}}$. In the IECM modelling framework, the fuel flow rate, F_{fuel}, is adjusted to meet the 500 MW capacity depending on the fuel input conditions. Different capture rates, R_{CCS} and co-firing fractions of biomass with coal, C_f, were considered. The properties of the biomass-coal mixture is first determined with the co-firing rate:

$$HHV_{bio,WM}(sr,b) = HHV_{bio}(b) \times (1 - MC_{pellet}(sr,b)) \tag{3.19}$$

$$HHV_{fuel}(sr,b) = HHV_{coal} \times (1 - Cf) + Cf \times HHV_{bio,WM}(sr,b) \tag{3.20}$$

$$C_{fuel}(sr,b) = C_f \times C_{bio}(b)(1 - MC_{pellet}(sr,b)) + (1 - C_f) \times C_{coal} \tag{3.21}$$

Polynomial fit functions of the fuel carbon content, $C_{fuel}(sr,b)$, heating value, $HHV_{fuel}(sr,b)$ and the power plant capture rate, R_{CCS}, were derived from IECM to calculate the power plant generation efficiency $\eta_{PP}(sr,b)$, net power output $NPO(sr,b)$ and the make-up

water flowrate $F_W(sr,b)$:

$$NPO(sr,b) = FIT_{NPO}(C_{fuel}(sr,b),HHV_{fuel}(sr,b),R_{CCS}) \tag{3.22}$$

$$F_{water}(sr,b) = FIT_{F_{water}}(C_{fuel}(sr,b),HHV_{fuel}(sr,b),R_{CCS}) \tag{3.23}$$

$$\eta_{PP}(sr,b) = FIT_{\eta_{PP}}(C_{fuel},HHV_{fuel}(sr,b),R_{CCS}) \tag{3.24}$$

$$F_{fuel}(sr,b) = \frac{NPO(sr,b)}{\eta_{PP}(sr,b) \times HHV_{fuel}(sr,b)} \tag{3.25}$$

CO_2 transport and storage

A high level description of the CO_2 transport and storage part of the BECCS value chain is included in MONET. BECCS facilities and CO_2 storage sites are collocated. A 100 km CO_2 transport distance is considered for CO_2 transport to a storage site. A 6% CO_2 leakage from CO_2 T&S is considered in the carbon footprint model to account for compression and injection energy use and its subsequent emissions [139]. A cost of \$15.4/tCO_2 is considered for CO_2 transport and was calculated based on the capital and operating costs of a 3 MtCO_2/yr capacity, 100k length, 20 years lifetime CO_2 transport pipeline [140]. A \$5/tCO_2 is assumed in addition for CO_2 storage.

3.2.3 BECCS water balance

Biomass green, blue and grey water footprints

The water footprint of a crop in a given region can be interpreted as the summation of three contributions: the green, blue and grey water. Two metrics specific to the crop and region (climate) are required for the computation of the green and grey water footprints: the annual crop water requirement $CWR(sr,b)$ and the effective precipitations that the crop receives, $Pr_{eff}(sr,m)$, after water run-off. We use Food and Agriculture Organisation (FAO) guidelines [141] to compute these metrics.

To calculate how much water is received and required by the crop growth, each crop's seasonal/annual growth cycle, including length of annual crop growth, $GCL(sr,b)$ (in days), first and end day of annual growth ($GSD(sr,b)$ and $GED(sr,b)$, respectively), length of each growth phase (initial growth, medium growth, late phase and end of growth), and crop coefficient, $Kc_{ini}(sr,b)$, $Kc_{mid}(sr,b)$, $Kc_{end}(sr,b)$ associated with each growth phase, were collected from the literature. The shape of the growth cycle is represented in Figure 3.5.

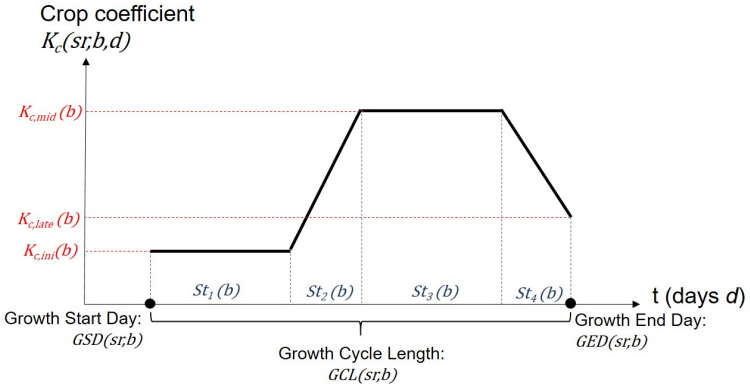


Figure 3.5: Illustration of a crop growth cycle.

The crop water requirement is calculated by multiplying a regional daily reference evapotranspiration rate $ET_0(sr,d)$ with the daily crop coefficient curve $K_c(sr,b,d)$:

$$CWR_{day}(sr,d) = K_c(sr,b,d) \times ET_{0,day}(sr,d) \tag{3.26}$$

$ET_0(sr,m)$ is calculated monthly using the Penman-Monteith equation, and daily assuming all days of the month have the same evapotranspiration rate:

$$ET_0(sr,m) = \frac{0.408\Delta(sr,m)(R_n(sr,m) - G(sr,m)) + 900\gamma(sr)u_{2m}(sr,m)\frac{e_s(sr,m)-e_a(sr,m)}{T_{mean}(sr,m)+273.15}}{\Delta(sr,m) + \gamma(sr) \times (1 + 0.34)u_{2m}(sr,m)} \tag{3.27}$$

where $\Delta(sr,m)$ is the slope of the saturation vapour pressure curve, $R_n(sr,m)$ the net solar radiation, $G(sr,m)$ the soil heat flux, $\gamma(sr)$ the psychometric constant of air at a given atmospheric pressure, $u_{2m}(sr,m)$, the wind speed at 2 meters, $e_s(sr,m)$, the mean saturation vapour pressure, $e_a(sr,m)$, the actual monthly average vapour pressure and

$T_{mean}(sr,m)$, the monthly average mean temperature. All metrics are calculated monthly for each sub-region sr, following the FAO guidelines [141], using monthly climate data including average low and high temperatures, average daily sunshine hours, average wind speed at 2 meters, monthly mean humidity, elevation of weather station, latitude of weather station, from a weather station in each region sr.

In MONET, we assume that the green water footprint is then determined by share of the crop water requirement fulfilled by precipitation received over the crop cycle. To calculate the total green water footprint per ton of pellet delivered at the power plant, we amortise this quantity over the total amount of pellets delivered over the project lifetime:

$$GreenWF(sr,sr',b,t) = \frac{\sum_{d \in GCL} min(CWR_{day}(sr,b,d), Pr_{eff,day}(sr,d)) \times PL}{tPellet(sr,sr'b,t)} \quad (3.28)$$

The blue water is assumed to be the amount of fresh water required in addition to the green water to compensate for the crop evapotranspiration, or the irrigation need over the growth cycle, $IN_{GC}(sr,b)$:

$$IN_{GC}(sr,b) = \sum_{d \in GCL} CWR_{day}(sr,b,d) - Pr_{eff,day}(sr,d) \quad (3.29)$$

$$BlueWF(sr,sr',b,t) = \frac{IN_{GC}(sr,b) \times PL}{tPellet(sr,sr'b,t)} \quad (3.30)$$

The last contribution, the grey water, accounts for water pollution resulting from farming. The main cause of water pollution is assumed to be nitrogen leaching from nitrogen-based fertilizer use [142]. Following the work of Mekonnen *et al.*, we calculate the amount of fresh water needed to dilute the water nitrates concentration to its usual background level [143]. Grey water footprint is thus a direct function of nitrogen-based fertilizer application rate (in kg/ha/yr), and nitrogen leaching, N_{leach}:

$$GreyWF = \frac{\sum_{a=1}^{a=PL} N_{leach} \times R_N(sr,b,a)}{0.01 \times tPellet(sr,sr',b,t)} \quad (3.31)$$

The total supply chain water footprint is calculated summing all three terms:

$$WF_{SC}(sr,sr',b,t) = BlueWF(sr,sr',b,t) + GreenWF(sr,sr',b,t) + GreyWF(sr,sr',b,t) \tag{3.32}$$

BECCS plant water use

Key drivers of a power plant's water intensity of power plant include the plant cooling system, plant performance and local climate conditions [144]. The three main cooling systems in use in power plants today, in order of decreasing water withdrawal, are the wet once-through, wet recirculating cooling tower and dry cooling (air). When comparing the water intensity of each cooling system, it is important to differentiate between water withdrawal and water consumption. The water consumed is the fraction of the total water withdrawn from the cooling source which is not returned to the source after use. Country-specific data on cooling systems and water withdrawal from electricity remains scarce. From the modelling of both 2005 and future cooling system shares available in Davies *et al.*, it is observed that recirculating wet cooling towers represents the highest present and future share in the USA China, Europe, India and Latin America [144]. Though the authors project a significant penetration of dry cooling systems, which are the least water consumptive, we assumed that all BECCS plants are built with a wet recirculating cooling tower, which is a state-of-the-art system.

In this study, the power plant hydrodynamic efficiency is assessed by the water intensity, $WI(sr,b)$, which is considered to be the amount of fresh water *withdrawn* per MWh of electricity generated.

$$WI_{PP}(sr,b) = \frac{F_{water}(sr,b)}{NPO(sr,b)} \tag{3.33}$$

BECCS plant water footprint, $WF_{PP}(sr,b)$ can also be calculated per ton of pellet:

$$WF_{PP}(sr,b) = \frac{F_{water}}{C_f \times F_{fuel}(b) \times (1 - MC_{pellet}(b))} \tag{3.34}$$

Total BECCS water footprint

BECCS total water footprint is calculated summing the biomass production water footprint, $WF_{SC}(sr,sr',b,t)$, with the water used within the power plant, $WF_{PP}(sr,b)$:

$$WF(sr,sr',b,t) = WF_{SC}(sr,sr',b,t) + WF_{PP}(sr,b) \tag{3.35}$$

The marginal water footprint, $MWF(sr,sr',b,t)$ is defined by the sum of the volumes of blue and grey water required in addition to green water:

$$MWF(sr,sr',b,t) = BlueWF_{SC}(sr,sr',b,t) + GreyWF(sr,sr',b,t) + WF_{PP}(sr,b) \tag{3.36}$$

3.2.4 BECCS energy balance

An energy balance is performed over the full BECCS value chain, accounting for direct and indirect energy uses along the BECCS biomass supply chain, and the electricity produced at the power plant gate.

Energy carrier, primary energy, and electrical energy equivalent

MONET builds upon various energy return on investment (or EROI) methodologies developed by Hall *et al.* [145, 146], Murphy *et al.* [147], Raugei *et al.* [148] and Dale *et al.* [149], to perform a dynamic accounting of the system energy inputs and outputs over time. Because of the variable nature and quality of the different energy inputs (*e.g.*, fuel, electricity or heat), a set e, of energy methods, was implemented to express the energy inputs and outputs under different boundary assumptions. To convert to use of a fuel j as an energy carrier, an embodied energy $EE_j(e)$ is used. It is equal to 1 when e='EC', and to the fuel supply chain energy use, or embodied energy, for e='PE' and e='EEQ'.

In the case of chemical inputs (fertilizers, lime, herbicide and pesticide), MONET explicitly considers them by including the manufacturing energy of these inputs. As these chemicals are usually made from natural gas, this embodied energy is considered both as an energy carrier and primary energy input [150].

To convert the use of electricity to primary energy, For electricity however, regional average power generation efficiencies, $\eta_{grid}(sr)$ were used [151, 152]:

$$C_{elec\rightarrow PE}(sr,'PE') = \frac{1}{\eta_{grid}(sr)} \tag{3.37}$$

$$C_{elec\rightarrow PE}(sr,'EC') = 1 \tag{3.38}$$

$$C_{elec\rightarrow PE}(sr,'EEQ') = 1 \tag{3.39}$$

Finally to convert energy carriers into electrical energy equivalents, conversation factors, $C_{j\rightarrow elec}(sr,e)$, specific to each fuel j, were obtained using the regional conversation efficiencies of this fuel j to electricity:

$$C_{j\rightarrow elec}(sr,'EC') = 1 \tag{3.40}$$

$$C_{j\rightarrow elec}(sr,'PE') = 1 \tag{3.41}$$

$$C_{j\rightarrow elec}(sr,'EEQ') = \frac{1}{\eta_{j\rightarrow elec}(sr)} \tag{3.42}$$

Decarbonisation of the energy system

To be consistent with time-evolving CO_2 removal targets, we consider the decarbonisation of both the electricity and transport/fuel sectors over time in each 1.5C representative pathway (P1 to P4). For the decarbonisation of the electricity, we computed the carbon intensity of the electricity using the IAMC 1.5 scenario explorer database [10], for Asia, Latin America and the OECD/EU (or ASIA, LAM and OECD/EU in the database). We computed the decreasing trend of the electricity carbon intensity relative to a 2020 value, and applied it to the model's BAU electricity carbon intensity in each region (for China and India using ASIA trends, Brazil using LAM trends, and the USA and EU using OECD/EU trends). The carbon intensity was considered to be zero when negative.

For fuel use at the biomass production (machinery) and transport (truck and shipping) levels, no clear decarbonisation pathway can be obtained from the IAMC 1.5°C scenario explorer database. In the IEA 'Modern Truck Scenario' (MTS), a combination of fuel switching and energy efficiency measures is projected to decrease road freight final energy demand from 36 EJ in 2015 to 27 EJ in 2050, while well-to-wheel GHG emissions drop from 3.1 $GtCO_2$ in 2015 to 1.2 $GtCO_2$ in 2050 [153]. This suggests a 52% drop in road freight transport CO_2 intensity per unit of energy by 2050. In adopting a conservative approach, we assumed a freight transport decarbonisation trajectory starting from 0% in 2030 and increasing with a 20% increment per decade (20% in 2040, 40%

in 2050, *etc.*) all to way to 100% in 2080. Decarbonisation options for freight road transport include 1) natural gas – in compressed (CNG) or liquefied (LNG) form, LNG being more suitable for higher mileage, larger payload vehicles [153], 2) hydrogen, 3) electric vehicle and 4) biofuels. In the IEA MTS, most of the decarbonisation is achieved through the switch to hybrid (approx. 30% of the heavy vehicle fleet) or fully electrified (approx. 35% of the heavy vehicle fleet) trucks, while biofuel meet 23% of final road transport energy demand in 2050 [153]. Transport decarbonisation not being the subject of this thesis, and recognising that the actual road transport decarbonisation will likely be different, we assume for simplicity that road transport decarbonisation is achieved through fuel switching to biofuels. In line with the theme of our study, we consider that biofuels are however not 100% carbon neutral, and have an associated supply chain emissions factor.
Owing to the uncertainty around shipping emissions reduction, we assume that shipping biomass in container ships remains undecarbonised.
For biomass drying, finally, we assume that natural gas ('NG') is used in 2030, and is switched to 100% wood drying as early as 2040. The cost of fuels remains however constant over time. We acknowledge that these assumptions might be oversimplifications, but they offer a conservative approach towards decarbonisation of transport, as an emission factor of biofuel is considered.

The embodied energy, $EE_{fuel}(e,time)$ (below as an example), emission factor, $EF_{fuel}(time)$, heating value, $LHV_{fuel}(time)$, and cost, $cost_{fuel}(time)$ of farming/processing fuel are thus calculated with a linear combination of diesel and biodiesel ('bioD'), based on the biofuel share, $frac_{biofuel}(time)$:

$$EE_{fuel}(e,time) = EE_{diesel}(e) \times (1 - frac_{biofuel}(time)) + EE_{bioD}(e) \times frac_{biofuel}(time) \tag{3.43}$$

The biodiesel emission factor is only considered to be the biofuel supply chain carbon footprint, as direct emissions are considered carbon neutral. For biomass drying, the embodied energy, $EE_{drying}(time)$ (below as an example), emission factor, $EF_{drying}(time)$, boiler efficiency, $\eta_D(time)$, and heating value, $LHV_{drying}(time)$, of the drying fuel are calculated in a similar fashion:

$$EE_{drying}(e,time) = EE_{NG}(e) \times (1 - frac_{biofuel}(time)) + EE_{wood}(e) \times frac_{biodry}(time) \tag{3.44}$$

Akin to biodiesel, the emission factor for wood pellets is considered to be the wood pellets supply chain carbon footprint, as direct emissions are considered carbon neutral.

For road transport, the emission factors in kgCO_2/t.km, $EF_{RT,f}(time)$ for all biomass formats $f \in$ {pellets, chips, bale } (or {pel, chip, bal }), are also calculated using $frac_{biofuel}(time)$:

$$EF_{RT,f}(time) = EF_{RTdiesel,f} \times (1 - frac_{biofuel}(time)) + EF_{RTbioD,f}(e) \times frac_{biofuel}(time) \quad (3.45)$$

The fuel efficiency, $FE_{RT,f}$ of using biodiesel or diesel for road transport is however assumed constant.

Supply chain energy demand

Both the direct and indirect energy demand of producing, processing, transporting and converting the biomass was considered in the energy balance. Direct energy inputs include diesel use for biomass farming, irrigation, size reduction, and transport in truck, heavy fuel oil used for biomass shipping, natural gas or wood pellets used for biomass drying, and electricity used for biomass pelleting process. Indirect energy inputs include the energy demand associated with the supply chain of input products such as seeds, fertilisers, lime and herbicides, typically manufactured using natural gas, as well as that of fuels (diesel, heavy fuel oil, natural gas).

The energy demand of each stage is first calculated for each year, a, per hectare:

- Application of inputs $i \in$ { seed, lime, herb, N, P_2O_5, K_2O }, with an embodied energy EE_i (or $EE_i(b)$ for switchgrass seeds/miscanthus rhizome/willow planting), and at a application rate $R_i(sr,b,a)$ in kg/ha (or in kg/ha for switchgrass seeds, rhizome/ha for miscanthus or planting/ha for willow):

$$ED_{inputs,ha}(sr,b,a,e,time) = C_{NG\rightarrow Power}(e).\sum_i R_i(sr,b,a).EE_i(b) + \sum_i R_i(sr,b,a) \times ER_{SupTrans} \times (1 + \frac{EE_{fuel}(e,time)}{LHV_{fuel}(time)}) \times C_{diesel\rightarrow elec}(sr,e) \quad (3.46)$$

  Seeds (or rhizome or plantings) and lime are only applied the first year of the crop cycle during land preparation ($Ind_{LandPrep}(sr,b,a)$), whilst herbicides are applied annually, and fertilisers during harvests ($Ind_{harv}(sr,b,a)$). This is reflected in the

application rate function of each products, $R_i(sr,b,a)$, which varies over time. The energy requirement to transport supplies, $ER_{SupTrans}$, in MJ/kg, in also considered.

- Farming operations, which includes the land preparation fuel requirement in L/ha, $FR_{LandPrep}(b)$, the harvest or collection (for residues) fuel requirement in L/ha, $FR_{harvest}(b)$, the irrigation energy in MJ/mm, ER_{irrig}, which is multiplied by the annual irrigation need in mm/ha/yr, $IN_{year}(sr,b)$, and the transport to the pelleting plant, which is assumed to be located at a distance D_{farm} of 25 km from the farm:

$$\begin{aligned} ED_{farm,ha}(sr,b,a,e,time) &= (FR_{Landprep}(b).Ind_{Landprep}(sr,b,a) \\ &+ FR_{harv}(b).Ind_{harv}(sr,b) + ER_{irrig} \times IN_{year}(sr,b) \\ &+ D_{farm} \times Yield_{WM}(sr,b,a) \times FE_{RT,f}(time) \\ &\times (EE_{fuel}(e,time) + LHV_{fuel}(time)) \times C_{diesel \rightarrow elec}(sr,e) \end{aligned} \quad (3.47)$$

- biomass feedstock size reduction (chopping/chipping) fuel requirement (diesel or biodiesel):

$$\begin{aligned} ED_{SR,ha}(sr,b,a,e,time) &= ER_{SR}(b) \times (1 + \frac{EE_fuel(e,time)}{LHV_{fuel}(time)}) \\ &\times Yield_{WM}(sr,b,a) \times C_{diesel \rightarrow elec}(sr,e) \end{aligned} \quad (3.48)$$

- biomass feedstock drying energy requirement in the form of fuel (natural gas or wood pellets) and power:

$$\begin{aligned} ED_{D,ha}(sr,b,a,e,time) &= ER_D(b) \times Bio_{proc,SR,WM}(sr,b,a) \times EE_{elec}(sr,e) \\ &+ FR_D(sr,b,time) \times (1 + \frac{EE_{drying}(e,time)}{LHV_{drying}(time)}) \times C_{NG \rightarrow elec}(e) \\ &\times Bio_{proc,SR,WM}(sr,b,a) \end{aligned} \quad (3.49)$$

where $FR_D(sr,b,time)$ is the fuel requirement determined by the dryer evaporation energy in MJ/tH_2O, $HR_{evap,D}$, biomass inlet moisture content, $MC_{proc,SR}(sr,b)$ and the biomass target moisture content TMC_D, which is required prior to pelleting or transport:

$$FR_D(sr,b,time) = \frac{HR_{evap,D}}{\eta_D(time)}\left(\frac{MC_{proc,SR}(sr,b)}{1-MC_{proc,SR}(sr,b)} - \frac{TMC_D(sr,b)}{1-TMC_D(sr,b)}\right) \tag{3.50}$$

$HR_{evap,D}$ was pre-determined using a dryer model described in Appendix A.

- biomass grinding, pelleting, cooling power requirement:

$$ED_{k,ha}(sr,b,a,e,time) = ER_k(b).Bio_{proc,k-1,WM}(sr,b,a).EE_{elec}(sr,e), \quad k \in \{G,P,C,PG\} \tag{3.51}$$

- biomass transport to the conversation plant (RT1, ST and RT2), depending on the transport mode t and the biomass transport format f:

$$ED_{RT1,ha}(set1,a,e,time) = RD1(set1) \times FE_{RT,f}(time) \times (LHV_D + EE_{fuel}(e,time)).C_{diesel\rightarrow elec}(e).Bio_{proc,P,WM}(sr,b,a) \tag{3.52}$$

$$ED_{ST,ha}(set1,a,e) = SD(sr,sr',p,p',t) \times FE_{HFO} \times EE_{HFO}(e) \times C_{HFO\rightarrow elec}(e).Bio_{proc,RT1,WM}(sr,b,a) \tag{3.53}$$

$$ED_{RT2,ha}(set1) = RD2(set1) \times FE_{RT,f}(time).(LHV_{fuel}(time) + EE_{fuel}(e,time)) \times C_{dieseltoelec}(e) \times Bio_{proc,ST,WM}(sr,b,a) \tag{3.54}$$

- biomass pellet grinding at the power plant prior to combustion:

$$ED_{PG,ha}(sr,b,a,e) = \begin{cases} ER_{PG} \times Bio_{proc,RT2,WM}(sr,b,a) \times EE_{elec}(e) \text{ if } sr \neq sr' \\ ER_G \times Bio_{proc,RT2,WM}(sr,b,a) \times EE_{elec}(e) \text{ if } sr = sr' \end{cases} \tag{3.55}$$

The annual, $tED_{SC,ha}$, cumulative, $CED_{SC,ha}$ and total supply chain energy demand per ton of biomass pellets over the project lifetime, tED_{SC}, can then be calculated:

$$ED_{SC,ha}(set1,a,e,time) = \sum_{k} ED_{k,ha}(set1,a,e,time) \tag{3.56}$$

$$CED_{SC,ha}(set1,a,e,time) = \sum_{a'=1}^{a} ED_{SC,ha}(set1,a',e,time) \tag{3.57}$$

$$tED_{SC}(set2) = \frac{CED_{SC,ha}(set1,PL,e,time)}{tPellet(sr,sr',b,t)} \tag{3.58}$$

To this energy demand must be added the energy demand from using coal instead of biomass, when the co-firing rate is lower than 100%:

$$ED_{coal}(sr,st',b,t,a,e) = Pellet(sr,sr',b,t,a) \times \frac{1}{C_f - 1} \times (1 + MC_{pellet}(sr,b) \times EE_{coal}(e) \tag{3.59}$$

$$tED_{coal}(sr,st',b,t,e) = \sum_{a=1}^{PL} ED_{coal}(sr,sr',b,t,a,e) \tag{3.60}$$

BECCS total value chain energy demand thus becomes:

$$ED_{ha}(set1,a,e,time) = ED_{SC,ha}(set1,a,e,time) + ED_{coal}(sr,st',b,t,a,e) \tag{3.61}$$

$$CED_{ha}(set1,a,e,time) = \sum_{a'=1}^{a} ED_{ha}(set1,a',e,time) \tag{3.62}$$

$$tED(set2) = \frac{CED_{ha}(set1,PL,e,time)}{tPellet(sr,sr',b,t)} \tag{3.63}$$

Energy generation

BECCS energy production can be expressed in total raw bioenergy production (at harvest), bioenergy production (in the form of bio pellets prior to combustion), and electricity generation.

The annual, EG_{bio}, and cumulative raw bioenergy production, CEG_bio are calculated from the annual biomass yield:

$$EG_{bio}(sr,b,a) = Yield(sr,b,a) \times HHV_{bio}(b) \times 1000 \tag{3.64}$$

$$CEG_{bio}(sr,b,a) = CYield(sr,b,a) \times HHV_{bio}(b) \times 1000 \tag{3.65}$$

The annual, EG_{pellet} and cumulative, CEG_{pellet}, bioenergy production in the form of pellets are calculated from the annual and cumulative biomass pellet production:

$$EG_{pellet}(sr,sr',b,t,a) = Pellet(sr,sr'b,t,a) \times HHV_{bio}(b) \times 1000 \tag{3.66}$$

$$CEG_{pellet}(sr,sr',b,t,a) = CPellet(sr,sr',b,t,a) \times HHV_{bio}(b) \times 1000 \tag{3.67}$$

The BECCS plant annual, EG_{PP}, cumulative, CEG_{PP}, and total electricity generation over the project lifetime, tEG_{PP} can be calculated:

$$EG_{PP}(sr,sr',b,t,a) = \frac{Pellet(sr,sr',b,t,a)}{1 - MC_{pellet}(sr,b)} \times HHV_{fuel}(b)) \times \eta_P(sr,b) \tag{3.68}$$

$$CEG_{PP}(sr,sr',b,t,a) = \sum_{a'=1}^{a} EG_{PP}(sr,sr',b,t,a) \tag{3.69}$$

$$tEG_{PP}(sr,sr',b,t) = CEG_{PP}(sr,sr',b,t,PL) \tag{3.70}$$

BECCS net energy balance

Different indicators are computed to assess BECCS performance in terms of energy production:

- The energy Return on Investment $EROI(set1,a,e,time)$, the ratio of the cumulative supply chain primary energy demand to the cumulative primary energy generated (in the form of biomass pellets):

$$EROI(set1,a,e,time) = \frac{CEG_{pellet}(sr,sr',b,a)}{CED_{SC,ha}(set1,a,'PE',time)} \tag{3.71}$$

- Electricity Return on Investment $E_lROI(sr,b,yr)$, the ratio of the cumulative primary energy demand to the cumulative electricity generated:

$$E_lROI(set1,a,e,time) = \frac{CEG_{PP}(sr,sr',b,t,a)}{CED_{ha}(set1,a,'PE',time)} \tag{3.72}$$

- The cumulative net Electricity Balance $CNEB(set1,a,e,time)$, the difference between the electricity generated by the system and the cumulative electricity demand along BECCS value chain:

$$NE_lB(sr,b,yr) = CEG_{PP}(sr,sr',b,t,a) - CED_{ha}(set1,a,'EEQ',time) \tag{3.73}$$

- Electricity breakeven time BET_E, the time required for the E_lROI to be above one:

$$BET_E(set1,a,time) = \sum_a \{a|E_lROI(set1,a,time) < 1\} \tag{3.74}$$

  Similarly, another definition is the time required for the net cumulative electricity balance to be positive:

$$BET_E(set1,a,time) = \sum_{yr} \{yr|CNE_lB(sr,b,yr) < 0\} \tag{3.75}$$

Figure 3.6 provides an overview of the BECCS energy model and its key indicators.

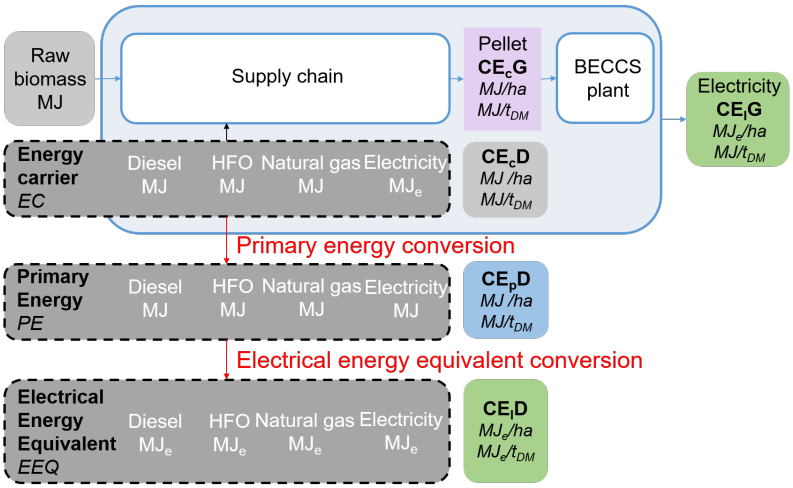


Figure 3.6: Net Electricity Balance, Electricity Return On Investment and Electricity Pay-Back Time are calculated based on these metrics.

3.2.5 BECCS carbon balance

BECCS supply chain GHG emissions

The same methodology is applied for the accounting of GHG emissions along BECCS value chain, with the following changes:

- For each input i, the embodied energy term, EE_i (or $EE_i(b)$ for seeds/rhizome/-plantings), are replaced by the carbon footprint term, CF_i (or $CF_i(b)$ for seeds/rhizome/plantings)
- For each fuel j, the embodied energy term, $EE_j(e)$, is replaced by the emission factor term, EF_j, for fossil fuels including natural gas, diesel and HFO, or by a carbon footprint term, CF_j, for biofuels including biodiesel and wood pellets. The energy methods set, e, is no longer used as no distinction are longer made between energy carriers, primary energy and electrical energy equivalent for emissions accounting,
- For each transport mode, $m \in \{\text{RT, ST }\}$, and biomass transport format, $f \in \{\text{pel, chip, bal }\}$, fuel efficiencies, $FE_{m,f}$ are replaced by emission factors $EF_{m,f}$
- two additional emission sources are accounted in the balance, including 1) direct and indirect land use change emissions from land conversion, 2) direct N_2O emissions from fertiliser application. These additional emission sources are described below,
- BECCS supply chain annual carbon footprint, $CF_{SC,ha}(set2', time)$, is calculated as the summation of all emissions terms up to the power plant,
- BECCS supply chain total carbon footprint, $tCF_{SC}(set2', time)$, is calculated as

the summation of all emissions terms up to the power plant, and divided by the total number of dry pellets delivered at the plants, $tPellet(sr,sr',b,t)$, over the BECCS project lifetime, PL,

Land use change To account for direct land use changes, conversion emission factors in tCO_2/ha for each land type were taken from the literature [76, 85]. These LUC emissions factors were assumed constant per land type and biomass type across all MONET regions. This is an approximation as these factors are likely to be highly dependent on the region/climate (*e.g.*, variation in vegetation density) as well as on which crop the land is converted to. Whilst some regional projects provide direct emissions factors for specific land transitions (for example the ELUM project in the UK, which provides direct emissions factors for grassland to wheat production and short rotation forestry [154]), no existing source provides emissions factors for all MONET regions using the same set of assumptions. When averaging emissions factors from Fargione *et al.* and Plevin *et al.*, we find an average grassland direct emissions factor of 13.6 tCO_2 per hectare. To compare these values with those of the ELUM project for example, transitioning from grassland to wheat and short rotation forestry (SRF) in the UK can generate a net emissions factor up to 40 tCO_2/ha for wheat and 20 tCO_2/ha for SRF in some UK regions, but the transition factors for most of the UK remain below 12 tCO_2/ha for wheat, and 0.05 tCO_2/ha for short rotation forestry. This suggests that the numbers used in our analysis might be conservative estimates for some of MONET regions.
Indirect land use change emissions factors are even for difficult to asses. They also depend on the initial use of the land, and the biomass crop the land is transitioned to, but equally depend on where the activity is reallocated. Land types were thus classified into two categories; managed land, *i.e.*, already allocated to an activity, and unmanaged land. If converting part of a managed land – cropland or grassland – to biomass production, an ILUC conversion factor in tCO_2 was attributed. When converting a land unallocated to any activity, ILUC was considered to be zero. This is not a conservative estimate as accessing this unused land is likely to involve establishing a logistic chain (*e.g*, building roads), and could potentially involve indirect land use change by trespassing over used land. ILUC conversion factors in tCO_2/ha are not found as such in the literature. Indirect land use change emissions have been thoroughly investigated in the context of biofuels in which conversion factors are expressed in tCO_2/MJ, and are a function of the biofuel energy yield MJ/(ha.yr), time horizon (in years), fraction of land displaced (in $\%_{ha}$) and average emission factor resulting from the activity displaced (in tCO_2/ha). Two different sources were used: an analysis by Plevin *et al.* based on corn bioethanol in the US [85], and an analysis from Overmars *et al.* based on bioethanol production in Europe, from three different feedstocks: wheat and sugar beet grown in Europe and sugarcane imported from Brazil and Pakistan [89]. As ILUC

factors are expressed in $kgCO_2eq/MJ$ of biofuels in both analysis, the data provided in the studies was used to derive land ILUC factors in $kgCO_2eq$ per hectare cultivated for bioenergy. These factors can then be used independently from biomass yield and project time horizon. When average net displacement factors (ha displaced/ha of biofuels) and emission factors (tCO_2eq/ha) were provided [85], the land ILUC factor was obtained by multiplying these two parameters. When the data provided was less straightforward [89], the land ILUC factor was obtained by multiplying the ILUC factor by the time horizon and bioenergy yield. Plevin *et al.* described two additional analyses on US bioethanol from maize [155] and corn [77] and these results were also included in the ILUC coefficient data set to ensure the consistency of the statistical analysis. Figures 3.7 and 3.8 provides further details on the methodology and data used.
We acknowledge the high uncertainty around these emission factors. Bearing in mind these caveats, we do not aim at quantifying the absolute impact of direct and indirect land use change, but we are rather interested in the potential impact on CO_2 removal breakeven time, when high indirect land use change values are considered.

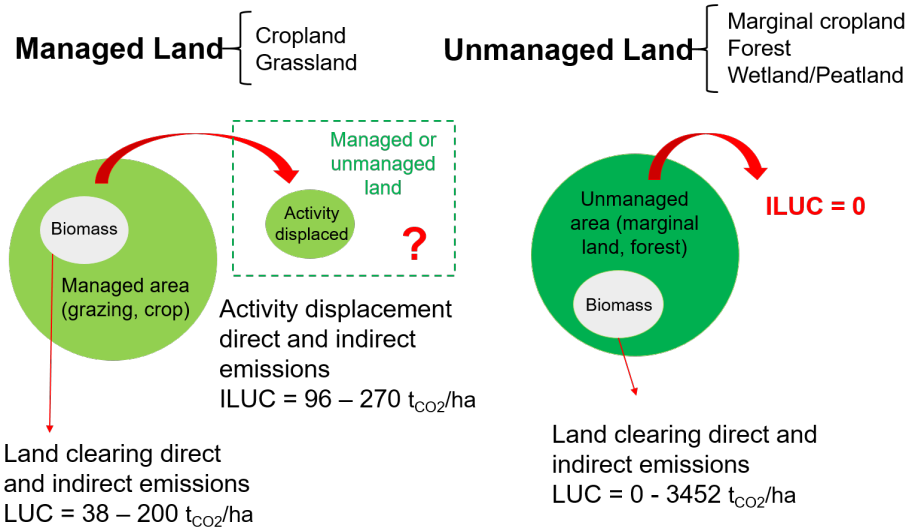
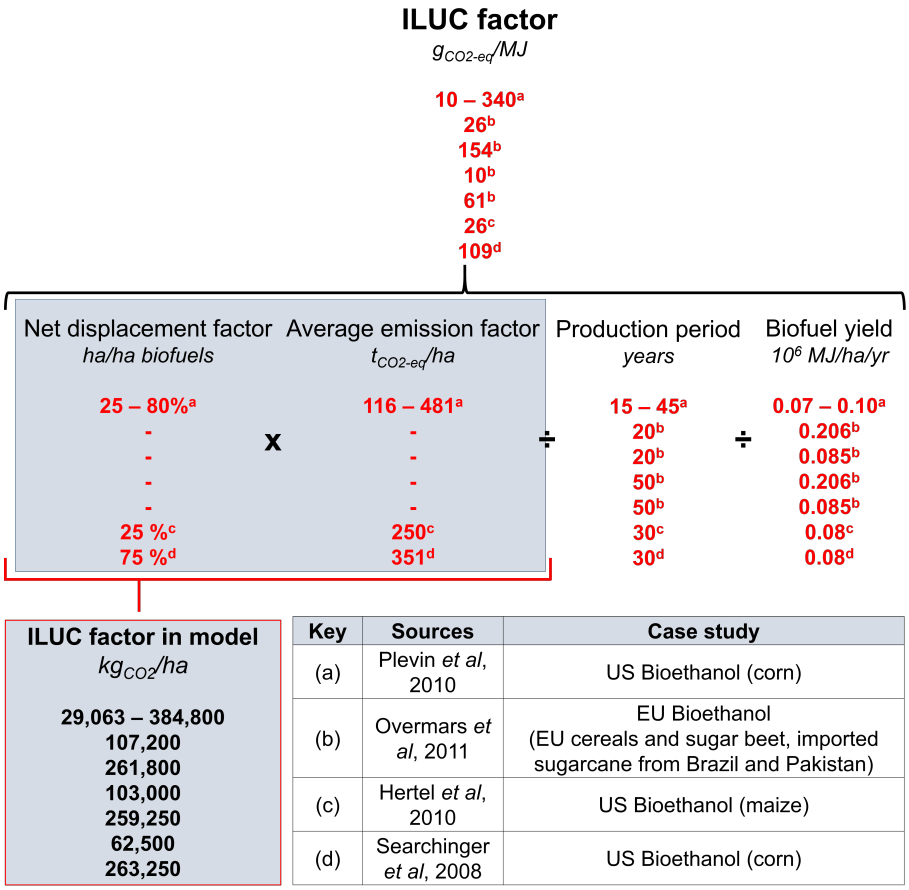


Figure 3.7: Methodology of direct and indirect land use change effects accounting. Upon considering indirect land use change, clearing a managed land could be as bad as clearing a more dense unmanaged land such as a forest. Indirect land use changes wide uncertainty range in turn impacts the uncertainty of the model.

N_2O emissions evaluation Nitrogen fertilizer application (in kg/(ha.yr)) is considered to cause N_2O-N direct formation, N_2O-N formation from NH_3-N and NO_x-N volatization, and N_2O-N formation from N leaching or runoff. The following expression



Key	Sources	Case study
(a)	Plevin *et al*, 2010	US Bioethanol (corn)
(b)	Overmars *et al*, 2011	EU Bioethanol (EU cereals and sugar beet, imported sugarcane from Brazil and Pakistan)
(c)	Hertel *et al*, 2010	US Bioethanol (maize)
(d)	Searchinger *et al*, 2008	US Bioethanol (corn)

Figure 3.8: Methodology for the derivation of ILUC conversion factors in $kgCO_2eq/ha$. Values derived from Plevin *et al.* [85], Searchinger *et al.* [77], and Hertel *et al.* [155] were obtained for bioethanol production in the US, whereas the results from Overmars *et al.* are the lower and upper bounds obtained for bioethanol production in Europe, considering three different feedstocks: wheat and sugar beet grown in Europe and sugarcane imported from Brazil and Pakistan.

evaluates nitrogen-based fertilizer application contribution to biomass carbon footprint:

$$EF_{\mathrm{N_2O}} = EF_{\mathrm{N}} + EF_{\mathrm{NH_3-N-NO_x-N}} \times EF_{\mathrm{N,volatilized}} + EF_{\mathrm{N,leaching}} \times LP \tag{3.76}$$

$$CF_{N2O}(sr,sr',b,t) = \frac{GWP_{\mathrm{N_2O}} \times C_{\mathrm{N_2O-N}} \times EF_{\mathrm{N_20}} \cdot \sum_{a=1}^{PL} R_{\mathrm{N}}(sr,b,a)}{Pellet(sr,sr',b,t)} \tag{3.77}$$

where $R_N(sr,b,a)$ nitrogen application rate in kg/ha, C_{N_2O-N} molecular conversion factor, EF_N emission factor in kN_2O-N/kgN applied, $EF_{NH_3-N-NO_x-N}$ emission factor in kgNH_3-N-NO_x-N/kgN applied, $EF_{N,volatilized}$ volatization factor in kgN_2O-N/kgNH_3-N-NO_x-N, $EF_{N,leaching}$ leaching factor in kgN_2O-N/kgN leaching, and LP leaching proportion in kgN leaching/ kgN applied.

BECCS plant CO_2 emissions

The carbon intensity of the BECCS plant, $CI_P(b)$, is a function of the capture rate, R_{CCS}, the biomass co-firing rate, C_f, and the biomass carbon content, $C_{bio}(b)$:

$$CI_P(b) = \frac{F_{fuel}(b) \times ((1 - R_{CCS}) \times C_{fuel}(b) - C_f \times C_{bio}(b)) \times C_{C \to CO_2}}{NPO} \times 10^3 \quad (3.78)$$

We can also calculate the BECCS plant annual total, $ECO2_{ha}$, captured and stored, $SCO2_{ha}(sr,sr',b,t,a)$, biogenic, $EBioCO2_{ha}$, and fossil, $ECoalCO2_{ha}$, CO_2 emissions:

$$EBioCO2_{ha}(sr,sr',b,t,a) = Pellet(sr,sr',b,t,a) \times Cbio(b) \times C_{C \to CO2} \quad (3.79)$$

$$ECoalCO2_{ha}(sr,sr',b,t,a) = Pellet_{WM}(sr,sr',b,t,a) \times (\frac{1}{C_f} - 1) \times C_{coal} \times C_{C \to CO2} \quad (3.80)$$

$$ECO2_{ha}(sr,sr',b,t,a) = EBioCO2_{ha}(sr,sr',b,t,a) + ECoalCO2_{ha}(sr,sr',b,t,a) \quad (3.81)$$

$$SCO2_{ha}(sr,sr',b,t,a) = R_{CCS} \times ECO2_{ha}(sr,sr',b,t,a) \quad (3.82)$$

The carbon footprint associated to coal use, $CF_{coal}(sr,sr',b,t,a)$, including direct and indirect emissions, is the following:

$$CF_{coal}(sr,sr',b,t,a) = (1 - R_{CCS}) \times ECoalCO2_{ha}(sr,sr',b,t,a) \quad (3.83)$$

$$+Pellet_{WM}(sr,sr',b,t,a) \times (\frac{1}{C_f} - 1) \times HHV_{coal} \times EF_{coal} \quad (3.84)$$

A 6% CO_2 leakage from CO_2 T&S, EF_{CO2T}, is also considered in the carbon footprint model to account for compression and injection energy use and its subsequent emissions

[56]:

$$CF_{CO2T}(sr,sr',b,t,a) = SCO2_{ha}(sr,sr',b,t,a) \times EF_{CO2T} \tag{3.85}$$

BECCS annual,CF_{ha}, and total carbon footprint over BECCS project lifetime, $tCF(set2',time)$, including coal and CO_2 transport carbon footprints, are the following:

$$CF_{ha}(set2,time) = CF_{SC,ha}(set2,time) + CF_{CO2T}(sr,sr',b,t,a) + CF_{coal}(sr,sr',b,t,a) \tag{3.86}$$

$$tCF(set2',time) = \sum_{a=1} PL \frac{CF_{ha}(set2',time)}{tPellet(sr,sr',b,t)} \tag{3.87}$$

BECCS carbon balance

To measure BECCS performance in terms of CO_2 removal, three metrics are calculated: total CO_2 removal over the project lifetime, $tRCO2$, BECCS CO_2 breakeven time, BET_{CO2}, and BECCS CO_2 efficiency, $t\eta_{CO2}$. BECCS annual, $RCO2_{ha}$, cumulative, $CRCO2_{ha}$, and total, $tRCO2$ over the BECCS project lifetime, net CO_2 removal, are calculated :

$$RCO2_{ha}(set2,a,time) = SCO2_{ha}(sr,sr',b,t,a) - CF_{ha}(set2,a,time) \tag{3.88}$$

$$CRCO2_{ha}(set2,a,time) = \sum_{a'=1}^{a} RCO2_{ha}(set2,a',time) \tag{3.89}$$

$$tRCO2(set2,a,time) = \frac{CRCO2_{ha}(set2,PL,time)}{tPellet(sr,sr',b,t,a)} \tag{3.90}$$

BECCS CO_2 breakeven time is calculated as the number of years required for a BECCS project to be net CO_2 negative:

$$BET_{CO2}(set1) = \{\sum a \| CRCO2_{ha}(set2,a,time) \geqslant 0\} \tag{3.91}$$

BECCS CO_2 efficiency is calculated as the ratio of cumulative CO_2 removal to cumulative CO_2 biologically sequestered, $CBioCO2$:

$$CBioCO2(sr,b,a) = CYield(sr,b,a) \times C_bio(b) \times C_{C\rightarrow CO_2} \tag{3.92}$$

$$\eta_{CO2}(set2,a,time) = \frac{CRCO2_{ha}(set2,a,time)}{CBioCO2(sr,b,a)} \tag{3.93}$$

$$t\eta_{CO2}(set1) = \eta_{CO2}(set2,PL,time) \tag{3.94}$$

From a BECCS facility perspective, the net carbon intensity of the plant, CI, as well as the amount of CO_2 removed per hour, $RCO2_{hr}$, can also be calculated:

$$CI(sr,b,l,p) = \frac{tRCO2(set2,a,time)}{tEG_{PP}(sr,sr',b,t)} \tag{3.95}$$

$$\begin{aligned} RCO2_{hr}(set1) = &-F_{fuel} \times (-C_{fuel}(b) \times C_{C\rightarrow CO_2} \times (1 - R_{CCS}) \\ &- C_f \times tCF(sr,b,l,p) \times (1 - MC_{pellet}(sr,b)) \\ &+ C_f \times C_{bio}(b) \times C_{C\rightarrow CO_2} \times (1 - MC_{pellet}(sr,b)) \end{aligned} \tag{3.96}$$

3.2.6 BECCS cost model

Biomass feedstock cost model

The same methodology is applied for the calculation of BECCS cost, with the following changes:

- For each input i, the embodied energy terms, EE_i (or $EE_i(b)$ for seeds/rhizome/-plantings), are replaced by a cost term, $cost_i$ (or $cost_i(b)$ for seeds/rhizome/-plantings)
- For each fuel j, the embodied energy terms, $EE_j(e)$, are replaced by a cost term, $cost_j$. The energy methods set, e, is no longer used as no distinction are longer made between energy carriers, primary energy and electrical energy equivalent for cost calculation,
- For each transport mode, $m \in \{\text{RT, ST }\}$, and biomass transport format, $f \in \{\text{pel, chip, bal }\}$, fuel efficiencies, $FE_{m,f}$ are replaced by a cost term $cost_{m,f}$
- two additional cost terms are accounted for in the cost calculation, including 1) the cost of land, and 2) the capital and labor costs of farming and pelleting operations,
- BECCS annual supply chain cost, $cost_{SC,ha}(set2',time)$, is calculated as the summation of all cost terms up to the power plant,
- BECCS total supply chain cost, $tcost_{SC}(set2',time)$, is calculated as the summation of all cost terms up to the power plant, and divided by the total number

of dry pellets delivered at the plants, $tPellet(sr,sr',b,t)$, over the BECCS project lifetime, PL,

Land cost Annual land rents in \$/ha/yr, $cost_{land}(sr,l)$ were collected for cropland, grassland and forests in different regions. The land rent for marginal land and for wheat straw from wheat production was considered to be zero:

$$cost_{land,ha}(sr,b,l,a) = cost_{land}(sr,l) \text{ for } b \neq \text{'wheat' and } l \neq \text{'marginal'} \quad (3.97)$$

Farming and pelleting machinery and labor costs For farming, the machinery capital cost term in \$/ha, CAP_{mach}, the number of labor hours in hrs/ha, Lab_{farm}, and the cost of labor in agriculture in \$/hrs, $cost_{lab}$ are added to the equation:

$$\begin{aligned} cost_{farm,ha}(sr,b,a,time) &= (FR_{Landprep}(b).Ind_{Landprep}(sr,b,a) + FR_{harv}(b) \\ &\times Ind_{harv}(sr,b) + \frac{ER_{irrig}}{LHV_{fuel}(time)} \times IN_{year}(sr,b)) \times \boldsymbol{cost_{fuel}(time)} \\ &+ D_{farm} \times Yield_{WM}(sr,b,a) \times \boldsymbol{cost_{RT,f}(time)} \\ &+ \boldsymbol{CAP_{mach}(sr,b) + Lab_{farm}(sr,b) \times cost_{lab}(sr)} \end{aligned} \quad (3.98)$$

Pelleting capital and labor costs For pelleting, the total plant capital cost in \$/t_{WM}, CAP_{PeP} (or the dryer cost, in \$/t_{WM}, CAP_D, if sr $=$ sr'), and the pelleting plant operation and maintenance cost including of regional labor costs, OM_{PeP}, are considered in addition to the energy cost:

$$cost_{CapPeP,ha}(sr,sr',b,a) = \begin{cases} CAP_{PeP}(sr) \times Bio_{proc,SR,WM}(sr,b,a) \text{ if } sr \neq sr' \\ CAP_D(sr) \times Bio_{proc,SR,WM}(sr,b,a) \text{ if } sr = sr' \end{cases} \quad (3.99)$$

$$cost_{OMPeP,ha}(sr,sr',b,a) = OM_{PeP}(sr) \times Bio_{proc,SR,WM}(sr,b,a) \text{ if } sr \neq sr' \quad (3.100)$$

BECCS plant cost and revenues model

The levelised capital and operating costs of BECCS plant in \$/MWh are calculated knowing the regional CAPEX, CAP_{PP}, O&M, OM_{PP}, load factor, $Loadf$, net power output, NPO and capital recovery factor, CRF_{PP}, of a BECCS plant, itself calculated based on the interest rate, IR_{PP} and the plant lifetime, LT_{PP}:

$$CRF_{inf} = \frac{IR_{inf} \times (IR_{inf}+1)^{LT_{inf}}}{(IR_{inf}+1)^{LT_{inf}} - 1} \tag{3.101}$$

$$cost_{PP,MWh}(sr,sr',b,time) = \frac{CAP_{PP}(sr',time) \times CRF_{PP} + OM_{PP}(sr')}{NPO(sr,b) \times 8760 \times Loadf} \tag{3.102}$$

The annual, $cost_{PP,ha}$, cumulative, $Ccost_{PP,ha}$ and total, $tcost_{PP}$ of a BECCS plant are then calculated based on annual electricity generation, EG_{PP}:

$$cost_{PP,ha}(sr,sr',b,t,a,time) = cost_{PP,MWh}(sr,sr',b,time) \times EG_{PP}(sr,sr',b,t,a) \tag{3.103}$$

$$Ccost_{PP,ha}(sr,sr',b,t,a,time) = \sum_{a'=1}^{a} cost_{PP,ha}(sr,sr',b,t,a',time)) \tag{3.104}$$

$$tcost_{PP}(sr,sr',b,t,time) = \frac{\sum_{a=1}^{CL} cost_{PP,ha}(sr,sr',b,t,a',time)}{tPellet(sr,sr',b,t)} \tag{3.105}$$

The revenues stream from selling electricity can also be calculated:

$$rev_{PP}(set1) = tEG_{PP}(sr,sr',b,t) \times cost_{elec}(sr') \tag{3.106}$$

CO_2 transport and storage cost

The annual, $cost_{CO2TS,ha}$, and total, $tcost_{CO2TS}$, CO_2 transport and storage costs are calculated using levelised CO_2 transport, $cost_{CO2T,SCO2}$, and storage, OP_{CO2S}, per ton of CO_2 captured and stored:

$$cost_{CO2TS,ha}(sr,sr',b,t,a) = (cost_{CO2T,SCO2}(sr') + OP_{CO2S}(sr')) \times SCO2_{ha}(sr,sr',b,t,a) \tag{3.107}$$

$$tcost_{CO2TS}(sr,sr',b,t) = \frac{\sum_{a=1}^{CL} cost_{CO2TS,ha}(sr,sr',b,t,a',time)}{tPellet(sr,sr',b,t)} \quad (3.108)$$

BECCS total cost and cost balance

BECCS annual, $cost_{ha}$, and total, $tcost$, are calculated summing up the biomass feedstock costs, power plant costs and CO_2 transport and storage costs:

$$cost_{ha}(set2,a,time) = cost_{SC,ha}(set2,a,time) + cost_{PP}(sr,sr',b,t,a,time) + cost_{CO2TS}(sr,sr',b,t,a) \quad (3.109)$$

$$tcost(set1) = \frac{Ccost_{ha}(set2,PL,time)}{tPellet(sr,sr',b,t,a)} \quad (3.110)$$

BECCS annual,CB_{ha}, and total, tCB, cost balance, accounting for the plant revenues, are calculated:

$$CB_{ha}(set1,a,time) = cost_{ha}(set1,a,time) - rev_{PP}(sr,sr',b,t) \quad (3.111)$$

$$tCB(set1,a,time) = \frac{\sum_{a=1}^{PL} CB_{ha}(set1,a,time)}{tPellet(sr,sr',b,t)} \quad (3.112)$$

Finally, assuming that the BECCS plant perceives a direct revenue for the service of CO_2 removal, in the form, for example, of a negative emissions credit (NEC), the breakeven credit required for the BECCS cost balance to equate zero, BE_{NEC}, can be quantified:

$$BE_{NEC}(set1) = \frac{tcost(set1) - (\sum_{a=1}^{PL} EG_{PP}(sr,sr',b,t)) \times cost_{elec}(sr')}{tRCO2(set1)} \quad (3.113)$$

Other relevant cost metrics calculated are BECCS total cost (including feedstock and CO_2 transport and storage costs) per MWh of electricity generated, $tcost_{MWh}$, CO_2 captured and stored, $tcost_{SCO2}$, and CO_2 removed, $tcost_{CO2}$:

$$tcost_{MWh}(set2time) = \frac{tcost(set2,a,time)}{\sum_{a=1}^{PL} EG_{PP}(sr,sr',b,t,a)} \tag{3.114}$$

$$tcost_{SCO2}(set2,a,time) = \frac{cost_{ha}(set2,a,time)}{\sum_{a=1}^{PL} SCO2_{ha}(sr,sr',b,t,a)} \tag{3.115}$$

$$tcost_{CO2}(set2,a,time) = \frac{cost_{ha}(set2,a,time)}{\sum_{a=1}^{PL} SCO2_{ha}(sr,sr',b,t,a)} \tag{3.116}$$

3.2.7 BECCS land balance

BECCS total land footprint is obtained by summing the biomass land footprint, LF_{SC}, with the power plant land footprint, LF_{PP}, based on the area of a 500 MW BECCS plant, $area_{PP}$, its lifetime, load factor and fuel flowrate:

$$LF_{SC}(sr,sr',b,t) = \frac{1}{tPellet(sr,sr',b,t)} \tag{3.117}$$

$$LF_{PP}(sr,b) = \frac{area_{PP}}{Loadf \times 8760 \times PL \times F_{fuel}(sr,b)} \tag{3.118}$$

$$LF(sr,sr',b,t) = LF_{SC}(sr,sr',b,t) + LF_{PP}(sr,b) \tag{3.119}$$

3.2.8 Key outputs for the optimisation framework

In order to solve the optimisation model, some key outputs of the value chain modelling framework are calculated per ton of CO_2 removed from the atmosphere, for each configuration $(set2',time)$:

- $Unit_{CO2}$ is the number of 500 MW units per ton of CO_2 removed.
- $SCO2_{CO2}$ is the amount of CO_2 captured and stored, in tCO_2/tCO_2 removed.
- WU_{CO2} is the total amount of water (blue, green and grey), in m^3/tCO_2 removed. In the case of biomass residues such as wheat straw, the blue water associated with straw production is allocated to the production of wheat, and therefore considered to be zero.
- MWU_{CO2} is the marginal amount of water (blue and grey), in m^3/tCO_2 removed.
- $LU_{SC,CO2}$ is the amount of land harvested for biomass at the field level, in ha/tCO_2. In the case of biomass residues such as wheat straw, the land footprint associated with straw production is allocated to the production of wheat, and therefore considered to be zero for straw.
- $LU_{PP,CO2}$ is the amount of land used by BECCS facilities, in ha/tCO_2 removed.

- EB_{CO2} is the amount of net electricity produced, accounting for the energy cost of BECCS value chain, in GJ/tCO_2 removed.
- $cost_{CO2}$ is BECCS total cost, in \$/tCO_2 removed.
- CB_{CO2} is BECCS total cost balance, including revenues from electricity generation, in \$/tCO_2 removed.
- PU_{CO2} is the amount of pellet used, in t/tCO_2 removed.
- BU_{CO2} is the amount of raw biomass used, in t/tCO_2 removed.
- $BioC(b)$ is the biomass carbon content in $\%_{\mathrm{DM}}$.
- $tRCO2$ is the cumulative net amount of CO_2 removed by a BECCS configuration, over its lifetime, per ton of biomass, in tCO_2/t. This metric is used to constrain the solution space to the carbon negative configurations.

These metrics are calculated with the following formule:

$$Unit_{CO2}(set1) = \frac{1}{RCO2_{hr}(set1) \times Loadf \times 8760} \tag{3.120}$$

$$SCO2_{CO2}(set1) = \frac{\sum_{a=1}^{PL} SCO2_{ha}(set2,a,time)}{tRCO2(set1)} \tag{3.121}$$

$$WU_{CO2}(set1) = \frac{WF(sr,sr',b,t)}{tRCO2(set1)} \tag{3.122}$$

$$MWU_{CO2}(set1) = \frac{MWF(sr,sr',b,t)}{tRCO2(set1)} \tag{3.123}$$

$$LU_{SC,CO2}(set1) = \frac{LF_{SC}(sr,sr',b,t)}{tRCO2(set1)} \tag{3.124}$$

$$LU_{PP,CO2}(set1) = \frac{LF_{PP}(sr,b)}{tRCO2(set1)} \tag{3.125}$$

$$LU_{CO2}(set1) = LU_{SC,CO2}(set1) + LU_{PP,CO2}(set1) \tag{3.126}$$

$$tEB_{CO2}(set1) = \frac{tEB(set1,time)}{tRCO2(set1)} \tag{3.127}$$

$$tcost_{CO2}(set1) = \frac{tcost(set1)}{tRCO2(set1)} \tag{3.128}$$

$$tCB_{CO2}(set1) = \frac{tCB(set1)}{tRCO2(set1)} \tag{3.129}$$

$$PU_{CO2}(set1) = \frac{1}{tRCO2(set1)} \tag{3.130}$$

$$BU_{CO2}(set1) = \frac{tYield(sr,b)}{tPellet(sr,sr',b,t) \times tRCO2(set1)} \tag{3.131}$$

3.3 BECCS deployment optimisation framework

3.3.1 Overview

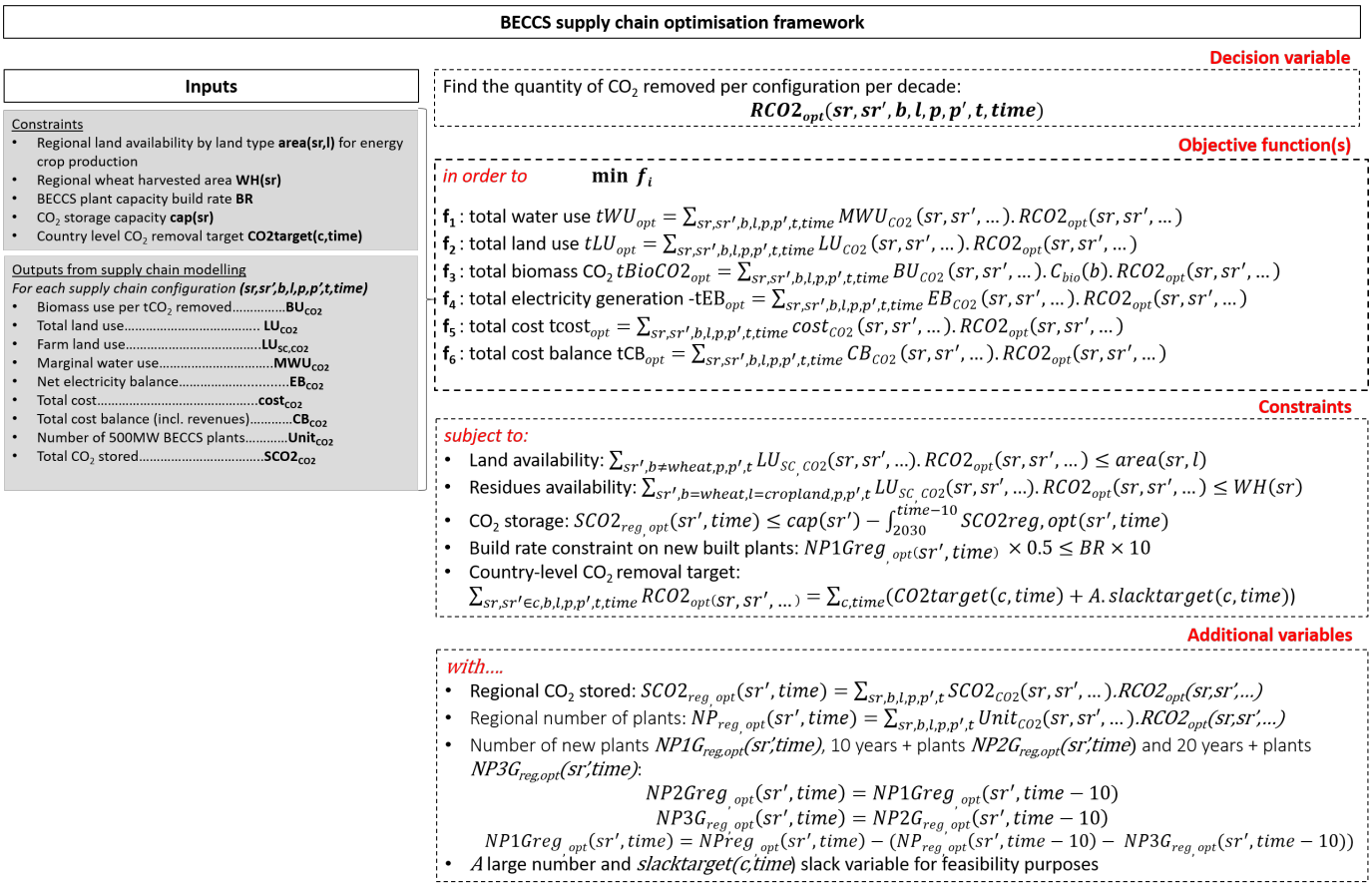


Figure 3.9: Overview of the BECCS deployment optimisation framework. Inputs per ton of CO_2 removed are pre-calculated by the supply chain model framework.

We assume perfect foresight in planning BECCS deployment between 2030 and 2100, *i.e.* all decades are solved simultaneously.

3.3.2 Objective functions

The purpose of this work is to determine the optimal BECCS value chain required to meet a regional and evolving CO_2 removal target, $CO2target$, by allocating the amount of CO_2 removed annually per configuration, $RCO2_{opt}$, while minimising or maximising different objective functions $[f_1, f_2, f_3, f_4, f_5, f_6]$:

- Minimisation of the total marginal water use, $tMWU_{opt}$, over the entire time horizon, $time$:

$$f_1 = tMWU_{opt} = \sum_{set1} MWU_{CO2}(set1) \times RCO2_{opt}(set1) \tag{3.132}$$

- Minimisation of total land use, tLU_{opt}, over the entire time horizon, $time$:

$$tLU_{opt} = \sum_{set1} LU_{CO2}(set1) + \times RCO2_{opt}(set1) \tag{3.133}$$

  Similarly to fresh water use, the cultivated land associated with the production of wheat straw is allocated to wheat production. Wheat straw land footprint at the field level is therefore not accounted for in the summation.
- Maximisation of the total CO_2 efficiency $t\eta_{CO2,opt}$, over the entire time horizon, $time$, *i.e.*, the ratio of the amount of CO_2 permanently removed $tRCO_{2,opt}$ to the amount of CO_2 stored in the biomass, $tBioCO2_{opt}$. The latter is directly related to the amount of biomass used:

$$f_3 = tBioCO2_{opt} = \sum_{set1} BU_{CO2}(set1) \times BioC(b) \times C_{C\rightarrow CO_2} \times RCO2_{opt}(set1) \tag{3.134}$$

$$tRCO2_{opt} = \sum_{set1} RCO2_{opt}(set1) \tag{3.135}$$

$$t\eta CO2_{opt} = \frac{tRCO2_{opt}}{tBioCO2_{opt}} \tag{3.136}$$

  As the total amount of CO_2 removed is fixed, maximising $t\eta CO2_{opt}$ is equivalent to minimising $tBioCO2_{opt}$. As $t\eta_{CO2}$ is an nonlinear variable, $tBioCO2_{opt}$ is thus minimised to ensure the linearity of the model. It is also worth noting that, minimising the total amount of CO_2 stored in the biomass is equivalent to minimising the total amount of biomass used.
- Maximisation of the net electricity produced, tEB_{opt}, by the BECCS value chain, over the entire time horizon, $time$:

$$f_4 = tEB_{opt} = \sum_{set1} tEB_{CO2}(set1) \times RCO2_{opt}(set1) \tag{3.137}$$

- Minimisation of the total cost, $tcost_{opt}$, of the BECCS value chain, over the entire time horizon, $time$:

$$f_5 = tcost_{opt} = \sum_{set1} tcost_{CO2}(set1) \times RCO2_{opt}(set1) \tag{3.138}$$

- Minimisation of the total cost balance, tCB_{opt}, including revenues from electricity generation, of the BECCS value chain, over the entire time horizon, $time$:

$$f_6 = tCB_{opt} = \sum_{set1} tCB_{CO2}(set1) \times RCO2_{opt}(set1) \tag{3.139}$$

The preference-based procedure of using a weighted sum of the different objectives as a unique objective function was not used here for two reasons. First, the inherent diversity of the different objectives – land use, water use, CO_2 efficiency and net energy produced – make them complex to convert into one single objective. Secondly we estimated that preference of one objective over the others will be highly region specific, and choosing these factors arbitrarily could therefore give irrelevant results as to BECCS optimal value chain. Therefore, in the first instance, we chose to treat each of these objectives separately, and leave the multi-criteria, multi-stakeholder problem for future work. Thus, we have formulated six distinct scenarios which allow us to perform a series of thought experiments across the BECCS value chain.

3.3.3 Constraints

These six optimisation scenarios are subject to the following constraints.

CO_2 removal target constraint

First, the total amount of CO_2 removed must be equal to the set CO_2 removal target:

$$tRCO2_{opt} = \sum_{c,time} (CO2Target(c,time) + slacktarget(c,time)) \tag{3.140}$$

An equality constraint was chosen over an inequality constraint in Equation 17, as an inequality constraint would lead to BECCS being deployed over the CO_2 removal target in the energy maximisation scenario. $slacktarget$ is the slack variable added to ensure that the model solves in all scenarios.

CO_2 negativity constraints

In order to avoid the model choosing carbon positive configurations (configurations which never reach carbon negativity) in combination with very carbon negative configurations, while still meeting the CO_2 removal target, the configurations considered must be carbon negative within a relevant time-frame, *i.e.*, the $tRCO2$ calculated in the modelling module must be positive:

$$tRCO2(set1) \geqslant 0 \tag{3.141}$$

This constrains the initial choice set of configurations.

As a further constraint, the amount of net CO_2 removed annually by the configuration, $tRCO2_{opt}$, which is the decision variable of the optimisation framework, must be positive:

$$tRCO2_{opt}(set1) \geqslant 0 \tag{3.142}$$

Energy positivity constraint

In the first instance, we also constrained the configurations to be selected by the optimisation model to be energy positive:

$$tEB(set1) \geqslant 50 \tag{3.143}$$

As electricity production is not the primary service delivered by BECCS, this constraint may be relaxed if the optimisation problem cannot solve.

Land availability constraint

The amount of land harvested in each region for dedicated energy crops is limited by the land availability $LA(sr,l)$ of land type l in sub-region sr:

$$\sum_{b \neq Wheat,p} LU_{SC,CO2}(set1) \times RCO2_{opt}(set1) \leqslant LA(sr,l) \tag{3.144}$$

Wheat harvested area constraint

Though no land footprint is attributed to wheat straw production, the amount of harvested land for wheat is each region is limited the wheat area availability $WA(sr)$ in sub-region sr:

$$\sum_{p} LU_{SC,CO2}(sr,sr',wheat,cropland,p,p',t,time) \times RCO2_{opt}(set1) \leqslant WA(sr) \tag{3.145}$$

CO_2 storage capacity constraint

Decadal regional storage $RegSCO2(sr',time)$ is limited by regional CO_2 storage capacity $cap(sr')$ and cumulative CO_2 stored in previous decades $CRegSCO2(sr',time)$:

$$SCO2_{opt,reg}(sr',time) = \sum_{sr,b,l,p,p',t} SCO2_{CO2}(set1) \times RCO2_{opt}(set1) \tag{3.146}$$

$$CSCO2_{opt,reg}(sr',time) = CSCO2_{opt,reg}(sr',time-1) + 10 \times SCO2_{opt,reg}(sr',time-1) \tag{3.147}$$

$$\sum_{sr,b,l,p,p',t} SCO2_{CO2}(set1) \times RCO2_{opt}(set1) \leqslant cap(sr') - CSCO2_{opt,reg}(sr',time) \tag{3.148}$$

Existing infrastructure constraint

Once a BECCS plant is built somewhere, we assume it has to be operated throughout it whole lifetime (no stranded assets). Sufficient CO_2 storage therefore needs to be

available for the lifetime operation of these installed plants. The total number of BECCS plants per region at any given decade is $NP_{opt,reg}(sr',time)$:

$$NP_{opt,reg}(sr',time) = \sum_{sr,b,l,p,p',t} Unit_{CO2}(set1) \times RCO2_{opt}(set1) \tag{3.149}$$

The age of the BECCS fleet is tracked by three variables: the number of first generation plants (10 years or younger) $NP1G_{opt,reg}(sr',time)$, second generation plants (between 10 and 20 years) $NP2G_{opt,reg}(sr',time)$ and third generations plants (20 years and older) $NP3G_{opt,reg}(sr',time)$. The third generation plants are retired after 30 years:

$$\begin{aligned} NP1G_{opt,reg}(sr',time) = NP_{opt,reg}(sr',time) - (NP_{opt,reg}(sr',time-1) \\ + NP3G_{opt,reg}(sr',time-1)) \end{aligned} \tag{3.150}$$

$$NP2G_{opt,reg}(sr',time) = NP1G_{opt,reg}(sr',time-1) \tag{3.151}$$

$$NP3G_{opt,reg}(sr',time) = NP2G_{opt,reg}(sr',time-1) \tag{3.152}$$

The number of new-built plants need to be positive or equal to zero:

$$NP1G_{opt,reg}(sr',time) gesqland 0 \tag{3.153}$$

Plant built rate constraint

A 1 GW/yr build rate capacity constraint, BR, is imposed on new-built (1G) 500 MW BECCS plants in each sub-region sr:

$$NP1G_{opt,reg}(sr',time) \times 0.5 \leqslant BR \times 10 \tag{3.154}$$

This is equivalent to having two 500 MW BECCS plants being built every year in each country (in Europe) or province/state (USA, India, China and Brazil), which is ambitious relative to historical build rates of renewable technologies [156].

To avoid changing a linear problem into a mixed-integer linear programming, the numbers of plants, $NPG_{opt,reg}$, $NP1G_{opt,reg}$, $NP2G_{opt,reg}$, $NP3G_{opt,reg}$, were implemented as continuous variables instead of integer variables. This means that small scale BECCS plants (*e.g.*, $<$ 100 MW) could be deployed as an outcome of the optimisation program, even though all BECCS plants are assumed to have the same power generation efficiency and levelised capital and operating costs per ton of CO_2 captured. Considering the uncertainty around the power generation efficiency and costs of large scale BECCS power plants, in the absence of existing demonstration projects, model tractability and low computation time (maintaining MONET as a LP) was chosen over the deployment of same-size BECCS plants.

3.3.4 Pareto-front analysis

The ε-Constraint method was used to quantitatively evaluate the trade-offs between the four objective functions. For each combination of objective functions, f_j and f_k, the following optimisation problem was solved:

$$\min \quad f_j \tag{3.155}$$
$$\text{s.t.} \quad f_k \leqslant \varepsilon_k^m \quad \forall k \neq j \tag{3.156}$$

with ε the upper bound vector $[\varepsilon_k^1, \varepsilon_k^2, ..., \varepsilon_k^m]$ linearly distributed between the lower and upper bounds of f_k, m being the number of points chosen for the purpose of this analysis.

3.3.5 Integrating alternative CO_2 removal methods in MONET

Owing to the separation, within MONET, of the modelling and optimisation framework, it is possible to include additional CO_2 removal methods in the optimisation framework, as long as their KPIs (*e.g.*, their cost, land use or water use per ton of CO_2 removed) are known. The KPIs of each CDR method, CDR, could be calculated as a function of a set of options, $set(CDR)$ in a separate modelling module. The optimisation module would then have for objective to calculate the amount of CO_2 removed by each method, CDR, under each configuration, $set(CDR)$, in each decade, $time$, in order to minimise a set of objective functions, subject to global (*e.g.*, land availability, regional CO_2 removal target) and CDR method-specific (*e.g.*, biomass availability for BECCS, renewable electricity availability for DACCS) constraints.

3.4 Data collection and curation

3.4.1 Type of data

As is evident from the foregoing description, this model requires a significant amount of input data. Thus, a key activity was the collection and statistical analysis of these data. The model input parameters are of several types:

- Energy data: all indirect energy data – chemicals, seeds and fuels embodied energy – and direct energy data – fuel LHV, energy for irrigation, transport fuel efficiency and drying systems characteristics.
- Carbon data: all indirect emission data – chemicals, seed and fuels carbon footprint – and direct emissions data – fuel and transport emission factors, N_2O model emission factors, gas global warming potential and land conversion factors.
- Crop data: the physical properties of each biomass type – composition, Cp, HHV – as well as farming data – yields over lifetime and in different regions, moisture content, lifetime and harvest rotation cycle, crop coefficients and calendar, chemical input rates, in-field operations fuel efficiencies and processing energy requirements.
- Climate data: precipitations, altitude, longitude, sunshine hours, wind speed, average low and high temperature and relative humidity for each region.
- Land type for direct and indirect land use change evaluation.
- Cost data: includes the unit cost of inputs, electricity and fuels, the capital and operating costs of infrastructure (pelleting plant, BECCS plant, CO_2 transport and storage), transport costs, labour costs and land rents.

Some input parameters have a great impact on all aspects of the supply chain. Yield for example is a key parameter. As all supply chain inputs during the growth stage are in a per hectare basis (land use effects, chemicals input, in-field operations), biomass productivity (or yield) in dry tons per hectare will directly impact the extent of these contributions per dry ton or GJ of biomass delivered at the power plant. Another example is biomass moisture content. It directly impacts drying energy requirement, but also all of the processing and transport stages whose energy requirements depend on the incoming wet biomass mass flow, and are finally converted in MJ/dry ton.
The values for these parameters are reported over a wide range in the literature. Miscanthus in Europe for example has been widely investigated, and productivity as low as 4 t_{DM}/ha [157] and as high as 60 t_{DM}/ha [158] have been reported. To capture this uncertainty in the model, a database gathering the 150 input parameters, and their value according to different sources, was developed. 50 input parameters were selected on the basis of their impact on the model, number of sources and scatter. Normalized data series length and scatter of these parameters are presented in figure 3.10.

As can be observed in Figure 3.10, it is important to acknowledge the level of variability in some of the input data, for example, the embodied energy and carbon footprint of chemicals, land conversion emission factors, yield values. This uncertainty associated with key input parameters can clearly lead to a wide range of model outcomes. In order to evaluate the uncertainty in these outcomes, the model was evaluated with the lower bound and upper bound of the selected parameters. If the data series contained more than five sources, and in order to avoid unlikely data (very extreme yield value for example), the lower bounds and upper bounds chosen were the 95% confidence interval bounds. To use the example of Miscanthus productivity in Europe, the range 15.6-22.1 was used instead of the 4-60 found in the literature. For parameters with less than five sources, minimum and maximum values were taken as the uncertainty bounds. Tables B.8 to B.3 in Appendix B gather the average value and range of uncertainty of each input parameter of the model.

3.4.2 Data source

Climate data

The location and data of climate stations were obtained from the software CLIMWAT [127], and were attributed to each sub-region. Figure 3.4 provides the location of these stations. Climate data recorded by the weather stations, such as monthly precipitation, average low and high temperature, relative humidity, sunshine hours, wind speed, monthly precipitation, as well as the location and altitude of the stations, were then read in the software CROPWAT [159].

Yield data

Yield data for different regions of the world were collected for each dedicated energy crop from the literature. When available, yield datasets with high regional discretisation were used [119, 160]. When the yield data of a sub-region sr was unknown, the yield of the sub-region with the closest climate conditions, according to the Koppen Climate Classification [161] was used. Wheat grain yield was obtained at the country level from the FAO [78]. Low, median and high yields of each biomass type are provided in Tables B.11, B.12 and B.13 in Appendix B. In this analysis, biomass yield and land type were considered as independent variables. Considering the embedded range of uncertainties in yield values considered for each biomass, with data obtained on both suitable land crops [162] and marginal lands [163], it was considered that this range already captured yield potential variability with land type. As no data was found on willow growth in regions other than North America and Europe, the study of willow was limited to these regions.

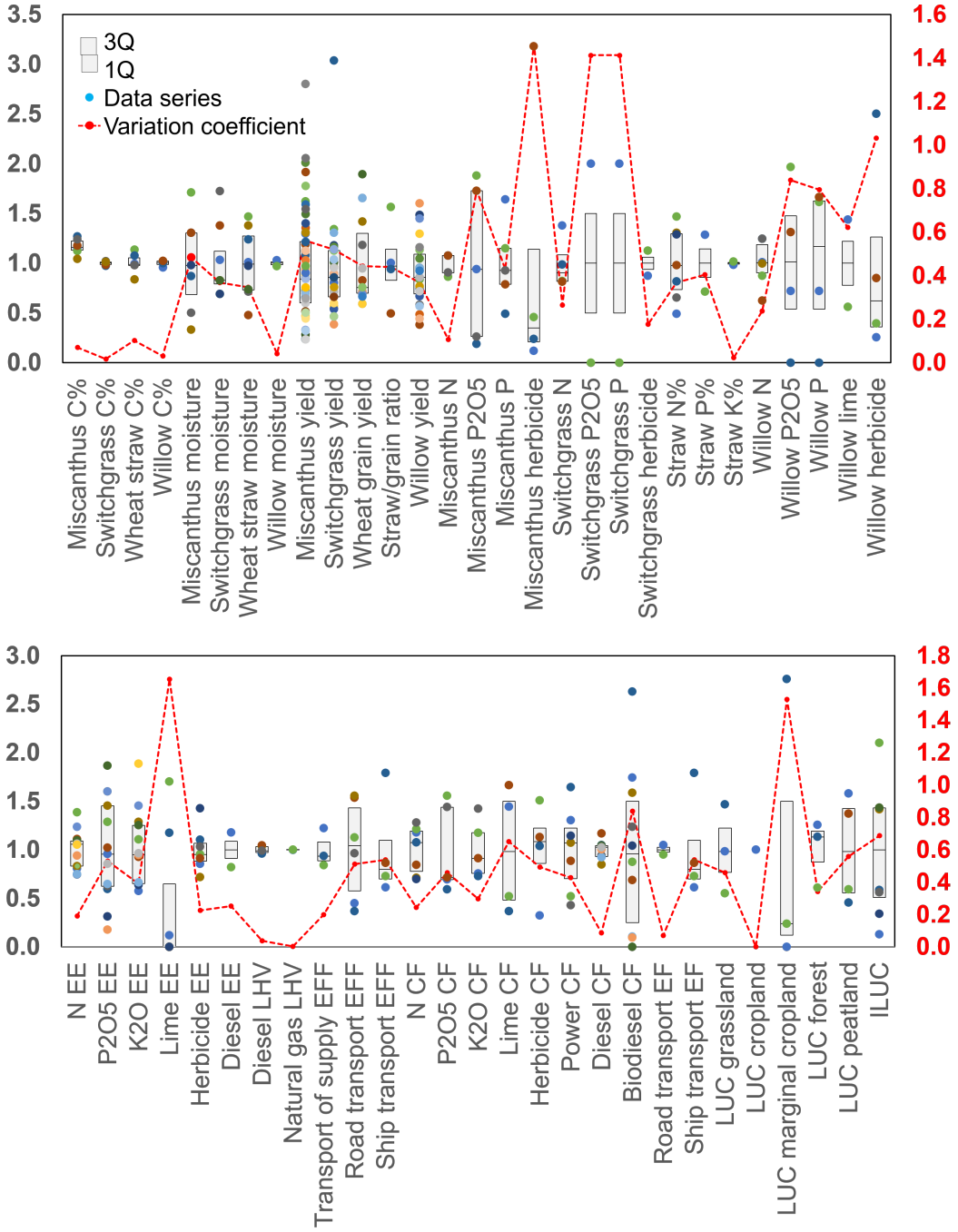


Figure 3.10: This figure presents the length and scatter of biomass(top) and GHG and energy (bottom) normalised data series of the 50 parameters selected for the model uncertainty evaluation. Biomass data include biomass carbon content, moisture content at harvest, and fertilizer and chemicals application rate. GHG and energy data include fertilizers, chemicals and fuel EE and CF, fuel LHV, transport fuel efficiency and emission factors, and LUC and ILUC conversion factors for different land types. Each circle in a data series corresponds to a value collected from the literature. Furnished series (Miscanthus yield) as opposed to scarce series (lime application rate), as well as scattered series (P_2O_5 application rate for Miscanthus), as opposed to unscattered series (straw potassium content) can be observed through the number and disposition of the circles relatively to the first and third quartiles. The variation coefficient is a last indication of scatter, with values over 1.5 for uncertain data such as LUC for marginal cropland or lime EE.

Land cover

In order to determine the total cropland, grassland and forest area available in each sub-region sr, the MODIS global land cover with a spatial resolution of 15 arc second geographic was used [164]. Tables B.14,B.15 and B.16 in Appendix B provide the land cover per cell adapted from the MODIS database. Forest area was calculated summing Evergreen/Deciduous Needleleaf/Broadleaf forests with the mixed forest categories. Grassland and cropland land cover were directly obtained from the land cover categories. As the use of cropland, grassland or forest, does not represent the base case of the analysis, but rather are exploratory scenarios where we consider the impact of land use change induced by BECCS, no slope or elevation constraint was considered.

Marginal land area

In order to use a consistent dataset for all regions, the marginal land dataset from the Cai *et al.* study was used in this work. As a conservative approach, and to be consistent with other literature sources, the lower bound values (Scenario 1 or "marginal mixed crop and vegetation land, part of abandoned land") from this study were considered [114]. Similarly to land cover and wheat harvested area, the 30 arc second resolution raster file was processed to obtain the marginal land area in each sub-region, sr. Data is supplied in Tables B.14,B.15 and B.16 in Appendix B. This marginal land dataset was used for the case study in Chapter 6.

Water stress

In the optimisation framework, no water availability constraint is considered. To account for potential water risk, the Overall Water Risk (OWR) factor developped by the AQUEDUCT Water risk Atlas, hosted by the World Resource Institute, was used to avoid bioenergy production in regions with high water stress [165]. The Overall Water risk index is a regional measure of both physical (water quantity and quality) and regulatory or reputational risks. The overall risk associated with the quantity of water available is assessed through the evaluation of baseline water stress, water stress variability (inter annual and seasonal), flood occurrence, drought severity, upstream storage and groundwater stress, while the quality of water is measured by upstream activity (*e.g.*, is the water available coming from a waste water stream or a protected land area). Regulatory risks are assessed through the density of media coverage on water issues in a particular region, the population's access to water, and the percentage of amphibian species classified as threatened, which is proxy to measure the fragility of a freshwater ecosystem. The overall water risk is computed by a weighted average of

all of these risks factors, with different weights as the function of the industry (69.7% for physical quantity, 9.1% for physical quality and 21.2% for regulatory risks across all sectors) [165]. This method results in a regional index between 0 and 5 (from low risk to extremely high risk). To avoid bioenergy production in regions with high water stress, a geospatial analysis was performed with the ARCGIS software to quantify the amount of set-aside land was available outside of high water stress regions (OWR$>$3, *i.e* high to very high water risk). A 30 arc geographic resolution map of set-aside land availability (Scenario 1 or "marginal mixed crop and vegetation land, part of abandoned land" in Cai *et al.* [114]) was intersected with a sub-basin level map of overall water risk [165], to determine the marginal land area per cell sr, outside of high water risk zones. The water stress constraint was only considered for the case study presented in Chapter 7.

Wheat harvested area

Wheat harvested area: in order to constrain the amount of wheat straw available per region, the map of the world wheat harvested area with a spatial resolution of 5 minute geographic, obtained from the SPAM model [166], was processed in ArcGIS [126] (Tables B.14,B.15 and B.16 in Appendix B). It is worth noting that the harvested area per cell can be greater than the cell size, in the case of multiple harvests per year.

Road tortuosity

The road distance was computed using euclidian distance, corrected by a tortuosity factor. Approximate tortuosity factors were computed for each sub-region sr, by dividing the road distance of the centroid to the nearest port, by the euclidian distance between these two points. Computed tortuosity factors are provided in Tables B.11, B.12 and B.13 in Appendix B.

Regionalisation of the cost data

All cost data was converted to 2018 US $ using dollars inflation rates and a euros to US dollars conversion rate of 0.85, a GBP to US dollars conversion rate of 1.42, and a INR (Indian Rupee) to US dollars of 0.014, a RMB (China Renminbi) to US dollars rate of 0.14, and a BRL (Brazil Real) to US dollars conversion rate of 0.30. Depending on the data availability, input data was added at the state level (US states, Chinese provinces, India states, Brazil states) or the country level (Brazil, China, EU countries, India, USA). When available, cost data was added at the state (*e.g.*, fuel and chemicals) were used. For some of the input parameters, when input data was only available for

the US, Purchasing Power Factors (PPF) were used to determine regional costs relative to those in the US. The input data for the cost model, as well further details on assumptions and sources, are gathered in Tables B.4, B.5, B.6, B.17, B.18 and B.19.

Global and regional CO_2 removal targets

Global CO_2 removal targets were taken from IAMC 1.5°C scenario explorer database [10], for IPCC 1.5°C representative scenarios P2, P3 and P4 [11] where negative emissions technologies other than afforestation are deployed: P2 (or SSP1), an optimistic scenario where BECCS deployment reaches 3.4 $GtCO_2/yr$ at the end of the century, P3 (or SSP2), a middle-of-the-road scenario where BECCS deployment reaches 12.4 $GtCO_2/yr$, and P4 (SSP5), a high energy demand fossil intensive scenarios, where BECCS deployment reaches 22.5 $GtCO_2/yr$. Deciding on a fair allocation of these global targets at the regional level depends on many factors, including past emissions, population, wealth, rate of emission reduction, *etc.* In this study, global targets were allocated based on absolute historical GHG emissions. Annual historic GHG emissions from 1850 to 2014 were collected for each country [167, 168]. Regional targets were then determined using the following formula:

$$CO2Target(c,time) = GTarget(time).\frac{Cum.GHGemissions(c)}{\sum_{c\ in\ World}\ Cum.GHGemissions(c)}$$
$$c\ in\ \{Brazil,\ China,\ EU,\ India,\ USA\} \quad (3.157)$$

To clarify, the regional target at a given year is exogenous, and does not change as a function of how much mitigation/removal is done in prior years. Furthermore, it was assumed that a regional CO_2 removal target is met where the CO_2 is physically stored and monitored. Table 3.1 summarises cumulative emissions per region and the computed regional share of global targets. As MONET only represents a subset of the world, annual CO_2 removal targets constraints considered in MONET are 58% – the sum of all individual shares based on a historical GHG emissions burden sharing of global targets – of the world annual CO_2 removal targets obtained from P2, P3 and P4 scenarios of the IPCC.

The CO_2 removal target is implemented as a step function in MONET. For each target scenario (P2 or P3), the values of the steps were adjusted so that the cumulative removal in MONET was equal to the cumulative removal in the IPCC scenario. Figure 3.11 represents the IPCC (full line) and the MONET (dotted line) CO_2 removal profiles.

Table 3.1: Regional cumulative GHG emissions and shares of global CO_2 removal targets in MONET

Regions	Cumulative GHG emissions 1850-2014 ($GtCO_2$)[a]	CO_2 removal target (% global target)
Brazil	122	4.3
China	336	11.9
EU	462	16.4
India	157	5.5
USA	571	20.2
Total MONET regions	1,647	58.3
Total World	2,826	100

[a]Historic GHG emissions from [167, 168]

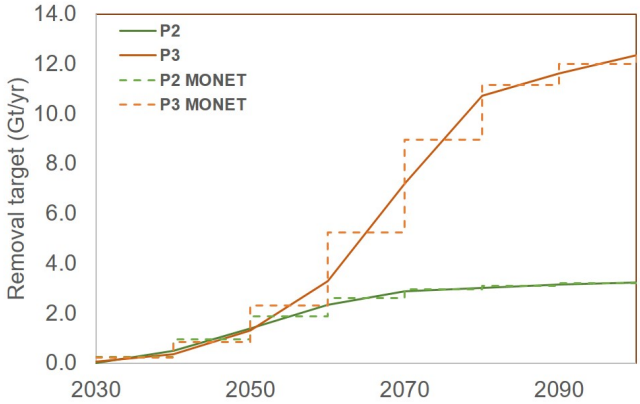


Figure 3.11: P2 and P3 CO_2 removal scenarios as in the IPCC (full line) and implemented in MONET (dotted line).

Based on these regional removal targets, it is possible to compute the algebraic difference between cost optimal regional removal – how much removal is done in the cost-optimal deployment – and regional removal targets. In this study, this is referred to as the CO_2 removal *surplus* – when positive – or *default* – when negative, and is calculated with the following formula:

$$CO_2RemovalSurplus/Deficit(c,time) = cRCO2_{opt}(c,time) - CO2Target(c,time) \tag{3.158}$$

where $cRCO2_{opt}$ is the optimal amount of CO_2 removal per region, and $CO2Target$ is the regional carbon dioxide removal target. When the regional surplus are non zero sum, the global target is not met.

BECCS cost data

Regional base year BECCS plants operating (O&M) and capital (CAPEX) costs were calculated from O&M costs and CAPEX of coal, coal + CCS and biomass plants data available in the International Energy Agency (IEA) 2018 World Energy outlook [169]. BECCS CAPEX was obtained by subtracting the CAPEX of a coal + CCS to that of coal plant, and adding this delta to that of a biomass plant. The same method was used to estimate BECCS operating cost. BECCS CAPEX reduction trends were computed from optimistic and pessimistic CAPEX reductions of biomass, coal, and coal CCS plants in 2020, 2040 and 2050, from the IEA World Energy Outlook [169]. To adopt a conservative approach, we assume that the CAPEX of these technologies in 2030 is what is referred as 'today's' CAPEX in the World Energy Outlook. The CAPEX in 2040 is then to be considered that in '2020' in the outlook, in 2050 that of '2030' and in 2060 that of '2040'. To further project the CAPEX of these technologies post-2060, we assume that CAPEX reductions follow the same rate as in the decade 2050-2060. BECCS CAPEX over time was then calculated from the CAPEX of the biomass, coal, and coal + CCS plants. Figure B.1 represents the CAPEX trends in both pessimistic and optimistic scenarios (shades), and the trend for the average CAPEX (lines), which was obtained from averaging the pessimistic and optimistic scenarios.

CO_2 storage

A BAU scenario and a high scenario were considered for the implementation of regional CO_2 storage capacity constraints in MONET:

- Brazil: To date, no national scale quantitative geological survey of Brazil. Only reliable quantitative estimates for the Campos basin, a depleted oil field, off the south-east coast of Brazil, which comprises 17 off-shore oil fields, with a total capacity of 950 $MtCO_2$ [170]. Based on geographic distribution, 16 of them (887.9 $MtCO_2$) were attributed to the the state of Rio de Janeiro, and one of them (61.3 $MtCO_2$) to the state of Espirito Santo, for modelling purposes. In the high scenario, an approximate CO_2 storage capacity quantification was performed using the methodology described in Wildenborg *et al.* [171], by multiplying each state basin area adapted from the Brazil geological survey [172] (adapated in ARCGIS) with a saline aquifer suitability probability of 50% and a CO_2 storage

density (or storage factor) of 0.2 $MtCO_2/km^2$. This new estimated CO_2 storage capacity was added to that of the Campos oil fields basin used in the BAU scenario.

- China: Data for the BAU and high scenarios was taken from a national scale geological survey, summing up CO_2 storage capacity in sedimentary basins (adapted from the US Geological survey [173]), in saline aquifers [117, 174] and in oil & gas fields [174]. CO_2 storage assessments data are provided in Tables B.21, B.22 and B.23.
- EU: Data for the BAU scenario was taken from the EU geocapacity geological survey [175], to the exception of the UK which was taken from the ETI UK CO_2stored database [176]. No alternative database was available for the optimistic scenario.
- India: To date, no national scale quantitative geological survey of India. In the high scenario, the same approach developed by Wildenborg *et al.* [171], and used for Brazil, was applied to sedimentary basin area in Indian states [177].
- USA: Data from the average and high CO_2 storage capacity scenarios in the US carbon storage ATLAS [178] were used for the BAU and high scenarios respectively.

CO_2 transport and storage cost

The cost of CO_2 transport, $cost_{CO2T,SCO2}$, was pre-calculated based on the capital and operating costs of a CO_2 transport pipeline, CAP_{CO2T}, with a 3 $MtCO_2/yr$ capacity, $Capa_{CO2T}$, 100k length, D_{CO2T}, a 20 years lifetime, LT_{CO2T}, and a 8% interest rate, IR_{CO2T} [140]:

$$cost_{CO2T,SCO2}(sr') = \frac{CAP_{CO2T}(sr') \times CRF_{CO2T} \times D_{CO2T}}{Capa_{CO2T}(sr')} + OP_{CO2T}(sr') \quad (3.159)$$

A cost of $5/$tCO_2$ was assumed in addition for CO_2 storage.

Cost of electricity

The cost of electricity in the industrial sector were used to calculate both the cost of using electricity at various stages of the biomass supply chain, and the revenues from generating electricity (as opposed to whole sale electricity prices, due their high volatility and low predictability). Data from the MME was used for Brazil [179], from the CEIC database for China [180], from the EUROSTAT database for the EU [181], from the Government of India for India [182], and for the EIA for the US [183].

3.5 Modelling and optimisation scenarios

3.5.1 Bioenergy availability: preventing land use change and water stress

In order to investigate BECCS economic-environmental impacts, three impact scenarios were considered in the optimisation framework:

- Impact I (or low impact): BECCS is only deployed via dedicated energy crops (DEC) grown on marginal land (MAL). Under this scenario, BECCS deployment does not cause land use change, and does not compete with other uses of agricultural residues (AR).
- Impact II (or average impact): BECCS is deployed via dedicated energy crops grown on marginal land and agricultural residues from cropland. BECCS economic-environmental impacts are limited to the use of agricultural residues.
- Impact III (or high impact): BECCS is deployed via dedicated energy crops from all land types, and agricultural residues from cropland. Under this scenario, BECCS deployment might compete with other markets and cause substantial land use change.

To evaluate the extent of land use change under each optimisation scenario, the variable $tLUC$ is calculated as the summation of all land types other than marginal land – *i.e.*, cropland, grassland and forest – used for the production of dedicated energy crops:

$$tLUC(time) = \sum_{sr,sr',b\neq wheat,l\neq MAL,p,p',t} LU_{SC,CO2}(set1,time) \times RCO2_{opt}(set1,time) \tag{3.160}$$

3.5.2 Supply chain assumptions

To capture the uncertainty and/or variability of some of the model input data, the MONET framework can be run under different data scenarios:

- Median scenario: the average values of all parameters are used for the calculations,
- Low scenario or 'Optimistic' scenario: values which minimise the water, land, CO_2 and energy intensities of BECCS value chain are used to perform the calculations. Lower bound values of the land use change emissions, biomass moisture content, carbon and energy intensities of chemicals and input products, fertiliser and chemical input rates, processing energy requirements, electricity carbon footprint, average power generation of the electricity are used. However, upper bound

values for biomass yield per region, biomass energy density and biomass carbon content are used.

- High scenario or 'Pessimistic' scenario: values which maximise the water, land, CO_2 and energy intensities of BECCS value chain are used to perform the calculations. Upper bound values of the land use change emissions, biomass moisture content, carbon and energy intensities of chemicals and input products, fertiliser and chemical input rates, processing energy requirements, electricity carbon footprint, average power generation of the electricity are used. However, lower values for biomass yield per region, energy density and carbon content are used.

To avoid including additional degrees of freedom to the model, no range of uncertainty or variability was implemented for marginal land availability, harvested wheat area, land cover, road tortuosity and climate data. Furthermore, owing to a lack of data describing inter-region and region-specific cost variation, all results in Chapter 7 were obtained by running MONET in a central cost scenario.

The following chapters 4, 5, 6, 7 use the MONET framework across different case studies to provide insights into the regional drivers of BECCS cost and sustainability.

Chapter 4

Carbon balance and resource efficiency of selected BECCS value chains

4.1 Introduction

4.1.1 Objectives of the chapter

This chapter explores the water-land-carbon nexus of BECCS to answer the following questions: 1) can BECCS deliver negative emissions? 2) in a relevant time frame, and 3) at a low resource cost. The purpose of this contribution is to present a spatially and temporally explicit, whole-systems assessment of selected BECCS value chains, accounting for the cultivation, harvesting, processing, transport, and conversion of biomass and the subsequent sequestration of the arising CO_2. We evaluate each distinct BECCS system on the basis of carbon, water, and land-use intensity, using the net removal of CO_2 from the atmosphere as a determining key performance indicator. This chapter is structured as follows. The remainder of this introduction gives an overview of existing biomass supply chain and BECCS water footprint modelling in the literature. Section 4.2 quantifies and qualifies the carbon, land and water footprint of selected biomass supply chains, and the resulting impact on the carbon, land, and water intensities of an integrated BECCS system. Finally, section 4.3 focuses on the dynamic accounting of GHG emissions over the system lifetime, on its sensitivities, and concludes with some perspectives on the implications for the potential of BECCS to result in the net removal of CO_2 from the atmosphere. Temporally, MONET is run under today's energy system. The impact of the decarbonisation of the energy sector is explored as alternative scenarios in section 4.3.3.

4.1.2 Bioenergy supply chain modelling in the literature

Before being combusted, biomass needs to be grown, harvested, processed (dried, densified for transport, *etc.*) and transported to the power plant. This results in substantial carbon costs, which will further decrease the CO_2 removal potential of a given BECCS project, on a whole-systems basis. Many studies have adopted various carbon accounting appoaches to determine biomass carbon footprint – direct and indirect CO_2 emissions to produce a ton of biomass. Bioenergy production has extended its potential feedstock from conventional cereal and oil crops, to cellulosic biomass, with both dedicated production and agriculture residues collection such as wheat straw [132, 184–186]. Among dedicated energy crops, perennial grasses and short rotation coppice have been extensively investigated. Both perennial grasses, miscanthus [119, 137, 157, 158, 187–200] and switchgrass [21, 56, 66, 184, 188, 192, 193, 201–208, 208–213] have been studied and compared at farming, processing or conversion level. Woody biomass such as short rotation willow has also been widely investigated for temperate climates [27, 150, 185, 193, 195, 214–219]. Studies based on transparent models with clearly outlined system boundaries, such as the Farm Energy Analysis tool (FEAT, [193]), the Biomass Emissions and Counterfactual (BEAC, [150]) and the Greenhouse Gases, Regulated Emissions, and Energy Use in Transportation Model (GREET, [220]) do exist. However, some studies only focus on a portion of the supply chain – adopting either a farm gate [193, 195, 217] or a power plant gate [137, 184, 221] perspective – and only a few include irrigation [199, 208] and drying [137, 184, 215]. Both processes could represent significant contributions in the biomass supply energy cost, and were included in this analysis. The extensive literature on the subject results in a high variability in carbon footprints and embodied energy values for a wide range of biomass. A detailed and transparent model of the entire BECCS value chain, including biomass conversion, with clear boundaries and assumptions, is required for the reliable evaluation of BECCS.

4.1.3 BECCS water footprint in the literature

The shift towards sustainable use of water in farming relies heavily on region-specific guidelines regarding crop irrigation need. One of the main methodologies is the blue, green and grey water footprint model developed by Hoesktra *et al.* [222]. Based partly on the crop evapotranspiration model developed by Allen *et al.* [141], this methodology enables the quantification of the water requirements of a given crop, based on the climate conditions (green water), ground and surface water local availability (blue water) and pollution (grey water) [142]. This methodology has been used to reliably determine the water footprint of a range of agricultural products [143, 223], including cellulosic biomass [224] and biofuels [225]. The water footprint of bioelectricity was also investigated [226], but did not include the power plant water requirement. Further, several studies have

focused on quantifying water use in the power generation sector [96, 220, 227]. Wu *et al.* developed a modelling framework to evaluate the blue water footprint as a function of cooling technologies, power plant type, and fuel, and included solid biomass as one of its case studies. Biomass upstream water requirement was however assumed to be met by rainfall, and biomass grey water footprint was not considered [220]. In order to evaluate BECCS overall water cost, both evaluations – biomass production and power generation water requirement – need to be integrated within the same framework.

4.2 The water-land-carbon nexus of BECCS

4.2.1 Case study

To capture the spatial dependence of BECCS value chain (*e.g.*, biomass productivity, climate, road and sea transport distance to the BECCS plant), we selected five regions of the world, associated with distinct climates, for this study: sub-tropical south-west Brazil (Sao-Paulo), continental temperate central China (Zhengzhou), temperate western Europe (Eindhoven), semi-arid northern India (Amritsar) and subtropical southern USA (Orlando). Table 4.1 presents the representative regions and specific cities used for the purpose of this case study.

Table 4.1: Regions and climates selected in the model

Country/Region	City	Climate
Brazil	Sao-Paulo	subtropical summer rainfalls
China	Zhengzhou	subcontinental temperate
Europe (Netherlands)	Eindhoven	oceanic temperate
India	Amritsar	semi-arid
The USA	Orlando (Florida)	subtropical summer rainfalls

4.2.2 BECCS water intensity

Validation of the water footprint model

We first validate the biomass water footprint model against existing water footprint evaluations in the literature. The evaluation of agriculture products water footprint has been carried out in the literature [143], and with a growing interest in biomass production, studies now also focus on modelling or measuring conventional and less-conventional biomass crops water footprints [211, 224, 228]. Studies however can differ

in input data (climate conditions, yield, fertilizer use, fertilizer leaching), boundaries (crop theoretical requirement, green and blue water footprints, grey footprint), and complexity of the model (water stress correction, soil water capacity and type). With these differences in mind, Table 4.2 compares model results within the literature. Overall results were found to be consistent with the sample of values selected from the literature.

Table 4.2: Water footprint model comparison with literature results

Crop, region[source]	Boundaries	Literature data	Model
Miscanthus, Netherlands [224]	CWR (m^3/t_{DM})	334	175-248 (205)[a]
Miscanthus, Florida [211]	GnWF + BWF (m^3/t_{WM})	330-495 (413)	289-373 (321)[b]
Switchgrass, Oklahoma [228]	CWR (mm/year)	521-786 (654)	414[c]-693[d]
Willow [195]	CWR (mm/year)	100-1790 (698)	628[c]-1034[d]
Wheat [223]	GnWF (m^3/t_{WM})	1277	728[c]-1712[d]
Wheat [223]	BWF (m^3/t_{WM})	342	255[c]-530[d]
Wheat [223]	GyWF (m^3/t_{WM})	207	62[c]-262[d]

[a]Model lower bound - upper bound (average) results for Europe, Netherlands.

[b]Model lower bound - upper bound (average) results for USA, Florida.

[c]Model average result for Europe, Netherlands.

[d]Model average result for USA, Florida.

The water use of the BECCS plant in MONET is derived from the IECM software [62]. Due to the lack of BECCS water footprint evaluation in the literature, we compare the water use of a coal fired power plant with a wet cooling tower and no CCS (base case) in IECM with the literature. Table 4.3 presents both water withdrawal and consumption values, and IECM results for this base case were found to be consistent with the literature.

Table 4.3: Comparison of IECM water intensity calculations with literature for a pulverized coal power plant with a wet cooling tower and no CCS

Source	Water withdrawal (m^3/MWh)	Water consumption (m^3/MWh)
IECM	2.4	1.5
Wu *et al.*, 2011 [220]	1.7-4.5	1.5-3.9
IEAGHG, 2013 [229]		1.2-1.9

Biomass water footprint

We begin with an evaluation of the blue and grey water footprint evaluation of each crop grown in each region – or more accurately in each climate. Blue and grey water footprints are presented in Figure 4.1. We consider wheat straw as a residues, thus with a zero blue and green water footprint at the farm level. The water footprint of wheat is represented here to compare the water footprint of energy crops with that of conventional crops. Energy dedicated crops water requirements per hectare were found to be higher on average than that of wheat: 830 mm/ha for miscanthus against 530 mm/ha for wheat. This is consistent with the BECCS water footprint analysis presented by Smith *et al.*, and can be explained in the difference in crop calendars and coefficients [36]. However, as pointed out by Smith *et al.*, this tendency changes when water footprints are expressed on a mass basis, due to the higher yield of energy dedicated crops as compared to that of conventional crops. Because of their low fertilizer input (impacts the grey water footprint) and relatively high yield, herbaceous biomass like miscanthus and switchgrass are thus found to be more sustainable water wise than conventional crops.

Among energy dedicated crops, SRC willow water footprint was found to be slightly higher than that of switchgrass and miscanthus, which is mainly due to willow lower yield per hectare. However, the feasibility of irrigating and fertilizing SRC willow by waste water has been investigated in Sweden [230, 231], which could considerably lower both grey and blue water footprints.

Energy dedicated crops are also characterized by a wider uncertainty range, relative to conventional crops. The difference lies in the greater uncertainty in input data (fertilizer use and yield) for the latter crops, derived from local experiments or simulations, as opposed to wheat data extracted from national or regional scales database on actual fertilizer use [232] and yield [78]. Switchgrass crop coefficients for example were not available in the literature, and, as suggested by Yimam *et al.*, coefficients of Sudan grasses [141], the closest species in terms of growth, were used [228].

Figure 4.1 shows the blue and grey water contributions in the growth of miscanthus, switchgrass, wheat, willow. The results are presented on a m^3/t_{DM} harvested crop basis.

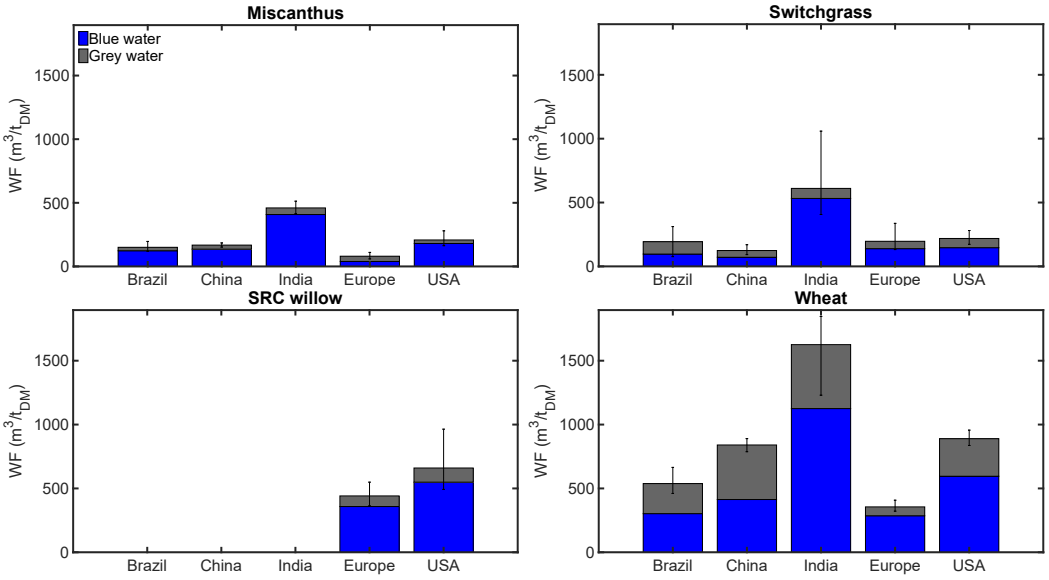


Figure 4.1: Blue and grey water footprints of four crops in different regions. Yield and nitrogen inputs are key contributors to the blue and grey water footprints which explains the poor performance of wheat relatively to perennial grasses, and to smaller extent willow. Water footprints are highly dependent on biomass type and regions, and all the more uncertain for energy dedicated crops.

BECCS net water use

We then quantify the water intensity of a BECCS plant, first without accounting for biomass water footprint, and represent the variation of the water intensity of a coal + CCS system with biomass co-firing proportion and CCS capture rate (figure 4.2).

It is observed in Figure 4.2 that co-firing and capture rate increases the water intensity, as such a system is likely to be less efficient, hence to burn more fuel per MWh of power generated, and therefore need more cooling water.

In a second instance, Figure 4.3 displays the water intensity of the power plant (in grey), and including the supply chain (in blue, yellow, red), within biomass water footprint uncertainty range. Wheat straw water footprint was considered to be zero, since all water withdrawal during biomass growth was allocated to wheat production.

It can be observed that the water footprint of the biomass supply chain far outweighs that of the actual power plant. At 90% co-firing and 100% biomass firing, water intensity can be up to 150 times higher when including biomass production water cost in the case of willow. This highlights the importance of performing a whole-systems assessment of any given BECCS option in order to ensure its sustainability, and of including water footprint in this assessment. This does not undermine, however, the importance of

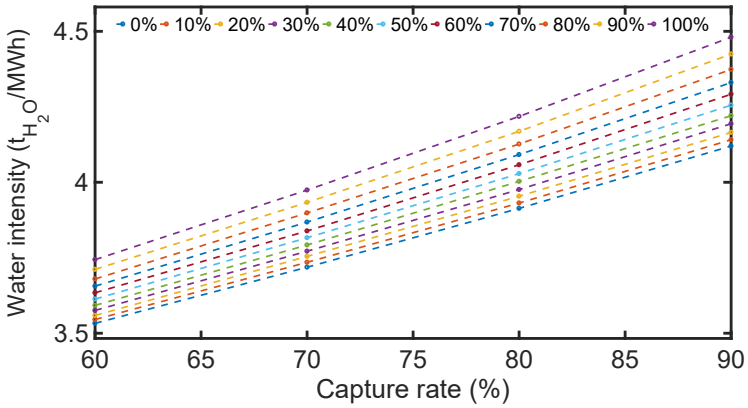


Figure 4.2: 500 MW supercritical coal-miscanthus pellets fired power plant water intensity as a function of capture and for different co-firing proportions. In a first instance, water withdrawal increases with capture rate, as steam is extracted from the steam cycle and used in the capture unit. To a smaller extent, water use increases with co-firing as a decrease in the fuel HHV increases the fuel flowrate required to generate the same amount of power.

reducing the cooling water intensity of power plants, which is already problematic, and likely to worsen, in certain areas with low water availability [58].

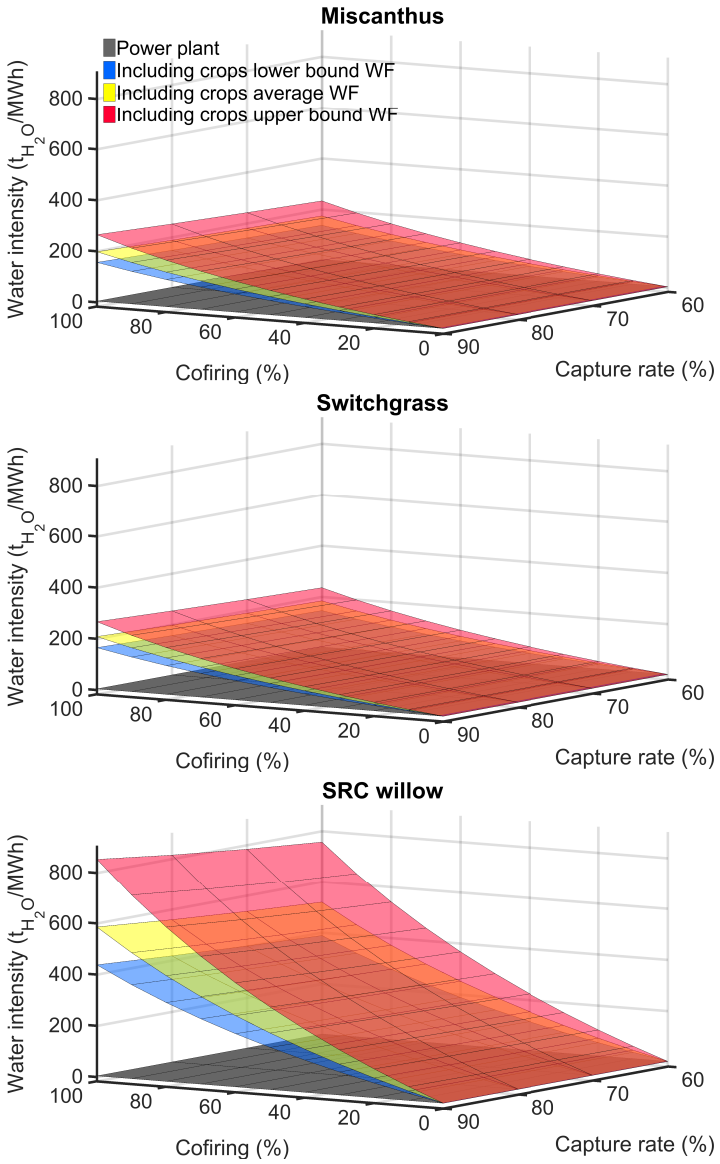


Figure 4.3: 500 MW supercritical coal - US miscanthus, switchgrass and willow pellets fired power plant water intensity as a function of capture rate and co-firing proportion, with and without supply chain. Biomass water footprint impact on the power plant water intensity is two orders of magnitude greater than that of the power plant cooling requirement.

4.2.3 BECCS carbon intensity

Validation of the carbon footprint model

The biomass carbon footprint model was first validated against existing evaluations from the literature in Table 4.4, evaluating the model under the same conditions (transport distance, region if possible, process included, *etc.*). Table 4.4 shows the great diversity in the results found in the literature, with field-to-plant carbon footprints found between 90 and 600 kg_{CO_2}/t_{DM}. To compare the model with each study, we quantified the carbon footprints obtained with the same supply chain structure used in the study (as detailed in the footnotes). With an average relative error between the model mean values and the literature results under 30%, and considering the results uncertainty range, the model results were considered consistent with the literature.

Table 4.4: Carbon footprint model comparison with literature results

Crop, region[source]	Units	Results	Model
Miscanthus, Germany [199]	kg_{CO_2}/t_{DM}	111.8	97-237 (152)[a]
Miscanthus, Ireland [137]	kg_{CO_2}/GJ_{HHV}	20.6	9.8-20.9 (14.5)[b]
Switchgrass, US [208]	kg_{CO_2}/t_{DM}	191-204	92-274 (162)[c]
Switchgrass, US [201]	kg_{CO_2}/t_{DM}	144.7-146.7	72-246 (139)[d]
Switchgrass, US [193]	kg_{CO_2}/t_{DM}	172	72-246 (139)[d]
Switchgrass, US [139]	kg_{CO_2}/t_{DM}	195-198	95-284 (168)[e]
Willow, UK-US [150]	kg_{CO_2}/GJ_e	118-242	147-396 [f]
Willow, average [193]	kg_{CO_2}/t_{DM}	89	87-253 (153)[d]
Wood pellets, Australia and Russia [215]	kg_{CO_2}/t_{DM}	143-594	166-603 (306)[g]
Wheat straw, UK [218]	kg_{CO_2}/GJ_e	66	26-53 (38)[h]

[a]Model lower bound - upper bound (average) results for Europe, production (bale), 100k transport, chopping and milling for combustion.

[b]Model lower bound - upper bound (average) results for Europe, production (bale) no irrigation, 100k transport, drying and pelleting.

[c]Model lower bound - upper bound (average) results for the US, production (bale or chopped).

[d]Model lower bound - upper bound (average) results for the US, production only no irrigation.

[e]Model lower bound - upper bound (average) results for US, production only no irrigation, 40k transport.

[f]Model lower bound (av. grassland) - upper bound (av. forest) results for Europe, production, LUC, no irrigation, processing, 25-75k transport.

[g]Model lower bound - upper bound (Europe-US) results, production, drying (50%), pelleting and transport.

[h]Model lower bound - upper bound (average) results for Europe, collection (bale), 40k transport, grinding.

Biomass carbon footprint without land use changes

We then evaluate the carbon footprint of selected BECCS configurations. Carbon footprints of different feedstock from different regions are presented in figure 4.4.

The addition of N_2O emissions, which have a large weight in the overall balance, underlines the double effect of fertilizers, both from their energy and carbon intensive production process, and from the subsequent emissions they cause after their application to the field. Biomass processing also has a higher weight in the carbon balance because of the relatively high electricity carbon intensity values chosen for this case study – 470-800 $kgCO_2$-eq/MWh [233, 234]. This input is highly dependent on the power source and region, and could be significantly improved in the context of a decarbonised electricity system.. Drying for high moisture biomass such as willow still

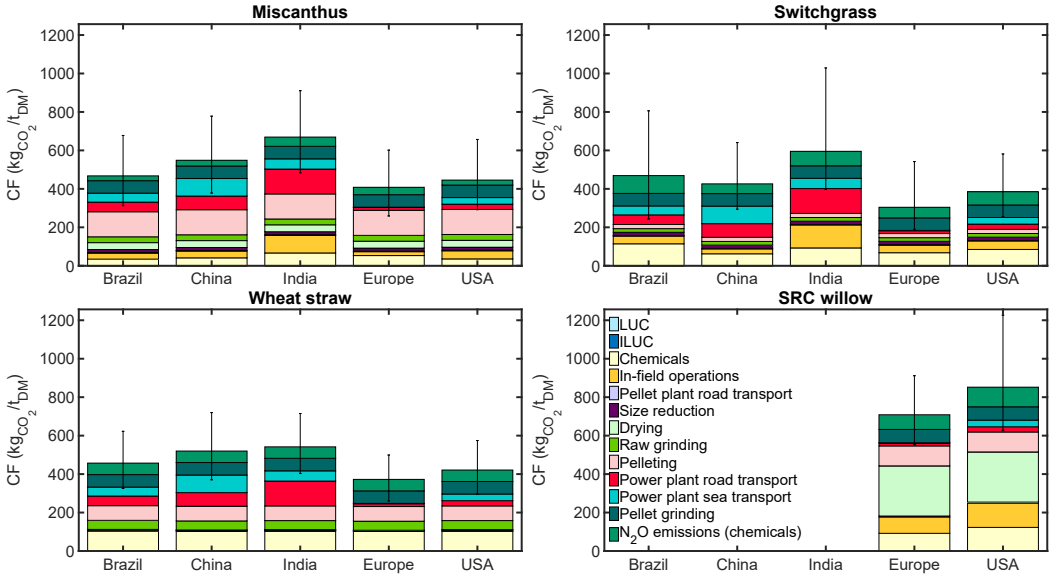


Figure 4.4: Carbon footprint of pellets from different regions without accounting for land use. In addition to road transport and drying, chemical application also represents a large portion of biomass carbon footprint, with a contribution from both chemical production and resulting N_2O emissions after application.

constitutes an important contribution. Aside from management practices like natural open-field or storage drying, this cost could be reduced by substituting natural gas with biomass in rotary dryers [215, 235]. These options are further investigated in section 4.3.

Effect of direct and indirect land use changes This study provides an evaluation of the potential impact direct and indirect land use change effects would have on the system. Net displacement and emission factors were considered the same for all managed land types (grassland or cropland), biomass types and regions. This is a first estimation to give indications as to the potential impact of including land use change. Applying this analysis to a certain case study in order to provide precise insight for a given region would require the use of region specific coefficients.

In can be observed from Figure 4.5 that direct and indirect land use changes have a substantial impact on the supply chain. When adding indirect land use change both the overall carbon footprint and uncertainty is up to three times higher than in the base case. It is important to note that as conversion factors are expressed on a per hectare basis, their impact is all the more important for lower yield biomass such as willow.

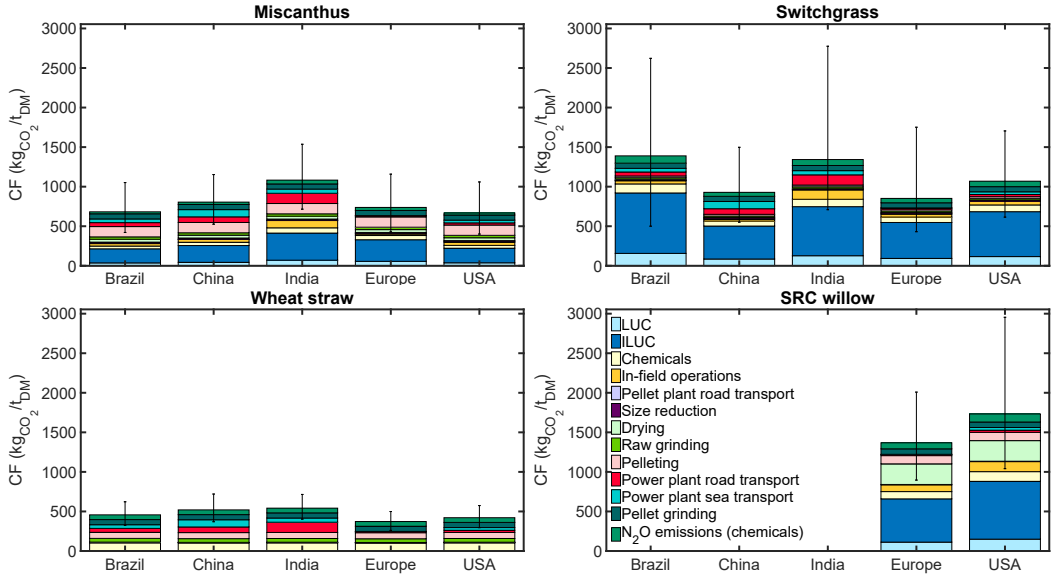


Figure 4.5: Carbon footprint of pellets from different regions, including both direct and indirect land use change effects (cropland). Other contributions are minor when compared to indirect land use change effects, which increase biomass carbon footprint value and uncertainty range by over 100%. Straw as a residue is not impacted by land use change, and is represented here to emphasise the impact of land use changes.

4.2.4 BECCS net carbon intensity

Figure 4.6 shows the evolution of the carbon intensity of a BECCS plant, first without considering the carbon footprint of the biomass feedstock.

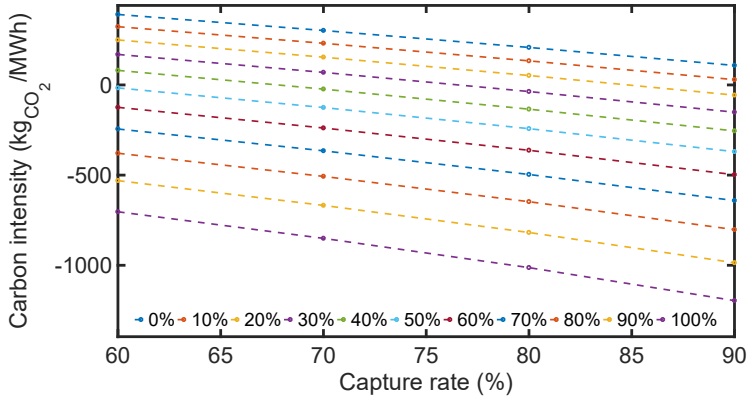


Figure 4.6: 500 MW supercritical coal-miscanthus pellets fired power plant carbon intensity as a function of capture and for different co-firing proportions. Naturally, increasing capture rate and biomass co-firing proportion both decrease the power plant carbon intensity.

As illustrated in Figure 4.6, carbon intensity decreases as coal gets displaced by biomass and carbon capture rate decreases. We then evaluate the impact of considering biomass supply chain emissions in the power plant carbon intensity. BECCS net carbon intensities as a function of biomass co-firing proportion and capture rate with and without land use changes are presented in Figures 4.7 and 4.8.

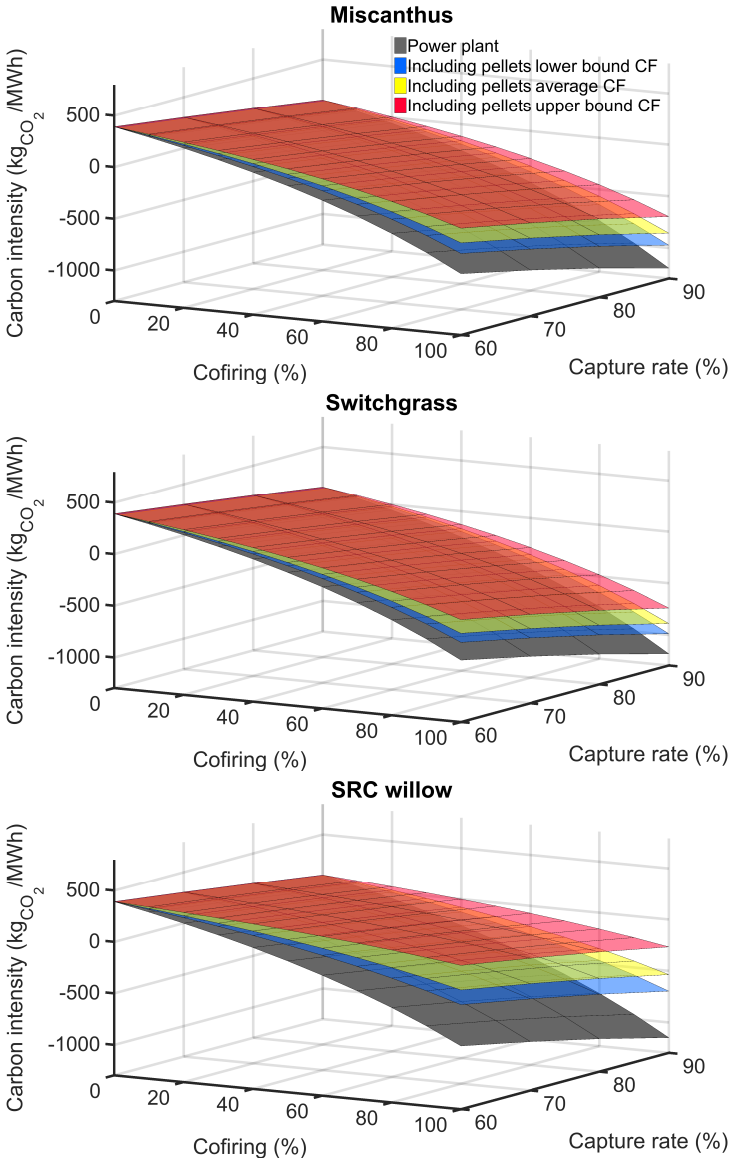


Figure 4.7: 500 MW supercritical coal - US biomass pellets fired power plant carbon intensity as a function of capture rate and co-firing proportion. Adding biomass supply chain emission can offset the power plant carbon negativity, which increase the minimum co-firing and capture rate values for the power plant to be carbon negative, hence decreasing its flexibility.

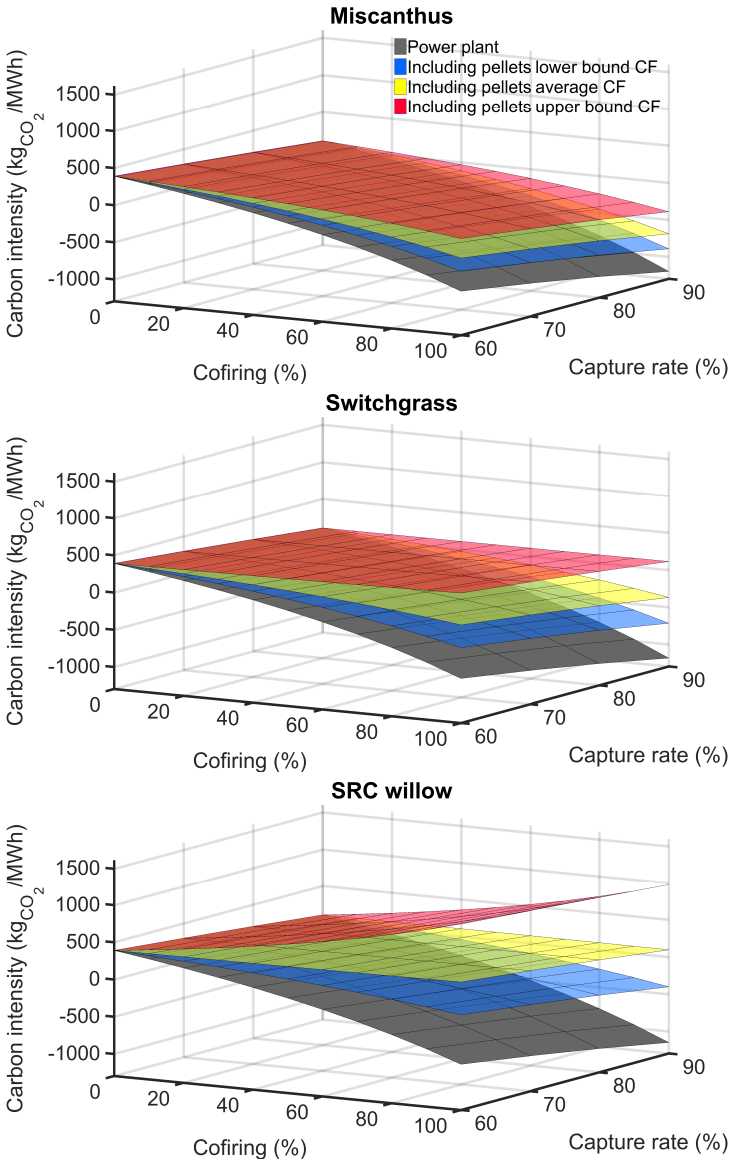


Figure 4.8: 500 MW supercritical coal - US biomass pellets fired power plant carbon intensity as a function of capture rate and co-firing proportion. The offset effect is exacerbated with indirect land use changes: BECCS systems do not reach carbon negativity in the upper bound scenarios.

As can be observed from Figures 4.7 and 4.8, whilst the majority of scenarios result in the net removal of CO_2 from the atmosphere, no two scenarios achieve an equivalent amount of net CO_2 removal. Importantly, it can be observed that some scenarios, such those relying upon willow in Figure 4.8, appear to be net carbon positive, resulting

in the net emission of up to 1,200 kg_{CO_2}/MWh. For comparison, an unabated coal-fired power plant might emit between 700 and 1,000 kg_{CO_2}/MWh. Thus, if the wrong choices are made throughout the supply chain, BECCS could indeed be substantially more carbon intense than an unabated coal-fired power plant. This is one of the core results of this study. At 90% capture rate, a willow-based BECCS system is, in the mean scenario, carbon negative within the 20%-100% co-firing range with no land use changes, carbon negative within the 30%-100% co-firing range with LUC, and always carbon positive with ILUC. In practical terms, this narrows the feasible range of a power plant operability – capture rate and co-firing proportion – for the system to be carbon negative, and ultimately decreases its flexibility. However, it is important to notice that BECCS systems including ILUC can still be carbon negative in the average scenario, within the 30%-100% co-firing range for a miscanthus-based system, and 40%-100% for a switchgrass-based system, at 90% capture rate. Limiting indirect land use changes effects as well as assuring high yield and low fuel, power and chemical input during biomass production will be capital for BECCS overall balance to be negative.

4.2.5 BECCS net carbon efficiency

If BECCS were a perfect system, one ton of CO_2 captured biologically would equate one ton of CO_2 sequestered geologically. However, this is not the case, and GHG direct and indirect emissions throughout the BECCS value chain carbon, as well as biomass dry mass loss, must be considered as this "carbon leakage" will decrease the net amount of CO_2 removed from the atmosphere. From this perspective, the notion of carbon efficiency can be considered: how many tons of CO_2 must be sequestered biologically in order to store 1 ton of CO_2 geologically? The carbon efficiencies of a switchgrass-based system from a marginal land and a central grassland are represented by Figure 4.9.

At can be observed in Figure 4.9, BECCS carbon efficiency reduces from 62% (marginal land) to 46% (grassland) when adding LUC and ILUC, with the latter accounting for over 26% of the carbon leakage. Upon adding land use changes, the facility is thus no longer carbon negative. This emphasises the fact that though efforts throughout BECCS supply chain must be made to reduce further carbon leakages (chemicals, transport, carbon capture), a better understanding and control of land use changes will be necessary to maximise BECCS carbon efficiency.

We have demonstrated the importance of including the biomass supply chain in the evaluation of the thermo- and hydrodynamic efficiencies, and carbon intensity of the overall system. Chemicals, road transport, drying and grinding were identified as important leakages in BECCS efficiencies, though negligible when compared to land use change effects. In the next section, a dynamic accounting of the GHG emissions is performed to evaluate BECCS efficiency at removing CO_2 from a time perspective.

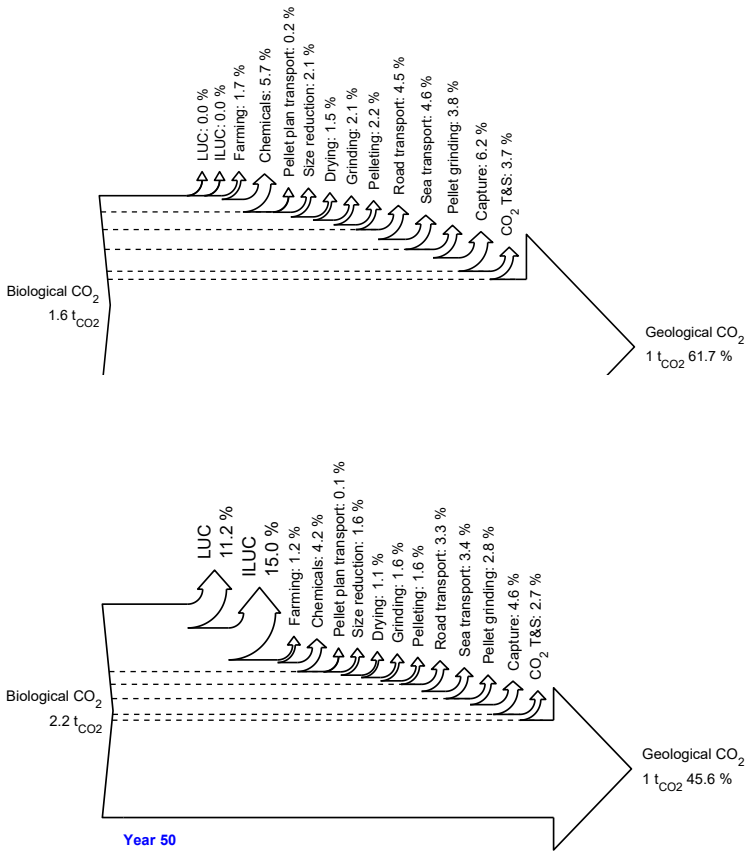


Figure 4.9: Carbon efficiency diagram of the carbon flux in a US switchgrass-based BECCS system from the biological storage in the biomass to the geological storage, with (bottom) and without (top) land use changes. In this case, accounting for land use change leads to a carbon positive system. Even with decreasing the carbon leakages resulting from the use of chemicals and biomass transport (about 11% of the losses), a substantial improvement to BECCS carbon efficiency will only be possible by limiting direct and indirect land use changes.

4.3 BECCS dynamic GHG emissions profile

We define the number of years required for the power plant cumulative emissions to reach zero as the biomass carbon breakeven time. To assess BECCS sustainability from a plant lifetime perspective and evaluate BECCS carbon breakeven time, a dynamic carbon balance was performed on the system.

4.3.1 Single dynamic balance

In this model, the land is cleared and the crop established at year 1, thus generating an initial carbon debt. The crop is harvested every n years, and therefore further biomass

processing, transport and capture is accounted for until the end-of-life for that crop in year 1+ N which is the crop end of life. As the land use change was considered to be amortised over a 50 year period, the dynamic carbon balance was performed oer 50 years. Figure 4.10 shows CO_2 cumulative emissions from a miscanthus fired BECCS power plant, from land conversion (year 1) to the power plant end of life (year 50).

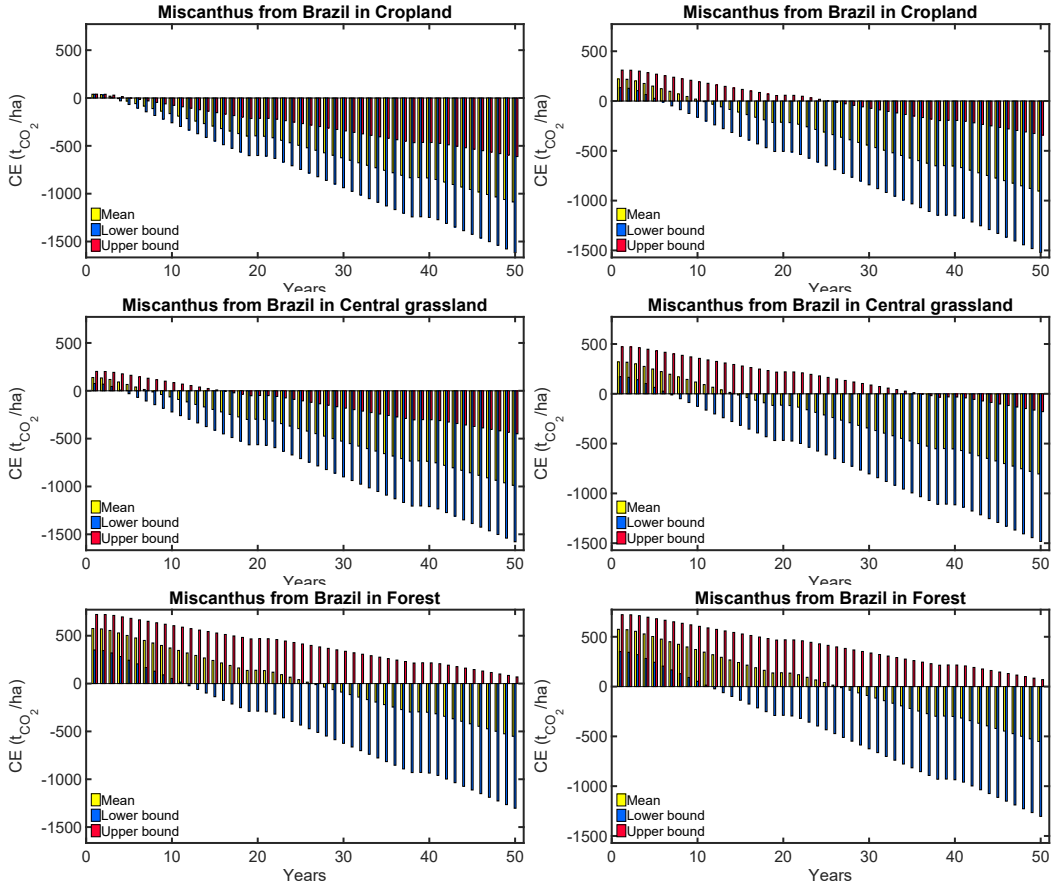


Figure 4.10: Miscanthus-based BECCS cumulative emissions in tCO_2/ha over 50 years for different land types including LUC (left) and ILUC (right). The system breakeven time increases from 1 to 26 years with direct land use changes. Miscanthus-based BECCS presents carbon positive scenarios before year 50 within the increased uncertainty range. Upon adding indirect land use changes, the system average breakeven time on a managed land increases by 7 years.

Miscanthus imported from Brazil breaks even after 3, 7 and 26 years, if grown on a cropland, central grassland and forest, respectively. When grown on a Brazilian forest, miscanthus is the only crop reaching carbon break even time before year 50. When including indirect land use changes effects for cropland and grassland in Figure 4.10, carbon breakeven time increases by seven years for cropland and grassland.

4.3.2 Multiple dynamic balances

Rather than simply representing average, lower bound and upper bound scenarios, it is important to evaluate the whole scope of BECCS outcomes. Four case studies were selected for this analysis:

1. Case A : Miscanthus from Brazil on marginal land (no LUC and ILUC),
2. Case B : Miscanthus from Brazil on central grassland (LUC and ILUC),
3. Case C : Willow from Europe on marginal land (no LUC and ILUC),
4. Case D : Willow from Europe on central grassland (LUC and ILUC).

Figure 4.11 represents the 729 outcomes when evaluating the model with the low, average and high values of biomass moisture content, carbon content, electricity carbon footprint, LUC conversion factor and ILUC conversion factors in those four case studies.

We can note from this analysis the diversity of possible outcomes, associated with a BECCS facility, as a function of the decisions made along the supply chain. In the case of miscanthus, which showed the lowest carbon footprint in the steady-state analysis, all scenarios are carbon negative over 50 years on a marginal land, with a carbon negative potential ranging from 0.7 to 1.6 ktCO_2/ha captured over 50 years. When including land use effects, the number of scenarios leading to a capture potential greater that 0.5 kt/ha was reduced to 648 out of 729, but no scenario led to a dynamic carbon positive balance. For the willow case study, which showed higher carbon footprints on a steady-state basis, the dynamic carbon balance was always negative on a marginal land, with a carbon capture potential ranging from 190 to 390 t/ha over 50 years. On a grassland however, the number of carbon negative scenarios dropped to 223. In terms of carbon breakeven time, without land use effects, the time required for BECCS to be negative varied on average between 1 year for miscanthus, to 3 years for willow. This became on average 15 times longer for miscanthus and willow when including land use changes. These results are presented in Table 4.5.

Table 4.5: Case studies dynamic GHG balance results repartition

Outcomes	Units	A	B	C	D
Positive scenarios		0	0	0	**460**
Negative scenarios		729	729	729	269
CO_2 removed	Mean *t/ha*	-1124	-805	-288	31
	Min *t/ha*	-1600	-1429	-392	-222
	Max *t/ha*	-718	-248	-186	285
Breakeven time	Mean *years*	1	15	3	46
	Min *years*	1	6	3	22
	Max *years*	2	32	3	**>50**

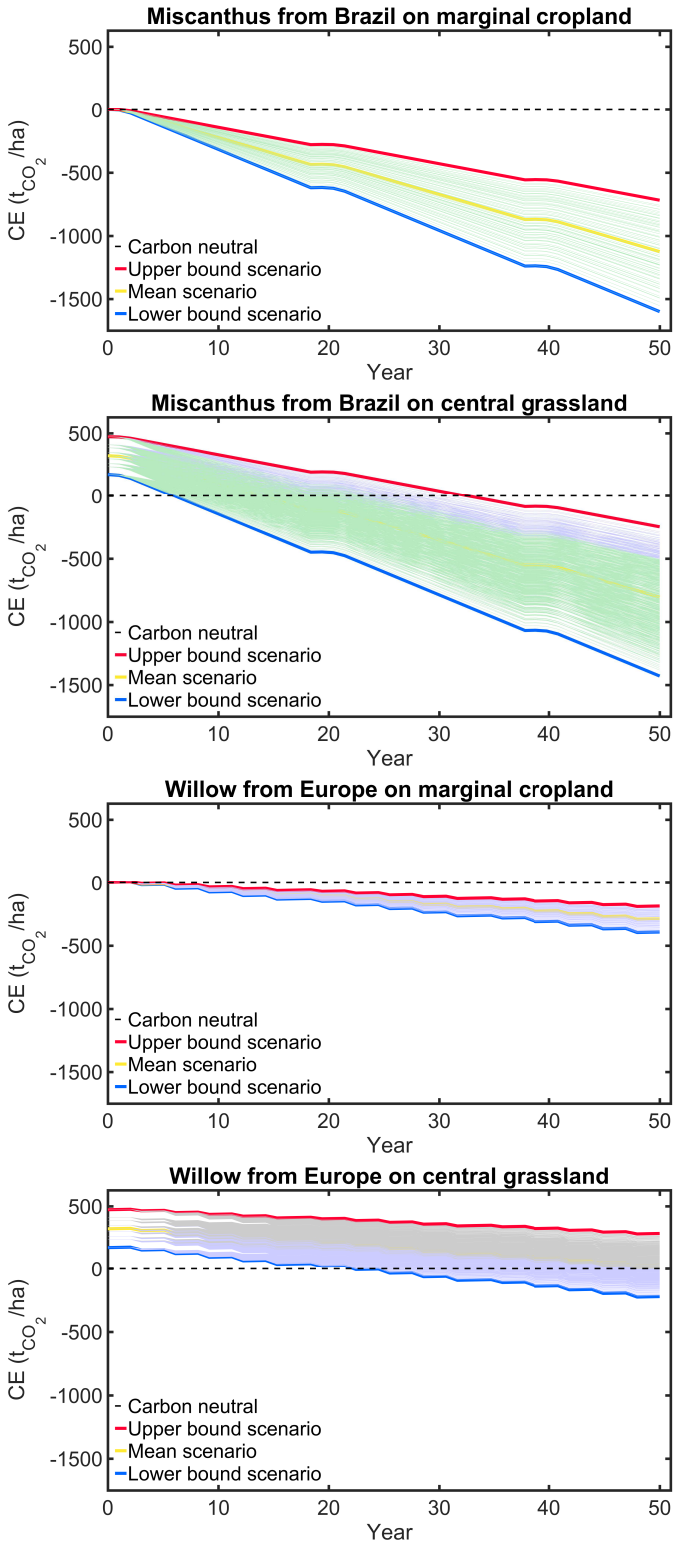


Figure 4.11: BECCS cumulative emissions in tCO_2/ha over 50 years for case studies A-D. Depending on the conditions, the system can be carbon positive (grey), slightly carbon negative – cumulative capture over 50 year below 0.5 $ktCO_2$ (purple), and very carbon negative – capture over 0.5 $ktCO_2$ (green). Upon including land use changes (moving from marginal land to grassland), the spectrum of potential outcomes substantially increases.

4.3.3 Sensitivity analysis and alternative scenarios

A sensitivity analysis was carried out in order to rank the parameters in terms of level of impact on the GHG dynamic emissions profile. The model was run with the lower, mean and upper values of 8 parameters: biomass carbon content, biomass moisture content, chemicals rate and footprint, fuel emission factors and carbon footprint, electricity footprint, yield, LUC and ILUC conversion emission factors. Figure 4.12 presents the dynamic emission profile of the 6,561 scenarios simulated for a miscanthus-based BECCS facility, coloured differently depending on the corresponding parameter. For each parameter, the profiles corresponding to the lower bound scenario are coloured in blue (red for yield and carbon content), to the mean scenario in yellow, and to the upper bound scenarios, in red (in blue for yield and carbon content).

As can be observed from both figures, ILUC is the primary determining factor, followed by LUC, yield, electricity footprint, biomass carbon content and biomass moisture content. Compared to these parameters, fuel emission factor and carbon footprints as well as chemicals rates and carbon footprints were found to have a limited impact on these results.

It is evident that LUC and ILUC conversion factors should be carefully evaluated on a case by case basis, but so should biomass yield, composition and electricity footprint. In practice, a crop yield is a complex function of a range of parameters, including climate, biomass properties, soil type, nutrient and water availability [236].

These results also indicate ways of improving BECCS sustainability. In order to evaluate the potential for improvements in BECCS, the following alternate scenarios were investigated:

1. Organic chemicals (no carbon footprint),
2. Biodiesel for in-field activities (100%) and road transport (blend 20% with conventional diesel B20),
3. Carbon neutral electricity,
4. Drying with biomass rather than natural gas.

Chemicals footprint and fuel emission factors ranges of uncertainty were relatively small compared to other parameters, which could explain their limited impact observed in the sensitivity analysis. For this reason, those parameters were included in the alternate scenarios. Table 4.6 summarises the ranges of impact on BECCS cumulative capture potential over 50 years in tCO_2/yr for each alternative scenario, as compared to the base case.

Due to the uncertainty around biodiesel carbon footprint, and the proportion limit to 20% in volume for biodiesel/diesel blend in road transport, bio-diesel impact was limited and even positive in some cases. Similarly to biodiesel, drying with biomass

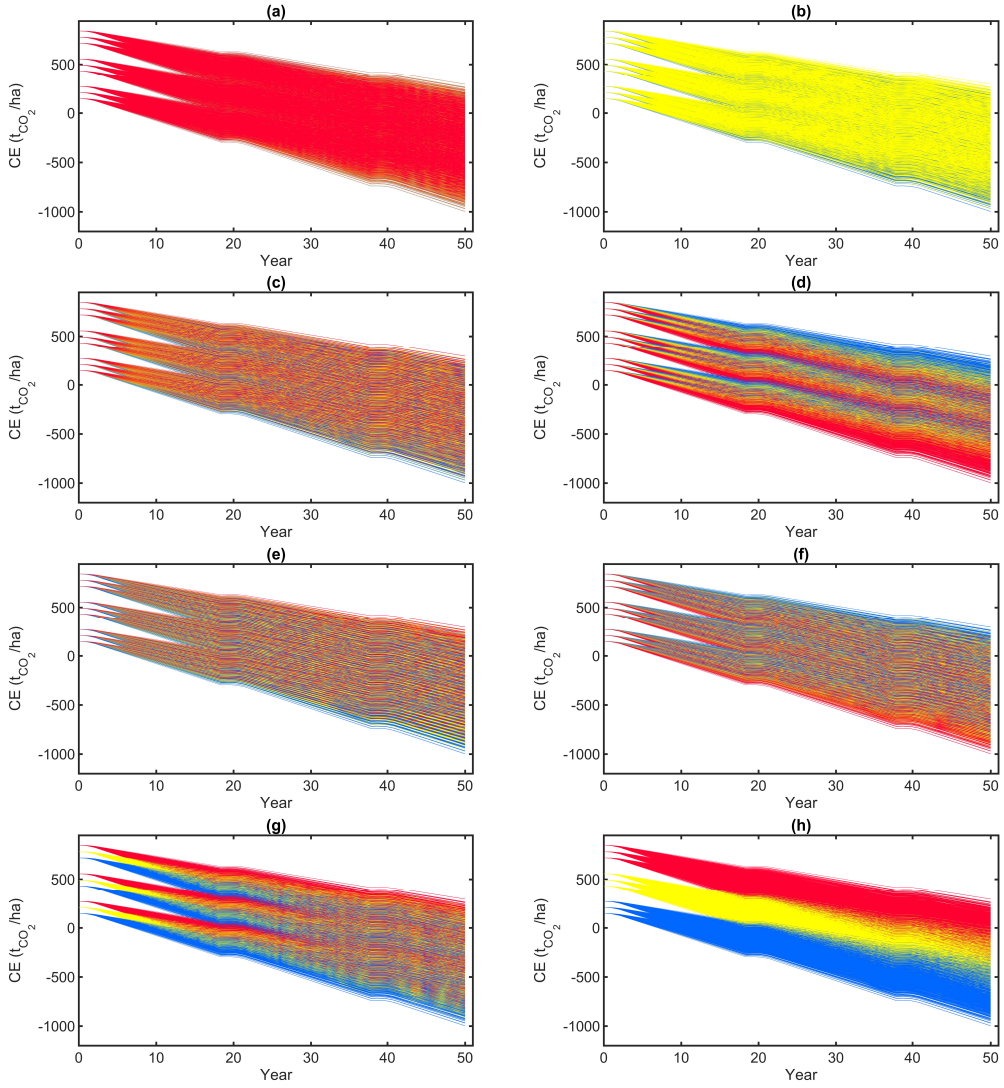


Figure 4.12: Sensitivity of miscanthus based-BECCS dynamic emission profile towards eight parameters (a: fuel footprint and efficiency, b: chemicals footprint and application, c: moisture content, d: yield, e: electricity footprint, f: biomass carbon content, g: LUC, h: ILUC). Emission profiles are coloured in red when the parameter is set to its upper bound (lower bound for yield and carbon content), yellow when set to its mean value, and blue when set to its lower bound (upper bound for yield and carbon content). Patterns indicate that ILUC is the determining factor, followed by LUC, yield, electricity carbon footprint and carbon content.

was found to have both a positive and negative impact. However, increasing the use of organic fertilisers for farming and carbon neutral electricity for biomass processing could bring substantial sustainability improvements to BECCS value chain. When land use changes are included in the case of willow, biomass carbon footprint is found to

Table 4.6: Alternative scenarios effect on BECCS carbon intensity over 50 years in tCO_2/ha. Using carbon neutral power had the most important impact on BECCS cumulative emissions, followed by farming with organic chemicals. Due to the variability in bioenergy carbon footprint, using biodiesel and drying with biomass could lead to both positive and negative impacts on BECCS cumulative emissions. This underlines the need for precise accounting of the GHG emissions associated with bioenergy materials production and supply.

Case study	Base case	Sc1	Sc2	Sc3	Sc4
A	-1124	-1158	-1192-**(-1119)**	-1364	-1158
B	-805	-839	-873-**(-800)**	-1044	-824
C	-288	-316	-313-(-306)	-348	-343
D	31	3	6-13	*-29*	**132**

be higher than that of natural gas, hence the negative effect (decrease) on the capture potential, rather than a positive effect (increase). Most importantly, a carbon positive case study such as willow on central grassland, could turn carbon negative by switching to carbon neutral electricity for biomass processing. This demonstrates the importance of intelligent management – organic chemicals, carbon neutral electricity, low carbon for transport and drying – to ensure bioenergy sustainability. This supports the assertion raised in Dale *et al.* that bioenergy can be sustainable when carefully managed [55].

4.4 Implications for resource mobilisation

In a given case study, the outcomes of BECCS sustainability analysis were observed to be very variable. In practical terms, this means that resource mobilisation to meet a mitigation target could vary widely from project to project. In order to stay within the 2°C scenarios, studies showed that the required level of deployment for BECCS was of the order of 12 $GtCO_2/yr$ by 2100 in the median scenario[36]. We evaluated the biomass, land, water, energy and nutrients requirements of BECCS given this annual carbon removal target. Smith *et al.* carried out a similar meta analysis in order to compare switchgrass-based BECCS and afforestation, given a removal target of 1 Gt_C/yr [56]. The difference with our analysis is that biomass supply chain results were obtained from various sources in the literature [139] and did not include direct and indirect land use changes. We performed the calculations on switchgrass and miscanthus from US and Brazil marginal lands (no direct and indirect land use changes), based on the same target and system boundaries in order to check the consistency of our results with the literature [36, 56]. The study by Smith *et al.* was not location and biomass specific, but most of the results were obtained for miscanthus [36]. Results for switchgrass in Smith *et al.* were adapted to the 12 $GtCO_2/yr$ target [56]. BECCS scenarios resulting in very variable dynamic emissions profile translated into different resources requirements in

terms of land, water and energy given a fixed mitigation target. As can be seen in 4.7, removing 3.3 Gt of carbon per year from the atmosphere using BECCS would require the annual mobilisation of 9 and 13 Gt_{DM} of processed switchgrass, 60 to 371 Mt of nutrients (N and P_2O_5), 1,250 to 2,490 Mha of marginal land in the US, and 7,800 to 15,700 Bm^3 of water. As a means of comparison, 17 Mt of N and P_2O_5 nutrients are used annually in the US, 721 Mha of land are harvested for cereal production in the world [78] (2014), and 7,980 Bm^3 of water is withdrawn – including green water – for the world agriculture [237]. This raises the question of water and land availability and whether marginal land will be sufficiently available and productive to enable biomass production at this scale, so as to avoid direct and indirect land use change effects. Using a higher yield crop such as miscanthus would lower the land and water requirements to 360-940 Mha and 3,600-9,700 Bm^3, respectively.

Furthermore, BECCS would need to be deployed at the scale of 1.7 to 2.4 TW. For reference, in 2017, the total installed coal-fired thermal power capacity was 2.1 TW[238]. Conversion of both coal and natural gas-fired power plants to dedicated biomass and biogas might well be necessary to meet these deployment targets. Furthermore, assuming a base load operation of the BECCS unit (85% load factor), this deployed capacity would represent an annual power generation of between 9,700 and 14,600 TWh, or between 41% and 62% of the global power demand in 2017 [239]. This result is highly dependent on BECCS annual load factor, and while a BECCS unit should run at full capacity to remove a maximum amount of CO_2 from the atmosphere, this value could potentially be dictated by the system short run marginal cost relative to that of the other power sources within the electricity market. Policies rewarding CO_2 removal from the atmosphere will be crucial in increasing BECCS competitiveness relative to other technologies, and in turn maximise BECCS load factor. However, from the annual power generation must be subtracted BECCS supply chain energy requirement. Within the uncertainty range, BECCS net energy balance could be both positive and negative, which needs to be considered when talking about BECCS energy supply potential.

It can be observed from table 4.7 that the model shows very good agreement with the literature for switchgrass [56]. However, though the model land requirement for miscanthus is in good agreement with the literature [36], water requirement and energy supply are found to be very different. The difference in water requirement can be explained by the different model assumptions. In Smith *et al.*, the contribution of bioenergy production to BECCS water footprint is evaluated at 80 $m^3/t_C/yr$, and the power plant + CCS contribution around 450 $m^3/t_C/yr$. This study assumes an evapotranspiration value for bioenergy between 1,176 and 1,822 $m^3/t_C/yr$ [36]. For reference, this value compares well with our model for which miscanthus evapotranspiration is 1240 m^3/t_C and total water footprint (evapotranspiration + grey water) 1635 m^3/t_C. The value of 80 m^3/t_C is then obtained by subtracting the evaporatranspiration of a refer-

ence grassland (the counterfactual) to bioenergy evapotranspiration [36]. However, if considered in the water balance, the counterfactual – leaving the land as is – would also need to be considered in the carbon balance, which would mean accounting for the CO_2 which would have been captured if the land had been left as is. As this was considered out of scope in this analysis, total evapotranspiration + grey water was selected as biomass feedstock water footprint. Furthermore the model evaluates the power plant + CCS water contribution at 14 m^3/t_C. It is assumed that the choice of a once-through cooling system – whose water consumption factor can be 30 times higher than that of a cooling tower system – as opposed to a recirculating cooling tower is the explanation behind this difference. For reference, the model would result in a power plant water requirement of 425 m^3/t_C with a once-through system. As for BECCS energy supply, BECCS was found to yield 170 EJ/yr at this deployment. However, this value does not include BECCS energy requirement which needs to be subtracted to BECCS energy supply.

Table 4.7: Comparison of the resource efficiency given a 12 $GtCO_2$/yr target removal of a BECCS utility operating at 100% load factor with literature, in two cases studies: switchgrass from the US and miscanthus from Brazil. Biomass is grown on marginal lands (no direct and indirect land use changes). Achieving this target would require between 1.7 and 2.4 TW of BECCS installed capacity, 1,250 and 2,400 Mha of marginal land, 7,800 and 15,700 Bm^3/yr, and 60 and 370 Gt of nutrients for a switchgrass-based system, which is in agreement with the literature. Such an installed capacity would result in a net energy output of 15 EJ/yr on average, but could also require 1 EJ/yr in the upper bound case. In the case of miscanthus, water requirement could be lowered to between 3,600 and 9,700, land requirement to 360 and 940 Mha. However a miscanthus based system could lead to an net energy use of 37 EJ/yr in the upper bound scenario.

Metrics	Switchgrass US	Smith *et al.* (2013)	Miscanthus Brazil	Smith *et al.* (2016)
Nb plants	3,413-4,852 (3,887)		3,323-5,758 (4,104)	
Biomass Gt_{DM}/yr	9.2-13.1 (11.1)		9.0-15.5 (10.5)	
Water Tm^3/yr	7.8-15.7 (10.4)	5.3-24.4 (14.5)	3.6-9.7 (5.5)	**0.072**
Land *Mha*	1,245-2,392 (1,630)	726-3,270 (1,910)	363-943 (538)	380-700
Energy *EJ/yr*	-22.4-1.0 (-15.1)		-15.3-37.0 (-0.01)	**-170**
Nitrogen *Mt/yr*	61-210 (112)		21-92 (42)	
Phosphate *Mt/yr*	0-161 (55)		8-98 (34)	
Sources		[56]		[36]

The same analysis was performed on grassland instead of marginal land, to account for land use changes. Figure 4.13 shows the amount of land, water, and BECCS capacity in order to meet the 12 $GtCO_2$ annual removal target, with (central grassland) and without (marginal land) land use change. Upon including land use changes (for *e.g.*, considering grassland instead of marginal land), resource mobilisation increases up to four times in the upper bound scenario.

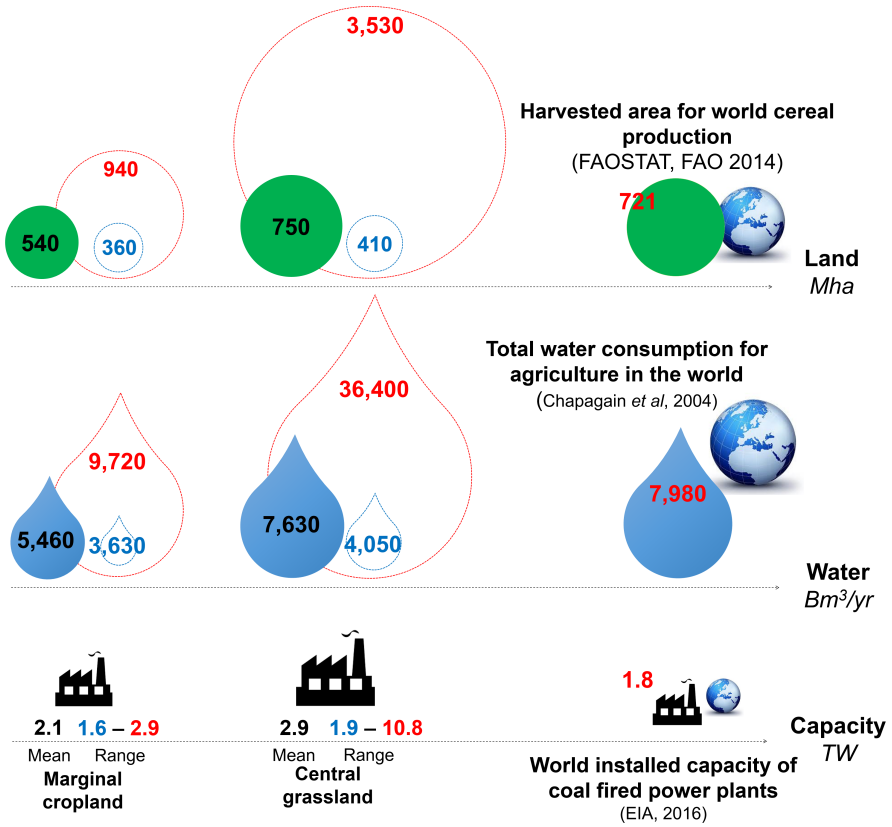


Figure 4.13: Water, land and capacity annual requirements of miscanthus-based BECCS to remove 12 $GtCO_2$/yr. Land use changes (grassland as compared to marginal land) increase resource mobilisation by up to four times in the upper bound scenarios.

4.5 Comparison with other carbon dioxide removal methods

The lower bounds and upper bounds results from the previous section were used to compare BECCS performance with other negative emission technologies, such as afforestation and DACCS. For afforestation, data was directly used from Smith *et al.*, 2013 [56]. As land requirement was expressed in ha/yr, the resulting afforested surface

over 50 years was considered in order to compare with BECCS land requirement. Data from the literature for land and energy requirement [36, 240–243] was adapted to this analysis. Table 4.8 summarises these results.

Given a CO_2 annual removal target, afforestation resulted in an overall similar land and water use than that of BECCS, though its land requirement corresponded to the upper range of BECCS results. Within the uncertainty range, BECCS net energy balance could be both positive and negative, but even when positive its energy intensity was found to be lower than that of DACCS. DACCS land requirement was several orders of magnitude lower than BECCS. However, the carbon footprint of the electricity used in the process, which would have had an impact on DACCS carbon efficiency, was not considered in the analysis. Using photovoltaic power could limit the carbon efficiency drop, but would on the other hand substantially increase DACCS land requirement. These trade-offs will have to be considered in detail when comparing BECCS and DACCS suitability for climate mitigation.

Table 4.8: Comparison of the performance of a BECCS facility operating at 100% load factor with afforestation and DACCS given a 12 $GtCO_2/yr$ target removal. BECCS results were obtained from the lower and upper bounds of miscanthus (Brazil) and switchgrass (US) simulations. Afforestation water and land requirements are similar to that of BECCS, though land requirement for afforestation corresponds more to BECCS upper bounds scenarios. DACCS land requirement is negligible compared to that of BECCS, but naturally has a higher energy requirement. From these simulations, BECCS maximum energy use is in all cases lower than the 145 to 247 EJ/yr required to remove the same amount of carbon with DACCS.

Metrics	BECCS	Afforestation	DACCS
Nb plants	3,323-5,758		3320
Water Tm^3/yr	3.6-15.7	5.3-11.6	
Land *Mha*	363-2,392	1,110-2,480	0.04-3.3
Energy *EJ/yr*	-22.4-37.0		81-274
Nitrogen *Mt/yr*	21-210	0.3-2.4	
Phosphate *Mt/yr*	0-161	0.7-2.5	
Sources		[56]	[36, 240–243]

4.6 Preliminary conclusions and discussion

In this part of the study, we used MONET through five thought experiments to quantify BECCS resource efficiency and carbon negativity under different scenarios.

The main conclusion of this study is the great variability in the possible outcomes of a BECCS project, both in terms of its cumulative net carbon removal over its lifetime, and also the time required for a given facility to start removing CO_2 from the atmosphere. Determining the sustainability or otherwise of a given BECCS project as a candidate for climate change mitigation is therefore only possible on a case-to-case basis. This has substantial implications for the regulation of those systems. The efficiency with which a BECCS project would remove CO_2 from the atmosphere is a first issue. Among carbon negative scenarios, it was observed that BECCS carbon intensity per hectare could vary greatly, which in turn means a great difference in the amount of resources (water, land, power plants) used to remove a ton of CO_2 from the atmosphere. For BECCS to be a valuable asset to the system, a minimum CO_2 removal efficiency might have to be defined to differentiate inefficient from efficient systems, therefore excluding scenarios that are not worth pursuing.

In terms of time horizon, depending on the conditions and due to biomass initial carbon cost to the ecosystem, BECCS does not necessarily start being a net carbon sink from year 1. If we consider that BECCS provides a service to the market – removing CO_2 out of the atmosphere, therefore avoiding future costs associated with climate change adaptation, it is reasonable to suggest that this service could be remunerated. However, it is also reasonable to suggest that this remuneration does not start until the facility is actually removing CO_2 from the atmosphere. Given that this breakeven time could be several years, this could well serve to complicate the delivery of BECCS projects, as the incentive for investing in BECCS might be otherwise insufficient.
Finally, in the case of a global deployment of an unintegrated BECCS value chain, this carbon crediting scheme would also need to acknowledge the diversity of stakeholders – biomass production, power generation, CO_2 transport and storage, and possibly countries, involved in BECCS value chain.

The next chapter explores another controversy associated with the large scale deployment of BECCS: is BECCS a net provider of energy?

Chapter 5

Is BECCS a threat to energy security?

5.1 Introduction

5.1.1 Objectives of the chapter

This chapter explores BECCS's ability to provide energy in a timely fashion. The purpose of this study is to deliver an analysis of the Energy Return on Investment (EROI) of BECCS, in order to provide insight into the circumstances under which BECCS can be net positive or negative, and to identify the key levers for improving the net energy balance. This chapter is structured as follows. The remainder of the introduction discusses the role of the EROI metric in the literature in general, and in the context of bioenergy in particular. Section 5.2.1 the details of the supply chain scenarios considered for this study. Section 5.2 presents the cumulative energy demand, power generation efficiency, cumulative EROI and cumulative net electricity balance of a UK-based BECCS facility using domestic or imported biomass pellets. In Section 5.3, an energy flow analysis provides insights as to the key levers of BECCS electricity balance improvement, including BECCS power generation efficiency. In meeting its long-term climate change commitments, the UK has set the target of achieving a net zero CO_2 economy by 2050. As the UK economy is not anticipated to be carbon neutral by 2050, meeting this target will rely on the net removal of CO_2 from the atmosphere, via the deployment of BECCS at the rate of 50 $MtCO_2/yr$ [244]. The impact of BECCS power generation efficiency on the net electricity balance, the BECCS capacity and amount of resources – land and water – required to remove these 50 $MtCO_2$ per year with UK-base BECCS fleets is also evaluated in section 5.3. Finally section 5.4 discusses the results and their socio-economic implications.

5.1.2 EROI for technology valuation

Energy systems follow the same rule as organic systems: in order to be viable, they need to produce at least as much useful energy as they consume [146]. This is measured by the Energy Return On Investment, which calculates the ratio of energy output of a system or resource to all the energy inputs required by this system, or to exploit this resource. It is thus a measure of the energy cost of energy: how much energy is required to provide energy in a specific form with a given technology? Deploying a technology with an EROI less than unity, would mean that overall, the technology uses more energy than it returns to society, which would result in the need for this technology to be complemented by other energy sources, preferably with a high EROI, to operate. Hall *et al.* suggest that fossil fuels could typically be used to compensate this energy deficit [146]. From this perspective, if, owing to poor management of the supply chain, BECCS EROI were to be found very low, deploying BECCS at the EJ scale could lead to an increase in fossil fuel use, which could hinder the potential environmental benefits of BECCS deployment, leading to further overshoot of emissions requiring the subsequent additional deployment of NETs, and so on, *ad infinitum*.

Though conceptually simple, there are, however, many caveats associated with the calculation of this metric. The first lies in the definition of the boundaries of the system for which EROI is calculated: what should be considered as the 'energy output' of the system, and similarly, what should be considered as 'energy inputs' [147]. Murphy *et al.* categorised fourteen EROI methodologies, defining three levels of energy output boundaries from extraction (or 'mine-mouth') to end-use or point of use, and five levels of energy inputs from direct energy and material inputs to auxiliary services consumption and environmental impacts [147]. As pointed out by the authors, the diversity in methodologies result in a great divergence in EROI values in the literature, with the EROI of modern coal being found between 20 and 67, between 1.6 and 12 for solar collectors power, and 0.8 and 10 for biofuels. Another consequence of this boundary definition is that the criteria of having an EROI above one at extraction or processing might not be enough, as the EROI at the point of use could therefore be lower than one. For example, Hall *et al.* propose that biofuels must provide a minimum EROI of 3:1 at processing in order to be a viable alternative to fossil fuels [146].

Another challenge lies in differentiating energy inputs and outputs in terms of energy quality. Considering that 1 joule of diesel has the same value as 1 joule of solar power overlooks the many attributes of an energy source; among service provided, scarcity, exergy, energy density, cleanliness, etc., which overall define its quality.[147] As a first approach, a common but fundamental distinction is made in studies between Primary Energy (PE) sources and Energy Carriers (EC): when calculating EROI based on energy carriers, 1 joule of electricity is equivalent to 1 joule of fuel, whereas in a primary en-

ergy methodology, all energy carriers vectors are converted back into the primary energy source from which they were generated [148, 150]. When the output of the system is electrical energy, considering the electrical equivalent energy (EEQ) of primary energy inputs is another method when performing EROI calculations. In calculating the net electricity balance and the E_IROI of solar photovoltaic (PV), Dale *et al.* considered the total electrical output, minus, or divided by, the cumulative primary energy use for the technology supply chain, converted into electrical energy equivalent [149]. Methodologies to convert energy inputs to weight them by quality, price-based adjustment or exergy-based adjustments are further examples which highlight the potential complexity of EROI calculation [147].

The quality of the energy source is equally important when comparing the EROI of different technologies, and can also be measured by the nature of the service provided by the energy source. Renewables such as wind and solar, which provide ready-to-use electricity, have typically a lower EROI than fossil fuels, which still need to be converted before delivering any form of energy. When comparing energy sources on the basis of similar service provided, the EROI of coal electricity for example, can be found between 12-24 [148], which is of the same magnitude of solar electricity, with values between 6 and 12 [148], and a median at 10 [145].

5.1.3 The EROI of bioenergy

There are many studies presenting energy analysis or EROI calculations of solid and liquid biofuels, as well as E_IROI calculations of bioelectricity. Moriarty *et al.* points out the wide range in these evaluations [93]. The EROI of short rotation willow in Europe is reported to be in the range 14.4 - 64.8, and that of miscanthus in Ireland, between 3.6 and 6.5. In terms of biofuels EROI, the authors report a range of 1.5-1.6 for US corn ethanol, up to 6 for US cellulosic ethanol, and Brazilian sugar cane ethanol at 5 [93]. These examples highlight the importance of explicitly considering specific region and feedstock when evaluating the EROI of resources, as biomass yield per hectare for example, may vary strongly from one region to another. Model boundaries also matter in the calculations. Table 5.1 gathers EROI values adapted from the literature, and highlights the importance of boundary choice when assessing bioenergy energy balance.

From this brief review of the literature, it can be observed that bioenergy EROI has been reported to have a wide range, with values between 2.3 and 84 as a function of biomass type, origin, and specific supply chain. However, when considering the whole value chain including pre-treatment and transport of the biomass, the range narrows to 3.6 to 15.9 for ready-to-use biomass pellets, and 2.3 and 4.2 for bioelectricity, when including pellet combustion. However, no ranges of EROI values for BECCS are reported in the literature.

Table 5.1: EROI values in the literature. Variations are observed depending on region of production, biomass type and supply chain boundaries.

Crop, region	EROI[a]	Boundaries
Miscanthus, average [193]	34.6	Raw biomass: production only no irrigation
Miscanthus, Poland [195]	23.4	Raw biomass: production only no irrigation, 4k transport
Miscanthus, Germany [199]	14.4	Bioelectricity: Production (bale), 100k transport, chopping and milling for combustion
Miscanthus, Ireland [137]	3.6	Pellet: production (bale) no irrigation, 100k transport, drying and pelleting
Switchgrass, US [208]	9.5-12	Raw biomass: production (bale or chopped) including irrigation
Switchgrass, US [201]	74-84	Raw biomass: production (bale) no irrigation, storage
Switchgrass, US [193]	16.4	Raw biomass: production only no irrigation
Switchgrass, US [139]	11-20	Raw biomass: production only no irrigation (bale, chopped), transport 40k
Willow, Sweden [245]	20.9	Raw biomass: production and 50k transport
Willow, average [193]	12	Raw biomass: production only no irrigation
Willow, Belgium [246]	11-54	Raw biomass: production only no irrigation
Wood pellets, Australia and Russia[215]	2.4-15.9	Pellet: production, drying (50% of the feedstock), pelleting and transport
Willow, Poland [195]	15.5	Raw biomass: production only no irrigation, 4k transport
Wheat straw, New Zealand [247]	4.2	Bioelectricity: Collection (bale), 90k transport, grinding, combustion
Wheat straw, UK [218]	2.3	Bioelectricity: collection (bale), 40k transport, conditioning, combustion

[a]EROI of biomass pellet or E_lROI of bioelectricity

5.1.4 The UK as a case study

As part of its transition to a low-carbon economy, the UK has committed to be net zero by 2050 [244]. Forecasts anticipate that in achieving this target, 50-130 $MtCO_2/yr$ of carbon dioxide could be sustainably removed from the atmosphere via BECCS, in order to offset remaining emissions from various sectors of the industry [244]. Building sustainable biomass supply value chains, as well as deploying an efficient CCS network, will be crucial in reaching this target. In 2015, the total EU pellet consumption reached 20 Mt of biomass pellets, with 6.2 Mt of imports, coming at 90% through the North America-EU trading route. In the UK, Drax power plant alone used 6.5 $MtCO_2$ of pellets in 2016 for its three biomass-dedicated 660 MW units. Though the majority of Drax feedstock originates from sawmill and forestry residues [40], and increasing biomass

demand in the UK, for both bioenergy and negative emissions purposes, will inevitably result in a diversification of the biomass feedstock, likely combining both domestic and imported agricultural residues and dedicated energy crops. On the CCS front, the UK boasts a diverse and well-characterised CO_2 offshore storage capacity in the North Sea. Results from the Energy Technology Institute UK CO_2 storage appraisal project indicate that the UK has a technical offshore CO_2 storage capacity of 80 $GtCO_2$ [176].

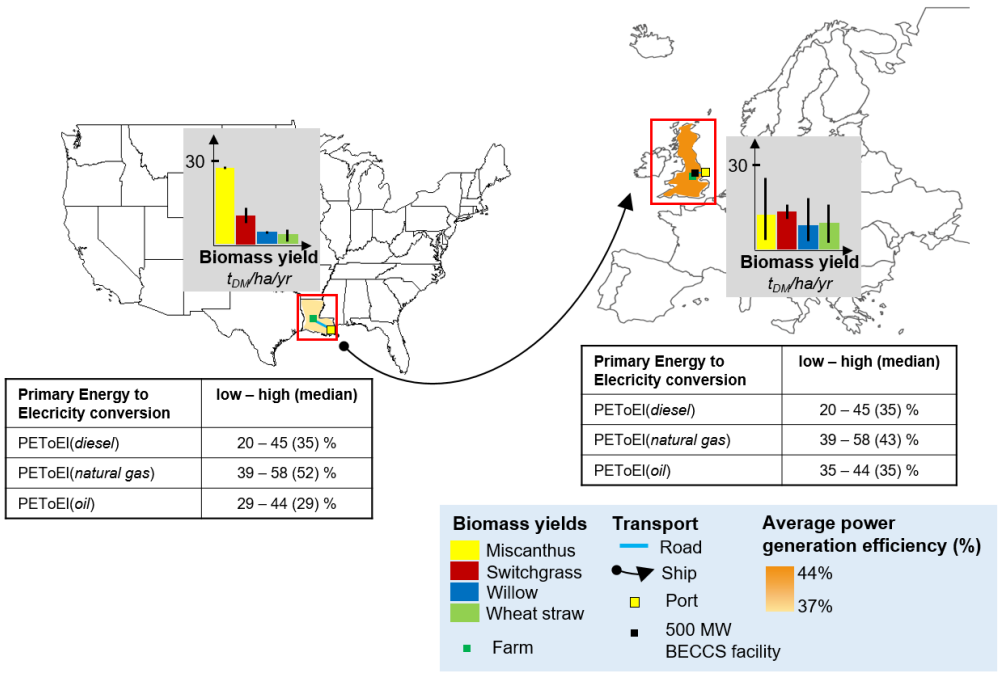
5.2 BECCS net electricity balance

5.2.1 Thought experiment

A UK-based 500 MW dedicated biomass pulverized fuel power plant, combined with amine-based post-combustion capture technology was considered as the main BECCS pathway for the UK in this analysis. Two archetypal feedstock supply chains were considered: domestic pellets and imported pellets from overseas. The purpose of these two scenarios is to compare the energy and carbon intensities of using local biomass, hence minimising transport, with importing biomass from a potentially more productive region, close to the coast, which requires oversea shipping. The region of import selected for the purpose of this study was Louisiana, as this is where the pelleting plants and port terminal owned by the UK DRAX power plant, which, in 2018, sourced over 50% of its pellet supply from the USA, are located [40].

Figure 5.1 gives a graphical representation of these two thought experiments, including key regional input data such as biomass yield, grid power generation efficiency, and primary energy to electrical energy conversion coefficients for the different fuels involved in BECCS value chain. As observed in Figure 5.1, biomass yield is on average higher in the oversea scenario, while the average efficiency of power generation is lower, which has a direct impact on the power to primary energy conversion when computing the EROI of the overall system. Both options were evaluated with the low, median and high values of the input parameters, resulting in a low, median and high scenarios for the results. It is worth noting that as more data was available for the UK than for Louisiana, the uncertainty ranges were usually larger for the UK.

Table 5.2 summarises the low, median and high values of some of the key model input data in both pellet supply chain scenarios, with their references.



Primary Energy to Elecricity conversion	low – high (median)
PEToEl(*diesel*)	20 – 45 (35) %
PEToEl(*natural gas*)	39 – 58 (52) %
PEToEl(*oil*)	29 – 44 (29) %

Primary Energy to Elecricity conversion	low – high (median)
PEToEl(*diesel*)	20 – 45 (35) %
PEToEl(*natural gas*)	39 – 58 (43) %
PEToEl(*oil*)	35 – 44 (35) %

Figure 5.1: Case study and input data considered in the model. Biomass yield (bar chart), primary energy to electricity conversion coefficients for each fuel (table), and average efficiency of the region power generation (region colouring) are given for each region in the low, median and high scenario. Biomass yield is on average higher in the oversea scenario, while the average efficiency of power generation is lower, which has a direct impact on the power to primary energy conversion when computing the EROI of the overall system. Higher yield variability in the UK is due to a higher availability of yield values in the literature for the UK than for Louisiana.

5.2.2 Energy model validation

In order to compare the different contributions, each energy input was calculated per dry ton of pellet delivered to the power plant. This distinction between the embodied energy GJ/t_{DM} harvested and delivered is important since it accounts for dry and wet mass loss along the supply chain. Comparing the embodied energy results with literature is only possible when the boundaries and assumptions (yield, moisture, transportation distance, etc.) of the models are known. For a proper comparison, the model was evaluated in the closest conditions to those of the source. The analysis presented in Table 5.3 indicates that our results are in good agreement with the literature.

Table 5.2: Energy model key input data

Parameter	Unit	Domestic Biomass	Imported Biomass	Sources
Willow yield	$t_{DM}/ha/yr$	4- - 17 (9)	5.1	see table
Switchgrass yield	$t_{DM}/ha/yr$	11 – 15 (13)	7.4 – 12.6 (10.8)	see tables B.12 and B.13
Miscanthus yield	$t_{DM}/ha/yr$	5 – 24.1 (12.8)	28.1	see tables B.12 and B.13
Wheat straw yield	$t_{DM}/ha/yr$	4.3 – 15.7 (9.4)	1.9 – 6.4 (4.1)	see tables B.12 and B.13
Electricity carbon footprint	kg_{CO_2}/MWh	349	400	[248, 249]
η_{grid}	%	44	37	[152]
$C_{elec \rightarrow PE}$	MJ/MJ	2.27	2.70	own calculation
$C_{diesel \rightarrow elec}$	%	20 – 45 (35)	20 – 45 (35)	[152]
$C_{NG \rightarrow elec}$	%	39 – 58 (52)	39 – 58 (43)	[151, 152]
$C_{HFO \rightarrow elec}$	%	29 – 44 (29)	35 – 44 (35)	[151, 152]
Road Distance (truck)	km	50	250	own calculation
Ship Distance (ship)	km	0	9,045	

For complete model data and references, see Appendix B. .

Table 5.3: Embodied energy model comparison with literature results

Crop, region[source]	Units	Results	Model
Miscanthus, average [193]	GJ/t_{DM}	0.52	0.31-1.02 (0.57)[a]
Miscanthus, Poland [195]	GJ/t_{DM}	0.77	0.32-1.03 (0.58)[b]
Miscanthus, Germany [199]	GJ/t_{DM}	1.25	0.86-2.00 (1.29)[d]
Miscanthus, Ireland [137]	GJ/GJ_{HHV}	0.28	0.08-0.14 (0.10)[e]
Switchgrass, US [208]	GJ/t_{DM}	1.5-1.9	0.7-1.8 (1.1)[f]
Switchgrass, US [201]	GJ/t_{DM}	0.2	0.4-1.4 (0.8)[g]
Switchgrass, US [193]	GJ/t_{DM}	1.1	0.4-1.4 (0.8)[g]
Willow, Sweden [245]	GJ/t_{DM}	0.86	1.5-2.6 (1.8)[h]
Willow, average [193]	GJ/t_{DM}	1.5	0.5-1.5 (0.9)[a]
Willow, Belgium [246]	GJ/(ha.yr)	3-16	6-12 (9)[a]
Wood pellets, Australia and Russia[215]	GJ/t_{DM}	1.13-7.5	3.7-8.0 (5.2)[i]
Willow, Poland [195]	GJ/t_{DM}	0.16	0.58-1.67 (1.01)[b]
Wood pellets [184]	MJ/t_{H_2O}	4455	4563 [j]
Wheat straw, New Zealand [247]	GJ/GJ_e	0.24	0.16-0.30 (0.22)[k]
Wheat straw, UK [218]	GJ/GJ_e	0.44	0.16-0.29 (0.22)[l]

[a]Model lower bound - upper bound (average) results for Europe, production only no irrigation.

[b]Model lower bound - upper bound (average) results for Europe, production only no irrigation, 4k transport.

[d]Model lower bound - upper bound (average) results for Europe, production (bale), 100k transport, chopping and milling for combustion.

[e]Model lower bound - upper bound (average) results for Europe, production (bale) no irrigation, 100k transport, drying and pelleting.

[f]Model lower bound - upper bound (average) results for the US, production (bale or chopped).

[g]Model lower bound - upper bound (average) results for the US, production (bale) no irrigation.

[h]Model lower bound - upper bound (average) results for Europe, production and 50k transport.

[i]Model lower bound - upper bound (Europe-US) results, production, drying (50%), pelleting and transport.

[j]Drying 45% to 15%.

[k]Model lower bound - upper bound (average) results for the US, collection (bale), 90k transport grinding, combustion.

[l]Model lower bound - upper bound (average) results for Europe, collection (bale), 40k transport grinding, combustion.

5.2.3 Cumulative energy demand of BECCS

The cumulative energy demand of BECCS was calculated in terms of energy carrier, primary energy and electrical energy equivalent, over the lifetime of a BECCS project which was considered to be fifty years, expressed in GJ/ha, or in GJ/t_{DM}. When expressed in GJ/t_{DM}, the cumulative energy demand is the same as the embodied energy (EE) of the dried pellet delivered at the power plant. These results are presented in Figure 5.2.

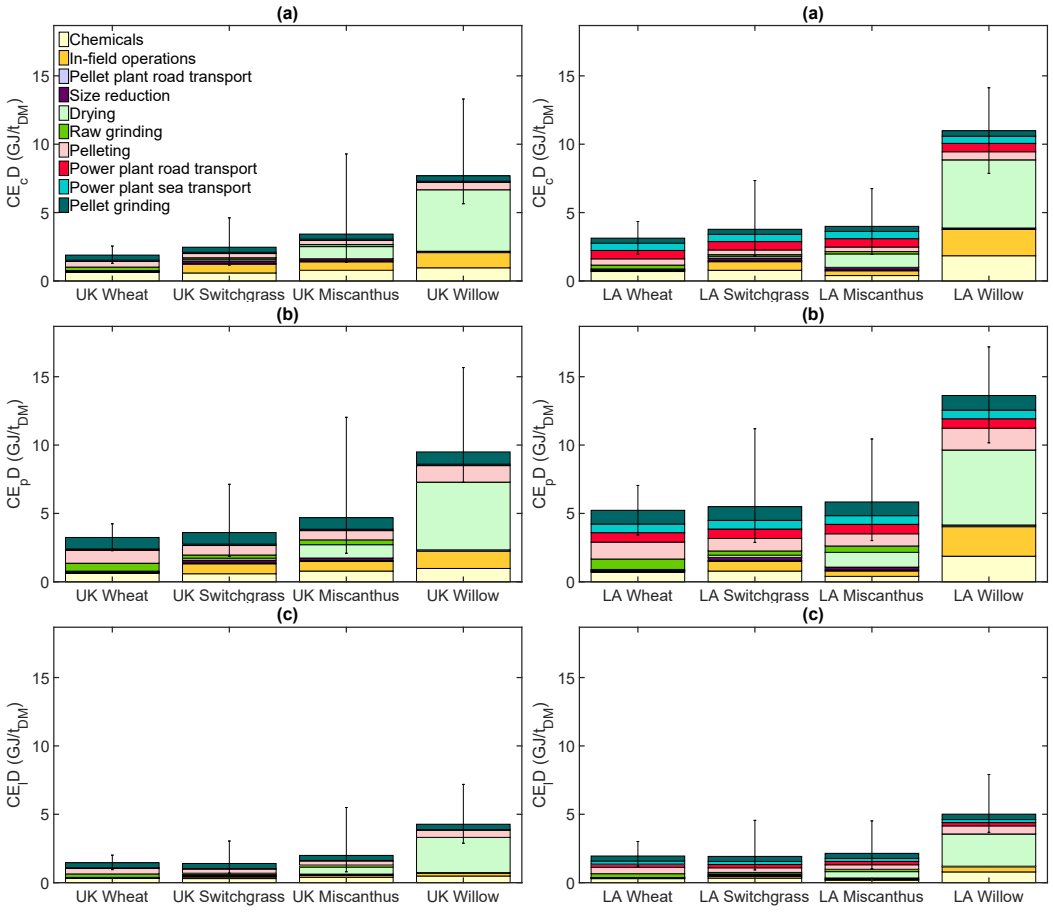


Figure 5.2: Cumulative energy demand of domestic (left) and imported (right) biomass pellets for different system boundaries: energy carrier (a), primary energy (b) and electrical energy equivalent (c). Cumulative energy demand is strongly dependant on the region, biomass and methodology chosen. Importing biomass pellet does not necessarily increase the energy demand as opposed to using domestic biomass. In the case of miscanthus, the transport energy contribution increase is almost compensated by the decrease of other contributions (chemicals, in field operations), due to a higher crop yield.

It was observed that the cumulative energy demand is strongly dependent on the region

of origin and biomass type. As expected, the cumulative energy demand expressed in terms of primary energy presents the numerically largest result, between 1.8 and 17.2 GJ/t_{DM}, with large contributions from the electricity inputs such as grinding, pelleting and pellet grinding. The cumulative energy demand in energy carrier results in a numerically smaller value, between 1.2 and 14.1 GJ/t_{DM}, with larger contributions from fossil fuel inputs such as farming, transport and drying. Finally, the energy demand in electrical energy equivalent is the lowest, with values between 0.7 and 7.9 GJ/t_{DM}. EROI methodology therefore impacts the total cumulative energy demand, as well as the main drivers of this energy demand. One must therefore be cautious when choosing one methodology over the other when identifying the key levers of improvement of BECCS net energy balance. The PE approach is assumed to be the most conservative approach when presenting EROI of pellets.

Wheat straw has the lowest cumulative energy demand. This can be explained by the fact that, in MONET, wheat straw is considered to be an agricultural residue, and all the energy inputs – fertilizer and in-field operations – associated with the production of wheat grain, are not allocated to the straw. However, straw collecting and additional fertilizer application due to removal of the straw from the field were accounted for.

Naturally, importing pellets from Louisiana as compared to using domestic pellet from the UK increases the transport contribution. Road transport, in particular, is what drives the transport cost. With a diesel fuel efficiency of about 1.65 MJ/(tons.km) in road transport, and a heavy fuel oil (HFO) efficiency of 0.05 MJ/(tons.km), 1 km of road shipping costs about 30 km of sea shipping. Therefore, transporting national biomass a distance of 400 km by road by road requires as much energy as shipping biomass over 13,000 km. Taking the road distance between the farm to the harbour and the harbour to the power plant into consideration, an equivalent journey in energy cost could be for example transporting feedstock grown within 100 km of the American east coast to Drax power plant in the UK. This shows that global supply chains should be designed so as to minimise their reliance on road transport (ocean and rail being preferred), and that the development of low carbon (or carbon negative via BTL+CCS) transport fuels will be vital in ensuring the sustainability of BECCS. Focusing on road and ocean transport highlights the importance of coastal as opposed to inland regions for bioenergy production. However, this conclusion could be nuanced when exploring the combination of rail and barge transport as an alternative to road transport. However, as can be seen in the case of miscanthus, the transport energy contribution increase can be almost compensated by the decrease of other contributions such as chemicals, and in field operations, due to a higher crop yield.

Willow stands out as unique in this study in that its embodied energy is primarily driven by drying. This is due to the fact that willow has a high average moisture content at harvest (52%), compared to 23% for miscanthus, 12% for switchgrass and 11% for wheat

straw. The moisture target at the drying stage was set to 15% in this analysis, in order to meet the moisture requirement of 10% for the pelleting process, and assuming a 5% moisture loss during grinding. This explains the absence of drying requirement for both switchgrass and wheat straw. In another supply chain scenario (bale or chips), biomass could be dried at a higher moisture content. However transportation energy cost and boiler efficiency penalty in the power plant would automatically be higher, which could potentially offset the energy saved at the drying stage. The embodied energy associated with the chemicals used also constitutes an important share contributing to above 10% of the overall embodied energy. This is due to the fact that willow is characterised by a relatively low yield for a high chemical input rate. Pellet grinding cost represents between 5 and 17% of the total production energy cost. Williams *et al.* showed that treatment on biomass pellets could reduce this cost by as much as a factor of four with steam-exploded pellets, and up to a factor of 25 with torrefied pellets [70]. Torrefied pellets grinding cost would therefore be over five times lower than that of coal on a mass basis, and four times lower on an energy basis. Torrefaction was not included in this analysis, but the trade-off between torrefaction energy requirement and improved power plant performance with torrefied biomass is clearly an area which warrants further study.

The relative magnitude of the uncertainty associated with the total embodied energy is observed to vary significantly between regions. For example, the calculated range for India is much greater than that for Europe. This observation is primarily driven by uncertainty in yield data. Yield data was widely available in Europe, which enabled the use of a 95% confidence interval as the uncertainty range, thus excluding extreme yield values. For India, yield values obtained experiments in arid or semi-arid climates in other regions were used [119, 250], but these data were scarce and highly variable.

5.2.4 E_lROI and Net Electricity balance

Having first calculated pellets' cumulative energy demand and BECCS cumulative electricity produced over the project lifetime, we calculated BECCS EROI and E_lROI as a function of time. Figure 5.3 presents the evolution of the values of biomass pellets EROI (a) and BECCS E_lROI (b) over time.

Two specific insights can be obtained from Figure 5.3: the median cumulative EROI and E_lROI values over the project lifetime, as well as the electricity pay-back time. It is observed that for electricity positive systems, the E_lPBT varies from 1 to 4 years. In the case of willow, upon importing pellets as opposed to using domestic pellets, the system becomes energy negative, as the lifetime E_lROI is found to be below one. The range of values obtained for the lifetime cumulative EROI and E_lROI are presented in Figure 5.4.

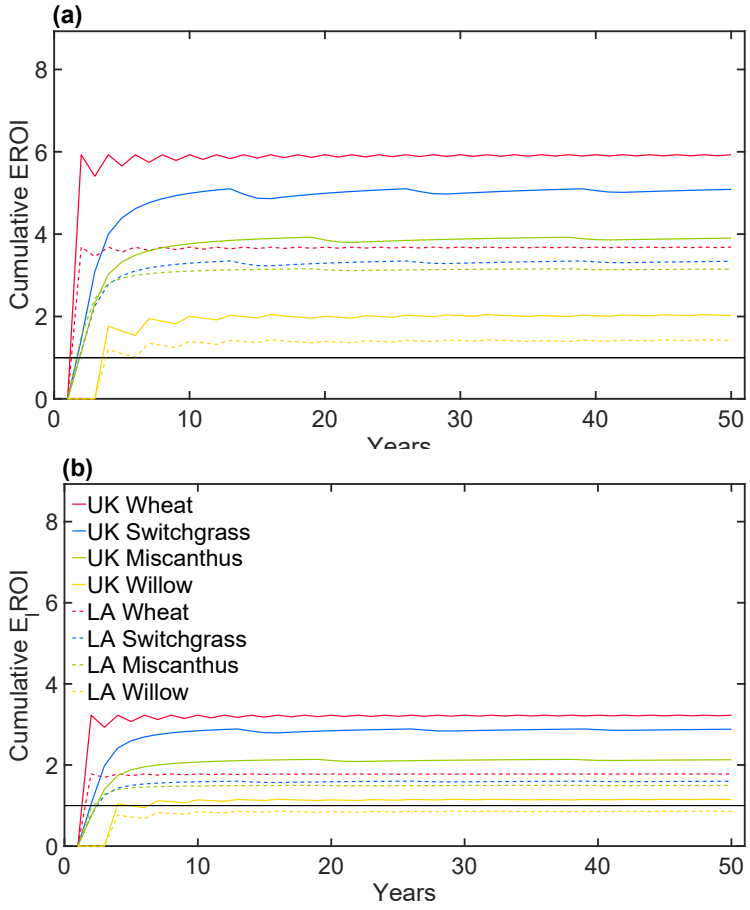


Figure 5.3: Dynamic EROI of biomass pellets (top) and dynamic E_IROI of abated bioelectricity (bottom) for the two feedstock case studies, in the median scenario. In the case of willow, upon importing pellets as opposed to using domestic pellet, the system becomes energy negative, as the lifetime E_IROI is found below one. For energy positive systems, the E_IPBT ranges from 1 to 4 years.

As observed in Figure 5.4, the median lifetime cumulative EROI varies from 1.1 to 10.3. These values are consistent with the biomass pellet EROI range of 3.6 to 15.9 reported in the literature, considering the variability in the input data and EROI calculation boundaries. In terms of lifetime cumulative E_IROI, values drop to 0.5 for willow from Louisiana, with maximal E_IROI attained for domestic switchgrass at 5.7.

Another way to look at the dynamic energy return is to analyse the net electricity balance of the system, over the course of a project lifetime. These results are presented in Figure 5.5.

As presented in Figure 5.5, depending on the region and feedstock scenario, but also on the model input data (yield, moisture content, chemical application rate, fuel efficiencies,

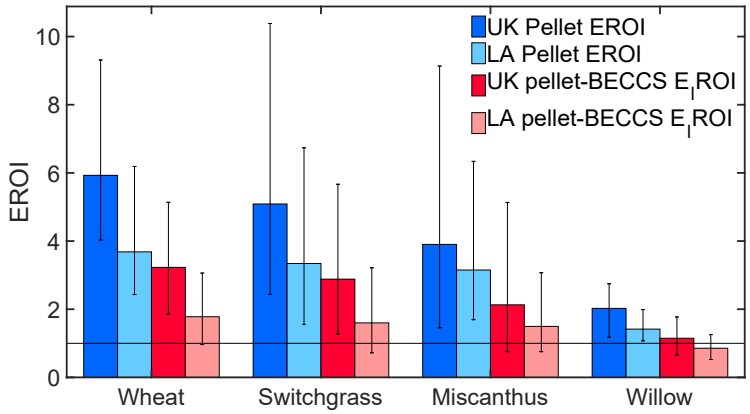


Figure 5.4: Lifetime EROI of biomass pellets (blue) and lifetime E_IROI of abated bioelectricity (red) for the two case studies. The lifetime cumulative EROI vary from 1.1 to 10.4, whereas the lifetime cumulative E_IROI values drop to between 0.5 to 5.7

embodied energy in fuel and chemicals, primary energy to electrical equivalent conversion coefficients, power generation efficiency, *etc.*), BECCS can lead to both negative and positive energy balances.

Overall, using agricultural residues such as wheat straw could be a promising option, as operating BECCS with this feedstock overall leads to a positive energy balance. However, this statement requires several caveats. First, the lifetime cumulative energy generation per hectare of such a system is low owing to a low straw yield per hectare, resulting in an inefficient use of the land for energy production via BECCS. Moreover, considering straw as a waste from grain production stands as long as wheat grain is not grown as an energy crop, which could be challenged if all wheat straw production was used for BECCS. Finally, BECCS deployment through agricultural residues will also be limited by regional wheat availability.

Using energy dedicated crops could be more challenging because of yield variability, as well as higher cumulative energy demand. In the case of willow, a lower yield, longer harvest cycle and higher cumulative energy demand result in a very low cumulative net power production in the mean and high scenarios, with an net energy negative balance in the mean scenario in the case of pellet imports from Louisiana. However, using higher productive grasses such as miscanthus and switchgrass could result in high cumulative net energy balance over fifty years, with values as high as 3,500 GJ/ha of net electricity produced in the case of miscanthus from the UK.

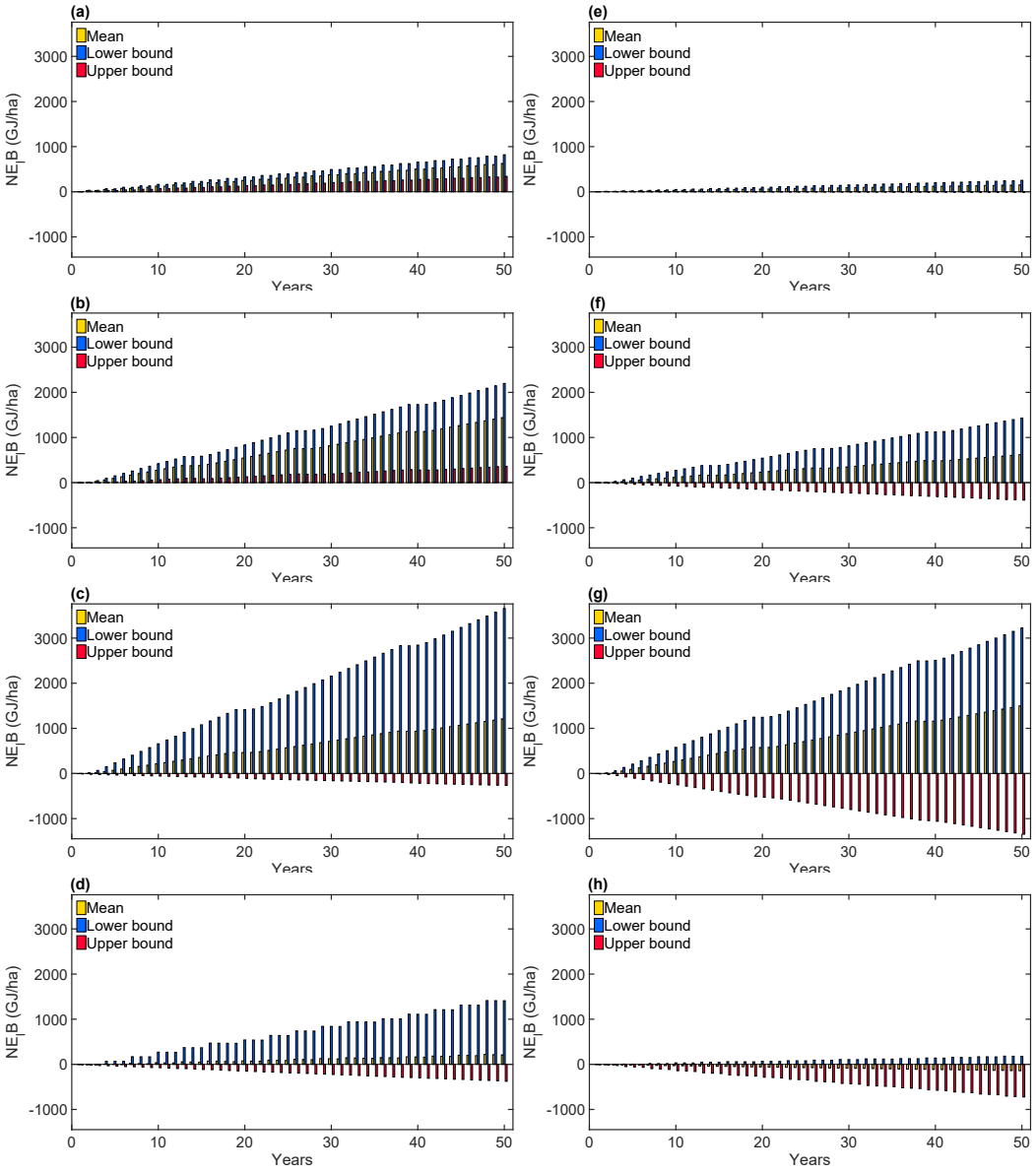


Figure 5.5: Cumulative net electricity balance of a BECCS facility using wheat straw (a and e), switchgrass (b and f), miscanthus (c and g), and willow (d and h) sourced from the UK (left) and Louisiana (right), in the high, mean and low scenarios. Depending on the scenario and case study, BECCS can lead to both positive and negative energy balances.

5.3 Improving BECCS net electricity balance

5.3.1 BECCS plant base efficiency

We calculated the plant power generation efficiency using the power plant model presented in 3. Figure 5.6 represents the power plant power generation efficiency η (in % HHV) as a function of the capture rate and co-firing rate.

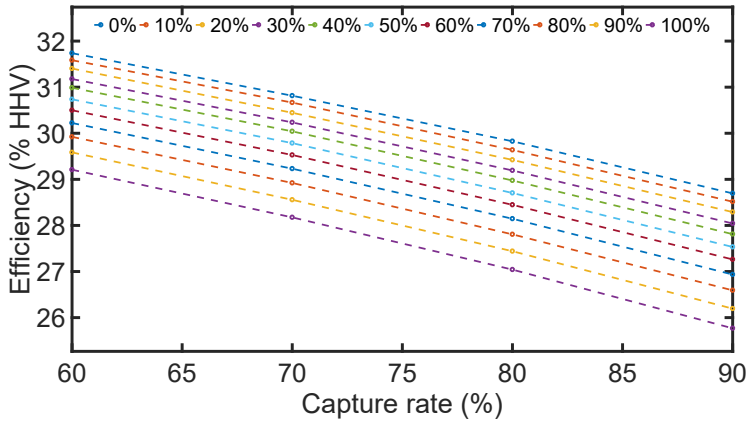


Figure 5.6: 500 MW supercritical coal-miscanthus pellets fired power plant efficiency (%HHV) as a function of capture and for different co-firing proportions. Efficiency decreases with capture rate, as the capture unit requires extra energy, and to a smaller extent with the increase in biomass share in the fuel.

As shown in figure 5.6, efficiency decreases with capture rate an co-firing proportion. This is explained by the efficiency penalty both imposed by the capture system and by the use of a lower quality fuel (lower HHV). It can be observed that the efficiency drop is more driven by the capture rate than by the co-firing increase: the efficiency drop is between 0.95 to 1.1% points for a 10% CO_2 capture rate increase, where it is between 0.15 to 0.40 for a 10% co-firing increase. With biomass pellets at 5% moisture and a power plant operating at 100% co-firing and 90% capture rate, the efficiency is found to be around 26%$_{\mathrm{HHV}}$ for all scenarios.

5.3.2 Identification of main energy losses

A energy flow analysis was performed on the system to identify the main energy losses along BECCS value chain, and their impact on BECCS electricity balance. Figure 5.7 presents the energy flow diagram of BECCS systems operating on domestic and imported biomass feedstock.

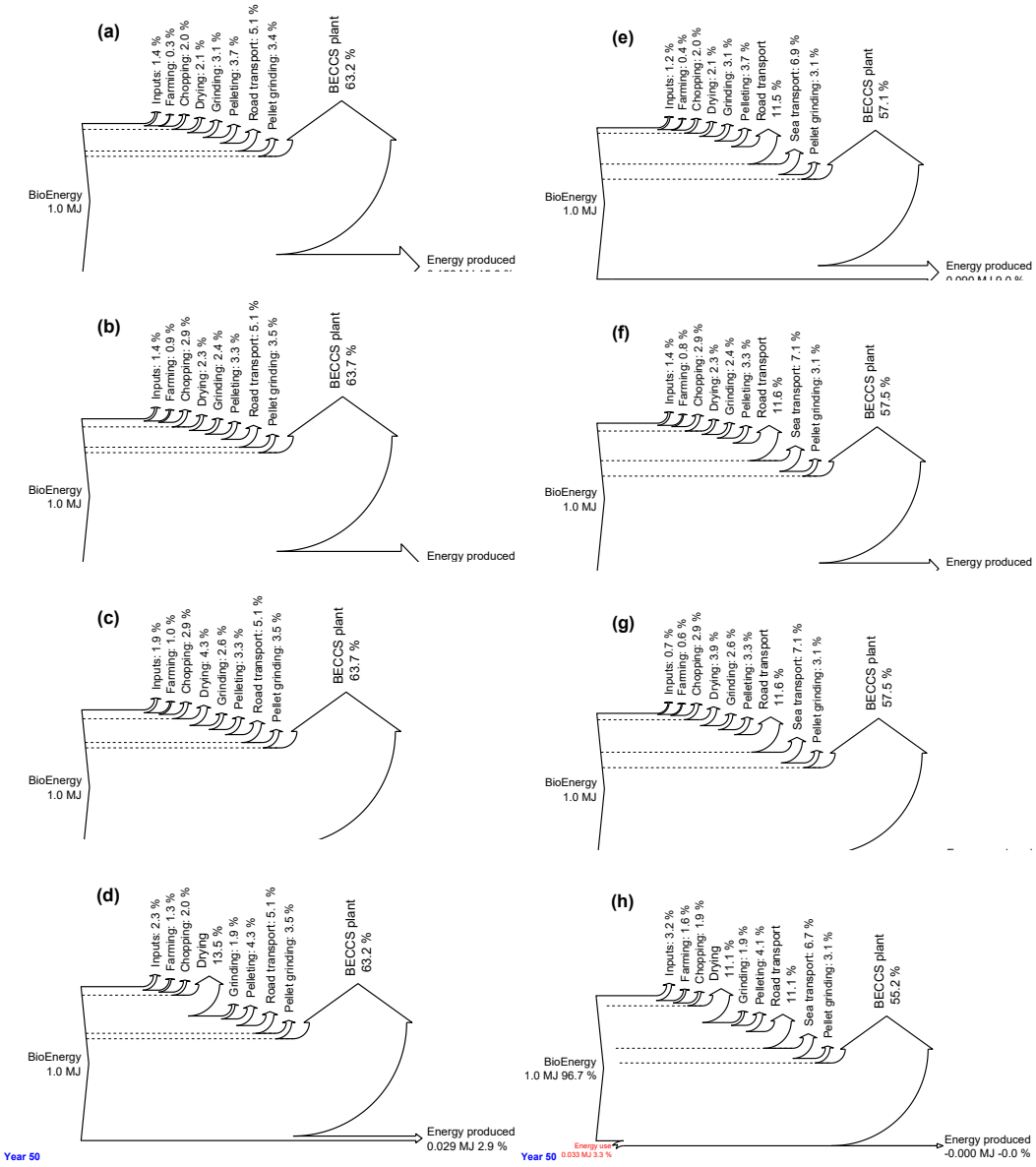


Figure 5.7: Energy flow diagram of BECCS value chain for domestic (left) and imported (right) wheat straw (a and e), miscanthus (c and g), and willow (d and h) pellets. Biomass conversion and CCS in the BECCS facility, followed by road transport, drying, and farming constitute the main energy losses along the chain. Power generation efficiency, transport fuel efficiency, moisture content and yield are therefore key levels to be optimized. In the case of miscanthus, an increase in transport energy losses for imported pellets, can almost be compensated by a decrease of farming losses because of an increased yield.

Biomass conversion and CCS in the BECCS facility, followed by road transport, drying, and farming (including inputs) constitute the main energy losses along the chain. Power

generation efficiency, transport fuel efficiency, moisture content and yield are therefore key parameters to be optimised when maximising BECCS net electricity balance. In terms of management of these levers, yield, moisture, and transport fuel efficiency are highly dependent on the feedstock and region of import, and can therefore be complex to predict and control. Power generation efficiency, however, as purely linked to the technology of the UK-based facility, constitutes a more tractable level to improve BECCS net electricity balance.

As shown by Bui *et al.*, BECCS efficiency can be increased by using advanced solvents with reduced heat duty, as well as by implementing heat integration options such as heat recovery from the exhaust gas to provide the solvent regeneration heat duty [49]. With such modifications, it was found that BECCS power generation efficiency could be increased to 38%$_{\mathrm{HHV}}$. This option was subsequently evaluated in MONET.

5.3.3 Power generation efficiency improvement and implications for resource mobilisation

In this section of the analysis, we calculate the annual net electricity production of a UK BECCS fleet operating to remove 50 MtCO_2 per year. Using MONET, this target scenario also enables the calculation of the annual land, water and BECCS capacity requirements to meet this carbon removal target.

Figure 5.8 represents the net energy balance, land use, water use, BECCS capacity and amount of CO_2 removed per unit per year for 26% (base case) and 38% efficient BECCS fleets, for all pellet supply scenarios. It is worth noting that the amount of CO_2 removed per unit per year, and BECCS deployed capacity, are inversely proportional.

As can be observed from Figure 5.8, BECCS capacity requirement and resource mobilisation in order to meet a given carbon removal target is entirely case specific. Meeting the UK's 2050 target will require between 8 - 14 GW of installed capacity, which represents 14 to 25% of the UK annual electricity generation by 2050 [251]. In terms of resources, between 2 - 175 Bm^3/yr of water and between 232 ha (when agricultural residues are used and the only land footprint considered is that of the power plant) and 22 Mha of land would be required, domestic wheat straw being the best case scenario, and imported willow pellets, the worse. It is important to note that these scenarios were considered to compare two archetypal supply chains, and no constraint on regional land and water availability were considered in their implementation. As a reality check, in the BECCS via domestic wheat straw scenario, 47 Mt of wheat straw, hence about 36 Mt of wheat grain, would be required per year, which is more than double the UK annual wheat production in 2014 [78]. A combination of wheat straw and energy dedicated crops would therefore be required to meet the UK carbon removal target via BECCS

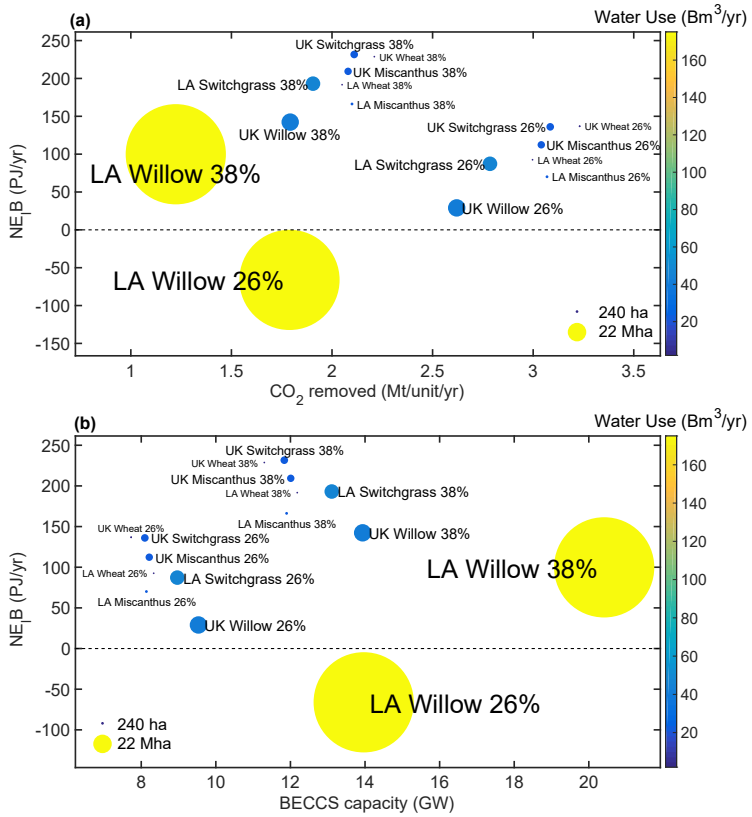


Figure 5.8: Mean net electricity balance (y-axis), water use (color scale), land use (marker size) as a function of CO_2 removed per unit per year (top) and capacity requirement (bottom), for a 26% and 38% efficient BECCS fleet. BECCS deployed capacity can be as high as 14 GW and as low as 8 GW, with annual water use between 2 and 175 Bm^3/yr, and the land use between 232 ha (when agricultural residues are used and the only land footprint considered is that of the power plant) and 22 Mha. The deployed BECCS fleet can generate up to 137 PJ/yr, but also require up to 66 PJ/yr in the case of willow pellets from Louisiana. Increasing BECCS power generation efficiency would improve the system net energy balance, but would also result in a lower CO_2 removal per BECCS unit, hence in a higher BECCS capacity, and to a smaller extent a higher amount of land and water required to meet a given carbon removal target.

with domestic biomass. Similarly, relying on imported willow pellets to meet the UK carbon removal target would lead to the mobilisation of 22 Mha of land in Louisiana. In this study, we assume that energy dedicated crops are grown on marginal land to avoid direct and indirect land use change. As the total area of Louisiana is approximately 13.5 Mha, there would not be enough land, let alone marginal land, to meet the UK removal target via this option. Designing optimal BECCS supply chains to meet a given carbon removal target will therefore need to consider a combination of regions, and specifically account for regional land and residue availability. It is also worth noting that wheat

straw very low land use and water use is also due to the fact that straw was considered as a waste from wheat grain production, therefore not accounting for land and water use for wheat farming in wheat straw CO_2, water and land balance. This assumption could be challenged if wheat straw use for BECCS started to impact wheat production for food.

In terms of net electricity generated, this BECCS fleet can generate up to 137 PJ/yr in the case of domestic wheat straw, but also require up to 66 PJ/yr in the case of willow pellets imported from Louisiana. To put these values in context, in 2014, electricity generation from bioenergy in the UK amounted to approximately 118 PJ [252]. Meeting the UK annual carbon removal target per year could thus potentially result in a 16% increase of bioelectricity supply when using domestic agricultural residues such as wheat straw, but could also consume the equivalent of 50% of the current UK bioelectricity supply when operating on willow pellets imported from southern USA. This could have profound implications as to UK electricity system design, with current forecast relying on BECCS as a net source of electricity, rather than as a net sink of electricity.

Increasing BECCS power generation efficiency would improve the system net energy balance, but would also result in a lower CO_2 removal per BECCS unit, hence requiring greater BECCS facility, as we have discussed previously [74], and to a smaller extent, a higher amount of land and water required to meet a given carbon removal target.

5.4 Preliminary conclusions and discussion

In this chapter, we evaluate the energy return on investment (EROI) of an archetypal BECCS facility. In order to highlight the importance of biomass sourcing, two feedstock scenarios are considered: use of domestic biomass pellets (UK) and import of biomass pellets from Louisiana, USA. We use the Modelling and Optimisation of Negative Emissions Technologies (MONET) framework to explicitly account for growing, pre-treating, transporting and converting the feedstock in a 500 MW BECCS facility. As an example, we illustrate how the net electricity balance (NE_1B) of a UK-based BECCS facility can be either positive or negative, as a function of supply chain decisions. Power plant efficiency, fuel efficiency for transport, transport distance, moisture content, drying method, as well as yield were identified as key factors that need to be carefully managed to maximise BECCS net electricity balance. A key insight of this contribution is that, given an annual carbon removal target, increasing BECCS' power generation efficiency by using a more advanced biomass conversion and CO_2 capture technology could improve BECCS net electricity balance, but at the cost of increasing the amount of BECCS capacity required to meet this target. BECCS optimal deployment pathway is thus heavily dependent on which service provided by BECCS is most valued: carbon

dioxide removal or power generation.

In this analysis, we found that BECCS E_IROI is highly variable depending on the feedstock and region of import scenarios considered, with values be as low as 0.5 and as high as 5.7. While lower bounds values are therefore energy negative (EROI below unity), upper bounds values were found in the range of solar PV. They remain however lower than the E_IROI of coal fired electricity, which was evaluated in the 12-24 range in Raugei *et al.* [148]. However, adding CCS to coal electricity could substantially lower the E_IROI of coal electricity [145]. This would mean that, in some scenarios, BECCS would be competitive with other low-carbon energy technologies, whilst also providing the additional service of atmospheric carbon dioxide removal. Though careful management of BECCS value chain can potentially lead to competitive E_IROI values, scenarios with low E_IROI could also be a reality. This would have several socio-economic implications. As observed by Hall *et al.*, biofuels with EROI values below 3:1 might need to be subsidised by fossil fuels, in the sense that their deployment would rely on the energy viability of fossil fuels, in order to provide value to the energy system [146]. This would mean that BECCS scenarios for which more energy is consumed than electricity is produced, could lead to an increase in fossil fuel use. This could threaten world energy security, as well as BECCS' carbon removal potential, as an increase in fossil fuel CO_2 emissions could offset the negative emissions provided by BECCS.

However, the implication may be nuanced when considering BECCS might not be solely deployed in the purpose of generating power, but also, and primarily, to remove CO_2 from the atmosphere. In Mac Dowell and Fajardy, it is shown that, providing a negative emissions credit is available to the operator of the BECCS facility, it is more profitable for a BECCS power plant to operate on a base-load fashion, therefore removing CO_2 constantly, and dispatching power on the electricity grid on a load following basis [74]. This underlines that BECCS' service of CO_2 removal, could be more important than energy generation.

It is also important to highlight that there are important trade-offs between carbon removal and power generation. As noted in the literature, less efficient power plant remove more CO_2 per year or per MWh_e generated than their more efficient counterparts [49, 74]. This was also observed in this analysis, as increasing BECCS efficiency improved BECCS net electricity balance and E_IROI, hence its value to the energy system, but also resulted in a decrease in the amount of CO_2 removed per facility per year, hence in a larger BECCS fleet required to meet an annual carbon removal target. To a smaller extent, resource mobilisation – land and water – also increased. Consequently, from an investment perspective, and depending on the source of the investment – negative emissions or energy sector – BECCS E_IROI might be less important than for other power generation technologies. To put BECCS net electricity balance in perspective, DACCS could require between 335 and 1,135 PJ/yr to remove 50 $MtCO_2$/yr [241, 242, 253],

which is still 5 to 17 times higher than BECCS energy requirement when deployed with willow from Louisiana.

Chapters 4 and 5 explored BECCS performance in terms of resource efficiency, carbon negativity, and energy positivity, under different scenarios, with no consideration of regional geophysical constraints to BECCS deployment. The next chapters explore BECCS optimal deployment to meet regional and global CO_2 removal targets, subject to resource and infrastructure constraints.

Chapter 6

Environmental trade-offs between optimal biomass supply chains in selected regions

6.1 Introduction

6.1.1 Objectives of the chapter

This chapter looks at BECCS optimal deployment within the BECCS performance trilemma: 1) technical performance, 2) resource efficiency, 3) environmental impacts, and presents a region-specific optimal allocation of resources – biomass feedstock, land, water, energy, CO_2 storage – to meet regional carbon dioxide removal targets via BECCS.

Given the UK's 2050 carbon removal target and identified available CO_2 storage in the North Sea, the design of optimal BECCS value chains for UK-based CO_2 removal from the atmosphere is the central case study investigated in this contribution. However, the framework is applicable to any region with identified CO_2 storage and CO_2 removal targets, and we further extend this work to present a series of thought experiments describing optimal supply chains were also determined to meet US and China-specific carbon removal targets, in Georgia and the Shanghai region, respectively. In a first thought experiment, we used the MONET framework to determine the optimal combination of feedstock type, region, land type, and transport route to a given region to remove CO_2 with a fleet of 500 MW UK, US and China-based pulverised combustion power plants, in conjunction with CO_2 capture and storage.

The remainder of this section introduces the role of multi-criteria optimisation in value

chain design. Section 6.2 presents the different optimal BECCS value chains to minimise either the total water use, land use and biomass use in selected regions. Section 6.3 investigates the trade-offs between these different environmental indicators, while section6.4 investigates the sensitivity of these indicators to the availabilities of marginal land and crop residues. Finally section 6.5 further investigates the relationship between the two services provided by BECCS – carbon dioxide removal and energy production – by highlighting the trade-offs between BECCS environmental performance indicators and energy production service.

6.1.2 Biomass supply chain design is a multi-criteria optimisation problem

Cost-based optimisation is a common approach in the field of supply chain design. In a study by Tagomori *et al.*, the authors investigated BECCS potential in Brazil by determining the cost-optimal CO_2 transport network, with CO_2 captured from biogenic sources [254]. Akgul *et al.* studied the optimisation of BECCS at the process scale, by determining the BECCS optimal technological pathway for power generation [27]. Through a pareto-front analysis, trade-offs between the cost and carbon intensity of the system were examined. Other studies have looked at spatially-explicit cost-optimal BECCS deployment pathways in South Korea [255], France [22] and the US [140, 256]. However, owing to the range of potential environmental impacts associated with BECCS, as well as services provided – power generation and carbon dioxide removal, BECCS key performance indicators (KPIs) are necessarily highly diverse. BECCS value chain optimisation is therefore inherently multi-objective, and by focusing either on cost, or on the trade-offs between economic and environmental performance, one could easily cloud the complex interactions existing between BECCS environmental impacts. In their work, Heck *et al.* presented a global land and biomass optimal allocation model for BECCS via B2H2 and B2L, in which the weighted sum of BECCS environmental impacts – freshwater use, forest loss, biosphere integrity and biochemical flows – resulting from achieving a fixed biomass harvest objective, was minimised. The results highlighted trade-offs between bioenergy production and negative emissions potential, as well as freshwater use and forest loss [79]. However, the difficulty with preference-based optimisation is that the optimisation results obtained are highly dependent on the values attributed to the weights, thus on the relative importance of each objective, which can be highly region specific. Furthermore, whilst the model carefully considered planetary boundaries and regional biomass production potential, BECCS downstream logistics, such as biomass processing and transport to potential CO_2 storage, were not included. This contribution thus addresses this gap via the development of a biomass supply chain optimisation model which explicitly accounts for biomass processing, transport and use in

the vicinity of CO_2 sinks, and investigates the trade-offs between BECCS KPIs through pareto-analysis.

6.2 Optimal biomass supply chain in the water-land-carbon nexus

In a first instance, this section presents different insights from the optimisation of the biomass supply chain required for BECCS to remove 50 Mt_{CO_2}/yr in the UK, under three different objective functions – water minimisation, land minimisation, and CO_2 efficiency maximisation, considering only DEC on MAL (impact I). To illustrate that the modelling framework can also be applied to meet other regional targets, this section includes the BECCS optimal supply chains required to meet US and China carbon removal targets, by storing CO_2 in southern USA, and in Eastern China, respectively. Figure 6.1 presents the selected regions, ports, as well as marginal land use density in each cell (fraction of the total land used by BECCS), biomass pellets transport fluxes (arrows) and amount of net CO_2 removed per region for each objective function, in the median scenario, to meet a UK target (black arrows). The coloured arrows illustrate how these optimal value chains may change as the location of the BECCS facility and CO_2 storage, and therefore the biomass transport distance, changes for the US (purple arrows) and China (blue arrows).

A first conclusion in that the structure of the optimal BECCS value chain changes substantially depending on which metric is prioritised. Under the water minimisation scenario, represented in Figure 6.1a, factors such a climate conditions, precipitation and yield play a central role in the water performance of each combination. In spite of substantial road and sea transport distance, regions from western and central Brazil are selected, owing to their combination of low carbon intensity of their electricity and high biomass yield, which highlights the strong trade-offs between transport and other supply chain parameters. As seen in Figure 6.1b, when minimising land use, yield and supply chain emissions have a strong impact on the results, and productive coastal regions from Brazil are selected. Similar results are obtained in the CO_2 efficiency maximisation scenario (Figure 6.1c), though domestic biomass is also selected in the balance to minimise CO_2 leakage from transport. When changing the CO_2 storage location from the UK to Georgia (US) or Shanghai (China), the change in biomass transport distance significantly changes the optimal configuration in the carbon efficiency maximisation scenario, in which biomass transportation represents an important share of the overall CO_2 leakages along the chain. However from a water and land minimisation perspective, the optimal regions do not change significantly, which further confirms the low weight of ship transport distance as compared to other more prevalent factors, when it comes

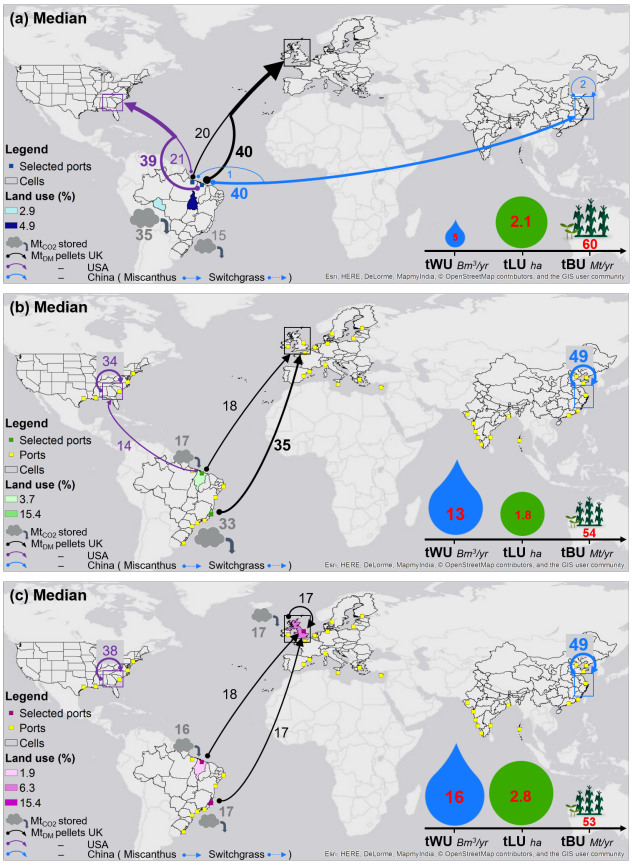


Figure 6.1: Optimal biomass supply chain to minimise global water use (a), land use (b) and CO_2 efficiency (c) in the median scenario to meet a 50 $MtCO_2$/yr removal target in three different regions - UK (black), Georgia (Purple) and Eastern China (blue). The arrows represent the biomass fluxes transported to the BECCS plant/CO_2 storage area of the matching colour, while the clouds present the share of removal achieved with each biomass supply. There are strong trade-offs between the resource efficiency indicators: water increases threefold from the water minimisation to the CO_2 maximisation scenario. Overall, biomass from regions with higher yield, lower grid carbon intensity and higher precipitation is chosen over indigenous biomass. Changing the storage location from the UK to Georgia or Shanghai brings significant changes to the optimal configuration in the CO_2 maximisation scenario, where transport plays an important role, but limited changes to the water and land minimisation configurations.

to resource conservation.

These results were also found highly dependent on the model input data, which can be observed in Figure 6.2 and 6.3. As regional yield, fertiliser use, and carbon footprint of the electricity change from the median to the optimistic scenario, thereby decreasing regional pellets' water and carbon footprints, other regions such as northern Europe are selected in the water minimisation scenario. In the land minimisation scenario, miscant-

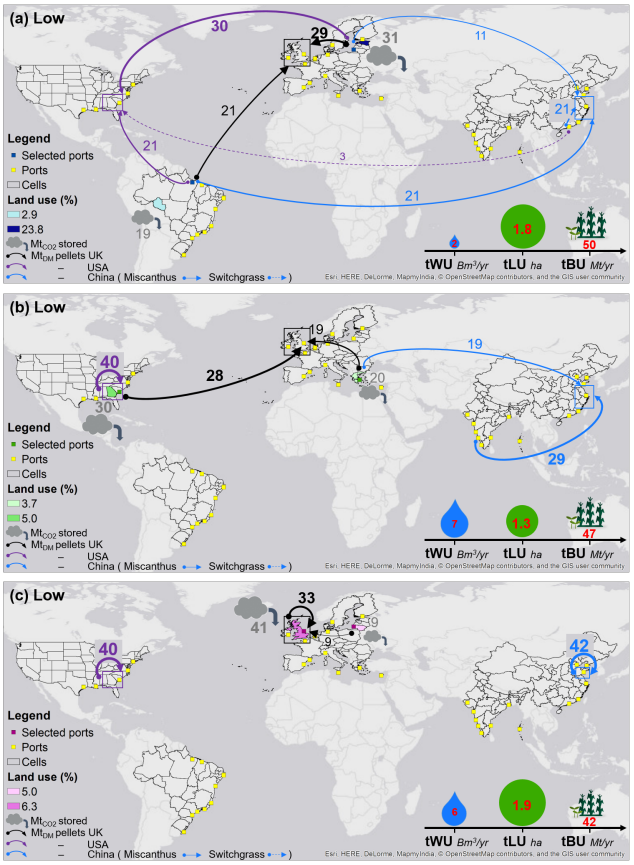


Figure 6.2: Optimal biomass supply chain to minimise global water use (a), land use (b) and CO_2 efficiency (c) in optimistic scenario.

hus from the US east coast and southern Europe is selected. This is highly dependent on the yield range considered for each region. In the CO_2 efficiency maximisation scenario, a balance of miscanthus from UK and Brazil are also selected in the optimistic and pessimistic scenarios. The trade-offs between these resources can be assessed by evaluating the total land use, water use, and biomass use under the three optimisation, which are also represented in Figure 6.1. It is observed that water use, and to a smaller extent land use and CO_2 efficiency, are highly dependent on which metric is optimised. Water use increases threefold in the CO_2 maximisation scenario, as compared to the water minimisation scenario. CO_2 efficiency and land use variations are less important: regardless of the optimised metric, land use remains within 1.8-2.8 Mha for all scenarios, and CO_2 efficiency, within 48-54%. The trade-off between CO_2 efficiency and land use is less extreme: in the pessimistic scenario, the supply chain required to minimise the land use is the same as the one required to maximise the CO_2 efficiency. The structure

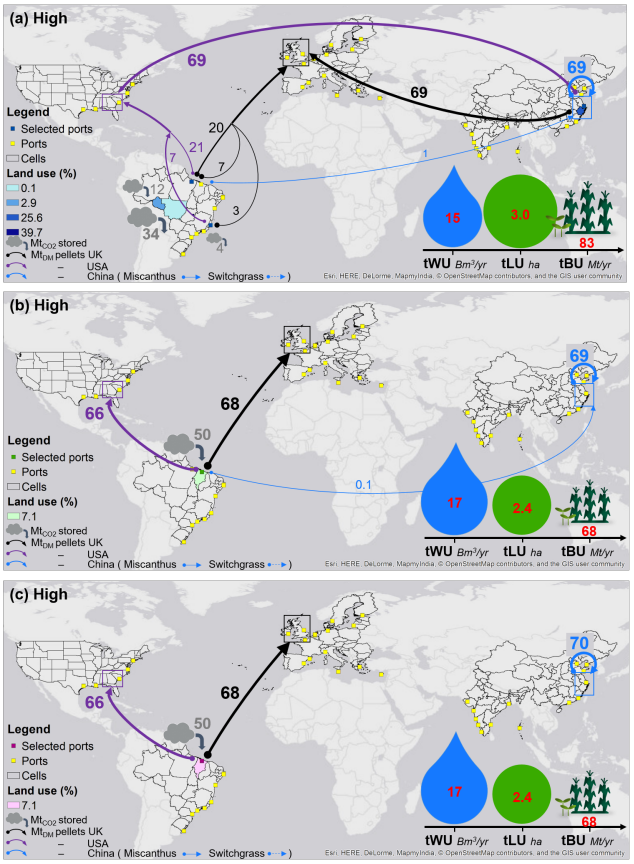


Figure 6.3: Optimal biomass supply chain to minimise global water use (a), land use (b) and CO_2 efficiency (c) in pessimistic scenario.

and the resource efficiency of BECCS optimal value chain are therefore very dependent on the objective function and parameters such as yield, fertiliser rate, climate and grid carbon intensity. Accurate weighing of each metric is required to determine an optimal biomass supply chain which reconciles all three metrics. Understanding which mechanisms might influence such decisions is therefore key to deploy BECCS optimally. Access to accurate data for the key model input parameters is also crucial.

6.3 Trade-offs within the water-carbon-land nexus

Trade-offs between the objective functions were quantitatively evaluated using the ε-constraint method, and pareto-fronts between each objective functions were generated. Figure 6.4 shows the pareto curves between f_1, f_2 and f_3 in the median, optimistic and pessimistic scenarios.

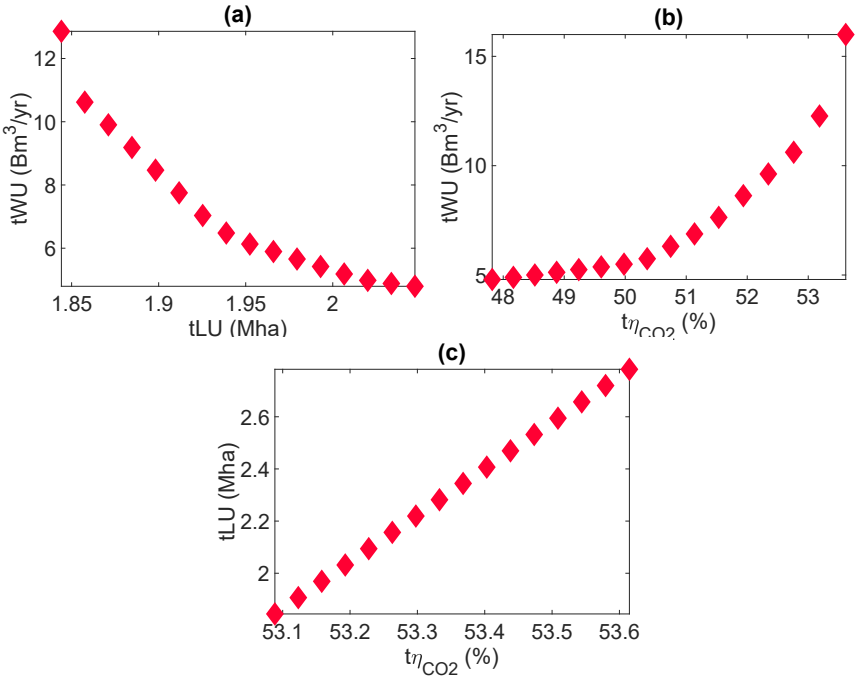


Figure 6.4: Pareto lines between water use, land use, and CO_2 efficiency, in the median scenario. There are strong trade-offs between water use and the other two objective functions. However, the trend of the pareto lines for these two relations ((a) and (b)) indicate the presence of tipping points which could reconcile the different objectives. CO_2 efficiency decreases marginally when land use increases, showing the proximity of these two optima.

As discussed in section 6.2, the pareto lines in Figure 6.4 indicate a strong trade-off between water use and the two other objective functions. When minimising water use, as total land use in constrained from 2.05 Mha to 1.85 Mha, water use increases from 5 to 13 Bm^3/yr. Moreover, as carbon efficiency is constrained from 48% to just under 54%, water use increases threefold. However, the shape of the pareto lines indicate the presence of tipping points: beyond 1.95 Mha and 50.1% efficiency, the rate of increase in water use significantly increases. In the case of land use against CO_2 efficiency, it is difficult to identify a tipping point, as the relationship is linear. However, the variation of the CO_2 efficiency is very limited for a given variation of land use, which shows that the optimal points are closed for both optimisation scenarios. This analysis shows the complex interactions between BECCS resource efficiency indicators. Deploying BECCS such that each indicator is maintained close to the tipping point, rather than optimised, could be a preferred option to maximise BECCS overall resource efficiency.

6.4 Sensitivity analysis

6.4.1 Limiting supply

As pointed out in the introduction, reliably quantifying the availability of marginal land is complex owing in part to the diversity in definitions, methodologies and datasets used. In 2013, Fritz *et al.* downgraded Cai *et al.* lower bound estimates by 69%, bringing the total marginal land availability from 320 Mha to 98 Mha [115]. Whilst the availability of agricultural residues can be evaluated with more certainty, determining which fraction of the residues is both recoverable from the field, and used for bioenergy without competing with other uses – for example soil enriching or fodder, is not straightforward. In a recent study on biomass production potential from Brazil [257], the author evaluated the harvestable proportion of agricultural residues to be below 50%, and the proportion of harvested resource available for bioenergy, below 10%. Owing to this complexity, we use this section to study the impact of constraining the availability of marginal land and agricultural residues on the total land use and total land use change in our various scenarios. Figure 6.5 shows the evolution of the total land use tLU in the land minimisation scenario, and the total land use change $tLUC$ for the three objective functions, as a function of marginal land and crop residues availability, in the impact scenario III. Figure 6.5a shows that the availability of residues plays a first order role in the system's total land use. When it is limited to 20%, total land use increases by several orders of magnitude. This can be explained by the fact that no land use at the field level, nor CO_2 emissions from farming, except from the additional fertiliser cost resulting from the removal of the residues from the field, were attributed to agricultural residues, as opposed to dedicated energy crops. As a grey water footprint is attributed to crop residues because of this additional fertiliser use, water use is decreased to a smaller extent. As far as land use change is concerned, when minimising land use and maximising the CO_2 efficiency, land use change only occurs when AR availability is limited below 20%. When minimising water use however, land use change can be high even in high marginal land availability. Though land use change results in higher lifecycle CO_2 emissions, as long as the the water consumption per CO_2 removed is still attractive, bioenergy crops planted on former cropland and grassland may still be preferable in the water minimisation scenario. This indicates the presence of trade-off between carbon removal and water use.

To provide further insight into this emergent behaviour, Figure 6.6 illustrates the evolution of BECCS optimal value chain in the water minimisation scenario at 0% residue use availability, and constraining marginal land availability from 100% to 10%. As marginal land availability decreases, it is interesting to see that the same regions from Brazil are used, but both the amount and proportion of grassland and cropland used increase, as

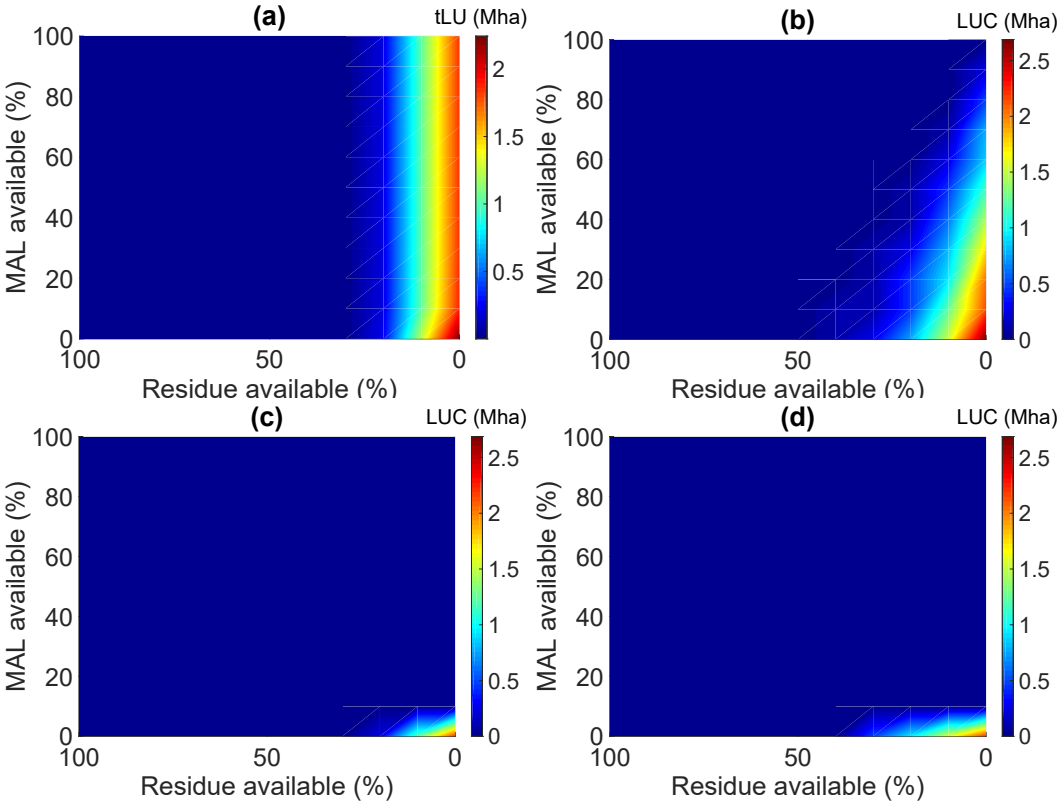


Figure 6.5: Total land use in the land minimisation scenario (a), and land use change in the water minimisation (b), land minimisation (c) and CO_2 efficiency maximisation scenarios, in impact scenario III. Residue availability has a first order impact on BECCS total land use. When minimising land use and maximising the CO_2 efficiency, land use change only occurs when AR availability is limited below 20%. When minimising water use however, land use change can be high even in high marginal land availability: there is a greater trade-off between carbon removal and water use.

well as the land use density. Other regions that had not been selected before, such as China, also start appearing in the results when land availability is drastically constrained, supporting the conclusion that the nearest regions are not necessarily the optimal regions from a water perspective.

This study has provided insight into the important trade-offs between BECCS resource efficiency and economic-environmental impacts. It was shown that using agricultural residues could drastically relieve BECCS pressure on land use. In order to obtain the same result while avoiding competition with other uses of agricultural residues, using high productivity-high carbon content biomass such as algae, could be a promising alternative [84]. A second important trade-off exists between water use and land use change: minimising water use for BECCS might result in high land use change, particularly when

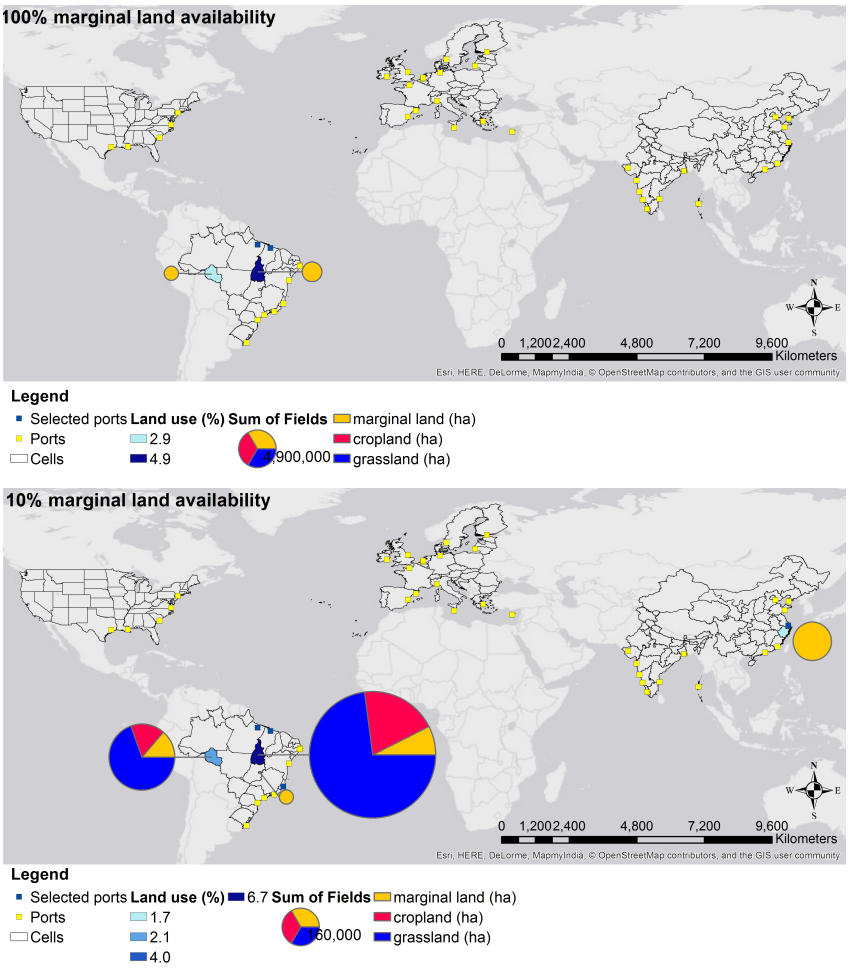


Figure 6.6: Evolution of BECCS optimal value chain in the water minimisation scenario at 0% AR availability, and constraining marginal land availability from 100% to 10%.

the availabilities of marginal land and crop residues are constrained. This conclusion builds upon the previous contribution of Heck *et al.*, where this potential compromise was first alluded to [79]. This further confirms that myopic focus on the trade-offs between BECCS environmental and economic performance is, at best, incomplete: there are complex interactions within BECCS environmental trade-offs which must be understood in order to deploy BECCS in a genuinely environmentally and ecologically benign manner.

6.4.2 Ramping up the carbon removal target

Whilst the UK projected a 50 $MtCO_2/yr$ target by 2050 in 2018, it is conceivable that more CO_2 might be stored in the UK for two reasons: 1) The UK's own target is likely to reach higher level – 130 $MtCO_2/yr$ – with the adoption of the economy-wide net zero target by 2050 [244], and 2) as regional storage availability is limited, other regions could be willing to store CO_2 in the UK as well. As a thought experiment, we investigate how ramping up the targeted amount of CO_2 to be stored in the UK impacts the key performance indicators of BECCS value chain under the three optimisation and impact scenarios. The resulting water use under the water minimisation scenario (a), land use under the land minimisation scenario (b), CO_2 efficiency under the CO_2 efficiency maximisation scenario (c), and total land use change in all three optimisation scenarios, in the impact scenario III, are presented in Figure 6.7.

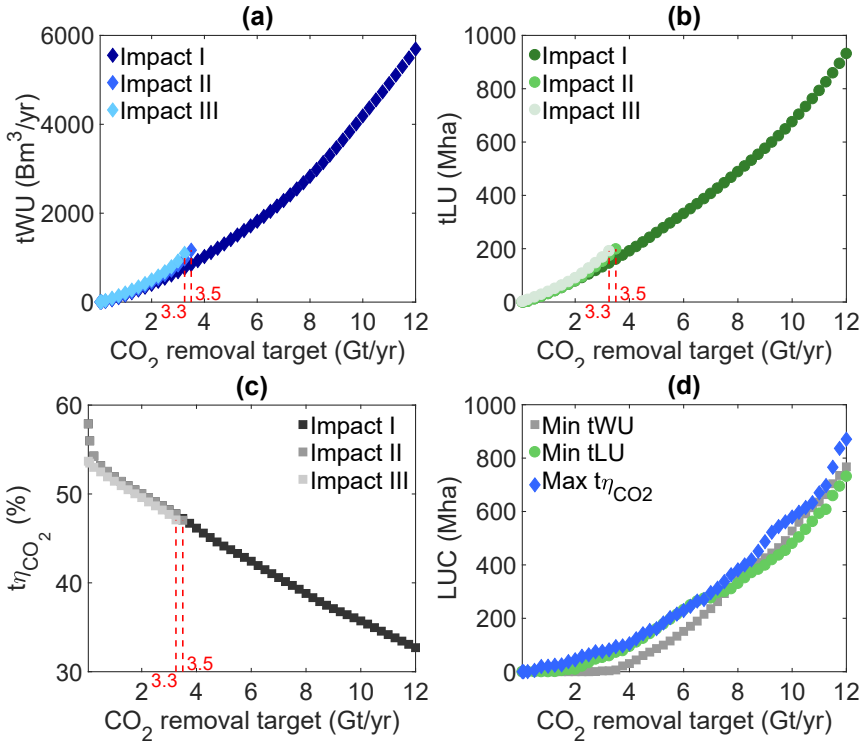


Figure 6.7: Minimal water use (a), minimal land use (b), maximal CO_2 efficiency (c) under impact scenario I (DEC on MAL), II (DEC on MAL and AR) and III (all land types, all crops) and land use change in impact scenario III under the three optimisation scenario (d).

Two insights can be derived from this thought experiment. First, the median world scale carbon dioxide removal can only be met in the impact scenario III, *i.e.*, when BECCS is deployed on all types of land and using crop residues in addition to dedi-

cated crops. As observed in Figure 6.7, by limiting bioenergy sourcing to dedicated energy crops from marginal land, up to 3.25 Gt_{CO_2}/yr can be removed by deploying BECCS and storing the CO_2 in the UK (a). Adding residues (b) – wheat straw in this study, only marginally increases BECCS carbon removal capacity, which reaches 3.5 Gt_{CO_2}/yr. Naturally, expanding the MONET framework by implementing other regions – Africa, Russia, Indonesia, Australia, in MONET, as well as climate-tailored biomass crops and agricultural residues would increase this carbon removal potential and nuance this statement, but this shows the potentially negative economic-environmental impacts associated with BECCS deployment at the gigatone scale.

Secondly, resource mobilisation and land use change increase exponentially with the CO_2 removal target. Removing 12 Gt_{CO_2}/yr would require at the minimum 5,700 Bm^3/yr, 930 Mha, and producing at the maximum 35 TJ/yr (net) at a maximum CO_2 efficiency of 33%, which, for comparison, is in the upper range of BECCS resource use in the literature. Smith *et al.* evaluated a land requirement of 380 – 700 Mha, and a marginal water requirement, as compared to the water consumption of a counter factual scenario, of 720 Bm^3 to meet a 12 Gt_{CO_2}/yr target [36]. In Heck *et al.*, removing 5 Gt_C/yr with bioenergy, resulting in a net removal of 8 to 10 Gt_{CO_2}/yr depending on the CO_2 efficiency of the process, requires between 1,000 and 4,000 km^3 of blue water use (no grey water considered), depending on the weighting of the objectives in the objective function [79]. This shows that though more CO_2 storage might be available in the UK, there is a limit beyond which CO_2 storage in the UK is no longer efficient, which confirms the need for multi-polar systems when deploying negative emissions at the gigatone scale.

6.5 Energy production or resource conservation?

In the final section of this paper, we focus on the technical element of the trilemma, *i.e.*, BECCS net electricity production potential. Figure 6.8 presents the total water use (a), land use (b), CO_2 efficiency (c), net electricity produced (d) and land use change (e) in the four optimisation scenarios, in the impact scenario I.

It is observed that energy maximisation presents much stronger trade-offs with the other metrics: water use, land use and land use change increase fivefold, and CO_2 efficiency decreases by 13 efficiency points, when maximising electricity production. This can be explained by the fact that, in order to maximise electricity production at a fixed CO_2 removal target, the ratio of energy production per amount of CO_2 removed needs to be maximised. This leads to the selection of regions featuring a high net electricity production, and/or a low net CO_2 removal, *i.e.*, in the latter, regions that are inefficient at removing CO_2 from the atmosphere. This results in a high water use, land use and low carbon efficiency. Another interesting insight from this analysis is that in the

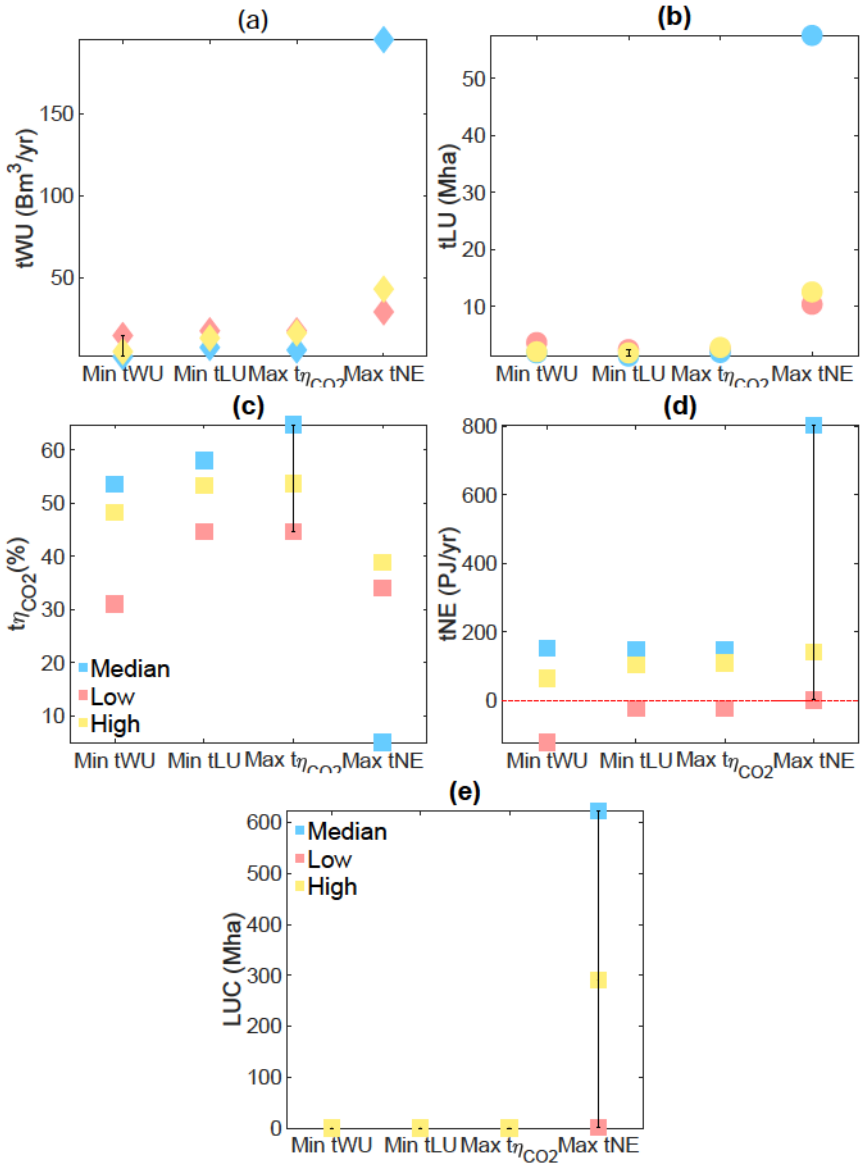


Figure 6.8: Total water use, land use, and CO_2 efficiency, in scenario I, and land use change (scenario III) under four objective functions, in the median, pessimistic and optimistic scenarios. Energy maximisation presents much stronger trade-offs with the other metrics: to maximise energy the ratio of energy production per CO_2 removed needs to be maximised, which results in a high water use, land use, low carbon efficiency and land use change. Only focusing on energy production and negative emissions is detrimental to BECCS environmental performance.

pessimistic scenario, the system cannot be net electricity positive.

All of these results highlight the strong trade-offs between net electricity production and CO_2 efficiency, which is consistent with what we observed in Chapter 5, and with other

studies in the literature [49, 74, 79]. In these studies, it was shown that BECCS services – CO_2 removal and electricity production – mutually exclude each other. However, this contribution takes the analysis further by showing that the duality is not only between electricity production and CO_2 removal, but for a given CO_2 removal target, between electricity production and BECCS land use, water use, CO_2 efficiency and land use change. One should therefore consider all of BECCS' KPIs when designing its supply chain, as focusing only on BECCS main services – CO_2 removal and electricity production – can ultimately counteract the ostensible positive environmental impact of BECCS.

Taking this point further, one can postulate the existence of a global BECCS supply chain which can satisfy both BECCS' energy production objectives and resource use constraints. Annual negative emissions requirements between 1.8 to 9.9 Gt_{CO_2} by 2050 have been predicted by integrated assessment models in order to maintain a 2°C trajectory, with median values around 7 Gt_{CO_2}/yr [37, 79]. Projections of primary energy delivered by BECCS in 2050 can be found between 35 and 120 EJ/yr depending on the scenario, with an average around 80 EJ/yr [11, 258, 259]. By removing 50 Mt_{CO_2}/yr in 2050, the UK would therefore be contributing to approximately 0.7% of the world CO_2 removal target. Assuming that the UK would remove CO_2 efficiently from the atmosphere, only 0.7% of the world marginal land available could therefore be mobilised to meet the UK CO_2 removal target. Using the 390-1,107 Mha from Cai *et al.* [114], the UK could therefore reasonably use up to 2.2-7.8 Mha of marginal land. By this contribution to global negative emissions, the UK should also theoretically supply 570 PJ/yr of primary energy, or generate approximately 170 PJ/yr of electricity. The droplets on Figure 6.9 represent the total electricity generated tE for different land constraints, under the energy maximisation scenario. Land use is separated in three zones: the 'safe' zone in green, where land use is constrained to 2.2 Mha, the uncertainty zone in yellow, where land use is constrained under 7.8 Mha, and the forbidden zone in red. The system's total water use is represented by the colour scale, and the total biomass use, by the size of the droplets. Energy production in the water, land and biomass minimisation are also represented for comparison by the triangles.

Figure 6.9 shows that, even while maintaining the total land use in a 'safe' zone (*i.e.*, inferior to 2.2 Mha), BECCS electricity production objective is met; the markers are outside of the grey area. Though maximising energy production drastically increases water, land and biomass use, it is nevertheless possible to reconcile BECCS energy generation objective with land use constraints. Similarly, the triangles representing the water, land and CO_2 efficiency minimisation and maximisation are also located in, or close to, the safe zone. Though there may be strong trade-offs between these resource efficiency indicators, they are all compatible with a safe land use. It is however worth noting that the same may not be said about other resources such as water, which

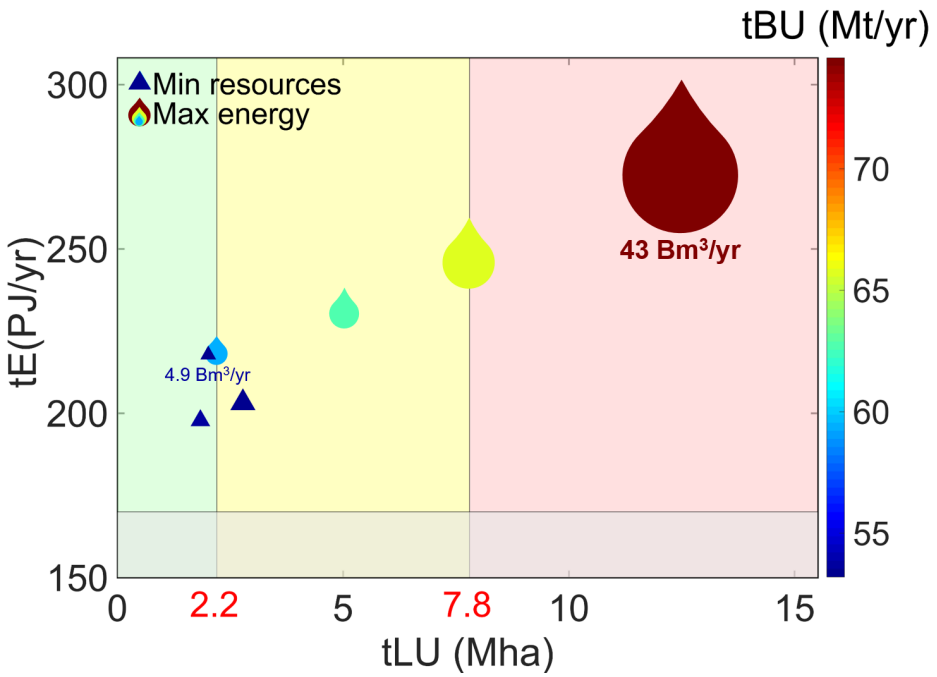


Figure 6.9: BECCS total electricity generated under different land constraints, in the energy maximisation scenario (droplets), and the water, land and CO_2 efficiency minimisation and maximisation scenarios (triangles). Water use is represented by the colour scale, and biomass use, by the markers' size. Even when land use is constrained to a 'safe' value (green zone), the UK electricity generation objective consistent with a 50 Mt_{CO_2}/yr target is met.

remains on the critical path to BECCS deployment.

6.6 Preliminary conclusions and discussion

In this chapter, we have identified the complex interactions existing between BECCS technical and environmental performance indicators. Assessing BECCS systems from a marginal cost per ton of CO_2 removed would therefore be incomplete. In particular, the strong trade-offs between water use and land use change, as well as between energy production and all of BECCS impacts, showed that one cannot optimise these systems from the perspective of a unique environmental impact. A sustainability standard which does not only regulate biomass maximum carbon intensity, but also BECCS water, land and CO_2 efficiencies, as well as land use change, will be required to ensure that BECCS is deployed within sustainable boundaries.

Growing perennial grasses on marginal land, whilst sustainable, might not be practical [260]. Actively engaging and incentivising all stakeholders of BECCS value chain, including farmers, will be crucial in unlocking BECCS deployment.

Furthermore, in meeting a regional carbon removal target, the prevalence of imported biomass in the optimisation results highlighted the predominance of parameters such as yield, CO_2 intensity of electricity, and climate data, over transport distance. Regions with good compliance with these parameters were repeatedly selected regardless of the CO_2 storage location. One implication of this is that BECCS policy frameworks will need to consider the logistics, and negative emissions accounting of a system where regions meet their carbon removal target with imported biomass. Another implication of this is, were CO_2 storage to be available in regions providing sustainable biomass, for example Brazil in this case study, a potential important share of the world carbon removal target could be achieved by a 100% Brazilian BECCS value chain. How much of the world carbon removal target could be met with this value chain, as well as the potential environmental and economic trade-offs between local and international value chains, are important research questions to tackle. If we take this thought experiment further in the context of meeting a global CO_2 removal target, it is conceivable that a region A meets its target using biomass feedstock from a region B to store CO_2 in a region C. Integrating the multi-polarity of negative emissions in the design of policy frameworks will likely be a crucial policy challenge for BECCS.

In the next chapter, we explore how these optimal BECCS value chains evolve in the context of meeting global CO_2 targets.

Chapter 7

Cost-optimal and sustainable BECCS deployment to meet global targets

7.1 Introduction

7.1.1 Objectives of this chapter

Whilst distinct in terms of economies and climates, China, India, USA, Brazil and the EU, according to IAMs, could be instrumental in deploying BECCS [261, 262]. In this Chapter, we explore the cost and resource optimal deployment of BECCS, and its evolution over time, under different cooperation and CO_2 storage availability scenarios. Our objectives are to (1) identify regional drivers of BECCS cost-optimal and sustainable deployment, and how it evolves overtime, with an evolving CDR target, changing energy system, and depletion of storage sites (section 7.2), (2) quantify the value of international collaboration on BECCS ability to deliver on climate targets at the lowest cost (section 7.3), and (4) explore the sensitivity of these results to regional CO_2 storage availability (section 7.4). The remainder of this introduction provides background on ways to allocate global targets to different regions, and BECCS cost evaluation in the literature.

7.1.2 Regional allocation of BECCS deployment

Peters and Geden *et al.* summarised BECCS optimal deployment across four IAMs, and show that China, USA, the EU, Brazil and India would provide alone between 33

and 65% of total CDR via BECCS [262], with on average China providing the highest share, followed by the USA, India, the EU and Brazil. It is however not clear that optimal deployment of BECCS (economic or otherwise) coincides with what regions *can sustainably* do (resource wise), nor with what they *should* do in terms of national climate targets.

For a range of bio-geophysical and socio-political reasons, not all regions are equally endowed in their ability to sequester CO_2 and produce biomass sustainably. For example, North America, Latin America, and Russia have been identified as regions with high potential for the production of energy crops on set-aside land [263, 264]. Whilst global CO_2 storage capacity is generally not considered as a bottleneck, regional assessments substantially vary in capacity and in reliability. Whilst the USA boasts over 8,000 $GtCO_2$ of storage with a 75-100% confidence, only 50 $GtCO_2$ have been identified in India, with a 56-75% confidence [41]. Futhermore, key IAMs assumptions including regional BECCS cost, carbon balance, as well as land and CO_2 storage availabilities remain relatively opaque [94]. For instance, 130 $GtCO_2$ of BECCS is deployed in India in some scenarios [262], which significantly exceeds current assessments of available CO_2 storage capacity in that region.

In addition to determining how much BECCS can be done in each region, in order to inform decision making, it is equally important to provide insight into how this CO_2 removal burden might be equitably distributed between a range of actors who are individually at different stages of development. The equitable allocation of carbon budgets is key in establishing the Nationally Determined Contributions (NDCs), and is a field of active research [262, 265, 266]. Burden sharing principles based on responsibility or inertia (present or historical CO_2 or GHG emissions), capacity (gross domestic product) or equality (population) have been proposed, but thus far no single principle has been unanimously agreed upon. A blended approach – for example weighting both population and emissions in the same equation [265] – provides an alternative, though 'fair' weighting factors are equally difficult to determine. What is already complex in the context of allocating emissions is even more so with carbon dioxide removal. A determining factor of this allocation will be whether CO_2 removal is done to a) offset past and residual emissions after maximum emissions mitigation efforts, or b) to compensate for today's lack of action and increasing emissions.

A prerequisite of these considerations is that climate change is globally tackled in a cooperative environment. Cooperation as a condition for effective climate change mitigation has been extensively discussed [267–270]. A common cooperative approach is that of 'climate clubs' [269], which are part of the wider category of 'public good' or 'voluntary' clubs. A climate club can be defined as a group of countries – typically smaller than the UNFCCC – that actively cooperate to reduce damages induced by climate change through international agreements (*e.g.*, an international carbon price),

and entice/maintain country membership through a set of club 'goods' or members-only incentives (*e.g.*, bilateral emissions trading or know-how exchange) [269]. Whilst, in principle, climate clubs involve all approaches to combat climate change, including mitigation, adaptation and removal, most of the literature focuses on climate change mitigation [269]. Studies have quantified the gains and identified the optimal structure of these climate clubs both at the global level [268, 270] and the state level (for example, cooperation between US states in Galan-Martin *et al.* [267]). As far as CO_2 removal is concerned, cooperation between countries is only mentioned in the context of research collaboration for advancing CCS, at the global scale [271] or the European scale [272]. However, there are inherent differences between the economic systems and enabling policies that deliver conventional mitigation and those that deliver carbon removal [8]. Both cooperation and collaboration involve countries working towards a common goal, but collaboration involves the creation of a physical output, through active exchanges between countries. Whilst mitigation can be done more effectively through cooperation alone, owing to the uneven distribution of key resources (*e.g.*, CO_2 storage or biomass), delivering large scale atmospheric removal of CO_2 is likely to require active collaboration.

7.1.3 BECCS cost in the literature

BECCS cost can vary significantly as a function of the technology, region and feedstock cost. In a recent review by Fuss *et al.*, BECCS costs in the literature could be found as low as \$17/tCO_2[1] and as high as \$446/tCO_2 [103]. BECCS pathways involving gasification (\$33-83/tCO_2), or fermentation (\$22-195/tCO_2) are typically cheaper than ones involving combustion of the biomass (98 to \$321/tCO_2), which can be explained by the lower cost of pre-combustion CO_2 capture or capture from fermentation, as compared to post- or oxy- combustion capture.

There are however significant overlaps between each technological route, and uncertainty ranges can be explained by different assumptions regarding counterfactual scenarios, feedstock cost, plant capital cost (CAPEX) and choice of boundaries for the cost and CO_2 balance. A significant amount of costs in the literature are presented as avoided costs, *i.e.*, the cost of the BECCS process (absolute or relative to an unabated technology) per ton of CO_2 avoided as compared to an unabated counterfactual. Abanades *at al.* calculates the cost of BECCS oxy-combustion plant with calcium looping to be between \$41 and \$83 per ton of CO_2 avoided as compared to a coal plant [273]. In Sanchez *et al.* the cost of CO_2 avoided of a BIGCC plant varies between \$69/tCO_2 when a coal IGCC plant is considered as the counter factual, and \$85/tCO_2 when a natural gas plant is considered as the counterfactual [274]. Whilst these values

[1] All cost data is in 2018\$

are relevant when comparing different decarbonisation technologies, there are not useful when comparing different carbon dioxide removal technologies.

To compare different dioxide removal technologies, calculating the absolute cost of CO_2 removal (*i.e.*, not inclusive of power generation revenues, or relative to an unabated counterfactual) is more insightful. However, the amount of CO_2 captured at the plant does not necessarily coincide with the amount of net CO_2 removal, when accounting for upstream supply chain. When accounting for the whole emissions, the amount of CO_2 removal can be much lower than the amount of CO_2 physically captured at the BECCS plant, which results in the cost of CO_2 removal being higher than cost of CO_2 captured. In Laude *et al.*, the cost of BECCS via bioethanol increases from \$51-154/tCO_2 when only CO_2 from fermentation is captured (case A), to \$231-256/tCO_2 when CO_2 from an auxiliary boiler using residual biomass (case B). However, a carbon balance on the whole value chain performed in this study shows that case A is actually not carbon negative when including the feedstock upstream emissions, and case B is only slightly carbon negative [275]. The cost of CO_2 removal would therefore actually be infinite in case A, and higher than \$231-256/tCO_2 in case B, which would be consistent with other CO_2 removal costs assessments for the same technology including value chain GHG emissions, which were evaluated between \$260 and \$432/tCO_2 [44]. Similarly, in Johnson *et al.*, the cost of BECCS increases from \$22-43 per ton of CO_2 captured, to about \$260-270/tCO_2 per negative emissions generated [140]. In Ranjan *et al.* a sensitivity analysis on BECCS avoided cost to upstream emissions is performed, and BECCS cost increases from \$173/tCO_2 with no upstream emissions, to \$460/tCO_2 when upstream emissions account for 60% of the CO_2 captured at the power plant [241].

Lastly, regional factors likely to directly impact BECCS cost are the capital cost of the BECCS plant, and the biomass feedstock cost. Among studies performed in a European or UK context, some CAPEX assumptions/calculations for BECCS power plants can be found as low as \$1,700-2,740/kW [276, 277]. In Yi *et al.*, it is assumed that adding CO_2 capture to a biomass plant only results in a \$56/kW CAPEX increment, as compared to the \$1,524/kW CAPEX increment between an unabated coal plant and a coal plant with CO_2 capture [276]. At the other end of the cost range, more conservative CAPEX values for BECCS power plants can be found around \$5,940-6,280/kW [278, 279], with cost reductions assumptions by learning and economies of scale resulting in costs around \$3,880-4,630/kW [278, 279][2]. In the IEA 2016 World Energy Outlook cost assumptions, CAPEX values for Europe and the US are significantly higher (\$3,722-6,380/kW) than CAPEX values in China or India (\$2,610-3,160/kW) [279]. This can be explained by differences in cost of capital, material and labour between regions.

[2]The CAPEX of a BECCS power plant was calculated using the differential CAPEX between a coal + CCS plant and coal power plant, and adding it to the CAPEX of a biomass power plant [279].

Another factor with a significant impact on BECCS cost is the biomass feedstock cost. Factors such as electricity and fuel costs, material and fertiliser cost, and biomass yield in the case of dedicated energy crop, result in a potential wide range of feedstock cost. Whilst prices for baled corn stover in China can be found as low as \$8/MWh of biomass primary energy [280], miscanthus pellets production costs in the UK can be found between \$17 and \$27/MWh [281]. Biomass feedstock cost also significantly increase with transport, with the cost of imported wood pellets in the UK between \$37 and \$52/MWh [278, 282]. Biomass feedstock cost is also likely to increase as the bioenergy demand increases [44]. In a BECCS cost IEAGHG report, biomass feedstock cost is projected to increase from \$20/MWh when global bioenergy demand is only 4 EJ, to \$260/MWh if global bioenergy demand increases to 74 EJ. Projecting the trajectory of BECCS cost over time is therefore not straightforward. Whilst technology learning and economies of scale could bring down the capital and operating costs of BECCS over time, the upward trajectory of biomass feedstock cost could cancel out/outweigh this trend.

There is therefore a great deal of heterogeneity among techno-economic assessments of BECCS when it comes to the following assumptions: 1) terminology/definition of the cost results presented, for example per ton of CO_2 avoided as opposed to captured; 2) counterfactual scenario chosen; 3) choice of boundaries to perform the cost balance, in particular which stages of the value chain are included in the economic analysis; 4) choice of boundaries to perform the carbon balance, in particular which supply chain emissions are considered to calculate the net negative emissions potential as opposed to the gross negative emissions potential of the process, and 5) critical cost assumptions including feedstock costs and plant capital cost. These result in a great variation in BECCS cost, and renders the comparison process from one study to another difficult.

7.2 Drivers of BECCS cost

7.2.1 BECCS cost in different regions

In order to explore the main drivers of BECCS cost, we first evaluate different supply chain configurations, and quantify the total cost per ton of CO_2 removed in different regions, using either local or imported biomass (Figure 7.1).

Overall, factors such as the plant CAPEX, feedstock processing and transport, are key drivers of BECCS cost. Whilst importing biomass from high productivity regions can be preferable from a resource minimisation perspective [6], using local biomass

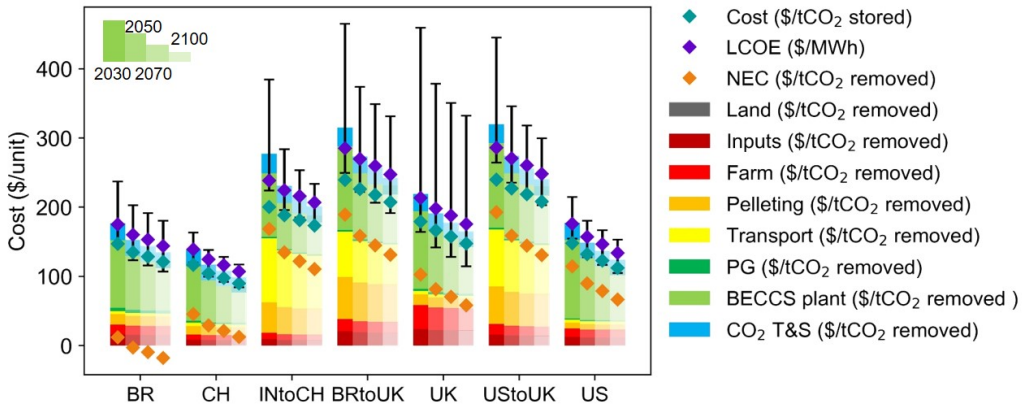


Figure 7.1: BECCS cost per ton of CO_2 removed (bars), per ton of CO_2 stored (green diamond), per MWh (purple diamond), and breakeven NEC (orange diamond) in Rio de Janeiro, Brazil ('BR'), Hainan, China ('CH'), Georgia, US ('US') and the UK ('UK'), using local or imported ('INtoCH', 'BRtoUK, 'UStoUK') biomass. Using imported biomass can substantially increase the cost of removal because of added cost and emissions of biomass transport. Cost variability (error bars) is largely driven by feedstock yield. BECCS cost decreases over time primarily because of CAPEX reduction, followed by reduced supply chain emissions due to decarbonisation of the energy system. In countries with low cost of BECCS and high cost of electricity, the NEC can become negative (*e.g* Brazil). (T&S = Transport and Storage)

consistently appears to be more cost effective, assuming these broader sustainability aspects are treated as externalities. The cost of removal in each region varies as a function of supply chain configuration. A key parameter impacting these variations is the feedstock yield. In the UK, a high yield range has been noted for energy crops in the literature [158, 191, 283], which explains the wider error bar. This shows that improved yield in the UK could bring BECCS cost close to that in other regions. Figure 7.1 also quantifies the total cost per ton of CO_2 stored, which is distinct to the cost per ton of CO_2 removed, emphasising the importance of considering BECCS value chain GHG emissions when evaluating BECCS cost. Importantly, as the energy system becomes decarbonised, the gap between the cost per ton of CO_2 removed and the cost per ton of CO_2 stored decreases.

If CO_2 removal is considered to be a common good, it is natural to assume that this service could be directly rewarded. Akin to the carbon price which penalises emitters, this incentive scheme could take the form, for example, of a negative emissions credit (NEC) [8, 74, 284, 285]. Figure 7.1 also represents the levelised cost of electricity of a BECCS plant, and the NEC required for the revenues from electricity generation and CO_2 removal equates the total system cost, referred to as 'breakeven NEC' in this study. In regions with low cost of BECCS and high electricity price (see Tables B.17, B.18 and

B.19 in Appendix B, the NEC becomes negative (*e.g.*, Brazil) in the second half of the century. BECCS cost is thus found to be region specific, with obvious implications for NEC trading.

7.2.2 BECCS deployment: where, when and how much?

In this section, we determine region-specific trajectories for the cost-optimal deployment of BECCS over time, subject to biomass and land availabilities, water risk and CO_2 storage capacity constraints, as well as an annual CO_2 removal target. Figure 7.2 illustrates cumulative biomass production (colouring) and CO_2 storage (markers) by the end of the century, for a low (7.2a,7.2b) and high (7.2c,7.2d) biomass availability, and a low (7.2a,7.2c) and high (7.2b,7.2d) CO_2 removal target.

At low targets, biomass is not a limiting factor and activity tends to be concentrated near CO_2 storage sites owing to the high cost of biomass transport. BECCS is primarily deployed in China and eastern US, whilst its deployment is limited in EU and Brazil, and non-existent in India. For the EU, this can be explained by higher costs and low availability of marginal land. For Brazil and India, it was considered that no or little CO_2 storage was available in Brazil and India, due to lack of quantitative data (see Tables B.21 and B.22 in Appendix B), which acts to limit BECCS deployment in these regions. At higher targets however, most regions become crucial in reaching higher levels of removal. BECCS is largely deployed in the EU, and biomass from regions with no/less CO_2 storage (Brazil, India) is shipped to closest storage sites. This naturally leads to a more expensive system, with a 57% increase in cumulative cost of removal (per tCO_2). Higher targets cannot be met only using energy crops on marginal land. When biomass supply is limited in this way, a maximum of 176 $GtCO_2$ (4.3 $GtCO_2$/yr by 2100) can be removed between 2030 and 2100, compared to the target of 237 $GtCO_2$ (58% of 408 $GtCO_2$, the P3 target). The target can only be met in the high biomass availability scenario, when additional land (*e.g.*, cropland, grassland or forests) is made available for biomass production, in addition to crop residues. In this case, with an average cost of electricity of \$103/MWh, and an average BECCS carbon intensity of -0.91 tCO_2/MWh, the global breakeven NEC decreases back to \$38/tCO_2. The expansion of bioenergy production on managed and natural land could, however, have unindented consequences on the economy or the environment.

BECCS cost-optimal deployment also varies with the configuration of the biomass supply chain (*e.g.*, yield). Figure 7.3 illustrates how cumulative biomass production, CO_2 storage, and total cost of removal changes as a function of these choices.

Total cost of removal is found to decrease by 16-18% in the optimistic scenario and increase by 26-27% in the pessimistic scenario, while the global breakeven NEC is found

as low as \$12/tCO$_2$ under a low target, and as high as \$163/tCO$_2$ under a high target. The structure of the supply chain, however, remains globally unchanged. This confirms that our findings regarding the relative importance of each region in deploying BECCS are robust.

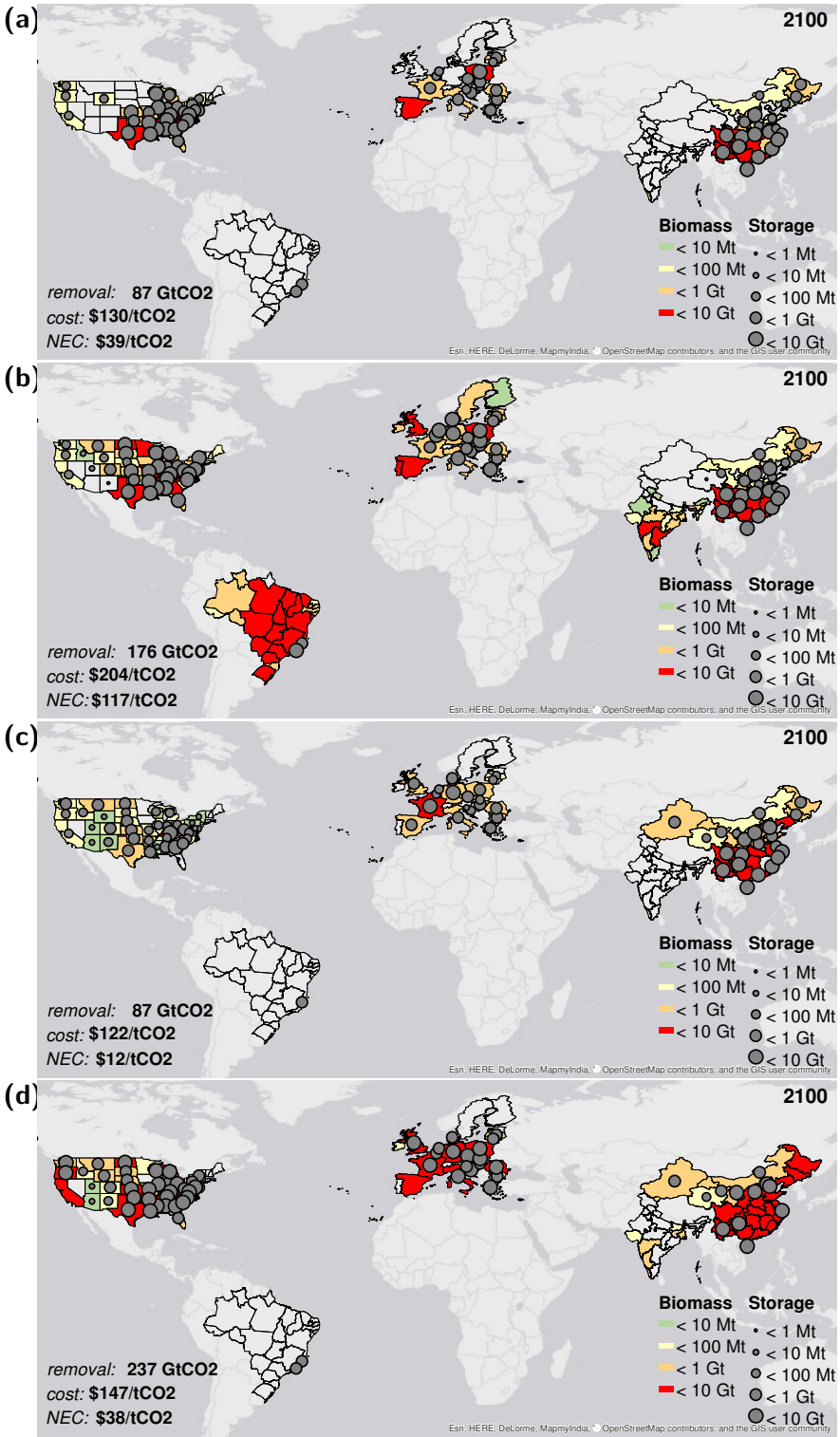


Figure 7.2: Cost-optimal BECCS deployment in a low (a,b) and high (c,d) biomass availability scenario, and for a low (a,c) and high (b,d) CO_2 removal target. Cumulative biomass production is represented by the colouring of the cells, while cumulative CO_2 storage by the size of the markers. At low targets, China and the US see most of BECCS deployment. Expanding biomass production on other types of land enables to meet both targets at lower costs, but could have unintended economic-environmental consequences.

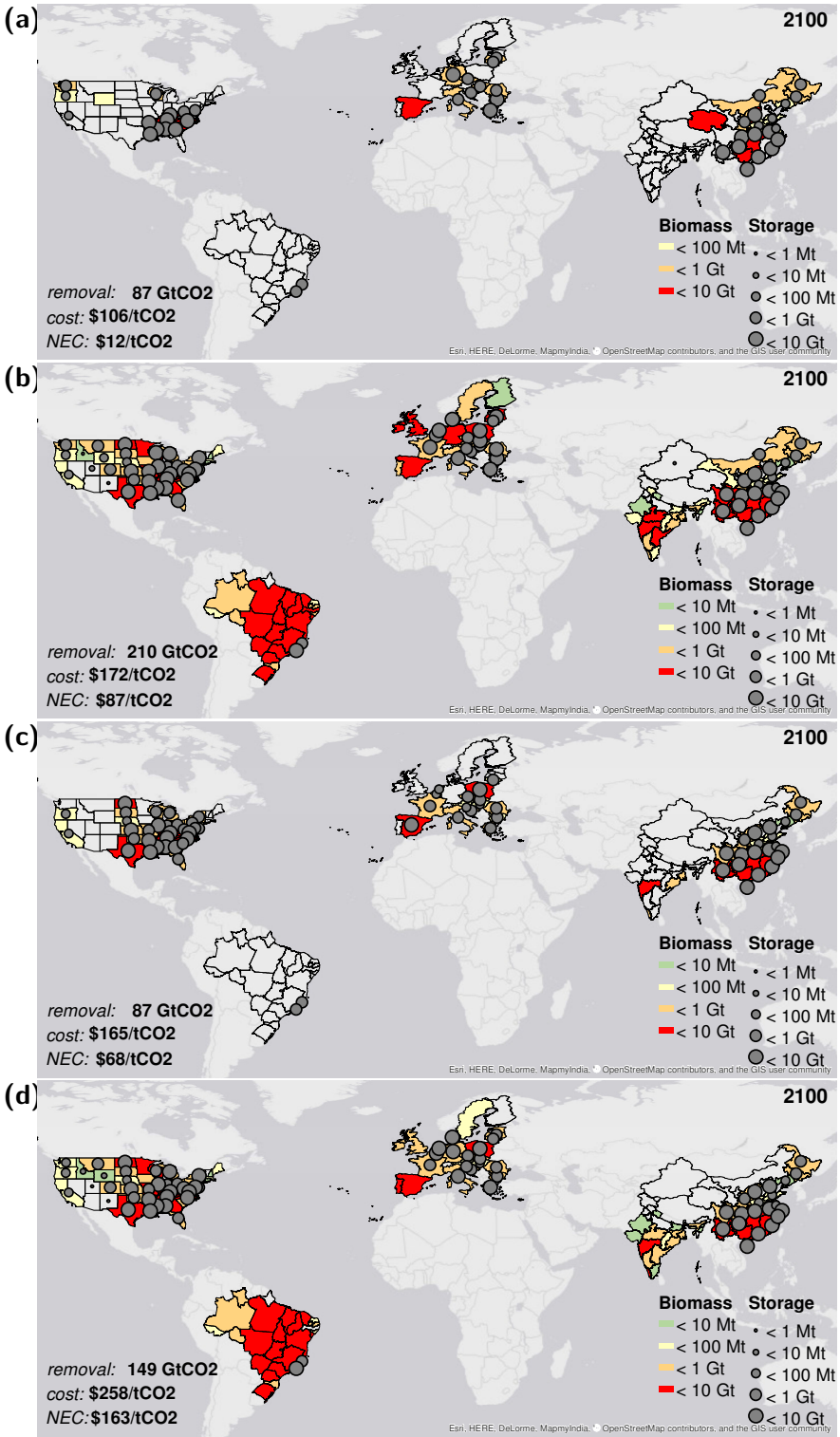


Figure 7.3: Cost-optimal BECCS deployment in the biomass supply chain sustainability optimistic (a,b) and pessimistic (c,d) scenarios, for low (a,c) and high (b,d) CO_2 removal targets, in the low biomass availability scenario. Cumulative biomass production is represented by the colouring of the cells, while cumulative CO_2 storage by the size of the markers. The total cost of removal is found to vary within 20% of the central scenario. The structure of the supply chain, however, remains globally the same.

7.2.3 BECCS cost curve

As shown in Figure 7.2b, BECCS average cost of removal can increase significantly when BECCS deployment impinges upon planetary boundaries. BECCS cost curve at the end of the century is represented in Figure 7.4, in a limited biomass scenario, for low (7.4a) and high (7.4b) targets. To account for revenues from electricity generation, the equivalent NEC cost curve is represented in Figures 7.4c and 7.4d. The colour of the dots indicates where the CO_2 is stored, while the coloured areas indicate cost ranges and potential of alternative CDR methods. While we acknowledge that alternative CDR methods might include biochar, enhanced weathering and land restoration, we only represent representative costs of afforestation and direct air capture, as examples of a natural CO_2 removal method (here afforestation) and a arguably more expensive engineered CO_2 removal method which does not face the same resource constraints as BECCS (here direct air capture).

At low targets, the cost of BECCS plants operating in different countries increases from \$100-110/tCO_2 removed in China, to \$120-140/tCO_2 removed in the USA/EU. In order to meet higher targets, biomass feedstock further from CO_2 storage sites is utilised, thereby increasing feedstock supply chain emissions and cost. Whilst Figure 7.2 shows that the average cost in this scenario is \$200/tCO_2 removed, Figure 7.4 shows that increasing CO_2 removal targets leads to the mobilisation of BECCS configurations removing increasingly marginal amounts of CO_2, at a removal cost higher than \$350/tCO_2 removed, and up to \$1,100/tCO_2 removed. To put these numbers in context, the cost range and CO_2 removal potential of alternative CDR methods [103], afforestation and direct air capture, are represented in Figure 7.4. BECCS cost curve is found to be higher than afforestation and lower than direct air capture. When accounting for revenues from electricity generation, the net cost of BECCS (equivalent to the NEC), is found to be competitive with afforestation in certain regions. This implies that a portfolio of CDR methods will be required, with the composition of this portfolio varying in time and space. It is important to note that the cost and potential values used for afforestation and direct air capture are estimates subject to the same case-to-case, and regional, variability as BECCS. Additionally, the portfolio of CDR methods is not limited to these three technologies, but also involves methods such as enhanced weathering, biochar and ocean fertilisation. Further research exploring the co-deployment of different CDR methods, under the same boundaries and set of assumptions, is required to determine how much and where the deployment of each technology is best suited, if at all, and to quantify and qualify the potential for synergies between different options.

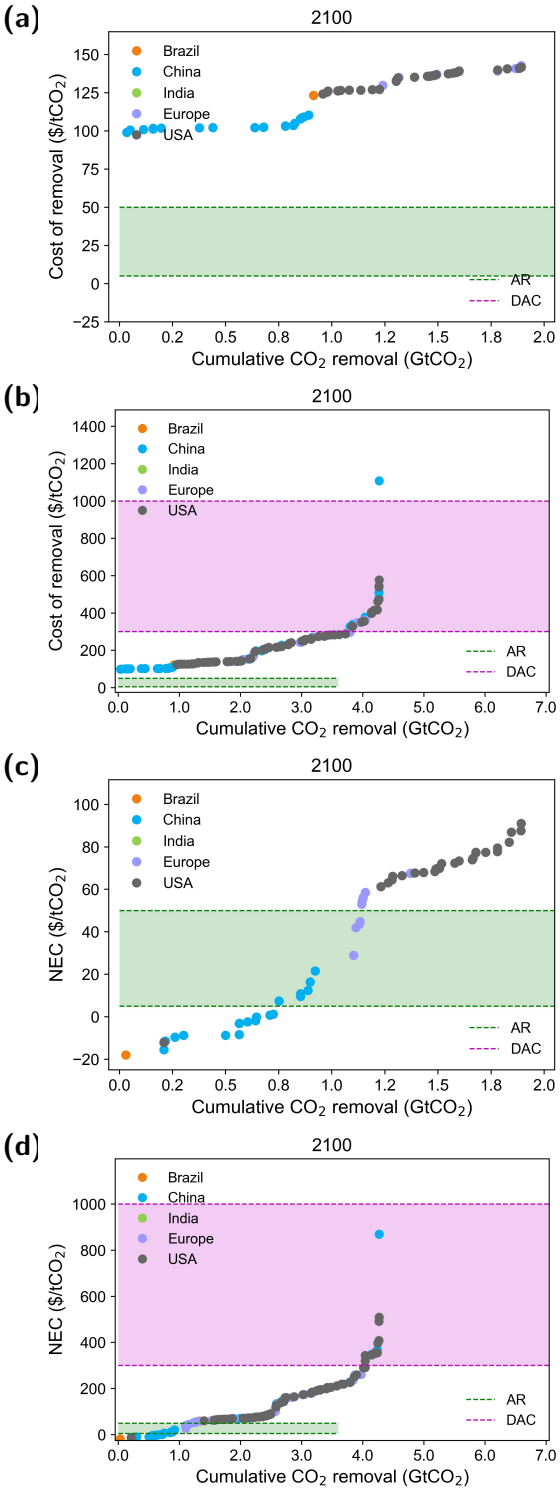


Figure 7.4: BECCS cost (a,b) and NEC (c,d) curves in 2100 with low biomass availability at a low target (a,c) and a high target (b,d). When biomass is limiting, BECCS is no longer cost effective, which indicates opportunities for alternative CDR methods (AR = afforestation, DAC = direct air capture, cost data ranges from Fuss *et al.* [103]).

7.2.4 Does electricity generation matter?

BECCS has the co-benefit of generating electricity in addition to removing CO_2 from the atmosphere. The value of electricity is greatly dependent on the structure of the electricity system, as well as the prevailing policy environment, and therefore robust prediction of electricity prices is challenging. In this thought experiment, we assume regional electricity prices remain constant over the century, and minimise the breakeven NEC, with results presented in Figure 7.5.

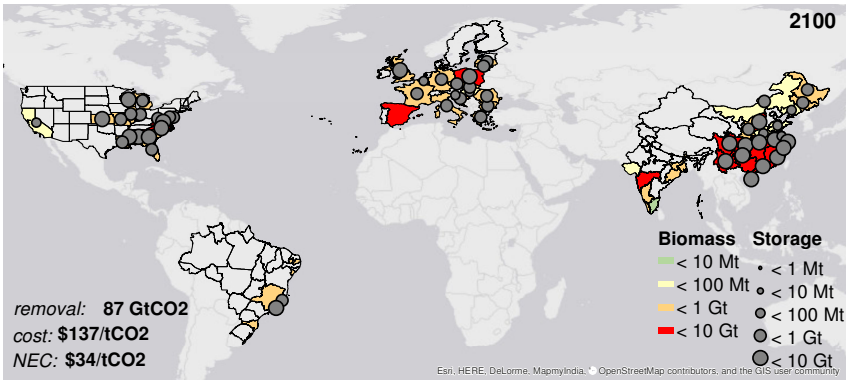


Figure 7.5: Cumulative biomass production (colouring) and CO_2 storage (markers) over time at low target, low biomass supply, when minimising cumulative net BECCS cost. Due to higher electricity prices, the EU plays a larger role, surpassing the US in terms of CO_2 removal, than when minimising total cost. With an average electricity price at \$96/MWh and an average BECCS carbon intensity at -0.93 tCO_2/MWh, the NEC decreases to \$34/tCO_2.

It is observed that when accounting for electricity revenues in BECCS total cost, China remains the main provider of CO_2 removal. However, a structural change in BECCS cost-optimal deployment is that the EU provides more CO_2 removal than the US, owing to higher electricity prices in the EU. The breakeven NEC decreases to \$34/tCO_2. Considering the value of electricity generation, higher BECCS cost regions such as the EU could play a more important role than might have otherwise been assumed.

7.3 CO_2 removal: *cui bono?*

Naturally, cost-optimal deployment might greatly differ from what a fair regional distribution of the global CO_2 target might be. In the previous section, a global CO_2 removal target was met in a cost-optimal and collaborative manner, regardless of the countries' individual target. Some regions might be providing more or less CO_2 removal than they ought to, effectively doing CO_2 removal on behalf of other regions, either because of a higher cost, or a lack of resources. In the context of mitigation, certain groups of

countries – EU Emissions Trading Scheme (EU ETS) is one example – are able to trade emissions at a market-adjusted carbon price, effectively having countries abating emissions on behalf of others. In a theoretical CO_2 removal climate club, countries could trade these negative emissions credits, effectively having regions removing CO_2 on behalf of others. Other membership benefits could involve, for example, trading biomass feedstock at preferential border tariffs. In this section, we attributed a CO_2 removal target to each region, and calculated the CO_2 removal 'surplus' or 'deficit' of each region (see section 3.4.2 in Chapter 3). Figure 7.6 shows annual levels of CO_2 removal surplus and annual CO_2 removal cost (right axis) under the four biomass availability/target scenarios.

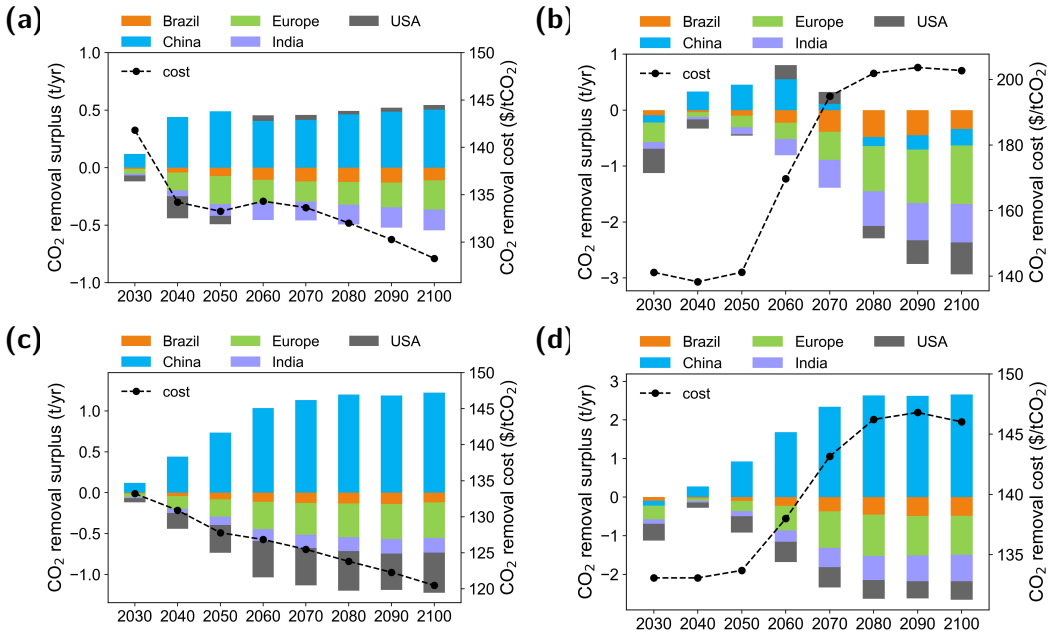


Figure 7.6: CO_2 removal surplus (left axis) and annual CO_2 removal cost (right axis) in the low (a,b) and high (c,d) biomass availability, and low (a,c) and high (b,d) CO_2 removal targets scenarios. Regions with high CO_2 storage and high low cost biomass availability (*e.g.*, China) provides most of the CO_2 removal surplus across the century.

At low targets (7.6a,7.6c), BECCS total cost does not significantly increase over time, which shows that CAPEX reductions of BECCS plants and decarbonisation of the energy system compensate for the increasing CO_2 removal target. However, the trend shifts at higher targets (7.6b,7.6d) when biomass and CO_2 storage supply become active constraints. An important conclusion is that countries with well distributed, high capacity, CO_2 storage, as well as cheap biomass supply (China in this study) accumulates significant surplus, thereby providing significant value to other regions.

The premise that a few countries may be doing CO_2 removal on behalf of others as-

sumes that countries are allowed to trade negative emissions credits. Equally, some scenarios rely on having countries or regions with low CO_2 storage capacity, but with abundant biomass supply (Brazil in this study), send biomass to regions with high CO_2 storage capacity, implicitly assuming biomass trading flows between regions. A lack of 'collaboration', by trading neither NEC nor biomass, could incur two risks: 1) unmet CO_2 removal target 2) higher cost of removal. Figure 7.7 explores the impact of collaboration on these two dimensions, by representing the total cost of removal as a function of cumulative CO_2 removal across the century, in different trading scenarios, at low (7.7a) and high (7.7b) targets. Squares represent scenarios where NEC trading is constrained, crosses where biomass trading is constrained, and diamonds where both are constrained.

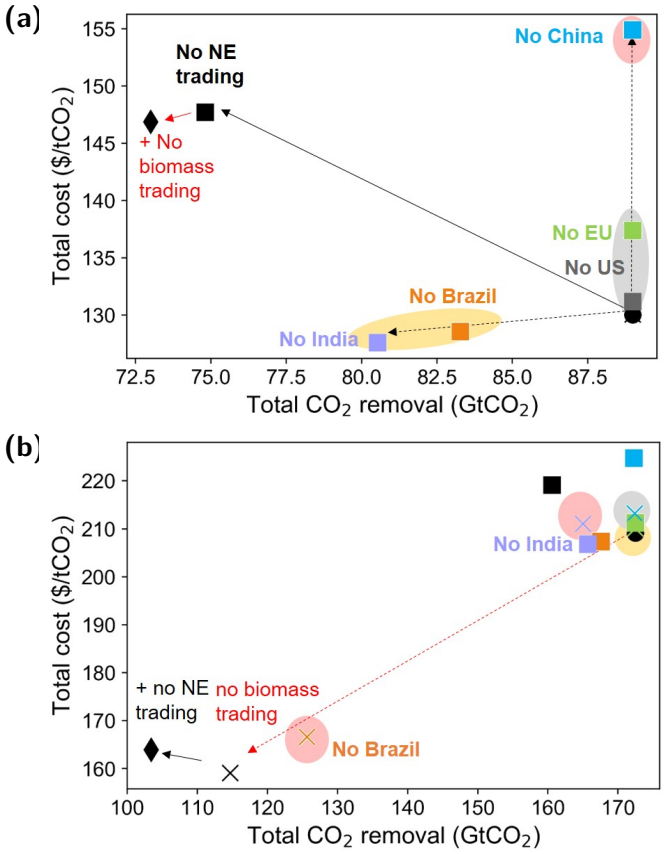


Figure 7.7: Total cost of removal and cumulative CO_2 removal under full collaboration (circle), negative emissions trading constraints (squares), biomass trading constraints (crosses) or both (diamonds), for specific (colours) or all (black), under a low target (a) and a high target (b) scenario. Without/with less collaboration, total cost of removal can increase by up to 14%, and cumulative CO_2 removal by down to 65 $GtCO_2$

At low targets (7.7a), trading NECs has a first order impact on CO_2 removal and cost

of removal. In a scenario without NEC trading, the global cumulative target is missed by 14 $GtCO_2$, and total cost of removal increases by 14%. Trading biomass however has a lesser impact, and constraining biomass trading in addition to NEC trading further decreases cumulative CO_2 removal by 1 $GtCO_2$.

We can also quantify the individual impact of integrating a particular region in the NEC trading market (coloured squares). In doing so, we see that different players bring different value when trading NECs. A first category of players stand out as 'Independent providers' (in red), *i.e.* regions with good storage availability, low cost and low carbon biomass close to storage sites (*e.g.*, China). Excluding these regions from the collaboration leads to a much higher cost (here 19%) as they can no longer provide surplus for other regions. Another emerging category includes the 'independent beneficiaries', *i.e.* regions with good storage and biomass availability but higher cost, (*e.g.*, EU and US). Excluding them from the collaboration leads to a higher cost if excluded as they have to fulfil their own targets, but the target is still met. Finally the 'dependent beneficiaries' are regions which are unable to meet their own targets due to lack of storage (*i.e.*, Brazil and India).

When targets are higher, and biomass becomes a limiting factor (7.7b), trading biomass (x) has a much higher impact than trading NECs (squares). When biomass cannot be traded, cumulative CO_2 removal decreases by 65 $GtCO_2$. The value of players in trading biomass also changes (coloured crosses). Regions with high biomass availability (*i.e.*, Brazil and India) emerge as critical biomass providers: limiting the trade of Indian, and to a greater extent Brazilian, biomass decreases total removal potential. In this scenario, regions such as China are non-critical biomass providers: limiting the trade of Chinese biomass slightly impacts the cost (1% increase) but does not compromise meeting the target. Finally, regions such as the EU and US are non-critical biomass beneficiaries: limiting the trade of EU and US biomass does not impact the cost nor the ability to meet the target.

The value of different regions in trading negative emissions and/or biomass therefore differs on CO_2 removal targets and which element – biomass or storage – is critical and/or limiting in achieving these targets. Some regions can be alternatively providers and beneficiaries, and in all cases, full collaboration leads to the highest chance of meeting global targets at the least cost. Whilst international cooperation is required to agree on regional responsibility to contribute to climate change mitigation and removal, active collaboration between regions, is essential to meet global CO_2 removal targets.

7.4 Sensitivity to CO_2 storage capacity

These results are highly dependent on assumptions as to how much CO_2 storage is available in each region. In this section, we explore the impact of having more storage in Brazil, and storage at all in India, on BECCS cost-optimal deployment Figure 7.8), and the value brought by each region to the collaboration (Figure 7.9).

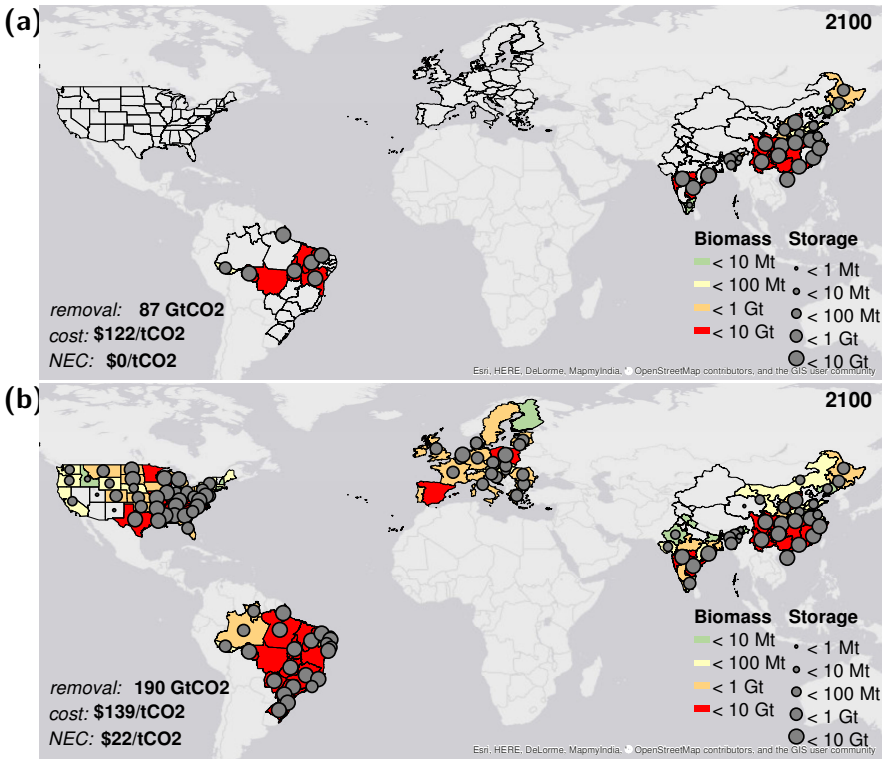


Figure 7.8: Cost-optimal BECCS deployment over time for a low (a) and high (b) CO_2 removal target, in the high CO_2 storage capacity scenario. Cumulative biomass production is represented by the colouring of the cells, while cumulative CO_2 storage by the size of the markers. With CO_2 storage available in all regions, Brazil, China and India become the key providers of CO_2 removal. The global breakeven NEC is zero at a low target (a).

At low targets (P2), if storage is available in India and Brazil, India, Brazil and China are the only regions providing CO_2 removal to minimise total cost. Total cost only decreases by 6% as compared to when storage is limited in India and Brazil. As Brazil provides a high share of the global removal target, the global breakeven NEC is found to be zero. At higher targets however, total cost decreases by 32% as compared to the base case scenario, and cumulative CO_2 removal potential increases by 14 $GtCO_2$. The value of players in trading negative emissions and biomass also changes with storage in Brazil and India, which is represented in Figure 7.9.

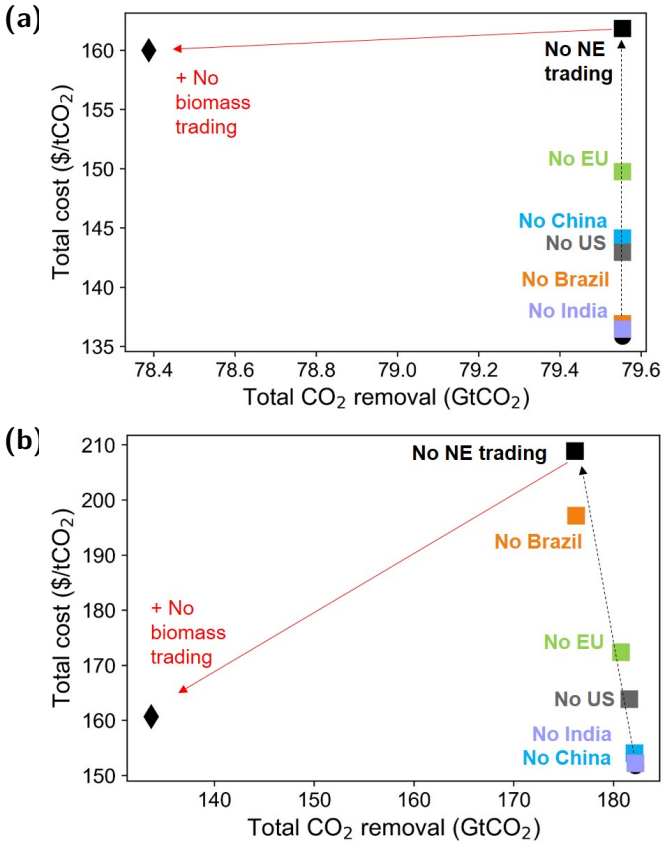


Figure 7.9: Total cost of removal and cumulative CO_2 removal under full cooperation (circle), negative emissions trading constraints (squares), biomass trading constraints (crosses) or both (diamonds), for specific (colours) or all (black), under a low target (a) and a high target (b) scenario, when CO_2 storage in Brazil and India is available. Brazil becomes a critical provider of negative emissions.

At low target (7.9a), the target is always met, except when neither negative emissions nor biomass trading is allowed between countries. Trading negative emissions with the EU becomes the larger cost driver, with the total cost increasing by 10% when the EU meets its target alone (independent beneficiary). At higher targets (7.9b), Brazil is a critical independent provider, with a cost increase of up to 29% when Brazil meets its target alone, and a 9 $GtCO_2$ decrease in CO_2 removal. This shows the importance of the availability of well distributed storage sites in lowering the cost of BECCS, and identifying the critical players in delivering cost-effective CO_2 removal.

7.5 Preliminary conclusions and discussion

In this Chapter, we elucidate the mechanisms behind cost-optimal BECCS deployment and how it evolves over time, with an increasing CO_2 removal target, the depletion of CO_2 storage sites and the decarbonisation of the energy sector. At low targets, when bioenergy supply is not a limiting factor, the cumulative cost of CO_2 removal decreases over time, which shows that decarbonisation of the energy sector and BECCS plant potential capital cost reductions may outweigh a potential cost increase from scaling up bioenergy production. At higher targets however, when reaching biophysical limits in biomass supply, BECCS removal cost can increase past the \$100-350/tCO_2 range, which indicate deployment opportunities for potentially more expensive, but less water and land intensive, carbon dioxide removal technologies (*e.g.*, direct air capture). It should be noted that these results are very sensitive to i) the amount of marginal/set aside land considered in this study, which is relatively uncertain and likely to vary over time, ii) the range of feedstock considered, which was limited to energy crops and wheat straw, and could be extended to all forestry and agriculture residues, wastes and marine biomass, iii) the burden sharing assumptions used to downscale the global target to the cumulative target of Brazil, India, China, the EU and the US (see section 3.4.2 in Chapter 3), iv) the fact that regions with potentially large BECCS potentials relative to their CO_2 removal targets (*e.g.*, Africa, Russia, Canada) have not been considered in this study. They however illustrate how pushing biomass availability boundaries can increase the total removal cost via BECCS.

When accounting for the value of electricity, the structure of the cost-optimal BECCS value changed, with the EU – with higher cost BECCS but also high wholesale electricity price – playing a larger role than the US in delivering negative emissions. These tendencies are naturally very dependent of the regional value of electricity, which is likely to evolve as the structure of regional energy system changes. The value of electricity will also greatly impact the incentives mechanisms required for BECCS systems to be financially viable.

It was observed that storage availability in India and Brazil would qualitatively and qualitatively impact BECCS cost-optimal deployment. This warrants for the need for a better characterisation of CO_2 storage sites at the regional level, particularly in regions which would are critical to meeting CO_2 removal targets at the lowest cost. This is particularly true in a collaborative world, where critical providers of CO_2 removal meet most of the world's target on behalf of other regions, in order to minimise resource and financial costs.

Finally, we quantified the value of critical regions collaborating within 'CO_2 removal clubs' to achieve CO_2 removal targets. An important finding is that inter-regional cooperation – in establishing regional targets – and collaboration – in trading negative

emissions credits and biomass – are central to sustainably and affordably meeting these targets, with important value creation opportunities for key providers of CO_2 removal.

Chapter 8

Conclusions

8.1 Conclusions and contributions made

In this dissertation, we have presented a modelling and optimisation framework of BECCS full value chain, from biomass production to CO_2 storage, and applied it to four case studies to answer the following questions: 1) Does BECCS deliver resource efficient negative emissions?, 2) Does BECCS provide energy?, 3) What are the trade-offs within BECCS resource nexus?, and 4) What are the geophysical and geopolitical drivers of BECCS cost-optimal deployment? In this section, we summarise the findings of the dissertation, and discuss the limitations of, potential improvements to, and further research questions which could be explored with the MONET framework.

8.1.1 Does BECCS deliver resource efficient negative emissions?

In Chapter 4, the modelling tool was first used in order to calculate the water and carbon footprints of a range of biomass fuels – miscanthus, switchgrass, willow, and wheat straw – grown on different land types and imported from selected regions of the world. Among energy dedicated crops, herbaceous biomass (miscanthus and switchgrass) were found to be more sustainable with respect to the three metrics, mainly because of the lower yield and higher moisture content of woody biomass. Overall, including direct and indirect land use changes had the most important impact, accounting for over 50% of biomass carbon footprint. Aside from land use change, important contributors to biomass carbon footprint were biomass transport for low moisture biomass, and transport, chemical input and processing for high moisture biomass. Drying and grinding energy costs are physically bound by biomass properties. Other biomass processing practices such as natural field drying, or torrefaction for grinding will have to be investigated to reduce these inputs.

Supply chain carbon, water and land footprints were implemented in the context of a 500 MW BECCS facility to evaluate the impact of the biomass supply chain on of the overall plant carbon intensity and water intensity. The results showed a substantial impact on water and carbon intensities at high co-firing proportions. Including direct and indirect land use changes had great impact on the power plant carbon intensity, narrowing the range of operability for the power plant to be carbon negative.

A dynamic carbon balance was carried out over a 50-year period to evaluate a BECCS powerplant carbon negative potential over its lifetime in different biomass-region-land type scenarios. Depending on the conditions of the simulation, carbon breakeven time could vary from 1 (marginal cropland) to 35 years (central grassland) for miscanthus from Brazil, and from 6 to over 50 years for willow from Europe. Within the uncertainty bounds considered for the input data, the key factors impacting the results were identified to be the land conversion factors, electricity carbon footprint, biomass yield and moisture content. The investigation of alternative scenarios such as using carbon neutral electricity, and organic chemicals, gave indications as to BECCS potential margin of improvements. However, BECCS overall results were driven by land use conversion factors, which indicate the need for thorough evaluations of these effects. Bypassing this issue with biomass growth on marginal land could be a potential solution. Yet, marginal land availability and uncertain biomass productivity response might not make them long term candidates for BECCS large-scale deployment.

Given the variable outcomes of BECCS sustainability analysis, BECCS large scale deployment was found to have very different implications in terms of resource mobilisation. Based on the analysis on switchgrass and miscanthus, within a scenario excluding direct and indirect land use changes, removing 12 $GtCO_2/yr$ with BECCS could annually require between 360 and 2,400 Mha of marginal lands, 3,600 and 15,700 Bm^3 of water, 30 to 360 Gt of nutrients, and 1.7 to 2.9 TW of installed BECCS capacity. As a means of comparison, the upper bounds of these values correspond respectively to over three times the world total harvested land for cereal production, twice the world annual water use for agriculture (including evapotranspiration), 20 times the US annual nutrients use, and 1.6 times the world total coal-fired power plants capacity. This underlines the challenges associated with the large scale deployment of BECCS, especially concerning water and nutrients consumption.

Overall it was shown that over a plant lifetime and when choosing the right conditions, BECCS can be a reliable option for the sustainable and permanent removal of CO_2 from the atmosphere, even when including supply chain, direct and indirect land use change effects. The high variability in BECCS CO_2 removal time and space efficiencies in the model outcomes underpinned the need for case-to-case analysis when it comes to BECCS sustainability assessment, especially for the determination of land use change factors. Policy implications of this conclusion are that regulating and attributing value

to these systems will have to integrate this regional specificity.

We have identified five key principles which could improve the sustainability of BECCS. The combination of a sensitivity analysis on the model combined with the investigation of alternate supply chain scenarios elucidated the following five key levers: 1) measuring and limiting the impacts of direct and indirect land use changes, 2) using carbon neutral power and organic fertilizers, 3) prioritizing sea and rail over road transport, 4) increasing the use of carbon negative fuels, and, 5) exploiting alternative biomass processing options, *e.g.*, natural drying or torrefaction. This indicates that regardless of the biomass and region studied, BECCS sustainability heavily relies on intelligent management.

8.1.2 Does BECCS provide energy?

With the case study presented in Chapter 5, we found that BECCS dynamic E_IROI profile is strongly case specific. Depending on the scenario, we found that lifetime E_IROI values could be found within the range of 0.5-5.7. This means that BECCS electricity could be equally of 'negative value' to the energy system – negative energy balance – as well as competitive with PV and decarbonised thermal power plants (coal or gas with carbon capture and storage). Large-scale deployment of low E_IROI scenarios without due consideration of this nuance could represent a risk to both energy security and carbon dioxide removal, with a potential increase of fossil fuel use, and subsequent CO_2 emissions, to compensate for BECCS net electricity negativity. Given that we have shown that BECCS can be both carbon positive and negative (Chapter 4) and both energy positive and negative (Chapter 5), the scope for unintended consequences is vast.

This case study also highlighted the main energy losses along BECCS value chain: biomass conversion and CCS, followed by transport (road), drying, and farming (including inputs) represented over 80% of the energy losses for high moisture and low yield biomass such as willow pellets. Power plant efficiency, fuel efficiency for transport, transport distance, moisture content, drying method, as well as yield were thus identified as key parameters that need to be carefully controlled to maximise BECCS net electricity balance. There are also important trade-offs between these levers. In most cases, a greater travel distance from a region naturally resulted in a higher cumulative energy demand of the value chain, therefore decreasing the EROI and E_IROI. However, it was found that greater travel distances could almost be compensated for by a reduction in energy requirement for farming, when importing biomass from a region with superior yield. In summary, given the manifold contributions which determine the net energy balance of BECCS, it is important to resist the temptation to draw broad, general conclusions from a potentially narrow range of specific case studies.

Finally, we found that improving BECCS power generation efficiency could drastically reduce BECCS energy losses, but would also increase the amount of BECCS installed capacity required to meet an annual carbon removal target, and thus the financial cost associated with meeting that target. There is therefore a clear trade-off between BECCS annual carbon removal potential and power generation, and consequently between BECCS annual carbon removal potential and E_IROI. As BECCS uniquely has the potential to provide both carbon removal and electricity, a lower E_IROI could thus be compensated by a higher annual carbon removal, and *vice versa*. BECCS value to the system, as well as optimal deployment pathway, will therefore strongly depend on the nature of the service for which BECCS is primarly deployed, carbon removal or power generation.

8.1.3 What are the trade-offs within the BECCS resource nexus?

By highlighting the trade-offs between BECCS resource efficiency, environmental performance and technical performance, Chapter 6 showed that the design of BECCS value chain needs to be performed in the prism of all BECCS KPIs. Strong trade-offs with tipping points were identified between water use and the other two resource efficiency indicators in particular. How to build an objective function which reconcile all of BECCS' KPIs, while accounting for how BECCS performance may vary from one region to another, is therefore a key research challenge to be addressed.

Another conclusion is that, factors such as yield, carbon intensity of power, and high precipitation led to the selection of imported biomass over indigenous biomass. The design of policy frameworks considering the carbon accounting implications of using foreign biomass to store CO_2 in a given region, thereby meeting this region's carbon removal target, are paramount to facilitate local BECCS deployment. What is already complex at the megatone scale becomes manifold at the gigatone scale: how to regulate systems where biomass is imported from a productive region A, CO_2 is stored in region B with abundant storage, to meet the CO_2 removal target of a region C, is a key research question to be investigated.

The availability of sufficient marginal land and agricultural residues were observed to be of paramount importance to our results. However, it is also recognised that their availability is controversial, at best. To provide insight into the impact of their respective availability, a sensitivity analysis of the optimisation results to the availability of marginal land and agricultural residues was performed. A first insight from this analysis is that agricultural residues exerted a first order impact on BECCS land use; residues being attributed low agricultural carbon and water footprints, total land use decreased by several orders of magnitude when using agricultural residues. Assessing precisely how much agricultural residues could be used for BECCS, without trespassing on other uses,

could drastically relieve the pressure of BECCS on land use. A strong trade-off between water use and land use change was also identified: when minimising water use, using non-marginal land from low water footprint regions, and therefore causing land use change emissions, was preferable to using marginal land from higher water footprint regions. Water use and land use change being two critical sustainability indicators for BECCS, one should therefore be careful with potential direct and indirect land use effects when deploying BECCS from a water-saving perspective, and *vice versa*.

When ramping up the CO_2 removal target, it was found that the world median CO_2 removal target of 12 Gt_{CO_2}/yr was only achievable by storing CO_2 in the UK when residues and all land types were considered for BECCS. It was also found that water use, land use and CO_2 efficiency did not increase linearly with the CO_2 removal target, as marginal land from 'sustainable' regions get depleted as the CO_2 target increases, thus leading to the selection of other types of land or less sustainable regions. This shows that, though the UK has the storage capacity to achieve more CO_2 storage than its current target, there will be a clear trade-off between how much and how efficient carbon dioxide removal from the UK will be. This further confirms the need for multi-polar systems when deploying negative emissions at the gigatone scale. Implementing other storage sites in MONET will be required to investigate the optimal structure of the world CO_2 network for carbon dioxide removal.

Finally, maximising net energy production led to a drastic increase in the system's water use, land use, and land use change, as well as a decrease in CO_2 efficiency. This is explained by the fact that, at a given CO_2 removal target, regions which are less efficient at removing CO_2 are selected to maximise the amount of energy produced. A key insight from this result is that focusing exclusively on energy production and CO_2 removal is detrimental to BECCS resource efficiency and impact on ecosystems.

As a final thought experiment, we considered the proportional share of marginal land available, to what the UK is contributing to the world global carbon removal target by 2050, as a safe land use boundary in the context of UK CO_2 removal target. Were BECCS in the UK to be deployed subject to this land use constraint, it was found that BECCS electricity production objectives were still met. What this last analysis shows is that, whilst BECCS KPIs may be negatively correlated, they are, however, not incompatible: providing the right choices are made along BECCS value chain, BECCS can be deployed in a way that meets altogether its carbon removal objective, electricity production objective, and land use constraints.

8.1.4 What are the geophysical and geopolitical drivers of BECCS cost-optimal deployment?

Finally, chapter 7 explored the cost-optimal deployment of BECCS to meet increasing CO_2 removal targets of five potential large contributors to carbon dioxide removal: Brazil, China, the EU, India and the USA.

We first quantified the total cost of BECCS in these regions, explicitely accounting for biomass production, processing and transport, BECCS plant capital and operation costs, and CO_2 transport and storage. Factors such as yield, labour cost, and electricity cost were found to be strong drivers of cost and required CO_2 removal credit to make a BECCS system economically viable. Regional differences between these factors led to significant BECCS cost variations between regions, with end of the century cost of removal as low as \$85/tCO_2 in South China in an optimistic biomass supply chain scenario (*e.g.*, high yield or low carbon footprint of inputs), and as high as \$450/tCO_2 in the UK in a pessimistic biomass supply chain configuration (*e.g.*, low yield or high carbon footprint of inputs), using local biomass. Biomass transport can also lead to a substantial increase in BECCS cost, up to 50% increase in the case of the UK importing biomass from Brazil, in the median scenario. Depending on regional CO_2 storage and biomass availability, these differences suggest a potential cost-optimal BECCS deployment structure where low cost BECCS regions provide CO_2 removal for higher cost BECCS regions.

In determining BECCS cost-optimal value chains with an increasing CO_2 removal target, the total cost of removal was found to decrease over time at low targets (P2). This suggests that potential BECCS CAPEX reductions as well as the decarbonisation of the energy system are key to reverse the projected tendency of BECCS cost of removal increasing with the CO_2 removal target. At higher targets however (P3), sustainable bionergy supply limits were reached, which led BECCS cost to increase well past the \$100-350/tCO_2 removed range. This represents the limits where BECCS is no longer cost competitive with alternative, non land-based, CDR technologies (*e.g.*, direct air capture).

Accounting for revenues from electricity generation was found to improve BECCS regional competitiveness. The negative emission credit required for a BECCS system to have a zero cost balance – or breakeven NEC – was found to be overall lower in the UK than in the US, though BECCS total cost was found lower in the US than in the UK. When minimising total cost including revenues from electricity, the structure of the cost-optimal BECCS value changed, with the EU – with higher cost BECCS but also high wholesale electricity price – playing a larger role than the US in delivering negative emissions. The value of electricity will also greatly impact the incentives mechanisms required for BECCS systems to be financially viable. In regions with low BECCS cost and

high electricity prices such as Brazil, negative emissions credit required for a BECCS system to breakeven were found negative, which highlight that not all countries will necessarily require a large incentives to deploy the BECCS technology.

The combination of low costs and the proximity of cheap and sustainable biomass supply to CO_2 storage sites led China to be the main provider of CO_2 removal in the cost-optimal configuration, followed by the USA and the EU. When optimising the BECCS value chain subject to biomass and negative emissions credits trading constraints, it was observed that different regions brought different value to CO_2 removal. As a function of regional CO_2 storage and biomass availability, different regions were identified as providers or beneficiaries, whilst full inter-regional collaboration in biomass and negative emissions trading led to highest chance of meeting global targets at the lowest cost. International trading, certification and governance frameworks will therefore have to be designed carefully to integrate a) how to agree on the fulfilling of regional CO_2 removal targets in the case of multi polar value chains, b) the tracking of CO_2 emissions along the value chain to determine the net removal achieved and c) a negative emissions credit exchange platform/market to encourage that BECCS be deployed in the most cost and resource efficient way.

8.2 Limitations of the thesis and future work

Naturally, there are numerous limits to the framework which was developed for the purpose of this dissertation. In this section we discuss the main limitations of the MONET framework, and how these could be improved in future work.

8.2.1 Biomass-to-x

In this dissertation, we chose to focus on a single BECCS pathway, which is biomass conversion to electricity in a large scale power plant. As it was described in Chapter 2, multiple pathways to negative emissions via BECCS exist, biomass to fuels or biomass to hydrogen being two examples. Pathways differ in cost, scale, range of suitable feedstock, efficiencies in removing CO_2, and value to the energy system, both in terms of energy production and CO_2 avoidance. Sustainable biomass being a limited resource, modelling different biomass conversion pathways in MONET could inform on the most efficient uses of biomass in different regions, as a function of the regions' energy system and mitigation targets.

8.2.2 Co-deployment of CDR methods

In the context of determining the extent to which each CDR method should be deployed, and where, MONET could integrate additional CDR methods, such as afforestation, direct air capture or enhanced weathering. Whilst all of these options could have a role in large-scale CDR in different regions, the co-deployment of these technologies could also bring about synergies, including, but not limited to 1) the potential of afforestation with forest management to provide feedstock for BECCS and biofuel, and 2) the potential of enhanced weathering and biochar to increase crop yield, thus freeing up land for bioenergy production. Capturing these synergies in MONET could inform on optimal co-deployment of CDR methods to remove CO_2 in the most resource and cost efficient way. Whilst an engineered CO_2 removal method such as DACCS could be added with limited changes to the model structure, we acknowledge that adding natural methods such as afforestation, land restoration, biochar, will require significant changes to the model structure. In particular, the introduction of feedback loops to capture synergies, as well as the dynamic modelling of CDR methods deployment to capture differences in CO_2 removal rates, are examples of changes which could be incorporated.

8.2.3 Biomass growth model

In MONET, two important assumptions are made when it comes to biomass productivity: a) biomass productivity is considered constant by region, regardless of the quality of the land, and b) irrigation is assumed to be always applied to meet the crop's regional water requirement. In practice biomass productivity is a complex function of factors such as soil type, soil nutrient content, irrigation practices, as well as terrain slope and elevation. In rain-fed regions, no irrigation is applied, potentially resulting in a lower yield, but also in a lower water footprint. Equally, biomass yield in likely to vary as a function of the quality of the land, *i.e.* be higher on cropland, and lower on marginal land. Distinguishing rain-fed from irrigated regions in MONET, and capturing the relationship between biomass productivity, water stress and soil quality/terrain profile, would give a more accurate quantification of BECCS water and land intensities in MONET. Integrating these nuances could be achieved by focusing on a single region with a higher spatial resolution.

8.2.4 Multi-objective optimisation of BECCS value chain

In both Chapter 6 where we explored the trade-offs between different sustainability indicators including water use, land use, land use change, energy and emissions, and Chapter 7 where we presented least-cost optimisation BECCS pathways under sustainability constraints, a single objective approach was used for the optimisation. Two

important limitations can be highlighted here. First, the set of indicators selected for this study does not span the whole range of BECCS identified environmental impacts, which also include, among others, biodiversity loss and soil nutrient depletion [79]. The rationale for excluding impacts on biodiversity and soil quality was that BECCS deployment was constrained to marginal land for the core scenario of this study. However, a higher spatial resolution and better representation of land cover and land use transitions, would enable to better capture these impacts, which are equally important in ensuring the deployment of BECCS (and other CDR methods) is done in a sustainable way. Additionally, while the single objective optimisation enabled to identify trade-offs between some of BECCS key performance indicators, it cannot provide any insights as to a "low regret" strategy for BECCS deployment, when considering all potential impacts. A multi-objective optimisation approach, for example by considering all of the identified indicators in a single objective function, rather than as externalities, would allow us to explore scenarios which conciliate all objectives. One of the key difficulties of such a method lies in the monetisation of non-economic indicators, such as water use, land use change, biodiversity loss, depletion in soil quality *etc.*, and how these weighing factors might vary from one region to another. More generally, the valuation of ecosystem services is a field of active research [286], and could be further explored in the context of the co-deployment of CDR methods, especially when considering landscape level approaches such as afforestation, soil carbon sequestration and biochar. Focusing on a single region at a higher resolution is also likely to be required to appropriately measure and value the aforementioned impacts.

8.2.5 Dynamic modelling in MONET

In the case study presented in Chapter 7, BECCS deployment is modelled across several decades to model the impact of increasing CO_2 removal target, the depletion of CO_2 storage sites, the decarbonisation of the energy system, and potential decrease in BECCS plant capital costs. The objective of MONET is not to provide projections of future BECCS deployment, but to identify resource and financial trade-offs between different regions. For this reason, these are the only parameters which were considered to evolve with time, and all other parameters, including power plant efficiency, biomass production energy, carbon and financial costs, labour costs, or biomass yield, which could have important impact on BECCS cost and sustainability, were considered constant. Several modifications could be implemented to improve the current representation of BECCS performance over time 1) Improve the current decarbonisation trends of the energy system, especially road transport and shipping, 2) model BECCS cost reduction over time with endogenous learning, instead of exogenous capital cost reductions, 3) include a sensitivity analysis around the temporal evolution of all of these parameters.

8.2.6 Broadening the scope of feedstock and regions

We use MONET to explore trade-offs between different BECCS value chains, and identify the drivers of BECCS technical, environmental and economic performance. Because MONET only focuses on a subset of biomass sources – excluding other sources such as forestry biomass, other agricultural residues, wastes [81], algae [84] – and on countries – excluding large regions of the world such as Africa, Russia and Oceania, MONET does not aim at providing exact quantifications of BECCS potential and costs. Widening the scope of feedstock and regions would allow to provide a fuller picture of the impact and costs of BECCS global deployment, as well as potential key players in delivering global CDR.

8.2.7 BECCS deployment: possible *vs.* probable

In this dissertation, we used the variability of various inputs of the value chain (*e.g.*, biomass productivity, inputs carbon and energy footprints), *etc.*, to inform on the breadth of potential outcomes, in terms of CO_2 removal, land and water use, energy production, and optimal deployment. Due to a limited number of data points per region, we were not able to perform a full stochastic analysis, to determine which of these outcomes are the most probable.

8.2.8 Accounting for BECCS social impact

For the sake of simplicity, we chose not to consider potential socio-economic impacts of BECCS deployment, such as economic growth, food prices, or broader human well-being (*e.g.*, employment) at the local level. Whilst assessing BECCS impact on the global economy (*e.g.*, food prices) would require partial or full equilibrium modelling, the value and job creation associated with BECCS deployment could be quantified using input/output based tools such as the Job and Economic Development Impact (JEDI), as it as been done in other BECCS deployment studies [287]. Accounting for the socio-economic dimension in MONET may influence geographic priorities of BECCS deployment, and serve as a useful initial decision-making tool to maximise the overall benefits of BECCS (or CDR) projects.

References

[1] Z. Hausfather, H. F. Drake, T. Abbott, and G. A. Schmidt. Evaluating the performance of past climate model projections. *Geophysical Research Letters*, (advance article). doi: 10.1029/2019GL085378.

[2] G. P. Peters, R. M. Andrew, J. G. Canadell, P. Friedlingstein, R. B. Jackson, J. I. Korsbakken, C. Le Quéré, and A. Peregon. Carbon dioxide emissions continue to grow amidst slowly emerging climate policies. *Nature Climate Change*, 2019. doi: 10.1038/s41558-019-0659-6.

[3] International Panel on Climate Change (IPCC). Global Warming of 1.5°C. Technical report, 2018. URL http://www.ipcc.ch/report/sr15/.

[4] M. Fajardy and N. Mac Dowell. Can BECCS deliver sustainable and resource efficient negative emissions? *Energy Environmental Science*, 10(6):1389–1426, 2017. doi: 10.1039/C7EE00465F.

[5] M. Fajardy and N. Mac Dowell. The Energy Return On Investment of BECCS: is BECCS a threat to energy security? *Energy & Environmental Science*, 11(6): 1581–1594, 2018. doi: 10.1039/C7EE03610H.

[6] M. Fajardy, S. Chiquier, and N. Mac Dowell. Investigating the BECCS resource nexus: delivering sustainable negative emissions. *Energy & Environmental Science*, 11(12):3408–3430, 2018. doi: 10.1039/C8EE01676C.

[7] M. Fajardy, P. Patrizio, H. Ahut Daggash, and N. Mac Dowell. Negative emissions: Priorities for research and policy design. *Frontiers in Climate*, 1:6, 2019. doi: 10.3389/fclim.2019.00006.

[8] H. A. Daggash, C. F. Heuberger, and N. Mac Dowell. The role and value of negative emissions technologies in decarbonising the UK energy system. *International Journal of Greenhouse Gas Control*, 81:181–198, 2019. doi: 10.1016/j.ijggc.2018.12.019.

[9] M. Fajardy, A. Köberle, N.l Mac Dowell, and A. Fantuzzi. BECCS deployment: a reality check. *Grantham Institute Briefing paper*, (No 28), 2019. URL https://www.imperial.ac.uk/media/imperial-college/grantham-institute/public/publications/briefing-papers/BECCS-deployment---a-reality-check.pdf.

[10] D. Huppmann, E. Kriegler, V. Krey, K. Riahi, J. Rogelj, S. K. Rose, J. Weyant, N. Bauer, C. Bertram, V. Bosetti, K. Calvin, J. Doelman, L. Drouet, J. Emmerling, S. Frank, S. Fujimori, D. Gernaat, A. Grubler, C. Guivarch, M. Haigh, C. Holz, G. Iyer, E. Kato, K. Keramidas, A. Kitous, F. Leblanc, J.-Y. Liu, K. Löffler, G. Luderer, A. Marcucci, D. McCollum, S. Mima, A. Popp, R. D. Sands, F. Sano, J. Strefler, J. Tsutsui, D. Van Vuuren, Z. Vrontisi, M. Wise, and R. Zhang. IAMC 1.5°C Scenario Explorer and Data hosted by IIASA. Integrated Assessment Modeling Consortium & International Institute for Applied Systems Analysis, 2018. doi: 10.22022/SR15/08-2018.15429.

[11] J. Rogelj, A. Popp, K. V. Calvin, G. Luderer, J. Emmerling, D. Gernaat, S. Fujimori, J. Strefler, T. Hasegawa, G. Marangoni, V. Krey, E. Kriegler, K. Riahi, D. P. van Vuuren, J. Doelman, L. Drouet, J. Edmonds, O. Fricko, M. Harmsen, P. Havlík, F. Humpenöder, E. Stehfest, and M. Tavoni. Scenarios towards limiting global mean temperature increase below 1.5°C. *Nature Climate Change*, 8(April): 1–8, 2018. doi: 10.1038/s41558-018-0091-3.

[12] J. C. Minx, W. F. Lamb, M. W. Callaghan, L. Bornmann, and S. Fuss. Fast growing research on negative emissions. *Environmental Research Letters*, 12(3): 035007, 2017. doi: 10.1088/1748-9326/aa5ee5.

[13] European Academies Science Advisory Council (EASAC). Negative emission technologies: What role in meeting Paris Agreement targets?, 2018. URL https://easac.eu/publications/details/easac-net/.

[14] M. Bui, C. S. Adjiman, A. Bardow, E. J. Anthony, A. Boston, Solomon Brown, P. S. Fennell, S. Fuss, A. Galindo, L. A. Hackett, J. P. Hallett, H. J. Herzog, G. Jackson, J. Kemper, S. Krevor, G. C. Maitland, M. Matuszewski, I. S. Metcalfe, C. Petit, Graeme Puxty, J. Reimer, D. M. Reiner, E. S. Rubin, S. A. Scott, N. Shah, B. Smit, J. P. M. Trusler, P. Webley, J. Wilcox, and N. Mac Dowell. Carbon capture and storage (CCS): the way forward. *Energy & Environmental Science*, 11:1062–1176, 2018. doi: 10.1039/C7EE02342A.

[15] R. H. Williams. Fuel Decarbonization for Fuel Cell Applications and Sequestration of the Separated CO_2. Technical report, Center for Energy and Environmental Studies, Princeton University, 1996. URL https://acee.princeton.edu/wp-content/uploads/2016/10/no-295.pdf.

[16] H. J. Herzog and E. M. Drake. Carbon dioxide recovery and disposal from large energy systems. *Annual Review of Energy and the Environment*, 21:145–166, 1996. doi: 10.1146/annurev.energy.21.1.145.

[17] M. Obersteiner, C. Azar, P. Kauppi, K. Möllersten, J. Moreira, S. Nilsson, P. Read, K. Riahi, B. Schlamadinger, Y. Yamagata, J. Yan, and J.-P. van Ypersele. Managing climate risk. *Science*, 294(5543):786–787, 2001. doi: 10.1126/science.294.5543.786b.

[18] F. Kraxner, S. Nilsson, and M. Obersteiner. Negative emissions from BioEnergy use, carbon capture and sequestration (BECS) – the case of biomass production by sustainable forest management from semi-natural temperate forests. *Biomass and Bioenergy*, 24(4-5):285–296, 2003. doi: 10.1016/S0961-9534(02)00172-1.

[19] International Energy Agency (IEA). Combining Bioenergy with CCS. Technical report, 2011. URL https://webstore.iea.org/combining-bioenergy-with-ccs.

[20] P. Read and J. Lermit. Bio-energy with carbon storage (BECS): A sequential decision approach to the threat of abrupt climate change. *Energy*, 30(14):2654–2671, 2005. doi: 10.1016/j.energy.2004.07.003.

[21] A. L. Robinson, J. S. Rhodes, and D. W. Keith. Policy Analysis Assessment of Potential Carbon Dioxide Reductions Due to Biomass - Coal Cofiring in the United States. *Environmental Science and Technology*, 37(22):5081–5089, 2003. doi: 10.1021/es034367q.

[22] S. Selosse and O. Ricci. Achieving negative emissions with BECCS (bioenergy with carbon capture and storage) in the power sector: New insights from the TIAM-FR (TIMES Integrated Assessment Model France) model. *Energy*, 76: 967–975, 2014. doi: 10.1016/j.energy.2014.09.014.

[23] Biomass with CO_2 Capture and Storage (Bio-CCS) The way forward for Europe. Technical report, Zero Emission Platform (ZEP), 2013. URL http://www.zeroemissionsplatform.eu/library/publication/206-biomass-with-co2-capture-and-storage-bio-ccs-%20the-way-forward-for-europe.html.

[24] J. S. Rhodes and D. W. Keith. Engineering economic analysis of biomass IGCC with carbon capture and storage. *Biomass and Bioenergy*, 29(6):440–450, 2005. doi: 10.1016/j.biombioe.2005.06.007.

[25] K. Mollersten, J. Yan, and J. R. Moreira. Potential market niches for biomass energy with CO_2 capture and storage - Opportunities for energy supply with

negative CO_2 emissions. *Biomass and Bioenergy*, 25(3):273–285, 2003. doi: 10.1016/S0961-9534(03)00013-8.

[26] C. Gough and P. Upham. Biomass energy with carbon capture and storage (BECCS): a review. Technical report, Tyndall Centre for Climate Change, University of Manchester, 2010. URL http://www.tyndall.ac.uk/publications/tyndall-working-paper/2010/biomass-energy-carbon-capture-and-storage-beccs-review.

[27] O. Akgul, N. Mac Dowell, L. G. Papageorgiou, and N. Shah. A mixed integer nonlinear programming (MINLP) supply chain optimisation framework for carbon negative electricity generation using biomass to energy with CCS (BECCS) in the UK. *International Journal of Greenhouse Gas Control*, 28:189–202, 2014. doi: 10.1016/j.ijggc.2014.06.017.

[28] T. Hasegawa, S. Fujimori, P. Havlík, H. Valin, B. L. Bodirsky, J. C. Doelman, T. Fellmann, P. Kyle, J. F. L. Koopman, H. Lotze-campen, D. M.-d Croz, Y. Ochi, I. P. Domínguez, E. Stehfest, T. B. Sulser, A. Tabeau, K. Takahashi, J. Takakura, H. V. Meijl, W. V. Zeist, K. Wiebe, and P. Witzke. Risk of increased food insecurity under stringent global climate change mitigation policy. *Nature Climate Change*, 8(August), 2018. doi: 10.1038/s41558-018-0230-x.

[29] A. Popp, K. Calvin, S. Fujimori, P. Havlik, F. Humpenöder, E. Stehfest, B. Leon, J. Philipp, J. C. Doelmann, M. Gusti, T. Hasegawa, P. Kyle, M. Obersteiner, A. Tabeau, K. Takahashi, H. Valin, S. Waldhoff, I. Weindl, M. Wise, El. Kriegler, H. Lotze-campen, O. Fricko, K. Riahi, and D. P. Van Vuuren. Land-use futures in the shared socio-economic pathways. *Global Environmental Change*, 42:331–345, 2017. doi: 10.1016/j.gloenvcha.2016.10.002.

[30] A. Wiltshire. Implications for food security of large scale BECCS deployment. Technical report, Met Office, 2016. URL http://www.avoid.uk.net/2016/06/implications-for-food-security-of-large-scale-beccs-deployment-d2c/.

[31] T. W. R. Powell and T. M. Lenton. Future carbon dioxide removal via biomass energy constrained by agricultural efficiency and dietary trends. *Energy & Environmental Science*, 5(8):8116, 2012. doi: 10.1039/c2ee21592f.

[32] Committee on Climate Change (CCC). Biomass in a low-carbon economy. Technical report, 2018. URL https://www.theccc.org.uk/publication/biomass-in-a-low-carbon-economy/.

[33] J. M. DeCicco, D. Y. Liu, J. Heo, R. Krishnan, A. Kurthen, and L. Wang. Carbon balance effects of U.S. biofuel production and use. *Climatic Change*, 138(3-4): 667–680, 2016. doi: 10.1007/s10584-016-1764-4.

[34] F. Creutzig, N. H. Ravindranath, G. Berndes, S. Bolwig, R. Bright, F. Cherubini, H. Chum, E. Corbera, M. Delucchi, A. Faaij, J. Fargione, H. Haberl, G. Heath, O. Lucon, R. Plevin, A. Popp, C. Robledo-Abad, S. Rose, P. Smith, A. Stromman, S. Suh, and O. Masera. Bioenergy and climate change mitigation: An assessment. *GCB Bioenergy*, 7(5):916–944, 2015. doi: 10.1111/gcbb.12205.

[35] N.E. Vaughan and C. Gough. Expert assessment concludes negative emissions scenarios may not deliver. *Environmental Research Letters*, 11(9):095003, 2016. doi: 10.1088/1748-9326/11/9/095003.

[36] P. Smith, S. J. Davis, F. Creutzig, S. Fuss, J. Minx, B. Gabrielle, E. Kato, R. B. Jackson, A. Cowie, E. Kriegler, D. P. van Vuuren, J. Rogelj, P. Ciais, J. Milne, J. G. Canadell, D. McCollum, G. Peters, R. Andrew, V. Krey, G. Shrestha, P. Friedlingstein, T. Gasser, A. Grubler, W. K. Heidug, M. Jonas, C. D. Jones, F. Kraxner, E. Littleton, J. Lowe, J. R. Moreira, N. Nakicenovic, M. Obersteiner, A. Patwardhan, M. Rogner, E. Rubin, A. Sharifi, A. Torvanger, Y. Yamagata, J. Edmonds, and C. Yongsung. Biophysical and economic limits to negative CO_2 emissions. *Nature Climate Change*, 6(1):42–50, 2016. doi: 10.1038/nclimate2870.

[37] K. Anderson and G. Peters. The trouble with negative emissions. *Science*, 354 (6309):182–183, 2016. doi: 10.1126/science.aah4567.

[38] J. Rogelj, M. den Elzen, N. Höhne, T. Fransen, H. Fekete, H. Winkler, R. Schaeffer, F. Sha, K. Riahi, and M. Meinshausen. Paris Agreement climate proposals need a boost to keep warming well below 2°C. *Nature*, 534(7609):631–639, 2016. doi: 10.1038/nature18307.

[39] S. Gollakota and S. McDonald. Commercial-scale CCS project in Decatur, Illinois - Construction status and operational plans for demonstration. *Energy Procedia*, 63:5986–5993, 2014. doi: 10.1016/j.egypro.2014.11.633.

[40] DRAX group plc. Annual report and accounts: Enabling a zero carbon, lower cost energy future. Technical report, 2018. URL https://www.drax.com/wp-content/uploads/2019/03/Drax-Annual-report-accounts-2018.pdf.

[41] Global CCS Institute. The Global Status of CCS: 2018. Technical report, 2018. URL https://indd.adobe.com/view/2dab1be7-edd0-447d-b020-06242ea2cf3b.

[42] D. Humbird, R. E. Davis, L. Tao, C. M. Kinchin, D. D. Hsu, A. Aden, P. Schoen, J. Lukas, B. Olthof, M. Worley, D. Sexton, and D. Dudgeon. Process Design and Economics for Biochemical Conversion of Lignocellulosic Biomass to Ethanol. Technical report, National Renewable Energy Laboratory, 2011. URL http://www.nrel.gov/biomass/pdfs/47764.pdf.

[43] G. Liu, E. D. Larson, R. H. Williams, T. G. Kreutz, and X. Guo. Making Fischer–Tropsch Fuels and Electricity from Coal and Biomass: Performance and Cost Analysis. *Energy & Fuels*, 25(1):415–437, jan 2011. doi: 10.1021/ef101184e.

[44] International Energy Agency Greenhouse Gas Programme (IEAGHG). Potential for Biomass and Carbon Dioxide Capture and Storage. Technical Report July, 2011. URL https://www.eenews.net/assets/2011/08/04/document_cw_01.pdf.

[45] P. Parthasarathy and K. S. Narayanan. Hydrogen production from steam gasification of biomass: Influence of process parameters on hydrogen yield – A review. *Renewable Energy*, 66:570–579, 2014. doi: 10.1016/j.renene.2013.12.025.

[46] International Energy Agency Greenhouse Gas Programme (IEAGHG). CO_2 Capture at Coal Based Power and Hydrogen Plants. Technical Report May, 2014. URL http://www.ieaghg.org/docs/General_Docs/Reports/2014-03.pdf.

[47] C. Koroneos, A. Dompros, and G. Roumbas. Hydrogen production via biomass gasification – A life cycle assessment approach. *Chemical Engineering and Processing: Process Intensification*, 47(8):1261–1268, 2008. doi: 10.1016/j.cep.2007.04.003.

[48] J. Hetland, P. Yowargana, S. Leduc, and F. Kraxner. Carbon-negative emissions: Systemic impacts of biomass conversion. A case study on CO_2 capture and storage options. *International Journal of Greenhouse Gas Control*, 49:330–342, 2016. doi: 10.1016/j.ijggc.2016.03.017.

[49] M. Bui, M. Fajardy, and N. Mac Dowell. Bio-Energy with CCS (BECCS) performance evaluation: Efficiency enhancement and emissions reduction. *Applied Energy*, 195(June):289–302, 2017. doi: 10.1016/j.apenergy.2017.03.063.

[50] C. Antonini, M. van der Spek, D. Sutter, A. Streb, M. Gazzani, and M. Mazzotti. Report on optimal plants for production of low-carbon H2 with state-of-the-art technologies. Technical report, 2018. URL https://www.sintef.no/globalassets/project/elegancy/deliverables/elegancy_d1.3.1_optimal-plants-low-carbon-h2.pdf.

[51] J. Bosch, S. de Jong, R. Hoefnagels, and R. Slade. Aviation biofuels: strategically important, technically achievable, tough to deliver. *Grantham Institute Briefing Paper*, (November), 2017. URL https://www.imperial.ac.uk/grantham/publications/briefing-papers/aviation-biofuels-strategically-important-technically-achievable-tough-to-deliver.php.

[52] K. Onarheim, S. Santos, P. Kangas, and V. Hankalin. Performance and costs of CCS in the pulp and paper industry part 1: Performance of amine-based post-combustion CO_2 capture. *International Journal of Greenhouse Gas Control*, 59: 58–73, 2017. doi: 10.1016/j.ijggc.2017.02.008.

[53] H. Mandova, P. Patrizio, S. Leduc, J. Kjärstad, C. Wang, E. Wetterlund, F. Kraxner, and G. William. Achieving carbon-neutral iron and steelmaking in Europe through the deployment of bioenergy with carbon capture and storage. *Journal of Cleaner Production*, 218:118–29, 2019. doi: 10.1016/j.jclepro.2019.01.247.

[54] P. C. Stoy, S. Ahmed, M. Jarchow, B. Rashford, D. Swanson, S. Albeke, G. Bromley, E. N.J. Brookshire, M. D. Dixon, J. Haggerty, P. Miller, B. Peyton, A. Royem, L. Spangler, C. Straub, and B. Poulter. Opportunities and Trade-offs among BECCS and the Food, Water, Energy, Biodiversity, and Social Systems Nexus at Regional Scales. *BioScience*, 68(2):100–111, 2018. doi: 10.1093/biosci/bix145.

[55] B. E. Dale, J. E. Anderson, R. C. Brown, S. Csonka, V. H. Dale, G. Herwick, R. D. Jackson, N. Jordan, S. Ka, K. L. Kline, L. R. Lynd, C. Malmstrom, R. G. Ong, T. L. Richard, C. Taylor, and M. Q. Wang. Take a Closer Look: Biofuels Can Support Environmental, Economic and Social Goals. *Environmental Science & Technology*, 48(13):7200–7203, 2014. doi: 10.1021/es5025433.

[56] L. J. Smith and M. S. Torn. Ecological limits to terrestrial biological carbon dioxide removal. *Climatic Change*, pages 89–103, 2013. doi: 10.1007/s10584-012-0682-3.

[57] C. Gough, S. G. Freites, C. Jones, S. Mander, B. Moore, C. Pereira, M. Röder, N. Vaughan, and A. Welfle. Challenges to the use of BECCS as a keystone technology in pursuit of 1.5°C. *Global Sustainability*, 1(forthcoming):1–9, 2018.

[58] K. Dooley and S. Kartha. Land-based negative emissions: Risks for climate mitigation and impacts on sustainable development. *International Environmental Agreements: Politics, Law and Economics*, 18(1):79–98, 2018. doi: 10.1007/s10784-017-9382-9.

[59] A. Singh and K. Stéphenne. Shell Cansolv CO 2 capture technology : Achievement from First Commercial Plant. *Energy Procedia*, 63:1678–1685, 2014. doi: 10.1016/j.egypro.2014.11.177.

[60] M. Campbell. Technology Innovation & Advancements for Shell Cansolv CO_2 capture solvents. *Energy Procedia*, 63:801–807, 2014. doi: 10.1016/j.egypro.2014.11.090.

[61] Y. Zhang, B. Freeman, P. Hao, and G. Rochelle. Absorber Modeling for NGCC Carbon Capture with Aqueous Piperazine. *Faraday Discussions*, 192:459–477, 2016. doi: 10.1039/C6FD00030D.

[62] M. B. Berkenpas, J. J. Fry, K. Kietzke, and E. S. Rubin. Integrated Environmental Control Model Getting Started. Technical report, Center for Energy and Evironmental Studies, Carnagie Mellon University. URL https://www.cmu.edu/epp/iecm/iecm_#doc.html.

[63] P. J. Tharakan, T. A. Volk, L. P. Abrahamson, and E. H. White. Energy feedstock characteristics of willow and hybrid poplar clones at harvest age. *Biomass and Bioenergy*, 25(6):571–580, 2003. doi: 10.1016/S0961-9534(03)00054-0.

[64] International Organization for Standardization. Solid biofuels: Fuel specifications and classes. Part 1: General requirements. Technical report. URL https://www.iso.org/obp/ui/#iso:std:iso:17225:-1:ed-1:v1:en.

[65] M. J. Stolarski, M. Krzyzaniak, S. Szczukowski, and J. Tworkowski. Willow biomass as a feedstock for gasification. *Journal of Research and Applications in Agricultural Engineering*, 58(1):168–171, 2013.

[66] A. Monti. *Switchgrass: A Valuable Biomass Crop for Energy*. Springer edition, 2012. URL https://www.springer.com/gp/book/9781447129028#aboutAuthors.

[67] H. Spliethoff and K. R. G. Hein. Effect of co-combustion of biomass on emissions in pulverized fuel furnaces. *Fuel Processing Technology*, 54(1-3):189–205, 1998. doi: 10.1016/S0378-3820(97)00069-6.

[68] P. McKendry. Energy production from biomass (part 1): Overview of biomass. *Bioresource Technology*, 83(1):37–46, 2002. doi: 10.1016/S0960-8524(01)00118-3.

[69] T. Heinzel, V. Siegle, H. Spliethoff, and K. R. G. Hein. Investigation of slagging in pulverized fuel co-combustion of biomass and coal at a pilot-scale test facility. *Fuel Processing Technology*, 54:109–125, 1998. doi: 10.1016/S0378-3820(97)00063-5.

[70] O. Williams, C. Eastwick, S. Kingman, D. Giddings, S. Lormor, and E. Lester. Investigation into the applicability of Bond Work Index (BWI) and Hardgrove Grindability Index (HGI) tests for several biomasses compared to Colombian la Loma coal. *Fuel*, 158:379–387, 2015. doi: 10.1016/j.fuel.2015.05.027.

[71] K. Savolainen. Co-firing of biomass in coal-fired utility boilers. *Applied Energy*, 74(3-4):369–381, 2003. doi: 10.1016/S0306-2619(02)00193-9.

[72] Y. Shao, J. Wang, F. Preto, J. Zhu, and C. Xu. Ash deposition in biomass combustion or co-firing for power/heat generation. *Energies*, 5(12):5171–5189, 2012. doi: 10.3390/en5125171.

[73] M. Pronobis. The influence of biomass co-combustion on boiler fouling and efficiency. *Fuel*, 85(4):474–480, 2006. doi: 10.1016/j.fuel.2005.08.015.

[74] N. Mac Dowell and M. Fajardy. Inefficient power generation as an optimal route to negative emissions via beccs? *Environmental Research Letters*, 12(4):045004, 2017. doi: 10.1088/1748-9326/aa67a5.

[75] A. B. Harper, T. Powell, P. M. Cox, J. House, C. Huntingford, T. M. Lenton, S. Sitch, E. Burke, S. E. Chadburn, W. J. Collins, E. Comyn-Platt, V. Daioglou, J. C. Doelman, G. Hayman, E. Robertson, D. van Vuuren, A. Wiltshire, C. P. Webber, A. Bastos, L. Boysen, P. Ciais, N. Devaraju, A.K. Jain, A. Krause, B. Poulter, and S. Shu. Land-use emissions play a critical role in land-based mitigation for Paris climate targets. *Nature Communications*, 9(1):2938, 2018. doi: 10.1038/s41467-018-05340-z.

[76] J. Fargione, J. Hill, D. Tilman, S. Polasky, and P. Hawthorne. Land Clearing and the Biofuel Carbon Debt. *Science*, 319(February):1235–1237, 2008. doi: 10.1126/science.1152747.

[77] T. Searchinger, R. Heimlich, R. A. Houghton, F. Dong, A. Elobeid, J. Fabiosa, S. Tokgoz, D. Hayes, and T. Yu. Use of U.S. Croplands for Biofuels Increases Greenhouse Gases Through Emissions from Land-Use Change. *Science*, 319 (5867):1238–1240, 2008. doi: 10.1126/science.1151861.

[78] Food and Agriculture Organization. FAOSTAT, . URL http://www.fao.org/faostat/en/#home. (accessed May 2016).

[79] V. Heck, D. Gerten, W. Lucht, and A. Popp. Biomass-based negative emissions difficult to reconcile with planetary boundaries. *Nature Climate Change*, 8:151–155, 2018. doi: 10.1038/s41558-017-0064-y.

[80] F. Monforti, E. Lugato, V. Motola, K. Bodis, N. Scarlat, and J. F. Dallemand. Optimal energy use of agricultural crop residues preserving soil organic carbon stocks in Europe. *Renewable and Sustainable Energy Reviews*, 44:519–529, 2015. doi: 10.1016/j.rser.2014.12.033.

[81] N. Pour, P. A. Webley, and P. J. Cook. Potential for using municipal solid waste as a resource for bioenergy with carbon capture and storage (BECCS). *International Journal of Greenhouse Gas Control*, 68(November):1–15, 2018. doi: 10.1016/j.ijggc.2017.11.007.

[82] S. Lossau, G. Fischer, S. Tramberend, H. V. Velthuizen, B. Kleinschmit, and R. Schom. Brazil' s current and future land balances : Is there residual land for bioenergy production? *Biomass and Bioenergy*, 81:452–461, 2015. doi: 10.1016/j.biombioe.2015.07.024.

[83] A. R. Milbrandt, D. M. Heimiller, A. D. Perry, and C. B. Field. Renewable energy potential on marginal lands in the United States. *Renewable and Sustainable Energy Reviews*, 29:473–481, 2014. doi: 10.1016/j.rser.2013.08.079.

[84] C. M. Beal, I. Archibald, M. E. Huntley, C. H. Greene, and Z. I. Johnson. Integrating Algae with Bioenergy Carbon Capture and Storage (ABECCS) Increases Sustainability. *Earth's future.*, 6(3):524–542, 2018. doi: 10.1002/2017EF000704.

[85] R. J. Plevin, M. O'Hare, A. D. Jones, M. S. Torn, and H. K. Gibbs. The greenhouse gas emissions from indirect land use change are uncertain, but potentially much greater than previously estimated. *Environmental Science & Technology.*, 44(21):8015–8021, 2010. doi: 10.1021/es101946t.

[86] T. Searchinger. Sound principles and an important inconsistency in the 2012 UK bioenergy strategy. Technical report, Woodrow Wilson School of Public and International Affairs, 2012. URL http://ww2.rspb.org.uk/Images/Searchinger_comments_on_bioenergy_strategy_SEPT_2012_tcm9-329780.pdf.

[87] H. Haberl, D. Sprinz, M. Bonazountas, P. Cocco, Y. Desaubies, M. Henze, O. Hertel, R. K. Johnson, U. Kastrup, P. Laconte, E. Lange, P. Novak, J. Paavola, A. Reenberg, S. van den Hove, T. Vermeire, P. Wadhams, and T. Searchinger. Correcting a fundamental error in greenhouse gas accounting related to bioenergy. *Energy Policy*, 45:18–23, 2012. doi: 10.1016/j.enpol.2012.02.051.

[88] European Commission. Impact Assessment. Technical report, 2012. URL http://ec.europa.eu/energy/en/topics/renewable-energy/biofuels/land-use-change.

[89] K. P. Overmars, E. Stehfest, J. P. M. Ros, and A. G. Prins. Indirect land use change emissions related to EU biofuel consumption: An analysis based on historical data. *Environmental Science and Policy*, 14(3):248–257, 2011. doi: 10.1016/j.envsci.2010.12.012.

[90] S. E. Tanzer and A. Ramirez. When are negative emissions negative emissions? *Energy & Environmental Science*, 12:1210–1218, 2019. doi: 10.1039/C8EE03338B.

[91] M. R. Withers, R. Malina, and S. R. H. Barrett. Carbon, climate, and economic breakeven times for biofuel from woody biomass from managed forests. *Ecological Economics*, 112:45–52, 2015. doi: 10.1016/j.ecolecon.2015.02.004.

[92] F. Cherubini, G. P. Peters, T. Berntsen, A. H. Strømman, and E. Hertwich. CO_2 emissions from biomass combustion for bioenergy: Atmospheric decay and contribution to global warming. *GCB Bioenergy*, 3(5):413–426, 2011. doi: 10.1111/j.1757-1707.2011.01102.x.

[93] P. Moriarty and D. Honnery. Review: Assessing the climate mitigation potential of biomass. *AIMS Energy*, 5(1):20–38, 2016. doi: 10.3934/energy.2017.1.20.

[94] A. Gambhir, I. Butnar, P. Li, P. Smith, and N. Strachan. A Review of Criticisms of Integrated Assessment Models and Proposed Approaches to Address These , through the Lens of BECCS. *Energies*, 12(9):1747, 2019. doi: 10.3390/en12091747.

[95] Y. Wada, I. E. M. de Graaf, and L. P. H. van Beek. High-resolution modeling of human and climate impacts on global water resources. *Journal of Advances in Modeling Earth Systems*, 8(2):735–763, jun 2016. doi: 10.1002/2015MS000618.

[96] International Energy Agency (IEA). Water for Energy: Is energy becoming a thirstier resource? In *World Energy Outlook*, pages 1–33. 2012. URL https://webstore.iea.org/world-energy-outlook-2012-2.

[97] United Nations Water. Coping with water scarcity: Challenge of the twenty-first century. *Waterlines*, 24(1):28–29, 2005. doi: 10.3362/0262-8104.2005.038.

[98] G. Fisher, H. T. van Velthuizen, M. M. Shah, and F. O. Nachtergaele. Global agro-ecological assessment for agriculture in the twenty-first century: Methodology and Results. Technical Report March, International Institute for Applied Systems Analysis, 2002. URL http://www.fao.org/landandwater/lwdms.stm#cd21.

[99] L. Zhuo, M. M. Mekonnen, A.Y. Hoekstra, and Y. Wada. Inter- and intra-annual variation of water footprint of crops and blue water scarcity in the Yellow River basin (1961-2009). *Advances in Water Resources*, 87:29–41, 2016. doi: 10.1016/j.advwatres.2015.11.002.

[100] Y. Wada, L. P. H. Van Beek, D. Viviroli, H. H. Drr, R. Weingartner, and M. F. P. Bierkens. Global monthly water stress: 2. Water demand and severity of water stress. *Water Resources Research*, 47(7):1–17, 2011. doi: 10.1029/2010WR009792.

[101] R. Séférian, M. Rocher, C. Guivarch, and J. Colin. Constraints on biomass energy deployment in mitigation pathways: The case of water scarcity. *Environmental Research Letters*, 13(5), 2018. doi: 10.1088/1748-9326/aabcd7.

[102] International Panel on Climate Change (IPCC). Climate Change and Land: an IPCC special report on climate change, desertification, land degradation, sustainable land management, food security, and greenhouse gas fluxes in terrestrial ecosystem. Technical report, 2019. URL https://www.ipcc.ch/srccl/.

[103] S. Fuss, W. F. Lamb, M. W. Callaghan, J. Hilaire, F. Creutzig, T. Amann, T. Beringer, W. D. O. Garcia, J. Hartmann, T. Khanna, G. Luderer, G. F. Nemet, J. Rogelj, P. Smith, J. L. V. Vicente, J. Wilcox, M. Z. Dominguez, and J. C. Minx. Negative emissions – Part 2 : Costs , potentials and side effects. *Environmental Research Letters*, 13:063002, 2018. doi: 10.1088/1748-9326/aabf9f.

[104] P. Psarras, H. Krutka, M. Fajardy, Z. Zhang, S. Liguori, N. Mac Dowell, and J. Wilcox. Slicing the pie: how big could carbon dioxide removal be? *WIREs Energy And Environment*, 6(5):253, 2017. doi: 10.1002/wene.253.

[105] J. Kemper. Biomass and carbon dioxide capture and storage: A review. *International Journal of Greenhouse Gas Control*, 40:401–430, 2015. doi: 10.1016/j.ijggc.2015.06.012.

[106] D. McLaren. A comparative global assessment of potential negative emissions technologies. *Process Safety and Environmental Protection*, 90(6):489–500, 2012. doi: 10.1016/j.psep.2012.10.005.

[107] R Slade, A. Bauen, and R. Gross. Global bioenergy resources. *Nature Climate Change*, 4(2):99–105, 2014. doi: 10.1038/nclimate2097.

[108] International Energy Agency Bioenergy. Bioenergy - a Sustainable and Reliable Energy Source. Technical report, 2009. URL http://www.ieabioenergy.com/wp-content/uploads/2013/10/MAIN-REPORT-Bioenergy-a-sustainable-and-reliable-energy-source.-A-review-of-status-and-prospects.pdf.

[109] T. Beringer, W. Lucht, and S. Schaphoff. Bioenergy production potential of global biomass plantations under environmental and agricultural constraints. *GCB Bioenergy*, 3(4):299–312, 2011. doi: 10.1111/j.1757-1707.2010.01088.x.

[110] Al. Strapasson, J. Woods, H. Chum, N. Kalas, N Shah, and F. Rossillo-Calle. On the global limits of bioenergy and land use for climate change mitigation. *GCB Bioenergy*, 9:1721–1735, 2017. doi: 10.1111/gcbb.12456.

[111] W. Steffen, K. Richardson, J. Rockström, S. E. Cornell, I. Fetzer, E. M. Bennett, R. Biggs, S. R. Carpenter, W. De Vries, C. A. De Wit, C. Folke, D. Gerten, J. Heinke, G. M. Mace, L. M. Persson, V. Ramanathan, B. Reyers, and S. Sörlin.

Planetary boundaries: Guiding human development on a changing planet. *Science*, 347(6223):1259855, 2015. doi: 10.1126/science.1259855.

[112] L. Boysen, W. Lucht, H. Schellnhuber, D. Gerten, V. Heck, and T. Lenton. The limits to global-warming mitigation by terrestrial carbon removal. *Earth's Future*, 5(5):463–474, 2017. doi: 10.1002/eft2.203.

[113] S. A. Edrisi and P. C. Abhilash. Exploring marginal and degraded lands for biomass and bioenergy production : An Indian scenario. *Renewable and Sustainable Energy Reviews*, 54:1537–1551, 2016. doi: 10.1016/j.rser.2015.10.050.

[114] X. Cai, X. Zhang, and D. Wang. Land Availability Analysis for Biofuel Production. *Environmental Science and Technology*, 45(January):334–339, 2011. doi: 10.1021/es103338e.

[115] S. Fritz, L. See, M. Van Der Velde, R.A. Nalepa, C. Perger, C. Schill, I. McCallum, D. Schepaschenko, F. Kraxner, X. Cai, X. Zhang, S. Ortner, R. Hazarika, A. Cipriani, C. Di Bella, A. H. Rabia, A. Garcia, M. Vakolyuk, K. Singha, M.E. Beget, S. Erasmi, F. Albrecht, B. Shaw, and M. Obersteiner. Downgrading recent estimates of land available for biofuel production. *Environmental Science and Technology*, 47(3):1688–1694, 2013. doi: 10.1021/es303141h.

[116] International Institute for Applied Systems Analysis (IIASA) and the Food and Agriculture Organisation (FAO). GAEZ v3.0 Global Agro-ecological Zones, 2012. URL http://www.gaez.iiasa.ac.at/.

[117] S. Li and C. Chan-Halbrendt. Ethanol production in (the) People' s Republic of China : Potential and technologies. *Applied Energy*, 86:S162–S169, 2009. doi: 10.1016/j.apenergy.2009.04.047.

[118] D. Zhuang, D. Jiang, L. Liu, and Y. Huang. Assessment of bioenergy potential on marginal land in China. *Renewable and Sustainable Energy Reviews*, 15(2): 1050–1056, 2011. doi: 10.1016/j.rser.2010.11.041.

[119] S. Xue, I. Lewandowski, X. Wang, and Z. Yi. Assessment of the production potentials of Miscanthus on marginal land in China. *Renewable and Sustainable Energy Reviews*, 54:932–943, 2016. doi: 10.1016/j.rser.2015.10.040.

[120] A. Strapasson, J. Woods, and K. Mbuk. Land use futures in Europe. *Grantham Institute briefing paper*, (17), 2016. URL https://www.imperial.ac.uk/media/imperial-college/grantham-institute/public/publications/briefing-papers/Land-Use-Futures-in-Europe---web-version-v3.pdf.

[121] A. A. Lovett, G. M. Sünnenberg, G. M. Richter, A. G. Dailey, A. B. Riche, and A. Karp. Land use implications of increased biomass production identified by gis-based suitability and yield mapping for miscanthus in england. *Bioenergy Research*, 2(1-2):17–28, 2009. doi: 10.1007/s12155-008-9030-x.

[122] A. W. Bauen, A. J. Dunnett, G. M. Richter, A. G. Dailey, Aylott, and E. M., Casella. Modelling supply and demand of bioenergy from short rotation coppice and Miscanthus in the UK. *Bioresource Technology*, 101(21):8132–8143, 2010.

[123] N. J. Glithero, P. Wilson, and S. J. Ramsden. Optimal combinable and dedicated energy crop scenarios for marginal land. *Applied Energy*, 147:82–91, 2015. doi: 10.1016/j.apenergy.2015.01.119.

[124] D. J. Muth and K. M. Bryden. An integrated model for assessment of sustainable agricultural residue removal limits for bioenergy systems. *Environmental Modelling and Software*, 39:50–69, 2013. doi: 10.1016/j.envsoft.2012.04.006.

[125] W. Wilhelm, J.M.F Johnson, J.L. Hatfield, W.B. Voorhees, and D.R. Linden. Crop and soil productivity response to corn residue removal: a literature review. *Agronomy Journal*, 96(1):1–17, 2004. doi: 10.2134/agronj2004.0001.

[126] Environmental Systems Research Institute. ArcGIS Release 10.5.1, 2012. URL http://desktop.arcgis.com/en/arcmap/.

[127] Food and Agriculture Organisation. CLIMWAT 2.0. URL http://www.fao.org/land-water/databases-and-software/climwat-for-cropwat/en/.

[128] T. Pacetti, L. Lombardi, and G. Federici. Water-energy Nexus: A case of biogas production from energy crops evaluated by Water Footprint and Life Cycle Assessment (LCA) methods. *Journal of Cleaner Production*, 101:1–14, 2015. doi: 10.1016/j.jclepro.2015.03.084.

[129] A. L. Borrion, M. C. McManus, and G. P. Hammond. Environmental life cycle assessment of bioethanol production from wheat straw. *Biomass and Bioenergy*, 47:9–19, 2012. doi: 10.1016/j.biombioe.2012.10.017.

[130] T. Ramjeawon. Life cycle assessment of electricity generation from bagasse in Mauritius. *Journal of Cleaner Production*, 16:1727–1734, 2008. doi: 10.1016/j.jclepro.2007.11.001.

[131] J. Dai, B. Bean, B. Brown, W. Bruening, J. Edwards, M. Flowers, R. Karow, C. Lee, G. Morgan, M. Ottman, J. Ransom, and J. Wiersma. Harvest index and straw yield of five classes of wheat. *Biomass and Bioenergy*, 85:223–227, 2016. doi: 10.1016/j.biombioe.2015.12.023.

[132] R. Parajuli, M. T. Knudsen, J. H. Schmidt, and T. Dalgaard. Life Cycle Assessment of district heat production in a straw fired CHP plant. *Biomass and Bioenergy*, 68(September):115–134, 2014. doi: 10.1016/j.biombioe.2014.06.005.

[133] M. de Wit and A. Faaij. European biomass resource potential and costs. *Biomass and Bioenergy*, 34(2):188–202, 2010. doi: 10.1016/j.biombioe.2009.07.011.

[134] X. Lu and H. Herzog. Biomass to Liquid Fuels Pathways: A Techno-Economic Environmental Evaluation. Technical report, 2015. URL http://sequestration.mit.edu/bibliography/BTL%20final%20compiled.pdf.

[135] T. Gebreegziabher, A. O. Oyedun, and C. W. Hui. Optimum biomass drying for combustion - A modeling approach. *Energy*, 53:67–73, 2013. doi: 10.1016/j.energy.2013.03.004.

[136] C. J. Roos. Biomass Drying and Dewatering for Clean Heat & Power. Technical Report September, US Department of Energy - CHP Technical Assistance Partnerships, 2008. URL http://northwestchptap.org/nwchpdocs/biomassdryinganddewateringforcleanheatandpower.pdf.

[137] F. Murphy, G. Devlin, and K. McDonnell. Miscanthus production and processing in Ireland: An analysis of energy requirements and environmental impacts. *Renewable and Sustainable Energy Reviews*, 23:412–420, 2013. doi: 10.1016/j.rser.2013.01.058.

[138] I. Obernberger and G. Thek. *The Pellet Hanbook, the production and thermal utilisation of biomass pellets*. Earthcan, 2010. URL https://books.google.co.uk/books?id=69QL45Hd8wEC&printsec=frontcover&hl=fr&source=gbs_ge_summary_r&cad=0#v=onepage&q&f=false.

[139] X. Qin, T. Mohan, M. El-Halwagi, G. Cornforth, and B. A. McCarl. Switchgrass as an alternate feedstock for power generation: An integrated environmental, energy and economic life-cycle assessment. *Clean Technologies and Environmental Policy*, 8(4):233–249, 2006. doi: 10.1007/s10098-006-0065-4.

[140] N. Johnson, N. Parker, and J. Ogden. How negative can biofuels with CCS take us and at what cost? Refining the economic potential of biofuel production with CCS using spatially-explicit modeling. *Energy Procedia*, 63:6770–6791, 2014. doi: 10.1016/j.egypro.2014.11.712.

[141] R. G. Allen, L.S. Pereira, D. Raes, and M. Smith. Crop evapotranspiration - Guidelines for computing crop water requirements. Technical report, 1998. URL http://www.fao.org/docrep/x0490e/x0490e00.htm#Contents.

[142] M. M. Mekonnen and A. Y. Hoekstra. Global Gray Water Footprint and Water Pollution Levels Related to Anthropogenic Nitrogen Loads to Fresh Water. *Environmental Science and Technology*, 49(21):12860–12868, 2015. doi: 10.1021/acs.est.5b03191.

[143] M. M. Mekonnen and A. Y. Hoekstra. The green, blue and grey water footprint of crops and derived crop products. Technical Report 47, UNESCO-IHE, 2010. URL https://waterfootprint.org/media/downloads/Mekonnen-Hoekstra-2011-WaterFootprintCrops_2.pdf.

[144] E. G. R. Davies, P. Kyle, and J. A. Edmonds. An integrated assessment of global and regional water demands for electricity generation to 2095. *Advances in Water Resources*, 52:296–313, 2013. doi: 10.1016/j.advwatres.2012.11.020.

[145] C. A. S. Hall, J. G. Lambert, and S. B. Balogh. EROI of different fuels and the implications for society. *Energy Policy*, 64:141–152, 2014. doi: 10.1016/j.enpol.2013.05.049.

[146] C.A.S. Hall, S. Balogh, and D.J.R. Murphy. What is the minimum EROI that a sustainable society must have? *Energies*, 2(1):25–47, 2009. doi: 10.3390/en20100025.

[147] D. J. Murphy, C. A. S. Hall, M. Dale, and C. Cleveland. Order from chaos: A preliminary protocol for determining the EROI of fuels. *Sustainability*, 3(10):1888–1907, 2011. doi: 10.3390/su3101888.

[148] M. Raugei, P. Fullana-i Palmer, and V. Fthenakis. The energy return on energy investment (EROI) of photovoltaics: Methodology and comparisons with fossil fuel life cycles. *Energy Policy*, 45:576–582, 2012. doi: 10.1016/j.enpol.2012.03.008.

[149] M. Dale and S. M. Benson. Energy balance of the global photovoltaic (PV) industry: is the PV industry a net electricity producer? *Environmental Science and Technology*, 47(7):3482–3489. doi: 10.1021/es3038824.

[150] A. L. Stephenson and D. Jc. MacKay. Life Cycle Impacts of Biomass Electricity in 2020. Technical Report July, Department of Energy and Climate Change, 2014.

[151] EURELECTRIC. Efficiency in Electricity Generation, 2003. URL http://dx.doi.org/10.1016/j.watres.2009.01.036.

[152] International Energy Agency (IEA). Energy Efficiency Indicators for Public Electricity Production from Fossil Fuels, 2008. URL https://www.iea.org/publications/freepublications/publication/En_Efficiency_Indicators.pdf.

[153] International Energy Agency (IEA). The Future of Trucks: Implications for energy and the environment. Technical report, 2017. URL https://www.iea.org/reports/the-future-of-trucks.

[154] M. Pogson, M. Richards, M. Dondini, E. O. Jones, A. Hastings, and P. Smith. ELUM: A spatial modelling tool to predict soil greenhouse gas changes from land conversion to bioenergy in the UK. *Environmental Modelling & Software*, 84: 458–466, 2016. doi: 10.1016/j.envsoft.2016.07.011.

[155] T. W. Hertel, A. A. Golub, A. D. Jones, M. O'Hare, R. J. Plevin, and D. M. Kammen. Effects of US Maize Ethanol on Global Land Use and Greenhouse Gas Emissions: Estimating Market-mediated Responses. *BioScience*, 60(3):223–231, 2010. doi: 10.1525/bio.2010.60.3.8.

[156] C. F. Heuberger, E. S. Rubin, I. Staffell, N. Shah, and N.I Mac Dowell. Power capacity expansion planning considering endogenous technology cost learning. *Applied Energy*, 204:831 – 845, 2017. doi: 10.1016/j.apenergy.2017.07.075.

[157] I. Lewandowski, J. C. Clifton-Brown, J. M O Scurlock, and W. Huisman. Miscanthus: European experience with a novel energy crop. *Biomass and Bioenergy*, 19(4):209–227, 2000. doi: 10.1016/S0961-9534(00)00032-5.

[158] J. Hillier, C. Whittaker, G. Dailey, M. Aylott, E. Casella, G. M. Richter, A. Riche, R. Murphy, G. Taylor, and P. Smith. Greenhouse gas emissions from four bioenergy crops in England and Wales: Integrating spatial estimates of yield and soil carbon balance in life cycle analyses. *GCB Bioenergy*, 1(4):267–281, 2009. doi: 10.1111/j.1757-1707.2009.01021.x.

[159] Food and Agriculture Organization. CROPWAT 8.0, . URL http://www.fao.org/nr/water/infores_databases_cropwat.html. (accessed May 2016).

[160] S. Kang, S. S. Nair, K. L. Kline, J. A. Nichols, D. Wang, W. M. Post, C. C. Brandt, S. D. Wullschleger, N. Singh, and Y. Wei. Global simulation of bioenergy crop productivity: Analytical framework and case study for switchgrass. *GCB Bioenergy*, 6(1):14–25, 2014. doi: 10.1111/gcbb.12047.

[161] M. Kottek, J. Grieser, C. Beck, B. Rudolf, and F. Rubel. World map of the Köppen-Geiger climate classification updated. *Meteorologische Zeitschrift*, 15 (3):259–263, 2006. doi: 10.1127/0941-2948/2006/0130.

[162] R. L. Graham, L. J. Allison, and D. A. Becker. ORECCL - Summary of a National database on energy crop landbase, yields, and costs, 1997. URL https://www.osti.gov/servlets/purl/501534.

[163] M. R. Schmer, K. P. Vogel, R. B. Mitchell, and R. K. Perrin. Net energy of cellulosic ethanol from switchgrass. *Proceedings of the National Academy of Sciences*, 105(2):464–469, 2008. doi: 10.1073/pnas.0704767105.

[164] S. Channan, K. Collins, and W. R. Emmanuel. Global mosaics of the standard MODIS land cover type data. URL http://glcf.umd.edu/data/lc/. (accessed May 2017).

[165] F. Gassert, M. Luck, M. Landis, P. Reig, and T. Shiao. Aqueduct Global Maps 2.0. URL https://www.wri.org/resources/data-sets/aqueduct-global-maps-20. (accessed May 2019).

[166] L. You, U. Wood-Sichra, S. Fritz, Z. Guo, L. See, and J. Koo. Spatial Production Allocation Model (SPAM) 2005 v3.2. URL http://mapspam.info. (accessed october 2017).

[167] J. Gtschow, L. Jeffery, R. Gieseke, and R. Gebel. The PRIMAP-hist national historical emissions time series (1850-2014). URL http://doi.org/10.5880/PIK.2017.001. (accessed January 2019).

[168] World Resources Institute. Climate Watch, 2018. URL https://www.climatewatchdata.org. (accessed January 2019).

[169] International Energy Agency (IEA). *World Energy Outlook 2018*. Paris, 2018. doi: https://doi.org/https://doi.org/10.1787/weo-2018-en. URL https://www.oecd-ilibrary.org/content/publication/weo-2018-en.

[170] G. C. Rockett, J. M. M. Ketzer, A. Ramírez, and M. Van Den Broek. CO_2 storage capacity of Campos Basin's oil fields, Brazil. *Energy Procedia*, 37:5124–5133, 2013. doi: 10.1016/j.egypro.2013.06.427.

[171] T. Wildenborg, S. Holloway, C. Hendriks, E. Kreft, A. Lokhorst, M. Brook, R. Brandsma, P. Egberts, and M. Larsen. Building the cost curves for CO_2 storage: European sector. Technical report, International Energy Agency Greenhouse Gas R&D Programme, 2005. URL https://www.globalccsinstitute.com/publications/building-cost-curves-CO2-storage-european-sector.

[172] J. M. M. Ketzer, C. X. Machado, G. C. Rockett, and R. S. Iglesias. Brazilian Atlas of CO_2 Capture and Geological Storage. Technical report, CEPAC, 2014. URL https://www.globalccsinstitute.com/archive/hub/publications/190903/brazilian-atlas-CO2-capture-geological-storage.pdf.

[173] S. Podwysocki. Coal-Bearing Regions and Structural Sedimentary Basins of China and Adjacent Seas: Structural sedimentary basins: U.S. Geological Survey Open-File Report 00-047. Technical report, U.S. Geological Survey, Reston, VA, 2000. URL https://pubs.usgs.gov/of/2000/of00-047/.

[174] R. T. Dahowski, X. Li, C. L. Davidson, N. Wei, and J. J. Dooley. Regional Opportunities for Carbon Dioxide Capture and Storage in China. Technical Report December, Pacific Northwest National Laboratory, 2009. URL https://energyenvironment.pnnl.gov/pdf/roccs_china_pnnl_19091.pdf.

[175] Geological Survey of Denmark and Greenland. Assessing European Capacity for Geological Storage of Carbon Dioxide - WP2 Report Storage Capacity. Technical report, 2009. URL http://www.geology.cz/geocapacity/publications/D16WP2Reportstoragecapacity-red.pdf.

[176] Energy Technologies Institute. A Picture of CO_2 Storage in the UK: Learnings from the ETI's UKSAP and derived projects, 2013. URL https://www.eti.co.uk/programmes/carbon-capture-storage/uk-storage-appraisal-project.

[177] S. Holloway, A. Garg, M. Kapshe, A. Deshpande, A. S. Pracha, and S. R. Khan. A regional assessment of the potential for CO_2 storage in the Indian subcontinent. Technical report, International Energy Agency Greenhouse Gas R&D Programme, 2008. URL https://hub.globalccsinstitute.com/sites/default/files/publications/95746/regional-assessment-potential-CO2-storage-indian-subcontinent.pdf.

[178] U.S. Department of Energy (DOE). Carbon Storage Atlas. Technical report, 2015. URL http://www.netl.doe.gov/technologies/carbon_seq/FAQs/carboncapture1.html.

[179] Office of Strategic Energy Studies. Monthly Energy Bulletin - Brazil, 2017. URL http://www.mme.gov.br/.

[180] CEIC Data. CEIC database. URL https://www.ceicdata.com/en/china/electricity-price%0A). (accessed 2019).

[181] European Commission. EUROSTAT. URL https://ec.europa.eu/eurostat/home? (accessed January 2019).

[182] Government of India. Evaluation Report on Rajiv Gandhi Grameen Vidyutikaran Yojana. Technical Report 224, 2014. URL http://planningcommission.nic.in/reports/peoreport/peo/peo_rggvy3107.pdf.

[183] Energy Information Agency (EIA). Electric power monthly. Technical Report March, 2019. URL https://www.eia.gov/electricity/monthly/current_month/epm.pdf.

[184] H. Shahrukh, A. O. Oyedun, A. Kumar, B. Ghiasi, L. Kumar, and S. Sokhansanj. Comparative net energy ratio analysis of pellet produced from steam pretreated biomass from agricultural residues and energy crops. *Biomass and Bioenergy*, 90: 50–59, 2016. doi: 10.1016/j.biombioe.2016.03.022.

[185] W. Schakel, H. Meerman, A. Talaei, A. Ramirez, and A. Faaij. Comparative life cycle assessment of biomass co-firing plants with carbon capture and storage. *Applied Energy*, 131:441–467, 2014. doi: 10.1016/j.apenergy.2014.06.045.

[186] T. L. T. Nguyen, J. E. Hermansen, and L. Mogensen. Environmental performance of crop residues as an energy source for electricity production: The case of wheat straw in Denmark. *Applied Energy*, 104:633–641, 2013. doi: 10.1016/j.apenergy.2012.11.057.

[187] W. Liu, J. Mi, Z. Song, J. Yan, J. Li, and T. Sang. Long-term water balance and sustainable production of Miscanthus energy crops in the Loess Plateau of China. *Biomass and Bioenergy*, 62:47–57, 2014. doi: 10.1016/j.biombioe.2014.01.018.

[188] I. E. Palmer, R. J. Gehl, T. G. Ranney, D. Touchell, and N. George. Biomass yield, nitrogen response, and nutrient uptake of perennial bioenergy grasses in North Carolina. *Biomass and Bioenergy*, 63:218–228, 2014. doi: 10.1016/j.biombioe.2014.02.016.

[189] F. Triana, N. Nassi o Di Nasso, G. Ragaglini, N. Roncucci, and E. Bonari. Evapotranspiration, crop coefficient and water use efficiency of giant reed (Arundo donax L.) and miscanthus (Miscanthus x giganteus Greef et Deu.) in a Mediterranean environment. *GCB Bioenergy*, pages 811–819, 2014. doi: 10.1111/gcbb.12172.

[190] M. B. Jones and M. Walsh. *Miscanthus for energy and fibre*. James & James (Science Publishers) Ltd, 2001.

[191] L. Price, M. Bullard, H. Lyons, S. Anthony, and P. Nixon. Identifying the yield potential of Miscanthus x giganteus: An assessment of the spatial and temporal variability of M. x giganteus biomass productivity across England and Wales. *Biomass and Bioenergy*, 26(1):3–13, 2004. doi: 10.1016/S0961-9534(03)00062-X.

[192] B. Gabrielle, L. Bamière, N. Caldes, S. De Cara, G. Decocq, F. Ferchaud, C. Loyce, E. Pelzer, Y. Perez, J. Wohlfahrt, and G. Richard. Paving the way for sustainable bioenergy in Europe: Technological options and research avenues for large-scale biomass feedstock supply. *Renewable and Sustainable Energy Reviews*, 33:11–25, 2014. doi: 10.1016/j.rser.2014.01.050.

[193] G. G. T. Camargo, M. R. Ryan, and T. L. Richard. Energy Use and Greenhouse Gas Emissions from Crop Production Using the Farm Energy Analysis Tool. *Bioscience*, 63(4):263–273, 2013. doi: 10.1525/bio.2013.63.4.6.

[194] M. A. Mehmood, M. Ibrahim, U. Rashid, M. Nawaz, S. Ali, A. Hussain, and M. Gull. Biomass production for bioenergy using marginal lands. *Sustainable Production and Consumption*, (August):1–19, 2016. doi: 10.1016/j.spc.2016.08.003.

[195] A. Grzybek. Modelling of biomass utilisation for energy purpose, 2010. URL https://nibio.brage.unit.no/nibio-xmlui/handle/11250/2460138.

[196] E. A. Heaton, J. Clifton-Brown, T. B. Voigt, M. B. Jones, and S. P. Long. Miscanthus for renewable energy generation: European Union experience and projections for Illinois. *Mitigation and Adaptation Strategies for Global Change*, 9(4):433–451, 2004. doi: 10.1023/B:MITI.0000038848.94134.be.

[197] D. G. Christian, A. B. Riche, and N. E. Yates. Growth, yield and mineral content of Miscanthus x giganteus grown as a biofuel for 14 successive harvests. *Industrial Crops and Products*, 28(3):320–327, 2008. doi: 10.1016/j.indcrop.2008.02.009.

[198] U. Bohmel. *Comparative Performance of Annual and Perennial Energy Cropping Systems Under Different Management Regimes*. PhD thesis, University of Hohenheim, 2007. URL https://core.ac.uk/download/pdf/56707081.pdf.

[199] I. Lewandowski, A. Kicherer, and P. Vonier. CO_2-balance for the cultivation and combustion of Miscanthus. *Biomass and Bioenergy*, 8(2):81–90, 1995. doi: 10.1016/0961-9534(95)00008-U.

[200] J. C. Clifton-brown, J. Breuer, and M. B. Jones. Carbon mitigation by the energy crop, Miscanthus. *Global Change Biology*, 13(11):2296–2307, 2007. doi: 10.1111/j.1365-2486.2007.01438.x.

[201] X. Lu, M. R. Withers, N. Seifkar, R. P. Field, S. R. H. Barrett, and H. J. Herzog. Biomass logistics analysis for large scale biofuel production: Case study of loblolly pine and switchgrass. *Bioresource Technology*, 183:1–9, 2015. doi: 10.1016/j.biortech.2015.02.032.

[202] S. Lettens, B. Muys, R. Ceulemans, E. Moons, J. Garcia, and P. Coppin. Energy budget and greenhouse gas balance evaluation of sustainable coppice systems for electricity production. *Biomass and Bioenergy*, 24(3):179–197, 2003. doi: 10.1016/S0961-9534(02)00104-6.

[203] D. Pimentel and T. Patzek. Ethanol production using corn, switchgrass, and wood; Biodiesel production using soybean and sunflower. *Natural Resources Research*, 14(1):65–76, 2005. doi: 10.1007/s11053-005-4679-8.

[204] N. Nassi o Di Nasso, M. V. Lasorella, N. Roncucci, and E. Bonari. Soil texture and crop management affect switchgrass (Panicum virgatum L.) productivity in the Mediterranean. *Industrial Crops and Products*, 65:21–26, 2015. doi: 10.1016/j.indcrop.2014.11.017.

[205] J. van Dam, A. P. C. Faaij, J. Hilbert, H. Petruzzi, and W. C. Turkenburg. Large-scale bioenergy production from soybeans and switchgrass in Argentina. Part A: Potential and economic feasibility for national and international markets. *Renewable and Sustainable Energy Reviews*, 13(8):1710–1733, 2009. doi: 10.1016/j.rser.2009.03.009.

[206] J. S. Tumuluru. Comparison of Chemical Composition and Energy Property of Torrefied Switchgrass and Corn Stover. *Frontiers in Energy Research*, 3 (November):1–11, 2015. doi: 10.3389/fenrg.2015.00046.

[207] R. Samson. Switchgrass Production in Ontario: A Management Guide. Technical report, Resource Efficient Agricultural Production (REAP) Canada, 2007. URL http://www.plantmanagementnetwork.org/pub/fg/review/2008/energy/.

[208] B. Kalita. *Life cycle assesment of switchgrass (Panicum virgatum L.) biomass production in Ontario*. PhD thesis, University of Guelph, 2012. URL https://atrium.lib.uoguelph.ca/xmlui/bitstream/handle/10214/3257/Binu%20Kalita%20thesis.pdf?sequence=4.

[209] C. S. Snyder, T. W. Bruulsema, T. L. Jensen, and P. E. Fixen. Review of greenhouse gas emissions from crop production systems and fertilizer management effects. *Agriculture, Ecosystems and Environment*, 133(3-4):247–266, 2009. doi: 10.1016/j.agee.2009.04.021.

[210] J. Daystar, C. Reeb, R. Gonzalez, R. Venditti, and S. S. Kelley. Environmental life cycle impacts of cellulosic ethanol in the Southern U.S. produced from loblolly pine, eucalyptus, unmanaged hardwoods, forest residues, and switchgrass using a thermochemical conversion pathway. *Fuel Processing Technology*, 138:164–174, 2015. doi: 10.1016/j.fuproc.2015.04.019.

[211] M. Wu and Y-W. Chiu. Developing County-Level Water Footprints of Biofuel Produced from Switchgrass and Miscanthus in the US. Technical report, Argonne National Laboratory, 2014. URL https://www.osti.gov/biblio/1177405.

[212] A. J. Ashworth, A. M. Taylor, D. L. Reed, F. L. Allen, P. D. Keyser, and D. D. Tyler. Environmental impact assessment of regional switchgrass feedstock production comparing nitrogen input scenarios and legume-intercropping systems. *Journal of Cleaner Production*, 87(C):227–234, 2015. doi: 10.1016/j.jclepro.2014.10.002.

[213] R. Samson and P. Duxbury. Assessment of pelletized biofuels. Technical report, Resource Efficient Agriculture Production (REAP) - Canada, 2000. URL https://www.reap-canada.com/online_library/feedstock_biomass/15%20Assessment%20of.PDF.

[214] M. Mobini, T. Sowlati, and S. Sokhansanj. A simulation model for the design and analysis of wood pellet supply chains. *Applied Energy*, 111:1239–1249, 2013. doi: 10.1016/j.apenergy.2013.06.026.

[215] R. Ehrig. *Analysis of Environmental and Economic Aspects of International Pellet Supply Chains*. PhD thesis, Technical University (TU) Berlin, 2014. URL https://d-nb.info/1067385681/34.

[216] P. Thornley, P. Gilbert, S. Shackley, and J. Hammond. Maximizing the greenhouse gas reductions from biomass: The role of life cycle assessment. *Biomass and Bioenergy*, 81(0):35–43, 2015. doi: 10.1016/j.biombioe.2015.05.002.

[217] R. W. Matthews. Modelling of energy and carbon budgets of wood fuel coppice systems. *Biomass and Bioenergy*, 21(1):1–19, 2001. doi: 10.1016/S0961-9534(01)00016-2.

[218] M. Elsayed, R. Matthews, and N. Mortimer. Carbon and energy balances for a range of biofuels options. Technical report, Resources Research Unit, Sheffield Hallam University, 2003. URL http://airburners.com/PUB/Sheffield-studie-mei2003.pdf.

[219] J. Wickham, B. Rice, J. Finnan, and R. McConnon. A review of past and current research on short rotation coppice in Ireland and abroad. Technical report, COFORD and Sustainable Energy Authority of Ireland, 2010. URL http://www.coford.ie/media/coford/content/publications/projectreports/SRC.pdf.

[220] M. Wu and M. J. Peng. Developing a Tool to Estimate Water Use in Electric Power Generation in the US. Technical report, 2011. URL https://publications.anl.gov/anlpubs/2011/02/69392.pdf.

[221] L. Gustavsson, P. Borjesson, B. Johansson, and P. Svenningsson. Reducing CO_2 emissions by substituting biomass for fossil fuels. *Energy*, 20(11):1097–1113, 1995. doi: 10.1016/0360-5442(95)00065-O.

[222] A.Y. Hoekstra, A. K. Chapagain, M. M. Aldaya, and M. M. Mekonnen. Water Footprint Manual State of the Art. Technical Report november, 2009. URL http://www.waterfootprint.org/downloads/WaterFootprintManual2009.pdf.

[223] M. M. Mekonnen and A. Y. Hoekstra. The green, blue and grey water footprint of crops and derived crop products. Volume 2 : Appendices. Technical Report 47, UNESCO-IHE, 2010. URL https://waterfootprint.org/media/downloads/Mekonnen-Hoekstra-2011-WaterFootprintCrops_2.pdf.

[224] P. W. Gerbens-Leenes, A. Y. Hoekstra, and T. van der Meer. The water footprint of energy from biomass: A quantitative assessment and consequences of an increasing share of bio-energy in energy supply. *Ecological Economics*, 68(4): 1052–1060, 2009. doi: 10.1016/j.ecolecon.2008.07.013.

[225] M. Wu, M. Mintz, M. Wang, and S. Arora. Water consumption in the production of ethanol and petroleum gasoline. *Environmental Management*, 44(5):981–997, 2009. doi: 10.1007/s00267-009-9370-0.

[226] P. W. Gerbens-Leenes, A. Y. Hoekstra, and T. H. van der Meer. The water footprint of bioenergy. *Proceedings of the National Academy of Sciences of the United States of America*, 106(25):10219–10223, 2009. doi: 10.1073/pnas.0812619106.

[227] J. Macknick, R. Newmark, G. Heath, and K. C. Hallett. Operational water consumption and withdrawal factors for electricity generating technologies: a review of existing literature. *Environmental Research Letters*, 7(4):045802, 2012. doi: 10.1088/1748-9326/7/4/045802.

[228] Y.T. Yimam, T. E. Ochsner, and V. G. Kakani. Evapotranspiration partitioning and water use efficiency of switchgrass and biomass sorghum managed for biofuel. *Agricultural Water Management*, 155:40–47, 2015. doi: 10.1016/j.agwat.2015.03.018.

[229] International Energy Agency Greenhouse Gas Programme (IEAGHG). Water Intensity of Power Generation, IEAGHG Information Paper. Technical report, 2013. URL http://content.ccrasa.com/library_1/2715%20-%202013-IP22%20Water%20Intensity%20of%20Power%20Generation.pdf.

[230] I. Dimitriou. *Performance and Sustainability of Short-Rotation Energy Crops Treated With Municipal and Industrial Residues*. PhD thesis, Swedish University of Agricultural Sciences, 2005. URL http://www.fao.org/forestry/16311-0befb3519578a3029f886963c54379981.pdf.

[231] L. Sevel, T. Nord-Larsen, M. Ingerslev, U. Jørgensen, and K. Raulund-Rasmussen. Fertilization of SRC Willow, I: Biomass Production Response. *Bioenergy Research*, 2014. doi: 10.1007/s12155-013-9371-y.

[232] P. Heffer. Assessment of Fertilizer Use by Crop at the Global Level. Technical Report August, International Fertilizer Industry Association (IFA), 2013. URL https://api.ifastat.org/reports/download/12246.

[233] Atlantic Consulting. LPG's Carbon Footprint Relative to Other Fuels - A Scientific Review, 2009. URL https://www.shvenergy.com/wp-content/uploads/2015/05/atlantic_consulting_scientific_review_carbon_footprint_june_2009.pdf.

[234] S. Hinchliffe, R. V. Diemen, C. Heuberger, and N. Mac Dowell. Transitions in Electricity Systems Towards 2030. Technical Report October, The Energy Centre of the Institution of Chemical Engineers (IChemE), 2015.

[235] VERSA. Personal communication, 2016. URL http://www.growversa.com/.

[236] C. Folberth, R. Skalský, E. Moltchanova, J. Balkovič, L. B. Azevedo, M. Obersteiner, and M. van der Velde. Uncertainty in soil data can outweigh climate impact signals in global crop yield simulations. *Nature Communications*, 7(May): 11872, 2016. doi: 10.1038/ncomms11872.

[237] A. K. Chapagain and A Y. Hoekstra. Water footprint of nations. Volume 1: Main report. Technical report, UNESCO-IHE, 2004. URL https://waterfootprint.org/media/downloads/Report16Vol1.pdf.

[238] International Energy Agency (IEA). Tracking power 2019. Technical report, 2019. URL https://www.iea.org/reports/tracking-power-2019/.

[239] International Energy Agency (IEA). IEA Statistics. URL https://www.iea.org/. (accessed July 2017).

[240] J. Wilcox. Direct Air Capture. In *CCS Leaders Forum*, London, 2016.

[241] M. Ranjan and H. J. Herzog. Feasibility of air capture. *Energy Procedia*, 4(2010): 2869–2876, 2011. doi: 10.1016/j.egypro.2011.02.193.

[242] R. Baciocchi, G. Storti, and M. Mazzotti. Process design and energy requirements for the capture of carbon dioxide from air. *Chemical Engineering and Processing*, 45:1047–1058, 2006. doi: 10.1016/j.cep.2006.03.015.

[243] Carbon Engineering. URL http://carbonengineering.com/our-technology/. (accessed July 2017).

[244] Committee on Climate Change (CCC). Net Zero – The UK' s contribution to stopping global warming. Technical report, 2019. URL https://www.theccc.org.uk/publication/net-zero-the-uks-contribution-to-stopping-global-warming/.

[245] P. Börjesson. Energy analysis of biomass production and transportation. *Biomass and Bioenergy*, 11(4):305–318, 1996. doi: 10.1016/0961-9534(96)00024-4.

[246] S. Njakou Djomo, O. El Kasmioui, T. De Groote, L. S. Broeckx, M. S. Verlinden, G. Berhongaray, R. Fichot, D. Zona, S. Y. Dillen, J. S. King, I. A. Janssens, and R. Ceulemans. Energy and climate benefits of bioelectricity from low-input short rotation woody crops on agricultural land over a two-year rotation. *Applied Energy*, 111:862–870, 2013. doi: 10.1016/j.apenergy.2013.05.017.

[247] V. Forgie and R. Andrew. Life Cycle Assessment of Using Straw to Produce Industrial Energy in New Zealand. Technical Report May, Landcare Research and New Zealand Centre for Ecological Economics, 2008. URL http://citeseerx.ist.psu.edu/viewdoc/download?doi=10.1.1.460.5188&rep=rep1&type=pdf.

[248] International Energy Agency (IEA). CO_2 emissions from fuel combustion. Technical report, 2017. URL https://www.iea.org/publications/freepublications/publication/CO2EmissionsfromFuelCombustionHighlights2017.pdf.

[249] Office of Atmospheric Programs. The emissions & generation resource integrated database. Technical Report February, Environmental Protection Agency, 2016. URL https://www.epa.gov/energy/emissions-generation-resource-integrated-database-egrid.

[250] L. Wang, Y. Qian, J. E. Brummer, J. Zheng, S. Wilhelm, and W. J. Parton. Simulated biomass, environmental impacts and best management practices for long-term switchgrass systems in a semi-arid region. *Biomass and Bioenergy*, 75:254–266, 2015. doi: 10.1016/j.biombioe.2015.02.029.

[251] The Department of Energy and Climate Change (DECC). The UK 2050 Calculator. URL http://2050-calculator-tool.decc.gov.uk/#/home. (accessed July 2017).

[252] Digest of UK Energy Statistics (DUKES). Renewable sources of energy, 2017. URL https://www.gov.uk/government/uploads/system/uploadsattachment_data/file/633782/Chapter_6.pdf.

[253] K. S. Lackner. The thermodynamics of direct air capture of carbon dioxide. *Energy*, 50(1):38–46, 2013. doi: 10.1016/j.energy.2012.09.012.

[254] I. S. Tagomori, F. M. Carvalho, F.T.F. da Silva, P. R. Paulo, P. R.R. Rochedo, A. Szklo, and R. Schaeffer. Designing an optimum carbon capture and transportation network by integrating ethanol distilleries with fossil-fuel processing plants in Brazil. *International Journal of Greenhouse Gas Control*, 68:112–127, 2018. doi: 10.1016/j.ijggc.2017.10.013.

[255] F. Kraxner, K. Aoki, S. Leduc, G. Kindermann, S. Fuss, J. Yang, Y. Yamagata, K. I. Tak, and M. Obersteiner. BECCS in South Korea-Analyzing the negative emissions potential of bioenergy as a mitigation tool. *Renewable Energy*, 61: 102–108, 2014. doi: 10.1016/j.renene.2012.09.064.

[256] E. Baik, D. L. Sanchez, P. A. Turner, K. J. Mach, C. B. Field, and S. M. Benson. Geospatial analysis of near-term potential for carbon-negative bioenergy in the United States. *Proceedings of the National Academy of Sciences*, page 201720338, 2018. doi: 10.1073/pnas.1720338115.

[257] A. Welfle. Balancing growing global bioenergy resource demands - Brazil's biomass potential and the availability of resource for trade. *Biomass and Bioenergy*, 105:83–95, 2017. doi: 10.1016/j.biombioe.2017.06.011.

[258] N. Bauer, K. Calvin, J. Emmerling, O. Fricko, S. Fujimori, J. Hilaire, J. Eom, V. Krey, E. Kriegler, I. Mouratiadou, H. Sytze de Boer, M. van den Berg, S. Carrara, V. Daioglou, L. Drouet, J. E. Edmonds, D. Gernaat, P. Havlik, N. Johnson, D. Klein, P. Kyle, G. Marangoni, T. Masui, R. C. Pietzcker, M. Strubegger, M. Wise, K. Riahi, and D. P. van Vuuren. Shared Socio-Economic Pathways of the Energy Sector – Quantifying the Narratives. *Global Environmental Change*, 42:316–330, 2017. doi: 10.1016/j.gloenvcha.2016.07.006.

[259] C. Azar, K. Lindgren, M. Obersteiner, K. Riahi, D. P. van Vuuren, K. M.G. J. den Elzen, K. Möllersten, and E. D. Larson. The feasibility of low CO_2 concentration targets and the role of bio-energy with carbon capture and storage (BECCS). *Climatic Change*, 100(1):195–202, 2010. doi: 10.1007/s10584-010-9832-7.

[260] T. Skevas, S. M. Swinton, and N.J. Hayden. What type of landowner would supply marginal land for energy crops? *Biomass and Bioenergy*, 67:252–259, 2014. doi: 10.1016/j.biombioe.2014.05.011.

[261] N.E. Vaughan, C. Gough, S. Mander, E. W. Littleton, A. Welfle, D. E.H.J. Gernaat, and D. P. Van Vuuren. *Environmental Research Letters*, (4):044014. doi: 10.1088/1748-9326/aaaa02.

[262] G. P. Peters and O. Geden. Catalysing a political shift from low to negative carbon. *Nature Climate Change*, 7(9):619–621, 2017. doi: 10.1038/nclimate3369.

[263] M. Hoogwijk, A. Faaij, B. Eickhout, B. De Vries, and W. Turkenburg. Potential of biomass energy out to 2100, for four IPCC SRES land-use scenarios. *Biomass and Bioenergy*, 29(4):225–257, 2005. doi: 10.1016/j.biombioe.2005.05.002.

[264] H. Yamamoto, J. Fujino, and K. Yamaji. Evaluation of bioenergy potential with a multi-regional global-land-use-and-energy model. *Biomass and Bioenergy*, 21 (3):185–203, 2001. doi: 10.1016/S0961-9534(01)00025-3.

[265] M. R. Raupach, S. J. Davis, G. P. Peters, R. M. Andrew, J. G. Canadell, P. Ciais, P. Friedlingstein, F. Jotzo, D. P. Van Vuuren, and C. Le Quéré. Sharing a quota on cumulative carbon emissions. *Nature Climate Change*, 4(10):873–879, 2014. doi: 10.1038/nclimate2384.

[266] M. G.J. den Elzen, J. G.J. Olivier, N. Höhne, and G. Janssens-Maenhout. Countries' contributions to climate change: Effect of accounting for all greenhouse gases, recent trends, basic needs and technological progress. *Climatic Change*, 121(2):397–412, 2013. doi: 10.1007/s10584-013-0865-6.

[267] A. Galán-Martín, C. Pozo, A. Azapagic, I. E. Grossmann, N. Mac Dowell, and G. Guillén-Gosálbez. Time for global action: An optimised cooperative approach towards effective climate change mitigation. *Energy and Environmental Science*, 11(3):572–581, 2018. doi: 10.1039/c7ee02278f.

[268] J. Hovi, D. F. Sprinz, H. Sælen, and A. Underdal. The Club Approach: A Gateway to Effective Climate Co-operation? *British Journal of Political Science*, (November 2016):1–26, 2017. doi: 10.1017/s0007123416000788.

[269] J. Hovi, D. F. Sprinz, H. Sælen, and A. Underdal. Climate change mitigation: A role for climate clubs? *Palgrave Communications*, 2(May), 2016. doi: 10.1057/palcomms.2016.20.

[270] W. Nordhaus. Climate Clubs : Overcoming Free-riding in. *American Economic Review*, 105(4):1339–1370, 2015. doi: 10.1257/aer.15000001.

[271] F. Karimi and R. Khalilpour. Evolution of carbon capture and storage research: Trends of international collaborations and knowledge maps. *International Journal of Greenhouse Gas Control*, 37:362–376, 2015. doi: 10.1016/j.ijggc.2015.04.002.

[272] I. Czernichowski-Lauriol, R. Berenblyum, S. Bigi, M. Car, M. Gastine, S. Persoglia, N. Poulsen, C. Schmidt-Hattenberger, R. Stead, C. J. Vincent, and T. Wildenborg. CO_2GeoNet actions in Europe for advancing CCUS through global cooperation. *Energy Procedia*, 154:73–79, 2018. doi: 10.1016/j.egypro.2018.11.013.

[273] J. C. Abanades, M. Alonso, and N. Rodríguez. Biomass Combustion with in Situ CO_2 Capture with CaO. I. Process Description and Economics. *Industrial & Engineering Chemistry Research*, 50(11):6972–6981, jun 2011. doi: 10.1021/ie102353s.

[274] Daniel L. Sanchez and Duncan S. Callaway. Optimal scale of carbon-negative energy facilities. *Applied Energy*, 170:437–444, 2016. doi: 10.1016/j.apenergy.2016.02.134.

[275] A. Laude, O. Ricci, G. Bureau, J. Royer-Adnot, and A. Fabbri. CO_2 capture and storage from a bioethanol plant: Carbon and energy footprint and economic assessment. *International Journal of Greenhouse Gas Control*, 5(5):1220–1231, 2011. doi: 10.1016/j.ijggc.2011.06.004.

[276] Q. Yi, Y. Zhao, Y. Huang, G. Wei, Y. Hao, J. Feng, U. Mohamed, M. Pourkashanian, W. Nimmo, and W. Li. Life cycle energy-economic-CO_2 emissions evaluation of biomass/coal, with and without CO_2 capture and storage, in a pulverized fuel combustion power plant in the United Kingdom. *Applied Energy*, 225(February): 258–272, 2018. doi: 10.1016/j.apenergy.2018.05.013.

[277] K. Al-qayim, W. Nimmo, and M. Pourkashanian. Comparative techno-economic assessment of biomass and coal with CCS technologies in a pulverized combustion power plant in the United Kingdom. *International Journal of Greenhouse Gas Control*, 43:82–92, 2015. doi: 10.1016/j.ijggc.2015.10.013.

[278] A. Bhave, R. H.S. Taylor, P. Fennell, W. R. Livingston, N. Shah, N. Mac Dowell, J. Dennis, M. Kraft, M. Pourkashanian, M. Insa, J. Jones, N. Burdett, A. Bauen, C. Beal, A. Smallbone, and J. Akroyd. Screening and techno-economic assessment of biomass-based power generation with CCS technologies to meet 2050 CO_2targets. *Applied Energy*, 190:481–489, 2017. doi: 10.1016/j.apenergy.2016.12.120.

[279] International Energy Agency (IEA). World Energy Outlook, 2016. URL https://www.iea.org/newsroom/news/2016/november/world-energy-outlook-2016.html.

[280] L. Ren, K. Cafferty, M. Roni, J. Jacobson, G. Xie, Leslie Ovard, and Christopher Wright. Analyzing and Comparing Biomass Feedstock Supply Systems in China: Corn Stover and Sweet Sorghum Case Studies. *Energies*, 8(6):5577–5597, 2015. doi: 10.3390/en8065577.

[281] A. Hastings. Economic and Environmental Assessment of Seed and Rhizome Propagated Miscanthus in the UK. *Frontiers in Plant Science*, 8(June):1–16, 2017. doi: 10.3389/fpls.2017.01058.

[282] BEIS. Electricity generation costs. Technical Report November, Department for Business Energy & Industrial Strategy, 2016. URL https://assets.publishing.service.gov.uk/government/uploads/system/uploads/attachment_data/file/566567/BEIS_Electricity_Generation_Cost_Report.pdf.

[283] A. Hastings, M. J. Tallis, E. Casella, R. W. Matthews, P. A. Henshall, S. Milner, P. Smith, and G. Taylor. The technical potential of Great Britain to produce lignocellulosic biomass for bioenergy in current and future climates. *GCB Bioenergy*, 6(2):108–122, 2014. doi: 10.1111/gcbb.12103.

[284] R. P. Cabral, M. Bui, and N. Mac Dowell. A synergistic approach for the simultaneous decarbonisation of power and industry via bioenergy with carbon capture and storage (BECCS). *International Journal of Greenhouse Gas Control*, 87(February):221 – 237, 2019. doi: 10.1016/j.ijggc.2019.05.020.

[285] H. A. Daggash and N. Mac Dowell. Higher Carbon Prices on Emissions Alone Will Not Deliver the Paris Agreement. *Joule*, 3(9):2120 – 2133, 2019. doi: 10.1016/j.joule.2019.08.008.

[286] S. K. Mishra, M. C. Negri, J. Kozak, J. F. Cacho, J. Quinn, S. Secchi, and H. Ssegane. Valuation of ecosystem services in alternative bioenergy landscape scenarios. *GCB Bioenergy*, 11(6):748–762, 2019. doi: 10.1111/gcbb.12602.

[287] P. Patrizio, S. Leduc, F. Kraxner, S. Fuss, G. Kindermann, S. Mesfun, K. Spokas, A. Mendoza, N. MacDowell, E. Wetterlund, J. Lundgren, E. Dotzauer, P. Yowargana, and M. Obersteiner. Reducing US coal emissions can boost employment. *Joule*, accepted:1–16, 2018. doi: 10.1016/j.joule.2018.10.004.

[288] H. Li, Q. Chen, X. Zhang, K. N. Finney, V. N. Sharifi, and J. Swithenbank. Evaluation of a biomass drying process using waste heat from process industries: A case study. *Applied Thermal Engineering*, 35(1):71–80, 2012. doi: 10.1016/j.applthermaleng.2011.10.009.

[289] Q. X. Xu and S. S. Pang. Mathematical Modeling of Rotary Drying of Woody Biomass. *Drying Technology*, 26(11):1344–1350, 2008. doi: Doi10.1080/07373930802331050.

[290] M. N. Haque. Simulation of Temperature and Moisture Content Profiles in a Pinus radiata Board during High-Temperature Drying. *Drying Technology*, 25 (4):547–555, 2007. doi: 10.1080/07373930701226922.

[291] J. Selivanovs, D. Blumberga, J. Ziemele, A. Blumberga, and A. Barisa. Research of woody biomass drying process in pellet production. *Environmental and Climate Technologies*, 10(1):46–50, 2012. doi: 10.2478/v10145-012-0017-7.

[292] E. M. W. Smeets, I. M. Lewandowski, and A. P. C. Faaij. The economical and environmental performance of miscanthus and switchgrass production and supply chains in a European setting. *Renewable and Sustainable Energy Reviews*, 13 (6-7):1230–1245, 2009. doi: 10.1016/j.rser.2008.09.006.

[293] R. E. Muller. Energy input-output simulations of crop production. In R. M. Peart and R. C. Brook, editors, *Energy in World Agriculture*. Elsevier, Amsterdam, vol. 5. edition, 1992.

[294] G. Kongshaug and T. K. Jenssen. Energy Consumption and Greenhouse Gas emissions in Fertilizer production. In *IFA Technical Conference*, Marrakech, 1998. URL https://fertiliser-society.org/proceedings/uk/Prc509.HTM.

[295] M. Q. Wang. Development and Use of GREET 1.6 Fuel-Cycle Model for Transportation Fuels and Vehicle Technologies. Technical report, 2001. URL https://greet.es.anl.gov/publications#B_GREET%20Manuals.

[296] N. Mortimer, P. Cormack, M. A. Elsayed, and R. E. Horne. Evaluation of the comparative energy, global warming and socio-economic costs and benefits of biodiesel. Technical report, Sheffield Hallam University, 2003. URL http://onlinelibrary.wiley.com/doi/10.1002/cbdv.200490137/abstract%5Cnhttp://www.northenergy.co.uk/c/pdf/Resources_Research_Unit-DEFRA_Biodiesel_Report_January_2003-4_1.pdf.

[297] M. S. Graboski. Fossil Energy Use in the Manufacture of Corn Ethanol. *National Corn Growers Association*, (August), 2002. URL www.ncga.com/ethanol/main.

[298] T. O. West and G. Marland. A synthesis of carbon sequestration, carbon emissions, and net carbon flux in agriculture: comparing tillage practices in the United States. *Agriculture, Ecosystems & Environment*, 91(1-3):217–232, 2002. doi: 10.1016/S0167-8809(01)00233-X.

[299] H. Shapouri. The 2001 net energy balance of corn ethanol. Technical report, U.S. Department of Agriculture (USDA), 2001. URL http://industrializedcyclist.com/Corn_Ethanol_E_Balance.pdf.

[300] T. Nemecek and S. Erzinger. Agricultural production systems. In *Special LCA Forum*, Lausanne, 2003. URL http://www.ecoinvent.org/fileadmin/documents/en/presentation_papers/agriculture_DF_eng.pdf.

[301] M. E. Walsh and D. Becker. BIOCOST: A software program to estimate the cost of producing Bioenergy crops. In *BIOENERGY '96 - The Seventh National Bionergy Conference: Partnerships to Develop and Apply*

Biomass Technologies, Nashville, 1996. URL https://www.osti.gov/biblio/478673-biocost-software-program-estimate-cost-producing-bioenergy-crops.

[302] Department for Environment, Food & Rural Affairs (DEFRA). Direct energy use in agriculture: opportunities for reducing fossil fuel inputs. Technical Report May, 2007. URL https://ukerc.rl.ac.uk/pdf/AC0401_Final.pdf.

[303] Energy Information Agency (EIA). Annual Energy Outlook 2016. Technical report, 2015. URL http://www.eia.gov/forecasts/aeo/data/browser/#/?id=12-AEO2016&cases=ref2016~ref_no_cpp&sourcekey=0\protect\T1\textdollar\delimiter"026E30F\protect\T1\textdollarnhttps://www.eia.gov/forecasts/aeo/electricity_generation.cfm.

[304] P. S. Mehta and K. Anand. Estimation of a lower heating value of vegetable oil and biodiesel fuel. *Energy and Fuels*, 23(8):3893–3898, 2009. doi: 10.1021/ef900196r.

[305] M. Q. Wang. The Greenhouse Gases, Regulated Emissions, and Energy Use in Transportation (GREET) Model Version 1.5. Technical report, 1999. URL https://greet.es.anl.gov/publications#B_GREET%20Manuals.

[306] J. E. A. Seabra, I. C. Macedo, H. L. Chum, C. E. Faroni, and C. A. Sarto. Life cycle assessment of Brazilian sugarcane products: GHG emissions and energy use. *Biofuels, Bioproducts and Biorefining*, 5:519–532, 2011. doi: 10.1002/bbb.289.

[307] C. Walsh and A. Bows. Size matters: Exploring the importance of vessel characteristics to inform estimates of shipping emissions. *Applied Energy*, 98:128–137, 2012. doi: 10.1016/j.apenergy.2012.03.015.

[308] G. P. Robertson, E. A. Paul, R. R. Harwood, L. E. Drinkwater, P. Wagoner, M. Sarrantonio, A. R. Mosier, D. Schimel, D. Valetine, K. Bronson, W. Parton, W. H. Schlesinger, A. R. Mosier, P. A. Matson, R. Naylor, I. Ortiz-Monasterio, R. A. Houghton, J. L. Hackler, and K. T. Lawrence. Greenhouse gases in intensive agriculture: contributions of individual gases to the radiative forcing of the atmosphere. *Science*, 289(5486):1922–1925, 2000. doi: 10.1126/science.289.5486.1922.

[309] R. Lal. Carbon emission from farm operations. *Environment International*, 30(7):981–990, 2004. doi: 10.1016/j.envint.2004.03.005.

[310] A. Moro and L. Lonza. Electricity carbon intensity in European Member States: Impacts on GHG emissions of electric vehicles. *Transportation Research Part D: Transport and Environment*, 64(October):5–14, 2017. doi: 10.1016/j.trd.2017.07.012.

[311] J. Sheehan, A. Aden, K. Paustian, J. Brenner, M. Walsh, and R. Nelson. Energy and Environmental Aspects of Using Corn Stover for Fuel Ethanol. *Journal of Industrial Ecology*, 7(3):117–146, 2004. doi: 10.1162/108819803323059433.

[312] P Balcombe, K. Anderson, J. Speirs, A. Hawkes, and N. Brandon. Methane and CO_2 emissions from the natural gas supply chain. Technical report, Sustainable Gas Institute, 2015. URL https://www.sustainablegasinstitute.org/methane-and-co2-emissions-gas-supply-chain/.

[313] C. De Klein, R.S.A. Novoa, S. Ogle, K.A. Smith, P. Rochette, T.C. Wirth, B.G. McConkey, A. Mosier, and K. Rypdal. Chapitre 11 : Émissions de N_2O des sols gérés, et émissions de CO_2 dues au chaulage et à l'application d'uree. *Lignes directrices 2006 du GIEC pour les inventaires nationnaux de gaz à effet de serre. Volume 4: Agriculture, foresterie et autres affectations des terres.*, pages 1–60, 2006. URL http://www.ipcc-nggip.iges.or.jp/public/2006gl/french/vol4.html.

[314] M. Duffy. Estimated Costs for Production, Storage and Transportation of Switchgrass. *Iowa State University Extension*, (February):1–8, 2008. URL https://www.extension.iastate.edu/agdm/crops/pdf/a1-22.pdf.

[315] The World Bank. World Development Indicators. URL https://datacatalog.worldbank.org/dataset/world-development-indicators. (accessed January 2019).

[316] Y-H. H. Chen, S. Paltsev, J. Reilly, J. Morris, V. Karplus, A. Gurgel, P. Kishimoto, E. Blanc, and M. H. Babiker. The MIT Economic Projection and Policy Analysis (EPPA) Model: Version 5, 2017. URL https://globalchange.mit.edu/publication/16620.

[317] A. Hu and Q. Dong. On natural gas pricing reform in China. *Natural Gas Industry B*, 2(4):374–382, 2015. doi: https://doi.org/10.1016/j.ngib.2015.09.012.

[318] International Labor Organisation. ILOSTAT. URL https://www.ilo.org/ilostat/. (accessed January 2019).

[319] The US Department of Agriculture. National Agriculture Statistics Services. URL https://www.nass.usda.gov/. (accessed January 2018).

[320] S. Xue, O. Kalinina, and I. Lewandowski. Present and future options for Miscanthus propagation and establishment. *Renewable and Sustainable Energy Reviews*, 49:1233–1246, 2015. doi: 10.1016/j.rser.2015.04.168.

[321] Crops for Energy. Crops4Energy. URL https://www.crops4energy.co.uk/. (accessed January 2019).

[322] A. Monti, S. Fazio, V. Lychnaras, P. Soldatos, and G. Venturi. A full economic analysis of switchgrass under different scenarios in Italy estimated by BEE model. *Biomass and Bioenergy*, 31(4):177–185, 2007. doi: 10.1016/j.biombioe.2006.09.001.

[323] D. Bradley, F. Diesenreiter, M. Wild, and E. Tromborg. World Biofuel Maritime Shipping Study. Report for IEA Task 40. Technical report, International Energy Agency, 2009. URL http://www.bioenergytrade.org/downloads/worldbiofuelmaritimeshippingstudyjuly120092df.pdf.

[324] C. Dupont, R. Chiriac, G. Gauthier, and F. Toche. Heat capacity measurements of various biomass types and pyrolysis residues. *Fuel*, 115(October 2015):644–651, 2014. doi: 10.1016/j.fuel.2013.07.086.

[325] S. V. Vassilev, D. Baxter, L.K. Andersen, and C. G. Vassileva. An overview of the chemical composition of biomass. *Fuel*, 89(5):913–933, 2010. doi: 10.1016/j.fuel.2009.10.022.

[326] Y. Zhang, A. E. Ghaly, and B. Li. Physical Properties of Wheat Straw Varieties Cultivated Under Different Climatic and Soil. *American Journal of Engineering and Applied Sciences*, 5(2):98–106, 2012. doi: 10.3844/ajeassp.2012.98.106.

[327] S. Sokhansanj, A. Kumar, and A. F. Turhollow. Development and implementation of integrated biomass supply analysis and logistics model (IBSAL). *Biomass and Bioenergy*, 30(10):838–847, 2006. doi: 10.1016/j.biombioe.2006.04.004.

[328] R. Samson, P. Girouard, and Y. Chen. Evaluation of switchgrass and short-rotation forestry willow in Eastern Canada as bio-energy and agri-fibre feedstocks, 1997. URL https://www.osti.gov/etdeweb/biblio/20008243.

[329] O. Williams, E. Lester, S. Kingman, D. Giddings, S. Lormor, and C. Eastwick. Benefits of dry comminution of biomass pellets in a knife mill. *Biosystems Engineering*, 160:42–54, 2017. doi: 10.1016/j.biosystemseng.2017.05.011.

[330] R. Michel, N. Mischler, B. Azambre, G. Finqueneisel, J. Machnikowski, P. Rutkowski, T. Zimny, and J. V. Weber. Miscanthus x Giganteus straw and pellets as sustainable fuels and raw material for activated carbon. *Environmental Chemistry Letters*, 4(4):185–189, 2006. doi: 10.1007/s10311-006-0043-4.

[331] N. G. Danalatos, S. V. Archontoulis, and I. Mitsios. Potential growth and biomass productivity of Miscanthus giganteus as affected by plant density and N-fertilization in central Greece. *Biomass and Bioenergy*, 31(2-3):145–152, 2007. doi: 10.1016/j.biombioe.2006.07.004.

[332] S. B. McLaughlin, R. Samson, D. Bransby, and A. Wiselogel. Evaluating physical, chemical, and energetic properties of perennial grasses as biofuels. In *Bioenergy '96-The Seventh National Bioenergy Conference*, 1996. doi: 10.1016/S0140-6701(98)96595-X.

[333] H. W. Elbersen. Switchgrass (Panicum virgatum L.) as an alternative energy crop in Europe - Initiation of a productivity network. Technical report, Agrotechnological Research Institute (ATO-DLO), 2001. URL https://www.switchgrass.nl/upload_mm/3/0/6/a0982a5d-bb01-4054-92bc-d7ba96c8fa7a_Elbersen%20et%20al%202003.%20Final%20report%20Eu%20switchgrass%20project.pdf.

[334] A. Teel and S. Barnhart. Switchgrass Seeding Recommendation for the Production of Biomass Fuel in Southern Iowa. Technical report, Iowa State University, 2003. URL http://www.extension.iastate.edu/Publications/PM1773.pdf.

[335] W. Guidi, E. Piccioni, and E. Bonari. Evapotranspiration and crop coefficient of poplar and willow short-rotation coppice used as vegetation filter. *Bioresource Technology*, 99(11):4832–4840, 2008. doi: 10.1016/j.biortech.2007.09.055.

[336] M. C. Heller, G. A. Keoleian, M. K. Mann, and T. A. Volk. Life cycle energy and environmental benefits of generating electricity from willow biomass. *Renewable Energy*, 29(7):1023–1042, 2004. doi: 10.1016/j.renene.2003.11.018.

[337] M. Manzone, G. Airoldi, and P. Balsari. Energetic and economic evaluation of a poplar cultivation for the biomass production in Italy. *Biomass and Bioenergy*, 33(9):1258–1264, 2009. doi: 10.1016/j.biombioe.2009.05.024.

[338] A. Don, B. Osborne, A. Hastings, U. Skiba, M. S. Carter, J. Drewer, H. Flessa, A. Freibauer, N. Hyvönen, M. B. Jones, G. J. Lanigan, U. Mander, A. Monti, S. N. Djomo, J. Valentine, K. Walter, Walter Z.-L., and T. Zenone. Land-use change to bioenergy production in Europe: Implications for the greenhouse gas balance and soil carbon. *GCB Bioenergy*, 4(4):372–391, 2012. doi: 10.1111/j.1757-1707.2011.01116.x.

[339] X. Li, N. Wei, Y. Liu, Z. Fang, R. T. Dahowski, and C. L. Davidson. CO_2 Point Emission and Geological Storage Capacity in China. *Energy Procedia*, 1(1):2793–2800, 2009. doi: 10.1016/j.egypro.2009.02.051.

Appendix A

Biomass drying model

For drying, a model was designed based on Gebreegziabher *et al.* [135] and Li *et al.* [288]. Biomass drying has been covered by many studies [136, 289–291], but a precise thermodynamic and kinetic model is hard to obtain in the lack of biomass properties data, such as specific heat capacity, diffusivity, equilibrium moisture content, *etc.* This model uses a thermodynamic approach based on the industrial data provided by Gebreegziabher *et al.* and Li *et al.* on wood drying.

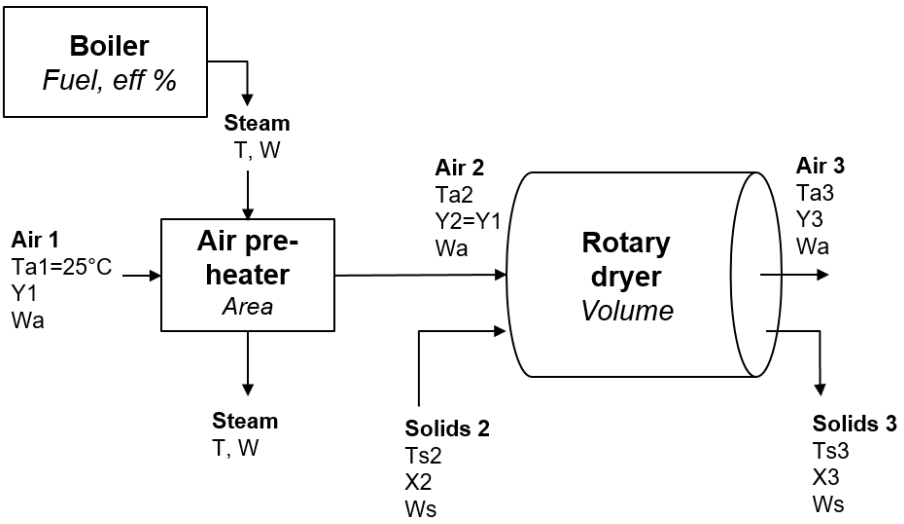


Figure A.1: Drying model

Chopped or chipped biomass is dried in a rotary dryer in contact with hot air. Air is heated through a heat exchanger from room temperature to about 60°C. Air inlet and outlet relative humidity RH_1 and RH_3 are known. Air moisture content Y_i at any

stage of the process is linked with air relative humidity through psychrometric relations, involving the saturated vapor pressure P_{ws_i}, and vapor pressure P_{w_i}:

$$P_{ws_i} = \frac{exp(77.345 + 0.0057(T_{a_i} + 273.15) - \frac{7235}{T_{a_i}+273.15})}{(T_{a_i} + 273.15)^{8.2}} \tag{A.1}$$

$$P_{w_i} = RH_i \times P_{ws_i} \tag{A.2}$$

$$Y_i = 0.62198\frac{Pa}{Pa - P_{w_i}}, i = 1,3 \tag{A.3}$$

where Pa is air pressure assumed constant throughout the process.

Considering a water mass balance on the pre-heater, air inlet moisture content is equal to air outlet moisture content:

$$Y_2 = Y_1 \tag{A.4}$$

Knowing biomass inlet MC_2 and outlet (target) MC_3 moisture content, these values can be converted into a dry basis moisture content:

$$X_i = \frac{MC_i}{1 - MC_i}, i = 2,3 \tag{A.5}$$

Because biomass quantity to dry W_s (dry basis) is also known, a water mass balance on the dryer give the required air quantity W_a (dry basis):

$$W_a(Y_3 - Y_2) = W_s(X_2 - X_3) \tag{A.6}$$

Finally the pre-heater heat rate Q_h can be determined with an energy balance on the heat exchanger:

$$Q_h = W_a(H_{a_2} - H_{a_1}) \tag{A.7}$$

H_{a_i} is the enthalpy of dry air;

$$H_{a_i} = Cp_{da} \times (T_{a_i} - T_{ref}) + Y_i(Cp_{v_i} \times (T_{a_i} - T_{ref}) + LH_w) \tag{A.8}$$

with Cp_{da}, Cp_{v_i} dry air and vapor specific heat capacity respectively, and LH_w water heat of vaporization, assumed constant in this range of temperature.

Assuming the heat exchanger uses steam generated by a boiler operating with an efficiency EFF_B, the specific boiler heat requirement is calculated:

$$ER_{drying,evap} = \frac{Q_h}{EFF_B \times W_s} \tag{A.9}$$

This value is implemented in the embodied energy model as drying heat requirement in MJ/t_{DM}. In this analysis, we assumed that the boiler operated with natural gas at a boiler efficiency of 90%. When wood pellets are used, an efficiency of 75% is considered. The overall fuel requirement $ER_D(sr,b,time)$ can then be determined:

$$ER_D(sr,b,time) = \frac{ER_{drying,evap} \times (\frac{MC_{proc,SR}(sr,b)}{1-MC_{proc,SR}(sr,b)} - \frac{MC_{proc,D}(sr,b)}{1-MC_{proc,D}(sr,b)})}{\eta_D(time)} \tag{A.10}$$

Appendix B

MONET input data

B.1 Energy, GHG and cost data

Table B.1: Mean values and ranges of uncertainty of energy data

Parameter	Unit	Mean	Range	Sources
Nitrogen fertilizer EE	MJ/kg	54.7	48.8-60.6	[193, 199, 203, 292–299]
Phosphate fertilizer EE	MJ/kg	10.2	6.8-13.5	[193, 199, 203, 292–299]
Potash fertilizer EE	MJ/kg	7.3	5.8-8.9	[193, 199, 203, 292–299]
Lime EE	MJ/kg	1.0	0.1-1.7	[193, 203, 297, 298]
Herbicide EE	MJ/kg	292.9	243.8-342.0	[193, 203, 297, 298, 300]
Miscanthus rhizome EE	MJ/rhizome	0.16	0.09-0.20	[199, 218, 292]
Switchgrass seed EE	MJ/kg	13.0	6.0-26.1	[193, 203, 292, 301]
Willow planting EE	MJ/cutting	0.10		[218]
Diesel EE	MJ/L	4.7	3.7-6.2	[217, 218]
Biodiesel EE	MJ/L	14.3		[218]
Natural gas EE	MJ/kg	4.7		[218]
Diesel LHV	MJ/L	37.4	35.9-39.1	[130, 199, 218, 302, 303]
Biodiesel LHV	MJ/L	34.8	33.7-37.3	[218, 304]
Natural gas LHV	MJ/kg	47.0	46.9-47.1	[305]
Transport of supplies (diesel)	MJ/kg	0.52	0.44-0.64	[195, 295]
Road transport diesel FE - pellet	L/(km.t_{WM})	0.041	0.028-0.06	[134, 137, 213, 218, 305]
Road transport diesel FE- chip	L/(km.t_{WM})	0.042	0.030-0.053	[134, 218]
Road transport diesel FE - bale	L/(km.t_{WM})	0.046	0.018-0.075	[130, 134, 199, 306]
Sea transport HFO efficiency - pellet	MJ/(km.t_{WM})	0.049	0.030-0.088	adapted from [218, 307]
Irrigation	MJ/mm	15.8	1.1-26.4	adapted from [128, 199, 235]

Table B.2: Mean values and ranges of uncertainty of GHG data

Parameter	Unit	Mean	Range	Sources
Nitrogen fertilizer CF	$kgCO_2eq/kg$	3.4	2.6-4.8	[193, 199, 209, 292, 295, 298, 308, 309]
Phosphate fertilizer CF	$kgCO_2eq/kg$	1.1	0.6-1.6	[193, 199, 292, 295, 298, 309]
Potash fertilizer CF	$kgCO_2eq/kg$	0.64	0.44-0.86	[193, 199, 295, 298, 309]
Lime CF	$kgCO_2eq/kg$	0.35	0.13-0.59	[193, 295, 296, 298, 309]
Herbicide CF	$kgCO_2eq/kg$	20.3	17.2-25	[193, 295, 298, 309]
Miscanthus rhizome CF	$kgCO_2eq/rhizome$	0.01		[193, 199]
Switchgrass seed CF	$kgCO_2eq/kg$	0.66	0.59-0.73	[193]
Willow planting CF	$kgCO_2eq/kg$	0.01		[218]
Coal CF	gCO_2eq/MJ	16		[310]
Wood chips (drying) CF	gCO_2eq/MJ	1.4	1.2-1.6	[218]
Diesel EF	$kgCO_2eq/L$	3.3	3.1-3.5	[91, 134, 193, 199, 210, 218, 295, 298, 309, 311]
Biodiesel EF	$kgCO_2eq/L$	0.9	0.6-1.2	[210, 218]
Natural gas EF	$kgCO_2eq/L$	64.2	59.1-69.3	[312]
Transport of supplies (diesel) EF	$kgCO_2eq/(km.t_{WM})$	0.05		[193, 295]
Road transport diesel EF - pellet	$kgCO_2eq/(km.t_{WM})$	0.086		own calculations
Road transport diesel EF - chip	$kgCO_2eq/(km.t_{WM})$	0.179		own calculations
Road transport diesel EF - bale	$kgCO_2eq/(km.t_{WM})$	0.145		own calculations
Road transport biodiesel EF - pellet	$kgCO_2eq/(km.t_{WM})$	0.022		own calculations
Road transport biodiesel EF- chip	$kgCO_2eq/(km.t_{WM})$	0.047		own calculations
Road transport biodiesel EF - bale	$kgCO_2eq/(km.t_{WM})$	0.038		own calculations
Sea transport HFO efficiency	$kgCO_2eq/(km.t_{WM})$	0.004	0.0025-0.0072	[307]
ILUC	$kgCO_2eq/ha$	183,030	117,010-249,040	adapted from [77, 85, 89, 155]
LUC grassland	$kgCO_2eq/ha$	136,330	75,000 - 200,000	[76, 85]
LUC cropland	$kgCO_2eq/ha$	37,500		[76]
LUC marginal land	$kgCO_2eq/ha$	25	0-69	[76]
LUC forest	$kgCO_2eq/ha$	573,170	350,000-719,500	[76, 85]
EF for N addition	$kgN_2O\text{-}N/kg_N$	0.01		[193, 313]
EF for N volatization	$kgN_2O\text{-}N/kgNH_3\text{-}N+NO_x\text{-}N$	0.01		[193, 313]
EF for NH_3-N+NO_x-N	$kgNH_3\text{-}N+NO_x\text{-}N/kg_N$	0.1		[193, 313]
EF for N leaching	$kgN_2O\text{-}N/kgN$	0.04	0.0075-0.075	[137, 193, 313]

Table B.3: Mean values and ranges of uncertainty of miscellaneous data

Parameter	Unit	Mean	Range	Sources
$C_{N2O-N \rightarrow N2O}$ conversion		1.57		[193, 313]
$C_{P \rightarrow P2O5}$ conversion		2.18		[132]
$C_{K \rightarrow K2O}$ conversion		1.21		[132]
$C_{C \rightarrow CO2}$ conversion		3.67		[302]
CCS plant area	ha	15		
DAC plant area for 10,000 t_{CO_2}/day	ha	13		
DAC energy requirement	MWh/t_{CO_2}	4.64	3.33-6.3	adapted from [241, 242]
Chopping solid recovery	$\%_{DM}$	98		
Drying solid recovery	$\%_{DM}$	98		
Drying target moisture	$\%_{DM}$	15		
Drying energy requirement	MJ/$t_{H_2Oevaporated}$	3734		own calculations
η_{NG}	%	90		
η_{wood}	%	75		
Grinding solid recovery	$\%_{DM}$	98		
Grinding moisture loss	%	5		
Pelleting solid recovery	$\%_{DM}$	98		
Pelleting moisture loss	%	5		
Road transport solid recovery	$\%_{DM}$	95		
Sea transport solid recovery	$\%_{DM}$	95		

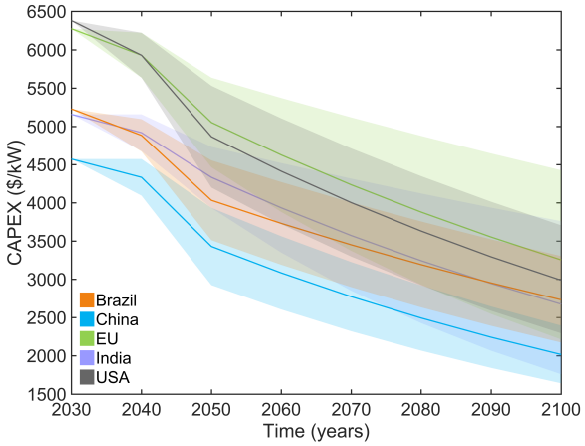


Figure B.1: Upper and lower (shades) as well as average (lines) BECCS CAPEX trends over time per region.

Table B.4: Country-level cost data

Region	N fertiliser[a] ($/kg)	P2O5 fertiliser[a] ($/kg)	K fertiliser[a] ($/kg)	Lime[a] ($/kg)	Herbicide[a] ($/kg)	Cropland[b] ($/ha/yr)	Grassland[b] ($/ha/yr)	Forest[b] ($/ha/yr)	Diesel[c] ($/L)	Natural gas[f] ($/MJ)	O&M Pellet Plant[g] ($/$t_{WM}$)	Labour farming[h] ($/hr)	Labour industry[i] ($/hr)	PPP[j]
Brazil	0.7	0.8	0.5	20.1	56.0	81.0	16.6	2.4	1.06	0.011	10.8	1.2	8.4	0.79
China	0.4	0.5	0.3	12.5	34.7	217.6	161.5	101.4	1.08	0.009	9.9	0.6	4.4	0.49
Austria	0.8	0.8	0.3	28.4	79.1	240.6	240.6	311.0	1.54	0.009	18.7	23.3	41.6	1.11
Belgium	0.8	0.8	0.6	28.2	78.6	151.0	151.0	125.7	1.64	0.007	20.7	25.5	49.7	1.11
Bulgaria	0.3	0.3	0.3	11.7	32.5	176.5	176.5	104.9	1.49	0.008	9.8	1.2	4.3	0.46
Croatia	0.3	0.3	0.3	23.6	65.8	122.6	122.6	56.0	1.51	0.008	11.2	4.7	10.1	0.70
Cyprus	0.9	0.8	0.6	18.2	50.8	67.9	67.9	95.8	1.52	0.008	13.3	10.2	18.8	0.93
Czech Republic	0.4	0.2	0.3	18.0	50.0	62.3	62.3	347.1	1.59	0.007	11.5	6.0	11.3	0.71
Denmark	0.8	0.8	0.4	34.4	95.7	472.6	472.6	490.0	1.72	0.009	20.2	48.4	47.7	1.35
Estonia	0.4	0.4	0.3	17.3	48.1	38.9	38.9	104.0	1.50	0.008	11.7	5.9	12.2	0.68
Finland	0.8	0.8	0.5	30.4	84.6	189.7	189.7	153.7	1.66	0.014	18.5	25.8	40.7	1.19
France	0.9	0.8	0.6	28.9	80.3	151.0	151.0	190.7	1.60	0.009	18.3	14.7	39.7	1.13
Germany	0.7	0.8	0.5	27.2	75.6	170.3	170.3	277.5	1.63	0.009	19.7	21.8	45.4	1.06
Greece	0.7	0.8	0.5	24.4	67.8	435.1	435.1	18.1	1.67	0.008	12.7	7.1	16.5	0.95
Hungary	0.7	0.3	0.3	15.5	43.1	117.9	117.9	108.5	1.60	0.007	11.0	5.8	9.0	0.61
Ireland	0.9	0.8	0.6	26.1	72.6	161.1	161.1	135.6	1.74	0.010	17.9	27.3	38.1	1.02
Italy	0.8	0.8	0.5	28.7	79.8	239.4	239.4	173.6	1.84	0.009	17.0	22.2	34.2	1.12
Latvia	0.4	0.3	0.2	16.4	45.7	47.4	47.4	103.1	1.45	0.009	10.8	3.1	8.3	0.64
Lithuania	0.4	0.4	0.3	15.2	42.3	67.5	67.5	327.2	1.42	0.009	10.8	3.7	8.3	0.60
Luxembourg	0.8	0.8	0.5	31.3	87.0	205.1	205.1	281.1	1.39	0.010	17.5	21.6	36.2	1.22
Malta	0.8	0.8	0.5	19.3	53.8	278.8	278.8	173.6	1.63	0.008	12.3	8.3	14.5	0.76
Netherlands	0.8	0.8	0.6	9.8	27.3	634.1	634.1	333.6	1.70	0.007	12.3	8.3	14.5	0.38
Poland	0.3	0.3	0.3	15.3	42.5	62.3	62.3	249.5	1.45	0.010	10.9	4.7	9.0	0.60
Portugal	0.7	0.8	0.5	21.0	58.5	38.9	38.9	386.9	1.62	0.009	11.6	7.3	11.5	0.82
Romania	0.4	0.3	0.3	12.3	34.3	119.4	119.4	125.7	1.50	0.006	10.1	1.7	5.5	0.48
Slovakia	0.4	0.3	0.3	17.0	47.2	36.6	36.6	174.5	1.61	0.009	11.7	4.7	12.2	0.96
Slovenia	0.3	0.3	0.3	21.5	59.9	118.0	118.0	161.8	1.55	0.009	13.2	12.0	18.5	0.66
Spain	0.7	0.7	0.5	24.5	68.3	122.6	122.6	66.9	1.48	0.009	14.7	22.2	24.7	0.84
Sweden	0.8	0.8	0.5	31.9	88.8	148.5	148.5	179.0	1.80	0.013	19.3	19.5	43.8	1.25
United Kingdom	1.0	0.7	0.5	27.7	77.0	199.6	199.6	167.2	1.93	0.008	18.6	23.2	41.1	1.08
India	0.3	0.3	0.2	8.0	22.2	331.8	523.6	22.6	0.84	0.009	9.2	0.7	1.7	0.31
USA	0.8	1.0	0.6	25.5	71.1	187.0	97.3	21.5	0.88	0.004	18.6	23.2	41.1	1.00

All cost data was converted to 2018 US $ using dollars inflation rates and a euros to US dollars conversion rate of 0.85, a GBP to US dollars conversion rate of 1.42, and a INR (Indian Rupee) to US dollars of 0.014, a RMB (China Renminbi) to US dollars rate of 0.14, and a BRL (Brazil Real) to US dollars conversion rate of 0.30.

[a]Fertiliser costs were obtained and adjusted from De Wit *et al.* [133] for EU countries, from Duffy *et al.* [314] for the USA, and calculated from US data and PPP factors [315] for India and Brazil. Lime and herbicide costs were obtained and adjusted from Duffy *et al.* [314] for the USA, and calculated from US data and PPP factors [315] for EU countries, India and Brazil.

[b]Land rents for cropland, grassland and forests for Brazil, India and the USA were obtained and adapted from Chen *et al.* [316], using the rents from the managed land (as opposed to natural). Land rents for cropland and grassland were considered equal in European countries, and obtained and adapted from arable land/permanent grassland rents from EUROSTAT [181]. For forest land rents in EU countries, the opportunity cost was considered, using the productive value of managed forests [181]. Land rents for marginal land were considered to be zero.

[c]Diesel cost per country for the period 2008-20016 was obtained from the World Bank database, averaged and inflated [315]. The cost of natural gas for the industrial sector was obtained from the EIA [183] for the USA, from the Ministry of Mines and Energy (MME) for Brazil [179], from EUROSTAT from the EU, and from Hu *et al.* for China [317]. The cost of natural gas in India was considered equal to that of China.

[d]The operation and maintenance cost (O&M) of pellet plants was calculated using data from Mobini *et al.* [214], by adjusting the personnel cost with regional wages in Manufacturing[e] and adding it to 'other O&M' cost in Mobini *et al.*

[e]Hourly compensation costs from the conference board and the International Labour Organisation [318] for all countries. Hourly compensation cost in agriculture from De Wit et al. [133] for EU countries, from the USDA [319] for the USA. When compensation cost in agriculture not available in China, Brazil and India, ratio of manufacturing to agriculture wages in region with closest GDP applied.

[f]PPP from the World bank [315]

Table B.5: Biomass production and transport costs

Cost item	Miscanthus	Switchgrass	Willow	Sources
Seed cost ($/unit)	0.15 (/rhizome)	29 (/kg)	0.21 (/planting)	Miscanthus [196, 292, 320, 321], Switchgrass [292, 314, 322] and Willow [321]
Machinery capital ($/ha/yr)	889	790	241	[322]
Labour hours (hrs/ha/yr)	6.6	9.7	5.1	[322]
Road transport pellet ($/ton$_{WM}$.km)	0.09	0.09	0.09	[201]
Road transport bale ($/ton$_{WM}$.km)	0.14	0.14		[201]
Road transport chip ($/ton$_{WM}$.km)			0.11	[201]
Sea transport pellet ($/ton$_{WM}$.km)	0.004	0.004	0.004	[323]

Table B.6: Other regional cost assumptions

Regions	All	Brazil	China	EU	India	USA	Sources
Interest rate	8%						Own assumptions
Lifetime power plant (yr)	30						Own assumptions
Lifetime pellet plant (yr)	20						Own assumptions
CO_2 T&S ($/t$CO_2$)	20.4						Own calculations/assumptions[a]
CAPEX pellet plant ($/ton$_{WM}$)	15.7						[214]
CAPEX dryer ($/ton$_{WM}$)	1.5						[214]
O&M Power plant ($/kW/yr)		223	154	218	175	234	adapted from the IEA World Energy outlook 2018 [169][b]
CAPEX Power plant (base year) ($/kW)		5229	4573	6275	5158	6381	adapted from the IEA World Energy outlook 2018 [169][b,c]

[a]15.4 CO_2 transport cost calculated based on the capital and operating costs of a 3 MtCO_2/yr capacity, 100k length, 20 years lifetime CO_2 transport pipeline [140]. A $5/t$CO_2$ was assumed in addition for CO_2 storage.

[b]Regional base year BECCS plants O&M and CAPEX were calculated from O& and CAPEX of coal, coal + CCS and biomass plants data available in the IEA World Energy outlook [169]. BECCS CAPEX (resp. O&M) was obtained by subtracting the CAPEX (resp. O&M cost) of a coal + CCS to that of coal plant, and adding this delta to that of a biomass plant.

[c]BECCS CAPEX reduction trends were computed from optimistic and pessimistic CAPEX reductions of biomass, coal, and coal CCS plants in 2020, 2040 and 2050, from the IEA World Energy Outlook 2016 [169]. To adopt a conservative approach, we assume that the CAPEX of these technologies in 2030 is what is referred as 'today"s CAPEX in the World Energy Outlook. The CAPEX in 2040 is then to be considered that in '2020' in the outlook, in 2050 that of '2030' and in 2060 that of '2040'. To further project the CAPEX of these technologies post-2060, we assume that CAPEX reductions follow the same rate as in the decade 2050-2060. BECCS CAPEX over time was then calculated from the CAPEX of the biomass, coal, and coal + CCS plants. Figure B.1 represents the CAPEX trends in both pessimistic and optimistic scenarios (shades), and the trend for the average CAPEX (lines), which was obtained from averaging the pessimistic and optimistic scenarios.

B.2 Biomass data

Table B.7: Mean values and ranges of uncertainty of wheat straw data

Parameter	Unit	Mean	Range	Sources
HHV	MJ/kg_{DM}	19.2	17.3-21.2	[64, 67]
Cp	$MJ/(kg_{DM}.K)$	1.3		[324]
C%	$\%_{DM}$	48.4	44.4-52.3	[64, 67, 69, 132, 325]
H%	$\%_{DM}$	5.5	5.0-6.1	[64, 67, 69, 132, 325]
O%	$\%_{DM}$	39.1	34.0-43.3	[64, 67, 69, 132, 325]
N%	$\%_{DM}$	0.61	0.50-0.71	[64, 67, 69, 132, 325]
P%	$\%_{DM}$	0.09	0.06-0.12	[132]
K%	$\%_{DM}$	1.08	0.38-1.5	[132]
S%	$\%_{DM}$	0.10	0.02-0.31	[64, 67, 69, 132, 325]
Cl%	$\%_{DM}$	0.32	0.01-0.73	[64, 67, 69, 132]
Ash%	$\%_{DM}$	4.5	1.6-7.3	[64, 67, 69, 325]
Moisture content at harvest%	$\%_{WM}$	10.9	5.2-16.0	[67, 69, 131, 132, 326]
Straw/grain ratio	$\%_{DM}$	1.3	0.64-2.03	[131]
Lifetime	years	1		
Rotation of harvests	years	1		
Growing cycle length	days	180 (Brazil, China, India) ; 335 (Europe) ; 120 (US)		[237]
Growing cycle starting month		11 (Brazil) ; 12 (China) ; 10 (Europe, India) ; 5 (US)		[237]
Growing cycle starting day		15 (Brazil, Europe, India, US) ; 1 (China)		[237]
Initial stage t_1		20 (Brazil, China, India) ; 160 (Europe) ; 15 (US)		[237]
Development stage t_2		80 (Brazil, China, India) ; 235 (Europe) ; 40 (US)		[237]
Mid-season stage t_3		150 (Brazil, China, India) ; 310 (Europe) ; 90 (US)		[237]
$K_{c,ini}$		0.7		[237]
$K_{c,mid}$		1.15		[237]
$K_{c,end}$		0.3		[237]
% N available in straw	$\%_N$	30		[132]
% P available in straw	$\%_P$	100		[132]
% K available in straw	$\%_N$	100		[132]
Collection (bales)	L/ha/harvest	4.4		[132]
Chopping (diesel)	MJ/t_{WM}	7.4		[132]
Drying (power)	MJ/t_{WM}	66	39-94	[214, 292]
Grinding (power)	MJ/t_{WM}	146	41-323	[184, 327]
Pelleting (power)	MJ/t_{WM}	300		[184, 328]
Pellet cooling (power)	MJ/t_{WM}	9		[214]
Pellet grinding (power)	MJ/t_{WM}	117		[329]

Table B.8: Mean values and ranges of uncertainty of miscanthus data

Parameter	Unit	Mean	Range	Sources
HHV	MJ/kg_{DM}	18.4	17.7-19.1	[64, 67, 68, 199, 330]
Cp	$MJ/(kg_{DM}.K)$	1.4		[324]
C%	$\%_{DM}$	47.8	45.1-50.4	[64, 67–69, 325]
H%	$\%_{DM}$	5.5	4.9-6.1	[64, 67–69, 325]
O%	$\%_{DM}$	42.3	40.2-44.3	[64, 67–69, 325]
N%	$\%_{DM}$	0.41	0.24-0.58	[64, 67–69, 325]
S%	$\%_{DM}$	0.22	0.04-0.37	[64, 67–69, 325]
Cl%	$\%_{DM}$	0.26	0.10-0.42	[64, 67–69]
Ash%	$\%_{DM}$	3.9	2.5-5.4	[64, 67–69, 325]
Moisture content at harvest%	$\%_{WM}$	23	15-31	[67–69, 195, 199, 331]
1st harvest yield proportion	%	21		[195]
2nd harvest yield proportion	%	64		[195]
Lifetime	years	18	16-21	[137, 195, 218]
Rotation of harvests	years	1		[195]
Growing cycle length	days	209	203-215	[189]
Growing cycle starting month		7 (N) ; 9 (S)	4-9 (N)	[189]
Growing cycle starting day		1		[189]
Initial stage t_1		45	42-48	[189]
Development stage t_2		67	64-70	[189]
Mid-season stage t_3		163	152-174	[189]
$K_{c,ini}$		0.4		[237]
$K_{c,mid}$		0.95		[237]
$K_{c,end}$		0.4		[237]
Lime rate	kg/ha	5764	4940-7413	[139, 210, 314]
Rhizome rate	rhizome/ha	20,000	10,000-20,000	[123, 195, 196, 281, 292]
Herbicide rate	kg/ha/yr	0.88	0.105-2.81	[137, 193]
Land preparation (diesel)	L/ha	75.1		[195]
Maintenance - harvest (bales)	L/ha/harvest	51.6		[195]
Chopping (diesel)	MJ/t_{WM}	108		[199]
Drying (power)	MJ/t_{WM}	66	39-94	[214, 292]
Grinding (power)	MJ/t_{WM}	125	68-182	[199]
Pelleting (power)	MJ/t_{WM}	125	52-232	[199, 213]
Pellet cooling (power)	MJ/t_{WM}	9		[214]
Pellet grinding (power)	MJ/t_{WM}	99		[329]

Table B.9: Mean values and ranges of uncertainty of switchgrass data

Parameter	Unit	Mean	Range	Sources
HHV	MJ/kg_{DM}	18.4	17.3-19.4	[68, 207]
Cp	$MJ/(kg_{DM}.K)$	1.3		[324]
C%	$\%_{DM}$	47.1	46.5-47.8	[66, 139, 325]
H%	$\%_{DM}$	5.9	5.4-6.3	[66, 139, 325]
O%	$\%_{DM}$	41.4	40.3-42.5	[66, 139, 325]
N%	$\%_{DM}$	0.8	0.51-1.1	[66, 139, 325]
S%	$\%_{DM}$	0.11	0.08-0.20	[66, 139, 325]
Cl%	$\%_{DM}$	0.13	0 - 0.16	[66, 139]
Ash%	$\%_{DM}$	5.7	5.2-6.1	[66, 139, 325]
Moisture content at harvest%	$\%_{WM}$	12	11-14	[139, 193, 201, 208, 332]
1st harvest yield proportion	%	21	11-30	[208, 333]
2nd harvest yield proportion	%	69	67-70	[208, 333]
Lifetime	years	12	10-15	[201, 207]
Rotation of harvests	years	1		[201, 207]
Growing cycle length	days	128	90-160	[207, 237]
Growing cycle starting month		5 (N) ; 9 (S)		[237]
Growing cycle starting day		1		[237]
Initial stage t_1		10		[237]
Development stage t_2		25		[237]
Mid-season stage t_3		100		[237]
$K_{c,ini}$		0.5		[141]
$K_{c,mid}$		1.03	0.9-1.15	[141]
$K_{c,end}$		0.98	0.85-1.1	[141]
Lime rate	kg/ha	5764	4940-7413	[139, 210, 314]
Seed rate	kg/ha/yr	0.8	0.4 - 1.1	[193, 203, 208, 218, 301, 334]
Herbicide rate	kg/ha/yr	0.48	0.42-0.54	[193, 208, 295]
Land preparation (diesel)	L/ha	15.7		[208]
Maintenance - harvest (bales)	L/ha/harvest	32.6		[208]
Chopping (diesel)	MJ/t_{WM}	135		[199]
Drying (power)	MJ/t_{WM}	66	39-94	[214, 292]
Grinding (power)	MJ/t_{WM}	99	52-162	[213]
Pelleting (power)	MJ/t_{WM}	127	72-211	[199, 213]
Pellet cooling (power)	MJ/t_{WM}	9		[214]
Pellet grinding (power)	MJ/t_{WM}	99		[329]

Table B.10: Mean values and ranges of uncertainty of short rotation coppice willow data

Parameter	Unit	Mean	Range	Sources
HHV	MJ/kg_{DM}	19.1	18.4-19.8	[64, 65, 193, 213, 217, 218]
Cp	$MJ/(kg_{DM}.K)$	1.5		[324]
C%	$\%_{DM}$	48.1	46-49.2	[64, 65, 325]
H%	$\%_{DM}$	5.9	5.3-6.4	[64, 65, 325]
O%	$\%_{DM}$	42.3	40.0-43.0	[64, 325]
N%	$\%_{DM}$	0.5	0.2-0.8	[64, 65, 325]
S%	$\%_{DM}$	0.05	0.02-0.1	[64, 65, 325]
Cl%	$\%_{DM}$	0.03	0.01-0.05	[64, 65]
Ash%	$\%_{DM}$	2.0	1.1-4.0	[64, 65, 213, 325]
Moisture content at harvest%	$\%_{WM}$	52	50-53	[63, 193, 195]
1st harvest yield proportion	%	72		[195]
2nd harvest yield proportion	%	100		[195]
Lifetime	years	16		[195, 217]
Rotation of harvests	years	3	2-4	[195, 213, 217]
Growing cycle length	days	150		[335]
Growing cycle starting month		5 (N) ; 9 (S)		[335]
Growing cycle starting day		15		[335]
Initial stage t_1		40		[335]
Development stage t_2		100		[335]
Mid-season stage t_3		130		[335]
$K_{c,ini}$		0.65		[335]
$K_{c,mid}$		1.6		[335]
$K_{c,end}$		0.90.93		[335]
Lime rate	kg/ha	5764	4940-7413	[139, 210, 314]
Cuttings rate	kg/ha/yr	608	284-875	[193, 218, 336, 337]
Herbicide rate	kg/ha/yr	0.43	0.11-1.08	[193, 202, 245, 336]
Land preparation (diesel)	L/ha	82.8		[195]
Maintenance - harvest (chips)	L/ha/harvest	164.2		[195]
Drying (power)	MJ/t_{WM}	66	39-94	[214]
Grinding (power)	MJ/t_{WM}	133		[214]
Pelleting (power)	MJ/t_{WM}	216		[214]
Pellet cooling (power)	MJ/t_{WM}	9		[214]
Pellet grinding (power)	MJ/t_{WM}	117		[329]

Table B.11: Regional road tortuosity and biomass yield (Brazil and China)

Sub-region *sr*	Road tortuosity[a]	Miscanthus yield[b]	Switchgrass yield[c]	Wheat yield[d]	Willow yield[e]
Acre	1.4	32.3 - 34.7 (33.5)	14 - 18 (16)	2.2 - 2.8 (2.6)	-
Alagoas	1.3	1 - 32.3 (14.6)	2 - 6 (4)	2.2 - 2.8 (2.6)	-
Amapa	2.2	32.3 - 34.7 (33.5)	14 - 18 (16)	2.2 - 2.8 (2.6)	-
Amazonas	2.4	15 - 41 (26.8)	10 - 18 (16)	2.2 - 2.8 (2.6)	-
Bahia	1.3	32.3 - 34.7 (33.5)	6 - 12 (8)	2.2 - 2.8 (2.6)	-
Ceara	1.5	32.3 - 34.7 (33.5)	8 - 14 (10)	2.2 - 2.8 (2.6)	-
Distrito Federal	1.3	32.3 - 34.7 (33.5)	14 - 18 (16)	2.2 - 2.8 (2.6)	-
Espirito Santo	1.4	32.3 - 34.7 (33.5)	10 - 14 (12)	2.2 - 2.8 (2.6)	-
Goias	1.4	12 - 22.8 (17.2)	14 - 18 (16)	2.2 - 2.8 (2.6)	-
Maranhao	1.3	32.3 - 34.7 (33.5)	14 - 18 (16)	2.2 - 2.8 (2.6)	-
Mato Grosso	1.5	32.3 - 34.7 (33.5)	14 - 18 (18)	2.2 - 2.8 (2.6)	-
Mato Grosso do Sul	1.1	12 - 22.8 (17.2)	10 - 18 (16)	2.2 - 2.8 (2.6)	-
Minas Gerais	1.4	12 - 22.8 (17.2)	6 - 14 (12)	2.2 - 2.8 (2.6)	-
Para	1.6	32.3 - 34.7 (33.5)	10 - 18 (18)	2.2 - 2.8 (2.6)	-
Paraiba	1.5	32.3 - 34.7 (33.5)	6 - 10 (8)	2.2 - 2.8 (2.6)	-
Parana	1.5	12 - 22.8 (17.2)	10 - 18 (12)	2.2 - 2.8 (2.6)	-
Pernambuco	1.1	1 - 32.3 (14.6)	1 - 6 (4)	2.2 - 2.8 (2.6)	-
Piaui	1.3	32.3 - 34.7 (33.5)	6 - 14 (10)	2.2 - 2.8 (2.6)	-
Rio de Janeiro	1.5	12 - 22.8 (17.2)	10 - 14 (12)	2.2 - 2.8 (2.6)	-
Rio Grande do Norte	1.5	12 - 22.8 (17.2)	6 - 10 (8)	2.2 - 2.8 (2.6)	-
Rio Grande do Sul	1.3	12 - 22.8 (17.2)	8 - 14 (10)	2.2 - 2.8 (2.6)	-
Rondonia	1.6	32.3 - 34.7 (33.5)	14 - 18 (16)	2.2 - 2.8 (2.6)	-
Roraima	2.5	32.3 - 34.7 (33.5)	10 - 14 (12)	2.2 - 2.8 (2.6)	-
Santa Catarina	1.4	12 - 22.8 (17.2)	10 - 18 (14)	2.2 - 2.8 (2.6)	-
Sao Paulo	1.3	12 - 22.8 (17.2)	10 - 18 (16)	2.2 - 2.8 (2.6)	-
Sergipe	1.3	32.3 - 34.7 (33.5)	1 - 6 (4)	2.2 - 2.8 (2.6)	-
Tocantins	1.3	32.3 - 34.7 (33.5)	14 - 18 (16)	2.2 - 2.8 (2.6)	-
Anhui	1.2	27.7 - 30 (28.9)	14 - 18 (16)	4.7 - 5.2 (5.0)	-
Beijing	1.1	25.4 - 27.7 (26.6)	2 - 10 (6)	4.7 - 5.2 (5.0)	-
Chongqing	1.4	23.1 - 27.7 (25.4)	14 - 18 (16)	4.7 - 5.2 (5.0)	-
Fujian	1.4	30 - 32.3 (31.2)	10 - 14 (12)	4.7 - 5.2 (5.0)	-
Gansu	1.2	0 - 0 (0)	0 - 2 (1)	4.7 - 5.2 (5.0)	-
Guangdong	1.3	30 - 32.3 (31.2)	10 - 18 (14)	4.7 - 5.2 (5.0)	-
Guangxi Zhuang	1.3	27.7 - 32.3 (30)	6 - 18 (12)	4.7 - 5.2 (5.0)	-
Guizhou	1.2	23.1 - 27.7 (25.4)	6 - 18 (16)	4.7 - 5.2 (5.0)	-
Hainan	1.1	32.3 - 34.7 (33.5)	2 - 6 (4)	4.7 - 5.2 (5.0)	-
Hebei	1.0	20.8 - 27.7 (24.3)	2 - 10 (6)	4.7 - 5.2 (5.0)	-
Heilongjiang	1.1	13.9 - 25.4 (19.6)	6 - 18 (14)	4.7 - 5.2 (5.0)	-
Henan	1.2	23.1 - 27.7 (25.4)	6 - 18 (12)	4.7 - 5.2 (5.0)	-
Hubei	1.4	25.4 - 32.3 (28.9)	10 - 18 (16)	4.7 - 5.2 (5.0)	-
Hunan	1.4	27.7 - 30 (28.9)	10 - 18 (12)	4.7 - 5.2 (5.0)	-
Inner Mongolia	1.4	0 - 13.9 (6.9)	0 - 10 (4)	4.7 - 5.2 (5.0)	-
Jiangsu	1.2	25.4 - 30 (27.7)	10 - 18 (16)	4.7 - 5.2 (5.0)	-
Jiangxi	1.3	27.7 - 30 (28.9)	10 - 14 (12)	4.7 - 5.2 (5.0)	-
Jilin	1.1	18.5 - 30 (24.3)	8 - 14 (12)	4.7 - 5.2 (5.0)	-
Liaoning	1.1	25.4 - 34.7 (30)	6 - 14 (10)	4.7 - 5.2 (5.0)	-
Ningxia Hui	1.2	13.9 - 18.5 (16.2)	2 - 6 (4)	4.7 - 5.2 (5.0)	-
Qinghai	1.3	0 - 0 (0)	0 - 2 (1)	4.7 - 5.2 (5.0)	-
Shaanxi	1.2	13.9 - 23.1 (18.5)	2 - 14 (8)	4.7 - 5.2 (5.0)	-
Shandong	1.1	23.1 - 27.7 (25.4)	6 - 12 (8)	4.7 - 5.2 (5.0)	-
Shanghai	1.5	32.3 - 34.7 (33.5)	14 - 18 (16)	4.7 - 5.2 (5.0)	-
Shanxi	1.2	13.9 - 20.8 (17.3)	2 - 6 (4)	4.7 - 5.2 (5.0)	-
Sichuan	1.3	13.9 - 25.4 (19.6)	0 - 18 (6)	4.7 - 5.2 (5.0)	-
Tianjin	1.0	30 - 32.3 (31.2)	6 - 10 (8)	4.7 - 5.2 (5.0)	-
Xinjiang Uyghur	1.3	0 - 0 (0)	0 - 2 (1)	4.7 - 5.2 (5.0)	-
Yunnan	1.3	23.1 - 32.3 (27.7)	0 - 18 (14)	4.7 - 5.2 (5.0)	-
Zhejiang	1.3	30 - 32.3 (31.2)	10 - 14 (12)	4.7 - 5.2 (5.0)	-

Table B.12: Regional road tortuosity and biomass yield (EU and India)

Sub-region *sr*	Road tortuosity[a]	Miscanthus yield[b]	Switchgrass yield[c]	Wheat yield[d]	Willow yield[e]
Austria	1.6	17.0 - 22.0 (19.5)	6.0 - 10.0 (8.0)	4.1 - 5.9 (4.9)	7.8 - 11.0 (9.4)
Belgium	1.1	16.0 - 16.0 (16.0)	10.0 - 14.0 (12.0)	8.4 - 8.9 (8.6)	4.0 - 17.0 (8.9)
Bulgaria	1.9	2.0 - 30.0 (14.3)	6.0 - 14.0 (8.0)	3.6 - 4.2 (3.8)	4.0 - 13.0 (8.4)
Croatia	1.4	18.0 - 18.0 (18.0)	6.0 - 10.0 (8.0)	4.0 - 5.3 (5.0)	11.0 - 11.0 (11.0)
Cyprus	1.8	12 - 27.7 (20.2)	0.0 - 6.0 (2.0)	2.2 - 3.1 (2.7)	1 - 11.0 (6.1)
Czechia	1.3	19.0 - 19.0 (19.0)	6.0 - 10.0 (8.0)	4.3 - 5.7 (5.0)	13.0 - 13.0 (13.0)
Denmark	2.5	5.0 - 22.0 (13.3)	4.3 - 10.0 (7.1)	6.5 - 7.4 (7.0)	8.0 - 8.0 (8.0)
Estonia	1.3	2.0 - 30.0 (14.3)	2.0 - 6.0 (4.0)	2.7 - 3.9 (3.3)	5.0 - 5.0 (5.0)
Finland	1.2	5.0 - 34.0 (17.1)	0.0 - 6.0 (2.0)	3.4 - 3.9 (3.8)	5.0 - 5.0 (5.0)
France	1.3	15.0 - 15.0 (15.0)	6.0 - 14.0 (9.5)	6.2 - 7.3 (6.8)	4.0 - 17.0 (8.8)
Germany	1.3	2.0 - 30.0 (14.4)	6.0 - 10.0 (8.0)	7.0 - 8.0 (7.4)	9.0 - 9.0 (9.0)
Greece	1.3	20.0 - 44.0 (31.2)	0.0 - 6.0 (2.0)	2.7 - 3.2 (2.8)	10.0 - 10.0 (10.0)
Hungary	1.3	2.0 - 30.0 (14.3)	10.0 - 14.0 (12.0)	3.7 - 4.6 (4.0)	8.0 - 8.0 (8.0)
Ireland	1.3	5.0 - 34.0 (14.5)	2.0 - 6.0 (4.0)	7.2 - 9.0 (8.4)	4.0 - 17.0 (8.6)
Italy	1.2	15.0 - 32.0 (25.7)	6.0 - 34.0 (13.6)	3.7 - 4.1 (4.0)	3.0 - 3.0 (3.0)
Latvia	1.4	2.0 - 30.0 (14.3)	2.0 - 6.0 (4.0)	3.0 - 4.4 (3.8)	5.0 - 5.0 (5.0)
Lithuania	1.1	2.0 - 30.0 (14.3)	6.0 - 10.0 (8.0)	3.3 - 4.8 (4.1)	9.0 - 9.0 (9.0)
Luxembourg	1.3	18.0 - 18.0 (18.0)	10.0 - 14.0 (12.0)	5.5 - 6.4 (5.9)	4.0 - 17.0 (8.8)
Malta	1.1	12.0 - 27.7 (20.2)	6.0 - 10.0 (8.0)	4.8 - 4.8 (4.8)	1.0 - 11.0 (6.1)
Netherlands	1.2	15.0 - 15.0 (15.0)	6.0 - 10.7 (8.3)	7.8 - 8.9 (8.5)	4.0 - 17.0 (8.9)
Poland	1.6	15.0 - 15.0 (15.0)	6.0 - 10.0 (8.0)	3.9 - 4.4 (4.2)	8.0 - 8.0 (8.0)
Portugal	1.2	20.0 - 20.0 (20.0)	6.0 - 10.0 (8.0)	1.3 - 1.8 (1.1)	1.0 - 1.0 (1.0)
Romania	1.5	16.0 - 16.0 (16.0)	6.0 - 10.0 (8.0)	2.7 - 3.7 (3.0)	8.0 - 8.0 (8.0)
Slovakia	1.5	16.0 - 16.0 (16.0)	6.0 - 10.0 (8.0)	3.3 - 4.6 (3.8)	7.0 - 7.0 (7.0)
Slovenia	1.3	16.0 - 16.0 (16.0)	6.0 - 10.0 (8.0)	4.4 - 5.4 (5.0)	10.0 - 10.0 (10.0)
Spain	1.2	14.0 - 34.0 (24.0)	2.0 - 6.0 (4.0)	2.4 - 3.6 (3.0)	8.0 - 8.0 (8.0)
Sweden	1.2	2.0 - 34.0 (16.2)	0.0 - 6.0 (1.0)	5.4 - 6.2 (5.8)	4.0 - 4.0 (4.0)
United Kingdom	1.4	5.0 - 24.1 (12.8)	2.0 - 14.6 (8.0)	6.7 - 7.7 (7.2)	4.0 - 17.0 (8.8)
Andhra Pradesh	1.1	5.0 - 34.7 (24.0)	6.0 - 14.0 (10.0)	2.8 - 3.2 (3.1)	-
Arunachal Prades	1.8	0.0 - 0.0 (0.0)	0.0 - 6.0 (2.0)	2.8 - 3.2 (3.1)	-
Assam	1.9	12.0 - 22.8 (17.2)	6.0 - 14.0 (12.0)	2.8 - 3.2 (3.1)	-
Bihar	1.4	12.0 - 22.8 (17.2)	6.0 - 10.0 (8.0)	2.8 - 3.2 (3.1)	-
Chhattisgarh	1.4	12.0 - 22.8 (17.2)	6.0 - 10.0 (8.0)	2.8 - 3.2 (3.1)	-
Delhi	1.2	5.0 - 34.0 (14.5)	6.0 - 10.0 (8.0)	2.8 - 3.2 (3.1)	-
Goa	1.4	32.3 - 34.7 (33.5)	6.0 - 10.0 (8.0)	2.8 - 3.2 (3.1)	-
Gujarat	1.4	0.0 - 34.0 (7.3)	6.0 - 10.0 (8.0)	2.8 - 3.2 (3.1)	-
Haryana	1.3	5.0 - 34.0 (15.9)	2.0 - 10.0 (6.0)	2.8 - 3.2 (3.1)	-
Himachal Pradesh	1.4	0.0 - 22.8 (8.6)	2.0 - 6.0 (4.0)	2.8 - 3.2 (3.1)	-
Jammu and Kashmir	1.4	0.0 - 0.0 (0.0)	0.0 - 2.0 (1.0)	2.8 - 3.2 (3.1)	-
Jharkhand	1.2	12.0 - 22.8 (17.2)	6.0 - 10.0 (8.0)	2.8 - 3.2 (3.1)	-
Karnataka	1.4	5.0 - 41.0 (19.5)	6.0 - 14.0 (9.0)	2.8 - 3.2 (3.1)	-
Kerala	1.4	32.3 - 34.7 (33.5)	10.0 - 14.0 (12.0)	2.8 - 3.2 (3.1)	-
Madhya Pradesh	1.2	5.0 - 34.0 (15.4)	6.0 - 14.6 (10.4)	2.8 - 3.2 (3.1)	-
Maharashtra	1.7	32.3 - 34.7 (33.5)	6.0 - 10.0 (8.0)	2.8 - 3.2 (3.1)	-
Manipur	2.4	12.0 - 22.8 (17.2)	6.0 - 14.0 (10.0)	2.8 - 3.2 (3.1)	-
Meghalaya	2.3	12.0 - 22.8 (17.2)	6.0 - 14.0 (10.0)	2.8 - 3.2 (3.1)	-
Mizoram	3.3	12.0 - 22.8 (17.2)	6.0 - 14.0 (10.0)	2.8 - 3.2 (3.1)	-
Nagaland	1.9	12.0 - 22.8 (17.2)	6.0 - 14.0 (10.0)	2.8 - 3.2 (3.1)	-
Odisha	1.5	32.3 - 34.7 (33.5)	6.0 - 10.0 (8.0)	2.8 - 3.2 (3.1)	-
Puducherry	1.3	32.3 - 34.7 (33.5)	6.0 - 14.0 (10.0)	2.8 - 3.2 (3.1)	-
Punjab	1.3	5.0 - 34.0 (14.5)	2.0 - 6.0 (4.0)	2.8 - 3.2 (3.1)	-
Rajasthan	1.3	0.0 - 0.0 (0.0)	6.0 - 10.0 (8.0)	2.8 - 3.2 (3.1)	-
Sikkim	1.3	5.0 - 34.0 (14.5)	10.0 - 14.0 (12.0)	2.8 - 3.2 (3.1)	-
Tamil Nadu	1.1	5.0 - 34.0 (14.5)	10.0 - 14.0 (12.0)	2.8 - 3.2 (3.1)	-
Tripura	4.0	12.0 - 22.8 (17.2)	6.0 - 14.0 (10.0)	2.8 - 3.2 (3.1)	-
Uttar Pradesh	1.2	12.0 - 22.8 (17.2)	6.0 - 10.0 (8.0)	2.8 - 3.2 (3.1)	-
Uttarakhand	1.3	12.0 - 22.8 (17.2)	2.0 - 10.0 (6.0)	2.8 - 3.2 (3.1)	-
West Bengal	1.4	32.3 - 34.7 (33.5)	6.0 - 10.0 (8.0)	2.8 - 3.2 (3.1)	-

Table B.13: Regional road tortuosity and biomass yield (US)

Sub-region *sr*	Road tortuosity[a]	Miscanthus yield[b]	Switchgrass yield[c]	Wheat yield[d]	Willow yield[e]
Alabama	1.3	27.7 - 27.7 (27.7)	14.0 - 18.0 (16.0)	2.9 - 3.2 (3.1)	5.6 - 5.6 (5.6)
Alaska	1.3	5.0 - 5.0 (5.0)	0.0 - 2.0 (1.0)	2.9 - 3.2 (3.1)	0.0 - 0.0 (0.0)
Arizona	1.2	2.4 - 2.4 (2.4)	2.0 - 6.0 (4.0)	2.9 - 3.2 (3.1)	0.0 - 0.0 (0.0)
Arkansas	1.2	12.0 - 22.8 (17.2)	10.0 - 14.0 (12.0)	2.9 - 3.2 (3.1)	5.9 - 5.9 (5.9)
California	1.2	28.1 - 28.1 (28.1)	0.0 - 6.0 (2.0)	2.9 - 3.2 (3.1)	0.0 - 0.0 (0.0)
Colorado	1.2	2.4 - 2.4 (2.4)	0.0 - 9.9 (5.8)	2.9 - 3.2 (3.1)	7.5 - 7.5 (7.5)
Connecticut	1.2	15.5 - 15.5 (15.5)	6.0 - 10.0 (7.7)	2.9 - 3.2 (3.1)	5.6 - 11.0 (7.9)
Delaware	1.3	12.0 - 22.8 (17.2)	9.4 - 18.0 (14.4)	2.9 - 3.2 (3.1)	5.6 - 5.6 (5.6)
Florida	1.2	12.0 - 22.8 (17.2)	10.0 - 14.0 (11.9)	2.9 - 3.2 (3.1)	5.5 - 5.5 (5.5)
Georgia	1.3	26.0 - 41.0 (31.9)	11.8 - 18.0 (14.9)	2.9 - 3.2 (3.1)	6.2 - 6.2 (6.2)
Hawaii	1.2	27.7 - 27.7 (27.7)	0.0 - 0.0 (0.0)	2.9 - 3.2 (3.1)	0.0 - 0.0 (0.0)
Idaho	1.2	2.4 - 2.4 (2.4)	0.0 - 6.0 (2.0)	2.9 - 3.2 (3.1)	0.0 - 0.0 (0.0)
Illinois	1.3	16.9 - 22.8 (19.9)	10.0 - 18.0 (13.4)	2.9 - 3.2 (3.1)	6.2 - 6.2 (6.2)
Indiana	1.3	16.9 - 22.8 (19.9)	10.0 - 14.0 (12.0)	2.9 - 3.2 (3.1)	6.2 - 6.2 (6.2)
Iowa	1.2	22.8 - 22.8 (22.8)	7.4 - 18.0 (13.0)	2.9 - 3.2 (3.1)	5.6 - 5.6 (5.6)
Kansas	1.1	18.3 - 18.3 (18.3)	6.0 - 18.0 (12.1)	2.9 - 3.2 (3.1)	6.1 - 6.1 (6.1)
Kentucky	1.2	27.7 - 27.7 (27.7)	6.0 - 14.0 (10.2)	2.9 - 3.2 (3.1)	5.9 - 5.9 (5.9)
Louisiana	1.1	28.1 - 28.1 (28.1)	10.0 - 18.0 (14.0)	2.9 - 3.2 (3.1)	5.1 - 5.1 (5.1)
Maine	1.2	15.5 - 15.5 (15.5)	6.0 - 10.0 (8.1)	2.9 - 3.2 (3.1)	5.5 - 5.5 (5.5)
Maryland	1.4	12.0 - 27.7 (20.2)	9.9 - 14.0 (11.5)	2.9 - 3.2 (3.1)	6.7 - 6.7 (6.7)
Massachusetts	1.1	15.5 - 15.5 (15.5)	10.0 - 14.0 (11.5)	2.9 - 3.2 (3.1)	6.2 - 11.0 (8.1)
Michigan	1.3	16.9 - 22.8 (19.9)	10.0 - 14.0 (11.7)	2.9 - 3.2 (3.1)	5.9 - 5.9 (5.9)
Minnesota	1.2	16.9 - 16.9 (16.9)	10.0 - 16.0 (12.8)	2.9 - 3.2 (3.1)	6.0 - 11.0 (8.0)
Mississippi	1.2	27.7 - 28.1 (27.9)	10.0 - 18.0 (13.5)	2.9 - 3.2 (3.1)	5.9 - 5.9 (5.9)
Missouri	1.2	12.0 - 22.8 (17.2)	10.7 - 18.0 (14.7)	2.9 - 3.2 (3.1)	5.6 - 5.6 (5.6)
Montana	1.2	2.4 - 2.4 (2.4)	0.0 - 6.0 (4.0)	2.9 - 3.2 (3.1)	0.0 - 0.0 (0.0)
Nebraska	1.1	12.0 - 12.0 (12.0)	6.0 - 14.0 (10.0)	2.9 - 3.2 (3.1)	6.6 - 6.6 (6.6)
Nevada	1.3	2.4 - 2.4 (2.4)	0.0 - 2.0 (1.0)	2.9 - 3.2 (3.1)	0.0 - 0.0 (0.0)
New Hampshire	1.3	15.5 - 15.5 (15.5)	6.0 - 10.7 (8.7)	2.9 - 3.2 (3.1)	5.9 - 11.0 (8.0)
New Jersey	1.2	15.5 - 15.5 (15.5)	9.9 - 14.0 (11.5)	2.9 - 3.2 (3.1)	7.5 - 7.5 (7.5)
New Mexico	1.1	2.4 - 2.4 (2.4)	2.0 - 6.0 (4.0)	2.9 - 3.2 (3.1)	0.0 - 0.0 (0.0)
New York	1.0	15.5 - 16.9 (16.2)	10.0 - 14.0 (11.5)	2.9 - 3.2 (3.1)	5.4 - 11.0 (7.8)
North Carolina	1.2	19.3 - 27.7 (22.6)	8.7 - 18.0 (14.2)	2.9 - 3.2 (3.1)	4.6 - 4.6 (4.6)
North Dakota	1.1	12.0 - 12.0 (12.0)	6.0 - 14.0 (10.4)	2.9 - 3.2 (3.1)	6.0 - 6.0 (6.0)
Ohio	1.4	16.9 - 22.8 (19.9)	10.0 - 14.0 (11.7)	2.9 - 3.2 (3.1)	5.3 - 5.3 (5.3)
Oklahoma	1.1	18.3 - 18.3 (18.3)	10.0 - 14.0 (12.0)	2.9 - 3.2 (3.1)	7.5 - 7.5 (7.5)
Oregon	1.6	12.0 - 27.7 (20.2)	0.0 - 11.1 (4.8)	2.9 - 3.2 (3.1)	5.8 - 5.8 (5.8)
Pennsylvania	1.2	15.5 - 16.9 (16.2)	6.0 - 14.0 (10.0)	2.9 - 3.2 (3.1)	7.4 - 7.4 (7.4)
Rhode Island	1.2	15.5 - 15.5 (15.5)	10.0 - 14.0 (11.6)	2.9 - 3.2 (3.1)	5.4 - 11.0 (7.8)
South Carolina	1.1	27.7 - 27.7 (27.7)	10.1 - 18.0 (14.5)	2.9 - 3.2 (3.1)	5.3 - 5.3 (5.3)
South Dakota	1.1	12.0 - 12.0 (12.0)	6.0 - 14.0 (10.6)	2.9 - 3.2 (3.1)	6.0 - 6.0 (6.0)
Tennessee	1.2	27.7 - 27.7 (27.7)	10.0 - 14.0 (11.6)	2.9 - 3.2 (3.1)	5.0 - 5.0 (5.0)
Texas	1.2	18.3 - 18.3 (18.3)	4.0 - 14.0 (9.2)	2.9 - 3.2 (3.1)	6.2 - 6.2 (6.2)
Utah	1.2	2.4 - 2.4 (2.4)	0.0 - 2.0 (1.0)	2.9 - 3.2 (3.1)	1.0 - 11.0 (6.3)
Vermont	1.3	15.5 - 15.5 (15.5)	6.0 - 11.1 (8.8)	2.9 - 3.2 (3.1)	5.4 - 11.0 (7.8)
Virginia	1.2	27.7 - 27.7 (27.7)	14.0 - 18.0 (16.0)	2.9 - 3.2 (3.1)	7.3 - 7.3 (7.3)
Washington	1.2	5.0 - 34.0 (17.3)	0.0 - 12.3 (5.1)	2.9 - 3.2 (3.1)	5.2 - 5.2 (5.2)
West Virginia	1.4	27.7 - 27.7 (27.7)	6.0 - 10.1 (8.5)	2.9 - 3.2 (3.1)	6.1 - 6.1 (6.1)
Wisconsin	1.2	12.0 - 27.7 (20.2)	8.0 - 16.0 (12.0)	2.9 - 3.2 (3.1)	5.2 - 11.0 (5.8)
Wyoming	1.2	5.0 - 34.0 (17.3)	0.0 - 6.0 (2.0)	2.9 - 3.2 (3.1)	5.4 - 11.0 (6.5)

[a]Own calculations. [b]Mean, low and high annual dry mass yield of miscanthus in t_{DM}/ha/yr. Data was adapted from [119, 122, 191, 192, 194, 196, 211, 283, 338]. When yield data for region *sr* is not available, yield data from regions with the closest climate are used. [c]Mean, low and high annual dry mass yield of switchgrass in t_{DM}/ha/yr. Data was adapted from [160, 162, 192, 196, 211, 338]. When yield data for region *sr* is not available, yield data from regions with the closest climate are used. [d]Mean, low and high annual dry mass yield of short rotation coppice willow in t_{DM}/ha/yr. Data was adapted from various willow yield datasets in the literature [122, 162, 338]. When yield data for region *sr* is not available, yield data from regions with the closest climate are used. [e]Mean, low and high annual dry mass yield of wheat in t_{DM}/ha/yr. Dry mass wheat yield data was obtained from the US Department of Agriculture [319]. To obtain the yield of wheat straw, a grain to straw conversion factor within the range 1.6 - 2.0 was used [131].

B.3 Land cover data

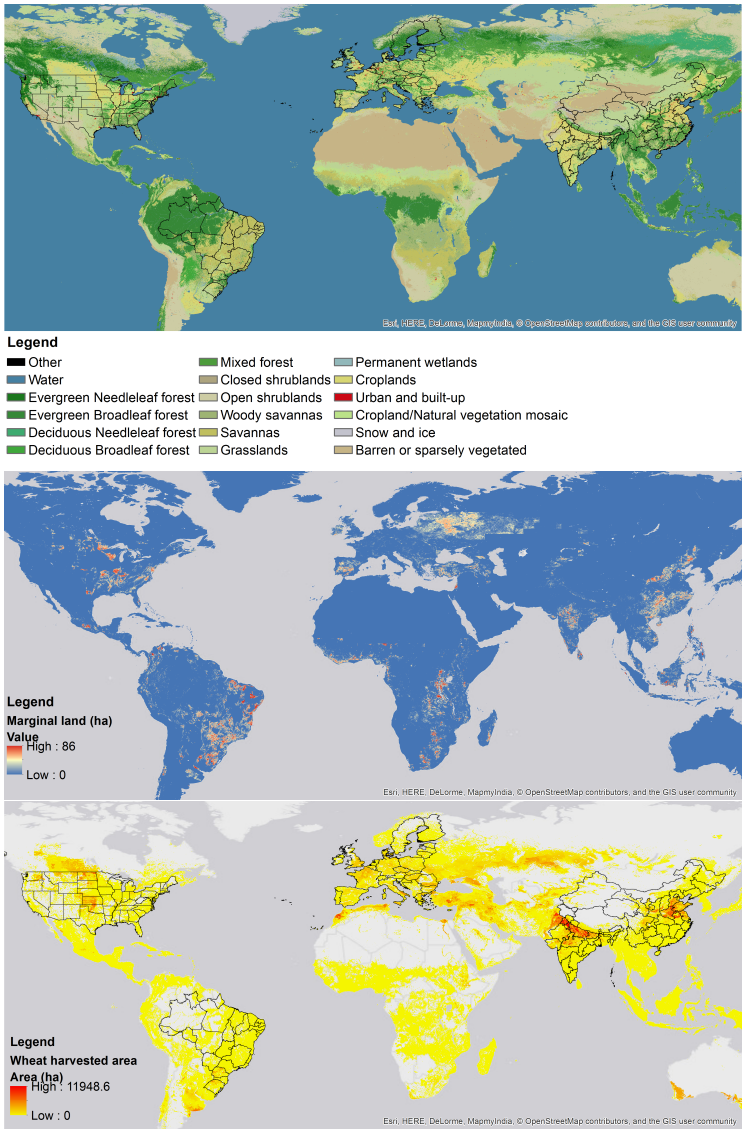


Figure B.2: Land cover with a resolution of 15 arc second geographic, adapted from the MODIS dataset [164], marginal land area with a resolution of 30 arc second geographic, adapted from Cai *et al.* [114], and harvested wheat area with a resolution of 5 minute geographic, adapted from MAPSPAM [166].

Table B.14: Land cover, marginal land and harvested wheat harvested area (Brazil and China)

Sub-region *sr*	Harvested wheat (ha)[a]	Cropland (ha)[b]	Grassland (ha)[b]	Forests (ha)[b]	Marginal land (ha)[c]	Marginal land - low OWR (ha)[d]
Acre	0	4529	8744	14796138	65464	65464
Alagoas	0	198379	104788	21278	538378	492540
Amapa	0	75662	99536	12048270	755909	755527
Amazonas	0	42148	264495	149210755	365120	365120
Bahia	139	2332945	2400444	2888010	7602747	7581625
Ceara	0	181331	126727	84689	1999432	1984798
Distrito Federal	2057	1368	786	21986	229625	229625
Espirito Santo	0	71259	42667	469747	617785	614718
Goias	12694	3256098	425759	188220	5852712	5852712
Maranhao	0	528157	156577	4809429	4763187	4763187
Mato Grosso	786	6351939	3312967	34375031	6428726	6428726
Mato Grosso do Sul	72331	1656405	4894778	1779656	7629190	7629190
Minas Gerais	16247	2313868	617202	2107767	9237942	9237942
Para	0	315938	296578	95045602	3428322	3416272
Paraiba	0	132971	277816	14484	639569	639569
Parana	1143865	3755553	1494937	4854533	5706602	5702059
Pernambuco	0	220129	421072	41975	990765	961456
Piaui	0	286497	128473	168498	3462185	3462185
Rio de Janeiro	0	93119	45561	791173	397731	396967
Rio Grande do Norte	0	167051	388911	8178	80691	80691
Rio Grande do Sul	851954	6038675	7898979	2952537	7876103	7876103
Rondonia	0	84925	351732	14417261	690893	690893
Roraima	0	23040	2278561	17130388	109482	109482
Santa Catarina	80420	547862	108752	4919658	1196099	1193191
Sao Paulo	62872	3426641	2921162	4024247	6118991	6118572
Sergipe	0	73177	192151	10946	1141001	985370
Tocantins	0	365163	1351570	795593	1369558	1369558
Anhui	1350540	9008590	53236	3584114	1240645	1195409
Beijing	37377	492158	235133	573765	163759	0
Chongqing	297372	1680121	12125	3868173	1380615	1314097
Fujian	5798	788547	62106	8141189	476468	457905
Gansu	649244	3626168	16539874	2687901	2306145	322923
Guangdong	4155	2175471	172886	7938579	1371573	1298031
Guangxi Zhuang	8483	1232313	55201	9722985	5379165	5378030
Guizhou	374575	2704320	126664	7237191	3620343	3620343
Hainan	0	302004	12377	1201111	930152	929428
Hebei	1137209	9208888	5640878	2278828	3039792	0
Heilongjiang	80519	17993228	1568397	16426106	558354	239576
Henan	2454033	12928238	155665	1986088	577474	10695
Hubei	460302	7266175	85837	8066266	1307885	1272333
Hunan	53940	3919821	77140	9784477	6191445	6191445
Inner Mongolia	431015	9129420	60913567	10450574	4567746	265022
Jiangsu	1146168	7828318	172257	426293	76925	34716
Jiangxi	13663	3711596	97963	8730602	2874002	2744951
Jilin	13946	7285991	1828079	7195687	541587	232838
Liaoning	16192	7576514	770886	3422504	1080172	5211
Ningxia Hui	195390	778026	3550427	35323	38509	0
Qinghai	87259	175418	49673691	122859	9721	9215
Shaanxi	820401	5021710	5487258	8947397	1862026	537194
Shandong	2179912	13244852	481401	222284	899162	19678
Shanghai	24371	426168	21090	11685	924	0
Shanxi	347502	5694177	6219109	2748386	4463694	1216620
Sichuan	1365270	7510980	18591401	18967825	1804046	1203745
Tianjin	83118	781202	95431	65487	232087	0
Xinjiang Uyghur	614630	6343242	38744012	972599	328036	0
Yunnan	296344	3296249	2467111	23357628	2062503	2062503
Zhejiang	52596	2010763	87662	6559833	2627207	1829519

Table B.15: Land cover, marginal land and harvested wheat harvested area (EU and India)

Sub-region *sr*	Wheat harvested area (ha)[a]	Cropland (ha)[b]	Grassland (ha)[b]	Forests (ha)[b]	Marginal land (ha)[c]	Marginal land - low OWR (ha)[d]
Austria	282813	1319031	842569	4675105	128706	128706
Belgium	214079	1024230	53644	774849	57725	57678
Bulgaria	1033864	5254531	252653	3297318	539360	481791
Croatia	175656	1354763	282974	2118367	168810	167736
Cyprus	3778	136242	109522	6023	0	0
Czech Republic	822510	2520362	32382	2734562	214332	214332
Denmark	637964	2657579	144640	534542	83300	82999
Estonia	84237	247227	136588	2791997	1135160	1134181
Finland	208661	241660	413429	16023481	8131	5157
France	5232675	25978359	1312489	11362939	965400	963138
Germany	3125000	10909863	439866	11744615	682462	681802
Greece	782626	4023178	936396	2491456	484050	452925
Hungary	1122858	5660820	25761	1218001	174406	139783
Ireland	92307	260390	5468795	945376	1521890	1516496
Italy	1403762	12011815	1691114	7546617	504537	398411
Latvia	190236	659162	87630	3490681	1412723	1412186
Lithuania	356901	2067600	45105	1911212	1590564	1590472
Luxembourg	13983	53896	2422	98199	1197	1197
Malta	1271	14076	4765	63	0	0
Netherlands	129071	877514	433984	502616	92373	92082
Poland	2231857	11508067	120279	9252908	2379125	2378547
Portugal	136834	2093644	383453	929271	1231336	1230691
Romania	2227876	11501556	178437	6645953	649723	576247
Slovakia	364508	1552104	23795	2256763	157578	157578
Slovenia	30460	158684	23056	1344556	33323	33323
Spain	2122749	18065148	3742814	6262563	6855073	6852712
Sweden	362669	1004257	1482953	23932037	457029	451412
United Kingdom	1871551	6737751	10162945	4223947	1548376	1513903
Andhra Pradesh	9656	13307665	148698	1226242	1822939	1142622
Arunachal Pradesh	3832	45325	498197	6873113	76598	76598
Assam	48111	2186102	182621	1517693	230982	230982
Bihar	1448068	7958426	80600	170385	98260	15219
Chhattisgarh	74003	3574992	26689	1851355	121831	109701
Delhi	19580	59652	975	0	668	0
Goa	0	16592	3366	79091	15565	15565
Gujarat	965926	11575614	629627	202106	1385494	37683
Haryana	1166419	4227329	1148	34914	1615	0
Himachal Pradesh	369177	368843	1099908	1621224	75187	12947
Jammu and Kashmir	255180	1371071	3725986	1685578	180611	22290
Jharkhand	40523	3990261	33766	595924	575933	531666
Karnataka	1907	11123324	122450	1207181	1062742	402873
Kerala	0	322889	3255	1492373	646538	524150
Madhya Pradesh	2681304	19787998	454460	1167565	4639474	855609
Maharashtra	752521	20504500	32319	1299262	4310811	2942568
Manipur	4	75316	6951	1838585	6912	6912
Meghalaya	2041	52606	15507	948206	113400	113400
Mizoram	6	1620	220	1894903	449	449
Nagaland	1179	5347	739	1319236	5319	5319
Odisha	5571	4668909	60187	1482198	625011	613994
Pondicherry	0	32020	440	598	3034	175
Punjab	1575621	4768287	1069	62908	7026	498
Rajasthan	2497183	20165145	641437	115671	1237793	19894
Sikkim	4383	2044	202531	315293	991	991
TamilNadu	0	4049505	45262	790576	645084	7620
Tripura	2576	40607	47	168152	29486	29486
Uttar Pradesh	5948565	22126919	120484	411306	106167	0
Uttarakhand	372507	543427	906279	2525426	206629	9316
West Bengal	173474	5937802	32272	369975	279391	275862

Table B.16: Land cover, marginal land and harvested wheat area (US)

Sub-region *sr*	Wheat harvested area (ha)[a]	Cropland (ha)[b]	Grassland (ha)[b]	Forests (ha)[b]	Marginal land (ha)[c]	Marginal land - low OWR (ha)[d]
Alabama	20123	398268	93544	5593855	1321772	1321196
Alaska	0	53534	22091691	12490700	1465	1395
Arizona	39139	426687	4690061	817390	0	0
Arkansas	143730	3420507	444584	5028882	2385539	2385539
California	115813	4272905	5856101	9065097	43884	20114
Colorado	780620	1102173	20027818	3811132	517109	515675
Connecticut	1	7801	739	985385	10051	9910
Delaware	20733	93339	4624	61178	340892	337646
Florida	3783	791771	537435	3669668	834105	831417
Georgia	60912	888444	104033	5173742	1244597	1244597
Hawaii	0	48014	156577	643340	0	0
Idaho	320812	1921733	11494023	7467668	47955	47955
Illinois	317882	10087503	30778	467639	2817237	2812533
Indiana	170056	5005968	21341	824892	511783	509139
Iowa	23168	12179716	5756	45639	358433	358433
Kansas	3656919	5615008	14634921	15695	1153356	1017246
Kentucky	143754	1874710	27727	3890270	1513903	1513903
Louisiana	49933	1953391	74687	3315499	647123	646708
Maine	0	35747	7014	7676144	98527	96318
Maryland	53500	240810	5504	755977	845353	792706
Massachusetts	0	14909	4985	1598136	99517	97691
Michigan	247566	1621019	51128	6890900	350089	217913
Minnesota	688062	10194383	96783	6001748	4858069	4852214
Mississippi	38206	1783635	45938	4278708	1733077	1732903
Missouri	321011	5507341	811555	3171928	3038770	3038770
Montana	1325102	1954948	27522033	7857145	1938973	1875857
Nebraska	689084	8139317	11445049	16387	96447	52975
Nevada	3646	187795	15611892	222819	2515	2515
New Hampshire	0	5536	2579	2235391	6674	6674
New Jersey	9632	100511	12157	819781	402441	399131
New Mexico	89403	389964	13555191	1196723	1411	1411
New York	38571	191208	12236	7235303	160895	148964
North Carolina	175674	875989	41818	5136186	2525415	2524324
North Dakota	3254269	13716895	3926992	38153	2072281	2027219
Ohio	357388	3888697	14626	1848257	184961	184961
Oklahoma	1639241	1285391	12604767	696497	606886	520774
Oregon	299564	1341064	10866425	11766586	22684	22666
Pennsylvania	58523	499219	11135	6103784	547859	547740
Rhode Island	0	5001	362	196382	16414	14934
South Carolina	60940	214200	51380	3274782	428381	428381
South Dakota	615808	8018063	11175820	368812	376552	354855
Tennessee	87527	1394394	35008	4274163	1789359	1789359
Texas	1058287	5602049	37201942	1626854	2780385	2732789
Utah	50872	498464	11978962	967047	3124	3124
Vermont	4	12125	2438	2060885	61	61
Virginia	63834	299991	18951	5710124	1118266	1114302
Washington	699836	1886521	4691697	9833514	93421	92662
West Virginia	1983	57765	15428	5037956	137764	137764
Wisconsin	84259	2436286	35165	5046464	3277713	3267378
Wyoming	56313	217786	22124670	2473527	41702	24638

[a]Obtained using harvested wheat area from MAPSPAM [166]. [b]Obtained using the MODIS dataset [164].[c]Obtained using marginal land dataset from Cai *et al.* [114]. Obtained using marginal land dataset from Cai *et al.* [114] (Scenario 1) and the Overall Water Risk index [165]

B.4 Electricity data

Table B.17: Electricity cost and carbon intensity over time (1/3)

Region	Electricity ($/MWh)[a]	CI BAU ($kgCO_2/MWh)[b]	CI 2030 ($kgCO_2/MWh)[c]	CI 2040 ($kgCO_2/MWh)[c]	CI 2050 ($kgCO_2/MWh)[c]	CI 2060 ($kgCO_2/MWh)[c]
Brazil	163	157	89	21	0.0	0
Anhui	112	657	214	44	0.0	0
Beijing	117	657	214	44	0.0	0
Chongqing	114	657	214	44	0.0	0
Fujian	107	657	214	44	0.0	0
Gansu	109	657	214	44	0.0	0
Guangdong	119	657	214	44	0.0	0
Guangxi Zhuang	127	657	214	44	0.0	0
Guizhou	101	657	214	44	0.0	0
Hainan	94	657	214	44	0.0	0
Hebei	94	657	214	44	0.0	0
Heilongjiang	117	657	214	44	0.0	0
Henan	99	657	214	44	0.0	0
Hubei	119	657	214	44	0.0	0
Hunan	119	657	214	44	0.0	0
Inner Mongolia	82	657	214	44	0.0	0
Jiangsu	114	657	214	44	0.0	0
Jiangxi	114	657	214	44	0.0	0
Jilin	125	657	214	44	0.0	0
Liaoning	122	657	214	44	0.0	0
Ningxia Hui	94	657	214	44	0.0	0
Qinghai	94	657	214	44	0.0	0
Shaanxi	99	657	214	44	0.0	0
Shandong	115	657	214	44	0.0	0
Shanghai	131	657	214	44	0.0	0
Shanxi	95	657	214	44	0.0	0
Sichuan	108	657	214	44	0.0	0
Tianjin	109	657	214	44	0.0	0
Xinjiang Uyghur	73	657	214	44	0.0	0
Yunnan	109	657	214	44	0.0	0
Zhejiang	118	657	214	44	0.0	0

Table B.18: Electricity cost and carbon intensity over time (2/3)

Region	Electricity ($/MWh)[a]	CI BAU ($kgCO_2/MWh$)[b]	CI 2030 ($kgCO_2/MWh$)[c]	CI 2040 ($kgCO_2/MWh$)[c]	CI 2050 ($kgCO_2/MWh$)[c]	CI 2060 ($kgCO_2/MWh$)[c]
Austria	82	164	62	18	0.1	0
Belgium	88	226	85	24	0.2	0
Bulgaria	94	498	188	53	0.3	0
Croatia	99	233	88	25	0.2	0
Cyprus	145	649	245	69	0.4	0
Czech Republic	85	521	197	56	0.4	0
Denmark	69	174	66	19	0.1	0
Estonia	86	1026	388	110	0.7	0
Finland	72	107	40	11	0.1	0
France	86	46	17	5	0.0	0
Germany	90	450	170	48	0.3	0
Greece	93	586	221	63	0.4	0
Hungary	86	274	104	29	0.2	0
Ireland	137	418	158	45	0.3	0
Italy	104	342	129	37	0.2	0
Latvia	95	145	55	15	0.1	0
Lithuania	82	186	70	20	0.1	0
Luxembourg	87	281	106	30	0.2	0
Malta	158	652	246	70	0.4	0
Netherlands	72	489	185	52	0.3	0
Poland	79	730	276	78	0.5	0
Portugal	91	346	131	37	0.2	0
Romania	83	340	128	36	0.2	0
Slovakia	93	169	64	18	0.1	0
Slovenia	81	265	100	28	0.2	0
Spain	118	293	111	31	0.2	0
Sweden	80	11	4	1	0.0	0
United Kingdom	114	349	132	37	0.2	0
India	36	771	252	52	0.0	0

Table B.19: Electricity cost and carbon intensity over time (3/3)

Region	Electricity ($/MWh)[a]	CI BAU ($kgCO_2/MWh$)[b]	CI 2030 ($kgCO_2/MWh$)[c]	CI 2040 ($kgCO_2/MWh$)[c]	CI 2050 ($kgCO_2/MWh$)[c]	CI 2060 ($kgCO_2/MWh$)[c]
Alabama	63	417	157	44	0.3	0
Alaska	179	422	159	45	0.3	0
Arizona	77	425	161	45	0.3	0
Arkansas	56	510	193	54	0.3	0
California	155	206	78	22	0.1	0
Colorado	73	671	254	72	0.5	0
Connecticut	138	228	86	24	0.2	0
Delaware	78	404	152	43	0.3	0
Florida	76	467	176	50	0.3	0
Georgia	62	457	173	49	0.3	0
Hawaii	262	696	263	74	0.5	0
Idaho	72	86	32	9	0.1	0
Illinois	66	370	140	40	0.3	0
Indiana	71	829	313	89	0.6	0
Iowa	83	456	172	49	0.3	0
Kansas	75	547	207	58	0.4	0
Kentucky	53	894	338	95	0.6	0
Louisiana	56	400	151	43	0.3	0
Maine	90	158	60	17	0.1	0
Maryland	79	463	175	49	0.3	0
Massachusetts	138	376	142	40	0.3	0
Michigan	71	502	190	54	0.3	0
Minnesota	80	464	175	50	0.3	0
Mississippi	63	428	162	46	0.3	0
Missouri	73	771	291	82	0.5	0
Montana	62	572	216	61	0.4	0
Nebraska	79	586	221	63	0.4	0
Nevada	81	350	132	37	0.2	0
NewHampshire	130	144	54	15	0.1	0
New Jersey	105	254	96	27	0.2	0
New Mexico	57	719	272	77	0.5	0
New York	61	211	80	23	0.1	0
North Carolina	64	396	150	42	0.3	0
North Dakota	85	760	287	81	0.5	0
Ohio	66	670	253	72	0.5	0
Oklahoma	53	476	180	51	0.3	0
Oregon	59	139	53	15	0.1	0
Pennsylvania	66	390	147	42	0.3	0
Rhode Island	148	396	149	42	0.3	0
South Carolina	53	287	108	31	0.2	0
South Dakota	82	235	89	25	0.2	0
Tennessee	53	453	171	48	0.3	0
Texas	59	479	181	51	0.3	0
Utah	68	744	281	79	0.5	0
Vermont	105	31	12	3	0.0	0
Virginia	69	372	141	40	0.3	0
Washington	52	85	32	9	0.1	0
West Virginia	65	904	341	97	0.6	0
Wisconsin	79	634	239	68	0.4	0
Wyoming	66	927	350	99	0.6	0

[a]The cost of electricity in the industrial sector were used to calculate both the cost of using electricity at various stages of the biomass supply chain, and the revenues from generating electricity (as opposed to whole sale electricity prices, due their high volatility and low predictability). Data from the MME was used for Brazil [179], from the CEIC database for China [180], from the EUROSTAT database for the EU [181], from the Government of India for India [182], and for the EIA for the US [183]. [b]2015 data from the IEA was used for the BAU Carbon intensity of electricity in China, EU countries, India and Brazil at the national level [248], and 2016 data from the Emissions & Generation Resource Integrated Database [249] was used for US states.[c]The carbon intensity of electricity in 2030 and after was calculated by applying regional electricity system's decarbonisation rates obtained from the IAMC 1.5 Scenario explorer database [10] to the BAU carbon intensity of electricity.

Table B.20: Energy conversion factors

Sub-region sr	η_{grid}[a]	$C_{elec \rightarrow PE}$[b]	$C_{diesel \rightarrow elec}$[c]	$C_{NG \rightarrow elec}$[c]	$C_{HFO \rightarrow elec}$[c]
Brazil	0.36	2.78	0.35 (0.20 - 0.45)	0.45 (0.39 - 0.58)	0.34 (0.34 - 0.44)
China	0.32	3.13	0.35 (0.20 - 0.45)	0.39 (0.39 - 0.58)	0.34 (0.34 - 0.44)
Austria	0.43	2.33	0.35 (0.20 - 0.45)	0.46 (0.39 - 0.58)	0.36 (0.36 - 0.44)
Belgium	0.45	2.22	0.35 (0.20 - 0.45)	0.51 (0.39 - 0.58)	0.41 (0.41 - 0.44)
Bulgaria	0.32	3.13	0.35 (0.20 - 0.45)	0.34 (0.39 - 0.58)	0.24 (0.24 - 0.44)
Croatia	0.32	3.13	0.35 (0.20 - 0.45)	0.34 (0.39 - 0.58)	0.24 (0.24 - 0.44)
Cyprus	0.32	3.13	0.35 (0.20 - 0.45)	0.34 (0.39 - 0.58)	0.24 (0.24 - 0.44)
Czech Republic	0.32	3.13	0.35 (0.20 - 0.45)	0.34 (0.39 - 0.58)	0.24 (0.24 - 0.44)
Denmark	0.43	2.33	0.35 (0.20 - 0.45)	0.45 (0.39 - 0.58)	0.40 (0.40 - 0.44)
Estonia	0.32	3.13	0.35 (0.20 - 0.45)	0.34 (0.39 - 0.58)	0.24 (0.24 - 0.44)
Finland	0.42	2.38	0.35 (0.20 - 0.45)	0.49 (0.39 - 0.58)	0.35 (0.35 - 0.44)
France	0.4	2.50	0.35 (0.20 - 0.45)	0.48 (0.39 - 0.58)	0.31 (0.31 - 0.44)
Germany	0.39	2.56	0.35 (0.20 - 0.45)	0.43 (0.39 - 0.58)	0.34 (0.34 - 0.44)
Greece	0.37	2.70	0.35 (0.20 - 0.45)	0.45 (0.39 - 0.58)	0.36 (0.36 - 0.44)
Hungary	0.35	2.86	0.35 (0.20 - 0.45)	0.39 (0.39 - 0.58)	0.33 (0.33 - 0.44)
Ireland	0.42	2.38	0.35 (0.20 - 0.45)	0.47 (0.39 - 0.58)	0.36 (0.36 - 0.44)
Italy	0.45	2.22	0.35 (0.20 - 0.45)	0.51 (0.39 - 0.58)	0.41 (0.41 - 0.44)
Latvia	0.32	3.13	0.35 (0.20 - 0.45)	0.34 (0.39 - 0.58)	0.24 (0.24 - 0.44)
Lithuania	0.32	3.13	0.35 (0.20 - 0.45)	0.34 (0.39 - 0.58)	0.24 (0.24 - 0.44)
Luxembourg	0.55	1.82	0.35 (0.20 - 0.45)	0.55 (0.39 - 0.58)	0.41 (0.41 - 0.44)
Malta	0.32	3.13	0.35 (0.20 - 0.45)	0.34 (0.39 - 0.58)	0.24 (0.24 - 0.44)
Netherlands	0.44	2.27	0.35 (0.20 - 0.45)	0.47 (0.39 - 0.58)	0.43 (0.43 - 0.44)
Poland	0.36	2.78	0.35 (0.20 - 0.45)	0.34 (0.39 - 0.58)	0.36 (0.36 - 0.44)
Portugal	0.43	2.33	0.35 (0.20 - 0.45)	0.54 (0.39 - 0.58)	0.38 (0.38 - 0.44)
Romania	0.32	3.13	0.35 (0.20 - 0.45)	0.34 (0.39 - 0.58)	0.24 (0.24 - 0.44)
Slovakia	0.31	3.23	0.35 (0.20 - 0.45)	0.35 (0.39 - 0.58)	0.23 (0.23 - 0.44)
Slovenia	0.32	3.13	0.35 (0.20 - 0.45)	0.34 (0.39 - 0.58)	0.23 (0.23 - 0.44)
Spain	0.39	2.56	0.35 (0.20 - 0.45)	0.50 (0.39 - 0.58)	0.35 (0.35 - 0.44)
Sweden	0.38	2.63	0.35 (0.20 - 0.45)	0.49 (0.39 - 0.58)	0.37 (0.37 - 0.44)
United Kingdom	0.44	2.27	0.35 (0.20 - 0.45)	0.52 (0.39 - 0.58)	0.29 (0.29 - 0.44)
India	0.28	3.57	0.35 (0.20 - 0.45)	0.41 (0.39 - 0.58)	0.26 (0.26 - 0.44)
USA	0.37	2.70	0.35 (0.20 - 0.45)	0.43 (0.39 - 0.58)	0.35 (0.35 - 0.44)

[a]Average power generation efficiencies from IEA 2008 [152].[b]Own calculations. [c]Fuel conversion efficiencies from [151, 152]

B.5 CO_2 storage data

Table B.21: CO_2 storage capacity in the BAU and high scenarios in Brazil and China

Sub-region *sr*	Capacity BAU ($GtCO_2$)	Capacity High ($GtCO_2$)	Notes and sources
Acre	0.0	20.8	▪ To date, no national scale quantitative geological survey of Brazil. ▪ Only reliable quantitative estimates for the Campos basin, a depleted oil field, off the south-east coast of Brazil, which comprises of 17 off-shore oil fields, with a total capacity of 950 $MtCO_2$[170]. ▪ Based on geographic distribution, 16 of them (887.9 $MtCO_2$) were attributed to the the state of Rio de Janeiro, and one of them (61.3 $MtCO_2$) to the state of Espirito Santo, for modelling purposes. ▪ In the high scenario, an approximate CO_2 storage capacity quantification was performed using the methodology described in Wildenborg *et al.* [171], by multiplying each state basin area adapted from the Brazil geological survey [172] (adapated in ARCGIS) with a saline aquifer suitability probability of 50% and a CO_2 storage density (or storage factor) of 0.2 $MtCO_2/km^2$. This new estimated CO_2 storage capacity was added to that of the Campos oil fields basin used in the BAU scenario.
Alagoas	0.0	19.9	
Amapa	0.0	20.7	
Amazonas	0.0	110.7	
Bahia	0.0	20.0	
Ceara	0.0	16.4	
Distrito Federal	0.0	0.0	
Espirito Santo	0.06	11.8	
Goias	0.0	4.6	
Maranhao	0.0	45.6	
Mato Grosso	0.0	43.1	
Mato Grosso do Sul	0.0	28.6	
Minas Gerais	0.0	32.2	
Para	0.0	53.0	
Paraiba	0.0	1.6	
Parana	0.0	16.8	
Pernambuco	0.0	6.1	
Piaui	0.0	20.8	
Rio de Janeiro	0.88	16.1	
Rio Grande do Norte	0.0	6.1	
Rio Grande do Sul	0.0	54.3	
Rondonia	0.0	7.2	
Roraima	0.0	7.4	
Santa Catarina	0.0	24.1	
Sao Paulo	0.0	41.9	
Sergipe	0.0	2.1	
Tocantins	0.0	9.0	
Anhui	100.5	100.5	▪ Data for the BAU and high scenarios was taken from a national scale geological survey, summing up CO_2 storage capacity in sedimentary basins (adapated from the US Geological survey [173]), in saline aquifers [174, 339] and in oil & gas fields [174].
Beijing	9.4	9.4	
Chongqing	20.3	20.3	
Fujian	11.0	11.0	
Gansu	36.7	36.7	
Guangdong	81.6	81.6	
Guangxi Zhuang	11.9	11.9	
Guizhou	1.5	1.5	
Hainan	58.6	58.6	
Hebei	163.0	163.0	
Heilongjiang	151.1	151.1	
Henan	114.0	114.0	
Hubei	35.0	35.0	
Hunan	20.5	20.5	
Inner Mongolia	236.1	236.1	
Jiangsu	145.4	145.4	
Jiangxi	0.0	0.0	
Jilin	61.9	61.9	
Liaoning	52.0	52.0	
Ningxia Hui	16.1	16.1	
Qinghai	21.7	21.7	
Shaanxi	108.7	108.7	
Shandong	170.0	170.0	
Shanghai	171.0	171.0	
Shanxi	43.6	43.6	
Sichuan	55.4	55.4	
Tianjin	38.4	38.4	
Xinjiang Uyghur	998.6	998.6	
Yunnan	0.8	0.8	
Zhejiang	171.0	171.0	

Table B.22: CO_2 storage capacity in the BAU and high scenarios in the EU and India

Sub-region *sr*	Capacity BAU ($GtCO_2$)	Capacity High ($GtCO_2$)	Notes and sources
Austria	0.0	0.0	▪ Data for the BAU scenario was taken from the EU geocapacity geological survey [175], to the exception of the UK which was taken from the ETI UK CO_2stored database [176]. ▪ No alternative database was available for the optimistic scenario.
Belgium	0.2	0.2	
Bulgaria	2.1	2.1	
Croatia	3.1	3.1	
Cyprus	0.0	0.0	
Czech Republic	0.8	0.8	
Denmark	2.8	2.8	
Estonia	0.0	0.0	
Finland	0.0	0.0	
France	8.7	8.7	
Germany	17.1	17.1	
Greece	0.8	0.8	
Hungary	0.5	0.5	
Ireland	0.0	0.0	
Italy	6.5	6.5	
Latvia	0.4	0.4	
Lithuania	0.0	0.0	
Luxembourg	0.0	0.0	
Malta	0.0	0.0	
Netherlands	2.0	2.0	
Poland	2.5	2.5	
Portugal	0.0	0.0	
Romania	9.0	9.0	
Slovakia	1.7	1.7	
Slovenia	0.1	0.1	
Spain	14.0	14.0	
Sweden	0.0	0.0	
United Kingdom	14.4	77.0	
Andhra Pradesh	0.0	6.5	▪ To date, no national scale quantitative geological survey of India. ▪ In the high scenario, the same approach developed by Wildenborg *et al.* [171], and used for Brazil, was applied to sedimentary basin area in Indian states [177].
Arunachal Pradesh	0.0	0.6	
Assam	0.0	3.2	
Bihar	0.0	0.0	
Chandigarh	0.0	0.0	
Delhi	0.0	0.0	
Goa	0.0	0.0	
Gujarat	0.0	12.7	
Haryana	0.0	0.0	
Himachal Pradesh	0.0	0.0	
Jammu and Kashmir	0.0	0.0	
Jharkhand	0.0	0.0	
Karnataka	0.0	0.0	
Kerala	0.0	0.0	
Madhya Pradesh	0.0	0.0	
Maharashtra	0.0	12.0	
Manipur	0.0	2.7	
Meghalaya	0.0	0.3	
Mizoram	0.0	2.6	
Nagaland	0.0	1.7	
Odisha	0.0	6.1	
Pondicherry	0.0	0.0	
Punjab	0.0	0.0	
Rajasthan	0.0	7.6	
Sikkim	0.0	0.0	
Tamil Nadu	0.0	6.0	
Tripura	0.0	1.3	
Uttar Pradesh	0.0	0.0	
Uttarakhand	0.0	0.0	
West Bengal	0.0	0.0	

Table B.23: CO_2 storage capacity in the BAU and high scenarios in the USA

Sub-region *sr*	Capacity BAU ($GtCO_2$)	Capacity High ($GtCO_2$)	Notes and sources
Alabama	367.7	830.3	▪ Data from the average and high CO_2 storage capacity scenarios in the US carbon storage ATLAS [178] were used for the BAU and high scenarios respectively.
Alaska	0.0	0.0	
Arizona	1.0	2.5	
Arkansas	24.8	69.4	
California	153.5	425.2	
Colorado	146.2	386.2	
Connecticut	0.0	0.0	
Delaware	0.1	0.1	
Florida	383.7	912.3	
Georgia	250.4	437.8	
Hawaii	0.0	0.0	
Idaho	0.5	1.4	
Illinois	88.8	230.2	
Indiana	73.5	144.1	
Iowa	0.0	0.0	
Kansas	38.1	91.8	
Kentucky	54.6	128.4	
Louisiana	930.1	2588.6	
Maine	0.0	0.0	
Maryland	2.6	3.0	
Massachusetts	0.0	0.0	
Michigan	46.3	67.0	
Minnesota	0.0	0.0	
Mississippi	521.3	1330.0	
Missouri	0.5	1.2	
Montana	384.1	944.1	
Nebraska	56.9	118.4	
Nevada	0.0	0.0	
New Hampshire	0.0	0.0	
New Jersey	0.0	0.0	
New Mexico	996.9	2778.6	
New York	4.9	4.9	
North Carolina	6.2	16.8	
North Dakota	147.4	256.1	
Ohio	12.2	13.2	
Oklahoma	89.6	222.2	
Oregon	44.3	125.2	
Pennsylvania	19.9	21.1	
Rhodelsland	0.0	0.0	
South Carolina	32.4	35.7	
South Dakota	8.3	14.5	
Tennessee	2.8	6.9	
Texas	3069.7	8450.0	
Utah	97.4	259.0	
Vermont	0.0	0.0	
Virginia	1.3	2.7	
Washington	247.1	698.4	
West Virginia	24.2	33.8	
Wisconsin	0.4	0.4	
Wyoming	632.6	1692.7	